RECORDS OF THE WESTERN AUSTRALIAN MUSEUM 40 001–046 (2025) DOI: 10.18195/issn.0312-3162.40.2025.001-046

Molecular and morphological assessment of the widely distributed legless gecko *Delma tincta* Kluge (Squamata: Pygopodidae), including a taxonomic revision

Mitzy Pepper[1*], Paul Doughty[2], Jade Fletcher[1] and J. Scott Keogh[1]

[1] Division of Ecology and Evolution, Research School of Biology, Australian National University, Canberra, Australian Capital Territory 2600, Australia.

[2] Collections and Research, Western Australian Museum, 49 Kew Street, Welshpool, Western Australia 6106, Australia.

Corresponding author: mitzy.pepper@anu.edu.au

ABSTRACT – The pygopodid lizard *Delma tincta* is widely distributed across Australia, including the arid zone, eastern seaboard and monsoon tropics. *Delma* is morphologically extremely conservative, and the highly cryptic *D. tincta* species complex presents a particular taxonomic challenge. Here, we use a large SNP molecular dataset and a detailed morphological dataset to evaluate variation in *Delma tincta* across its range. Our SNP data strongly support eight monophyletic populations, which we allocate to four species, based on a combination of morphological and genetic distinctiveness. Two of these species, including type *D. tincta*, have largely overlapping distributions over a vast area in central and northern Australia. The type specimen of *D. tincta* from Normanton in Queensland was collected 140 years ago and is in very poor condition. In the absence of other information, we elected to assign the name *tincta* to one of the two clades for which a tissue-sampled specimen was nearest to the type location. A specimen for which we had a sequence was collected 50 km from this locality, and we allocate the name *D. tincta* to this lineage. The other lineage we name *D. hades* sp. nov., with a sequenced specimen occurring as close as 200 km to the type location of *D. tincta*. These sympatric lineages, which are not each other's closest relatives, are morphologically cryptic and cannot be distinguished from one another without nuclear molecular data. Such cryptic species are a challenge for field ecologists and collection managers, and we provide recommendations for how to treat such taxa. We redescribe the lineage that occurs in eastern Queensland as *Delma reticulata* Garman. *Delma reticulata* is also challenging to distinguish from the two sympatric central species, but differs morphologically where they are geographically close to each other in southern Queensland. The most morphologically distinctive lineage is *Delma branchia* sp. nov., which occurs in the Pilbara and Gascoyne regions of Western Australia and is readily identified by a series of ventrolateral transverse bars that continue down the neck. The four species can be diagnosed from all congeners by unique fixed differences in nuclear SNPs and by aspects of colouration in some instances. Deep genetic structure and significant numbers of fixed and private allelic differences suggest additional species-level diversity may be present within three of the four taxa in the *D. tincta* species-group, requiring more detailed sampling in future. We comment on ecological and evolutionary patterns in *Delma*, including problematic patterns of introgression as observed here and in other groups. These new taxa bring the number of *Delma* species to 25, accounting for nearly half the species diversity of enigmatic pygopods.

KEYWORDS: Australian arid zone, monsoon tropics, cryptic species, molecular genetics, SNPs, gecko, Pygopodidae, Wet Tropics biogeographic barriers, fixed differences

urn:lsid:zoobank.org:pub:DB627045-E0D6-49B7-95A3-763E48C25097

INTRODUCTION

Australia harbours one of the most diverse lizard assemblages on the planet (Webb et al. 2015). In particular, geckos have undergone remarkable diversification in the arid zone, which supports the highest species richness across all four major gecko families found in the country (Norris et al. 2021). It was long assumed the superficially featureless deserts comprised young radiations with limited genetic diversity over vast areas (see Byrne et al. 2008). However, in recent decades, it has become clear that species with extremely wide distributions spanning

much of the arid zone comprise significant unrecognised taxonomic diversity (Oliver et al. 2009, 2014; Melville et al. 2021). The past two decades have seen integrative taxonomic revisions of many arid zone gecko groups, including *Heteronotia* (Pepper et al. 2013), *Diplodactylus* (Doughty et al. 2007; Hutchinson et al. 2009; Oliver et al. 2014), *Rhynchoedura* (Pepper et al. 2011), *Gehyra* (Doughty et al. 2018a; Kealley et al. 2018), *Lucasium* (Eastwood et al. 2020), *Nephrurus* (Oliver et al. 2022), *Oedura* (Oliver and Doughty 2016) and *Crenadactylus* (Doughty et al. 2016). In contrast to the deserts, the monsoon tropics of northern Australia are relatively depauperate of geckos, with the exception of the Kimberley region in Western Australia, which is a hotspot of gekkonine species richness (Norris et al. 2021). Indeed, intensive sampling across the monsoon tropics in recent years has identified many deeply divergent gecko lineages in *Gehyra* (Doughty et al. 2012, 2018b; Ashman et al. 2018; Oliver et al. 2020) and *Heteronotia* (Moritz et al. 2016). Together, these studies across central and northern Australia have resulted in the identification and description of dozens of new gecko species. Many of these newly described species differ only subtly in morphology. In the past, this variation was usually attributed to intraspecific variation within a wide-ranging taxon. However, integrative studies using a combination of molecular and morphological data and denser sampling often reveal a more complex picture with multiple taxa present, with many of these 'cryptic' species having, in hindsight, clear diagnostic morphological features.

The limbless pygopodid geckos are a group of 47 extant species that diversified in Australia (with two species occurring in New Guinea) (Brennan et al. 2016; Jennings 2021) and reach their highest species richness in the arid zone (Norris et al. 2021). With an elongate snake-like body plan, they bear little resemblance to their four-limbed relatives; however, several morphological characters such as fixed spectacles, fleshy tongues and two eggs per clutch have long suggested a close affinity with geckos (Kluge 1974). Molecular data have established that pygopods are an ancient sister lineage to the carphodactylid geckos (Jennings et al. 2003; Han et al. 2004; Oliver and Sanders 2009; Brennan et al. 2016), a relationship that is also supported by morphology (Daza and Bauer 2012).

Of the eight genera of pygopods, *Delma* is the most speciose, with 22 described taxa, many of which have geographically large distributions in the arid zone. One of the most widespread species is *Delma tincta* De Vis, occurring across central and northern Australia, and inhabiting a variety of semi-arid to arid habitats in far Western Australia (WA), the Northern Territory (NT) and Queensland (QLD), as well as occurring in northern South Australia (SA) and New South Wales (NSW) (Kluge 1974; Wilson and Swan 2021; Atlas of Living Australia). The species appears to be absent from the Great Sandy and Great Victoria deserts of WA, where the closely related *D. desmosa* replaces it; as such, the WA populations of *D. tincta* are geographically disjunct from those to the east. In his comprehensive revision of the genus *Delma*, Kluge (1974) found no significant morphological differences among populations of *D. tincta* across its vast distribution. Similarly, Shea (1991) examined many *D. tincta* specimens from central Australia and neighbouring regions and did not remark on any observable differences. However, the near continent-wide distribution of this taxon and the prevalence of cryptic species in other groups in the arid zone, as well as *D. tincta* being one of the oldest recognised pygopod species (De Vis 1888) warrants a genetic assessment of *D. tincta* populations from across its distribution.

Here, we use a combination of genetic data in the form of nuclear Single Nucleotide Polymorphisms (SNPs), as well as morphological evidence drawn from material collected across the geographic range of *D. tincta*, spanning nearly the entire arid zone and adjacent monsoon tropics. We found four deeply diverged lineages within *D. tincta* (*sensu lato*) and further structure within these main groups. Although the western lineage possesses useful diagnostic morphological characters, straightforward identification of the eastern taxa is problematic. They are highly conservative in traditional morphological characters used in pygopods, including meristic characters and size, and each exhibits significant intraspecific colour variation across their range and ontogenetic variation in head colour and pattern. The two most genetically divergent taxa are found in broad sympatry across the central and eastern arid zone, rendering geography an unreliable guide for species identification. We used a genotyped specimen collected ~50 km away from the type locality of *D. tincta* of Normanton, Queensland, to apply the name *tincta* to one of these lineages. Based on the strength of our molecular data, we raise *D. reticulata* Garman from north-eastern Australia from synonymy and describe two new species: a cryptic species that overlaps extensively with true *D. tincta* and another species from the Pilbara and Gascoyne regions of Western Australia. We also suggest ways for field workers and collection managers to cope with what appear to be truly cryptic species in the absence of genetic information to identify specimens.

MATERIALS AND METHODS

DNA ANALYSIS

Taxonomic sampling

We sampled 114 *D. tincta* tissues from collections of the Western Australian Museum (WAM), the South Australian Museum (SAMA), the Australian Museum (AMS), the Queensland Museum (QM) and the Museum and Art Gallery Northern Territory (MAGNT) to provide the broadest geographic sampling possible. We used *D. borea,* the sister taxon to *D. tincta* (Jennings 2021), as the outgroup for analyses.

SNP genetic data

We used the DArTseq (Diversity Array Technology sequencing) platform designed by Diversity Arrays Technology, Canberra, Australia (DArT) for genomic analysis and SNP genotyping. This technique involves a complexity reduction process that uses specific restriction enzymes to fragment the DNA, which is then sequenced using the Illumina HiSeq2500 system (for details on this method, see Kilian et al. [2012] and Georges et al. [2018]). The generated data includes thousands of 69 bp-long fragments associated with restriction sites and their accompanying SNPs. The utility of DArTseq data in assessing phylogeographic patterns and defining species boundaries is well-documented across multiple reptile studies (e.g. Melville et al. 2017; Georges et al. 2018; Zozaya et al. 2019; Chaplin et al. 2020; Esquerré et al. 2021; Pavon-Vazquez et al. 2022).

Preliminary phylogenetic analysis had identified some misidentified individuals that were not part of the *D. tincta* complex, so these were removed from the dataset (NTM R22310, WAM R174757, SAMA ABTC6580, SAMA R22934, SAMA ABTC60831 and SAMA ABTC60820) before filtering. We used the 'dartR 2.9.7' R package (Gruber et al. 2018) to filter our dataset as follows (in order). We first excluded SNPs that were found in the same fragment as other SNPs (to avoid linkage), and then excluded individuals with more than 60% missing data as a first pass to remove the poorest samples. We then excluded SNPs that had a reproducibility below 0.99, had a read depth below 4 or above 40, were missing in more than 90% of samples and whose minor allele was found in only one individual. Subsequently, we excluded individuals with more than 70% missing data. The following samples were excluded due to not meeting the individual call rate threshold: QM J80509, QM J84129, QM J90118, SAMA R22934, SAMA R67717, SAMA R42944, SAMA R42945, WAM R141584, WAM R141273, WAM R116545, WAM R138078, WAM R151060. In the Taxonomy section, holotypes and paratypes are denoted with '*'.

Phylogenetic analyses

Phylogenetic tree reconstruction on our filtered SNP dataset was conducted using two methods. We inferred the maximum likelihood (ML) tree in the program iq-tree 2.2.2.6 (Nguyen et al. 2015). We ran 10,000 ultrafast bootstrap replicates (Minh et al. 2013) and 10,000 replicates of the SH-like approximate likelihood ratio test (SH-aLRT; Guindon et al. 2010). Model selection was completed using Model Finder Pro with ascertainment bias correction (Kalyaanamoorthy et al. 2017). We also used the SNPs to model a lineage tree based on the multi-species coalescent. We used the program SVDQuartets (Chifman and Kubatko 2014), implemented in PAUP v.4.0 (Swofford 2003), assessing branch support with 10,000 bootstrap replicates.

Population structure

To infer population genetic structure and potential admixture, we used the Bayesian admixture analysis sNMF (Frichot et al. 2014) in the 'LEA 2.8.0' R package (Frichot and François 2015) to estimate ancestry coefficients (the proportion of an individual's genome that originates from a set of inferred ancestral populations). We tested nine combinations of the regularisation (α) and tolerance (ε) parameters, choosing that with the lowest cross-entropy. In these test runs, we performed ten repetitions for each value of K (number of theoretical populations) between 1–12. We then performed 100 repetitions for each of the 12 values of K with the best combination of α (1000) and ε (0.00001). We obtained the optimal value of K and individual ancestry coefficients from the run with the lowest cross-entropy. We also characterised population structure by performing a principal component analysis (PCA) with the 'gl.pcoa' function of 'dartR'.

Molecular species delimitation

The fixed difference at a locus occurs when two populations share no alleles, and as such, an accumulation of fixed differences between populations is a strong indicator of reproductive isolation (Georges et al. 2018). An important characteristic of fixed differences is that they enable clear identification of an individual's origin from a particular population or species, and alleles that are fixed and different between two populations are diagnostic characters. This ability to clearly distinguish between populations is especially useful in species delimitation studies (Georges et al. 2018; Unmack et al. 2019). We evaluated whether there are fixed allelic differences in the populations identified by sNMF and populations grouped into major lineages using the 'gl.fixed.diff' function of 'dartR'. We performed 1,000 simulation iterations where we identified true positives based on a threshold of 0.02 for the true minor allele frequency. We first performed this analysis on the four major groups ([P1–2, P7]; [P3–4, P6]; [P5]; [P8]) in pairwise comparisons to demonstrate their uniqueness. We then looked for fixed differences unique to each of these four major lineages by comparing each one to the other three lineages combined (e.g. P8 vs. P1, P2, P3, P4, P5, P6, P7). This latter analysis identifies diagnosable sequences that exclusively occur in a particular lineage. We filtered our data only to include sequences that occurred in more than 80% of the samples and excluded sequences shorter than 25 base pairs (because the probability of a sequence of 25 base pairs occurring more than once in a 2GB genome is $<10^{-6}$).

MORPHOLOGICAL ANALYSIS

Taxonomic sampling

We took linear measurements and counted meristic features in 142 specimens of *D. tincta* from across its distribution, which included all individuals genotyped in our SNP dataset that had associated specimens as well as high-quality specimens for which no tissue sample was available (Appendix 1 and type lists in the Taxonomy section). All specimens were from WAM, SAM, AMS and QM. A previous detailed assessment of *D. tincta*

and closely related species found sexual dimorphism in some linear measurements and meristic traits (Maryan et al. 2007), whereas an earlier study found little sexual dimorphism other than the number of ventral scales (Kluge 1974). We did not record sex and based our analyses on interspecific comparisons.

Morphological measurements and analysis

The following linear measurements are reported in mm and were taken with digital callipers, plastic ruler or string (for tails): snout-vent length (SVL) measured from tip of snout to vent, tail length (TailL) measured from tip of tail to vent and including both potentially original and regenerated tails (see further comments below), head depth (HeadD) measured from dorsal surface of head and ventral surface of throat at point immediately behind eye, head length (HeadL) measured from tip of snout to posterior margin of ear, head width (HeadW) measured from the widest point between the ears, snout length (SnoutL) measured from tip of snout to anterior margin of transparent spectacle and eye width (EyeW) horizontal distance measured from anterior to posterior extremities of transparent spectacle (measurement not including the circumocular granules). Three meristic counts were taken: number of 'hindlimb' (i.e. reduced 'flap') scales (HLS) counted from distal extreme and origin with body, number of midbody scale rows (MBS) counted entirely midway around body and number of ventral scales (VS) counted from immediately behind mental scale to vent. We exclude tail length from our summary descriptive statistics and analyses, as many tails were either recently broken or regenerated, as indicated by a clear break in colouration. For the formal descriptions, we provide only the original TailL for the longest TailL/SVL recorded in each species.

Colour and pattern were difficult to score as wide natural variation was coupled with variable fading in museum specimens. In general, hatchlings and juveniles always have a darkly marked head which fades with age to varying degrees among populations (Maryan et al. 2007; pers. obs.; see Results). Given the materials available to us, we examined available photographs of animals in life and preserved museum specimens to provide the best summation of colour and pattern possible.

We collected morphological data from genotyped specimens and did exploratory morphological analyses based on results from the genetic analyses. We excluded specimens smaller than 55 mm SVL to ensure we were measuring adult specimens (Maryan et al. 2007). These preliminary analyses of linear measurements and meristic data demonstrated that members of this species group are extremely morphologically conservative, as previously noted by Kluge (1974) and Shea (1991). We supplemented our morphological data set with additional non-genotyped specimens to maximise geographic coverage. Unfortunately, owing to the two central taxa's highly conservative morphology and sympatry, 52 specimens could not be confidently assigned to a taxon and were excluded from our analyses. However, we were able to include seven individuals of *D. reticulata,* which could be unambiguously assigned to this taxon based on geography and the lectotype of *D. tincta*. We did not record the sex of individuals, but our primary interest was in the differences between putative species. Therefore, our statistical analyses focus on differences between taxa. We did analyses of variance (ANOVA) to test for differences among putative species means for linear measurements, ventral scale number and relative sizes (ratios) of head length as a proportion of snout-vent length and relative head width, head depth, snout length and eye width as a proportion of head length.

RESULTS

DNA ANALYSIS

Preliminary phylogenetic analyses, including all *Delma* for which we had SNP data (*D. tincta*, *D. borea*, *D. desmosa*, *D. nasuta*, *D. butleri*, and *D. australis*), confirmed the monophyly of *D. tincta* (*sensu lato*). For all *D. tincta* samples, DArT scored 213,459 polymorphic SNPs. After filtering, 5020 SNPs and 96 individuals were retained and used for downstream analyses. Museum accession numbers and collection localities are given in Appendix 1.

Phylogenetic analyses

The ML analysis of the SNP dataset inferred *D. tincta* to be monophyletic with strong support (bootstrap = 100) (Figure 1). In addition, *D. tincta* individuals cluster within eight major lineages (P1–P8) that further cluster into four distinct, well supported clades: Pilbara-Gascoyne (P5; bootstrap = 100), QLD coast (P3–4, P6; bootstrap = 100), and two largely overlapping central/eastern desert clades (P1–2, P7; bootstrap = 99, P8; bootstrap = 100). The Pilbara-Gascoyne lineage was recovered as a sister to one of the central lineages (P8) with good support (bootstrap = 100), with the other central lineage (P1–2, P7) inferred as sister to these (bootstrap = 99). The QLD coast lineage (P3–4, P6) was recovered as sister to these three main lineages (bootstrap = 100). The coalescent lineage tree inferred using SVDquartets, where the lineages were defined *a priori* using the ML tree and the sNMF results (below), provided strong support for the grouping of populations 3, 4 and 6 (QLD coast), 1, 2 and 7 (central/eastern desert lineage 1), and the sister relationship between population 8 (central/eastern desert lineage 2) and 5 (Pilbara-Gascoyne) (Figure 2). However, the relationships among these major lineages were not strongly supported (bootstrap = 67).

In addition to the SNP dataset, we also collected Sanger sequenced data for the mitochondrial locus ND2 for the same individuals (unpublished data). These data showed rampant mito-nuclear discordance in line with ancient and recent hybridisation events between many lineages within the *D. tincta* species complex, as well as with the sister taxon *D. borea,*

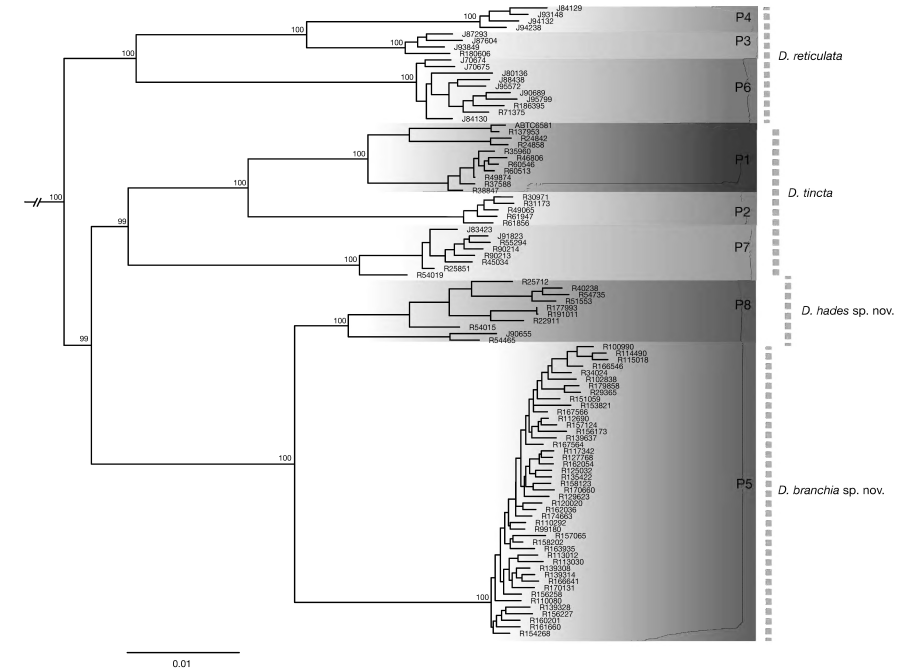

FIGURE 1 Maximum likelihood phylogeny of the *D. tincta* species complex inferred with IQ-Tree using 5020 SNPs. Branch support values correspond to ultrafast bootstraps. The outgroup is not shown. P1–P8 refer to the populations identified in the sNMF analysis.

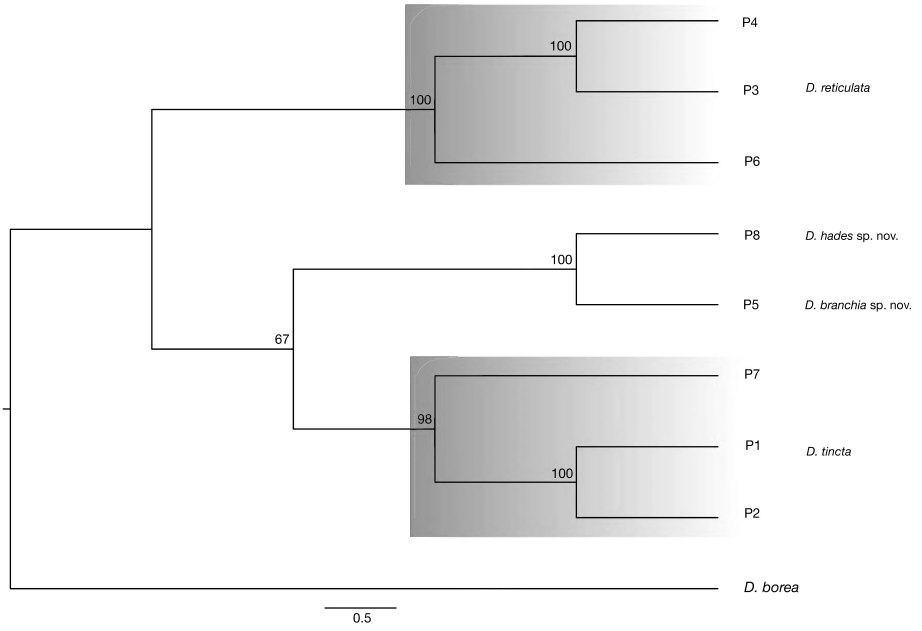

FIGURE 2 Nuclear DNA lineages of the *D. tincta* species complex based on a species tree (inferred with SVDQuartets).

and will be published elsewhere. Multiple instances of mitochondrial introgression have been identified within *Delma*, likely associated with the high frequency of sympatry, particularly between hypothesised sister taxa, and low morphological diversity (Brennan et al. 2016). Given this result, we do not refer to these ND2 data further and do not use these results to inform our species delimitation.

Population genetic analyses

Population genetic structure is highly concordant with our phylogenetic results. The best fitting model in our sNMF analysis indicated K = 8, with very little admixture between these clusters (Figure 3). This large number of populations reflects the significant deep structure within three of the four main lineages identified in the ML phylogenetic analysis. These clusters are readily identifiable in the PCoA plot of the first two PCs, which account for 36.2% and 13.4% of the variation, respectively (Figure 4).

Molecular species delimitation

The first fixed difference analysis comparing all six combinations of the four major groups revealed that all four lineages identified in the phylogenetic analyses have between 72 and 311 fixed differences between them (Table 2), far greater than the expected count of false positives for each comparison. For species diagnoses, we then report the diagnostic fixed differences unique to each lineage compared to all other groups (Appendix 2). The ICZN (International Code of Zoological Nomenclature) allows for any set of characters (including molecular ones) to serve as distinguishing features, provided they enable clear differentiation of taxa. We provide the diagnosable sequences and the position of the SNP, and if aligned, the position on the reference genome of *Gekko japonicus* in Appendices 2–3.

Morphological measurements and analysis

We present summary statistics and results of ANOVA analyses of the morphological data in Table 1. As anticipated, the analyses demonstrate these lineages are highly morphologically conservative in linear body measurements and meristic characters, conforming to a generalised *D. tincta* morphology. While several linear measurements show statistically significant differences in mean values among the four lineages (SVL, HeadL, HeadD, SnoutL), there is still extensive overlap in these values, rendering them of limited use for diagnostic traits. Body size did differ significantly, with the two central lineages reaching larger average body sizes than the western and eastern lineages; however, maximum SVLs were similar except for *D. reticulata,* which was smaller (Table 1). Analyses of relative HeadL and relative SnoutL show no significant differences, while relative HeadW and EyeW show significant differences. This is likely driven by a higher mean HeadW to HeadL ratio in the QLD lineage relative to the other putative species, but again, there is considerable overlap in values. Follow-up PCAs on linear measurements and ventral scale number, which do not identify groups a priori, showed near complete overlap among putative species and a DFA, with putative species identified, only reliably identified *D. reticulata* and *D. hades* sp. nov. at 85% and 86% accuracy, respectively, and performed more poorly on *D. branchia* sp. nov. (68%) and very poorly on *D. tincta,* with less than half of the individuals correctly identified (including the lectotype). Taken together, these analyses demonstrate that these taxa are morphologically extremely similar.

Cryptic species and criteria for species recognition

As discussed by De Queiroz (2007), different species concepts agree that the primary definition of a species is a group of metapopulations that are evolving independently; Maddison and Whitton (2023) also emphasise the persistence of a reproductive community through time with a recent history not shared by other lineages. Diagnosing such separately evolving entities for taxonomy is an issue for truly cryptic taxa that have no apparent morphological differences compared to close relatives (Bickford et al. 2007; Jörger and Schrödl 2013). Despite the prevalence of cryptic species across all animal phyla (Pérez-Ponce de León and Poulin 2016), they are often identified and differentiated but typically remain undescribed; they are '…the worst-case scenario of taxonomic incompleteness' (Delic et al. 2017). Nonetheless, there is strong agreement in the scientific community that cryptic species warrant thorough attention and appropriate taxonomic treatment, including naming them formally (see Delic et al. 2017).

Our SNP analyses identified four major lineages within what is currently recognised as *D. tincta* (Figure 5). Following the Generalized Lineage Concept (GLC; de Queiroz 1998), we consider each of these lineages as independently evolving entities and apply multiple criteria — including morphological and colour pattern differences, reproductive isolation and genetic divergence — to diagnose them as distinct species. In addition to clear phylogenetic and population genetic evidence (although not as deep as some eastern lineage differences), we found that colour and head pattern variation distinguish the western taxon, which is also geographically isolated from eastern populations by the western deserts. Taxonomic delineation is far from straightforward for the three remaining eastern populations (including *D. tincta* [*sensu stricto*]). The molecular evidence for divergent evolution, lack of admixture between groups and fixed allelic differences at a significant number of loci establishes the existence of metapopulations that no longer engage in reticulate evolution with neighbouring populations. That the two central taxa are not each other's closest relatives, and exist in broad geographic sympatry, presents a robust argument for valid biological species — the accumulation of many fixed differences between these lineages is a result of long-standing reproductive isolation. Further sampling in northern NSW and southern QLD may identify additional sympatry with the adjacent QLD lineage in the southern part of its distribution. Complicating this matter for field

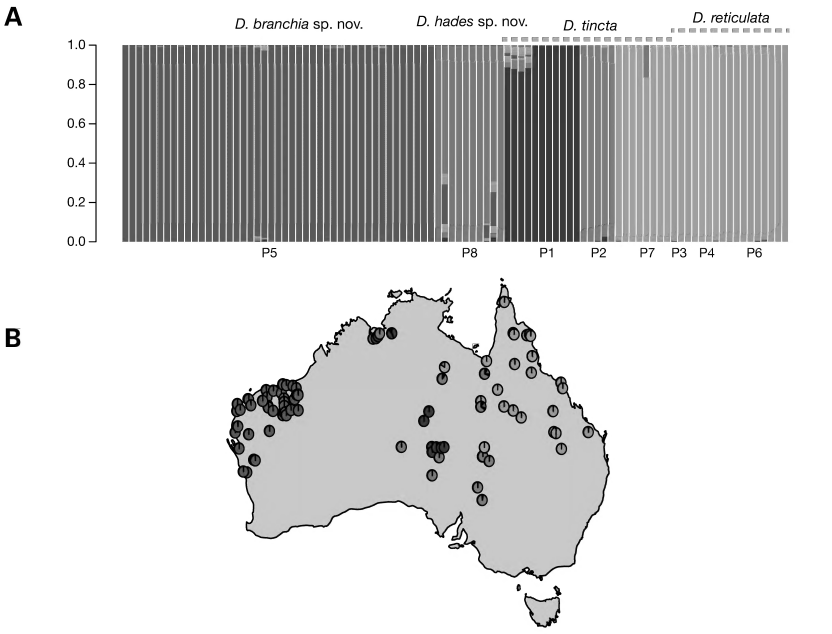

FIGURE 3 A) Ancestry coefficients of each of the eight identified genetic populations (K) for the *D. tincta* species complex, sorted by species. B) Distribution map of the genotyped specimens displayed as pie charts of their ancestry coefficients, to visualise the lack of geographic admixture.

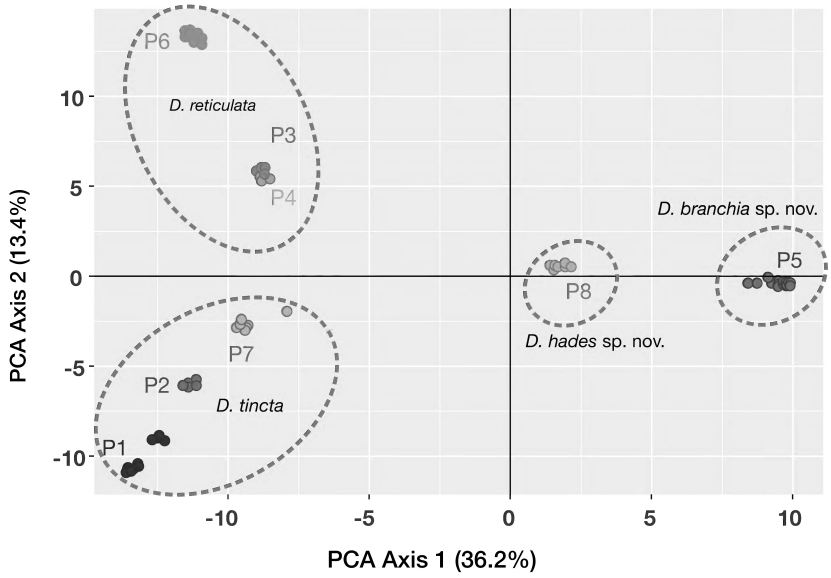

FIGURE 4 Principal coordinates analysis (PCoA) plot of genetic structure based on genetic distances among the 8 populations within the *D. tincta* species complex. Percentages of genetic variation explained by each PCoA axis are shown in parentheses.

TABLE 1 Summary statistics for characters and ratios measured for members of the *D. tincta* species complex. Mean ± SD (range) See text for abbreviations of characters used.

Character	*D. hades* sp. nov.	*D. reticulata*	*D. tincta*	*D. branchia* sp. nov.	Statistics
Sample size	8	13	17	42	
SVL	78 ± 13 (56–95)	69 ± 10 (55–84)	76 ± 12 (56–96)	70 ± 8 (55–93)	F3,80=3.177, P=0.0288
HeadL	8.3 ± 1.0 (6.6–9.2)	7.3 ± 0.8 (6.0–8.1)	7.8 ± 0.7 (6.4–8.8)	7.5 ± 0.6 (6.3–8.8)	F3,80=4.212, P=0.0082
HeadD	3.9 ± 0.6 (2.6–4.6)	3.4 ± 0.4 (2.6–4.1)	3.4 ± 0.5 (2.6–4.4)	3.3 ± 0.4 (2.6–4.3)	F3,80=5.052, P=0.0030
HeadW	4.9 ± 0.6 (3.7–5.5)	4.6 ± 0.7 (3.3–5.6)	4.7 ± 0.8 (3.4–6.0)	4.3 ± 0.5 (3.3–5.6)	F3,80=2.6537, P=0.0546
SnoutL	3.3 ± 0.4 (2.7–3.6)	2.9 ± 0.3 (2.3–3.2)	3.1 ± 0.3 (2.5–3.5)	3.0 ± 0.3 (2.1–3.5)	F3,80=4.4369, P=0.0063
EyeW	1.1 ± 0.1 (1.0–1.3)	1.2 ± 0.1 (0.9–1.4)	1.1 ± 0.1 (1.0–1.4)	1.2 ± 0.1 (1.0–1.4)	F3,80=0.0797, P=0.9708
HeadL/SVL	0.1 ± 0.0 (0.1–0.1)	0.1 ± 0.0 (0.1–0.1)	0.1 ± 0.0 (0.1–0.1)	0.1 ± 0.0 (0.1–0.1)	F3,80=1.657, P=0.1848
HeadW/HeadL	0.6 ± 0.0 (0.6–0.6)	0.6 ± 0.1 (0.6–0.7)	0.6 ± 0.1 (0.5–0.7)	0.6 ± 0.0 (0.5–0.6)	F3,80=4.3382, P=0.0071
SnoutL/HeadL	0.4 ± 0.0 (0.4–0.4)	0.4 ± 0.0 (0.4–0.4)	0.4 ± 0.0 (0.4–0.4)	0.4 ± 0.0 (0.3–0.4)	F3,80=0.9396, P=0.4259
EyeW/HeadL	0.1 ± 0.0 (0.1–0.2)	0.2 ± 0.0 (0.1–0.2)	0.2 ± 0.0 (0.1–0.2)	0.2 ± 0.0 (0.1–0.2)	F3,80=5.6045, P=0.0016
VS	67.8 ± 2.9 (63–72)	64.9 ± 2.5 (61–69)	69.7 ± 4.2 (63–78)	68.8 ± 2.9 (61–75)	F3,79=6.6280, P=0.0005
MBS	14 (100%)	14 (84.6%), 15 (15.4%)	14 (100%)	13 (14.6%),14 (82.9%), 15 (2.4%)	
HLS	2 (14.3%), 3 (85.7%)	3 (100%)	2 (6.3%), 3 (62.5%), 4 (31.3%)	3 (100%)	
Supralabial scales (R)	6 (100%)	5 (18.2%), 6 (81.8%)	5 (5.9%), 6 (94.1%)	5 (2.4%), 6 (95.2%), 7 (2.4%)	
Infralabial scales (R)	7 (100%)	4 (18.2%), 5 (72.7%), 6 (9.1%)	4 (11.8%), 5 (88.2%)	4 (23.8%), 5 (76.2%)	
Supralabial scales (L)	6 (100%)	5 (8.3%), 6 (83.3%), 7 (8.3%)	6 (100%)	6 (100%)	
Infralabial scales (L)	4 (14.3%), 5 (85.7%)	4 (8.3%), 5 (91.6%)	4 (5.9%), 5 (94.1%)	4 (7.1%), 5 (90%), 6 (2.4%)	

identification in central Australia, our morphological data indicate widely overlapping characters with no clear way to diagnose an ungenotyped individual reliably. In addition, multiple instances of mito-nuclear discordance identified in preliminary mtDNA analyses also render mtDNA barcoding an unreliable tool for species identification (unpublished data). Thus, for this truly cryptic species complex, we have relied heavily on the substantial molecular evidence from the nuclear SNPs and the diagnostic fixed differences for recognising the three eastern taxa (Table 2 and Appendices 2–3). While several deeply divergent lineages exist within three of the four major lineages, our current genetic sampling is geographically limited, and few genotyped specimens are available for morphological assessment, particularly in remote central Australia. In addition, small sample sizes can lead to an excess of fixed differences. Therefore, we grouped lineages together so each was represented by at least 10 samples. Until broader geographic and genetic sampling can clarify their evolutionary and ecological distinctiveness, we conservatively retain them within our proposed framework of four species in the *D. tincta*

TABLE 2 The fixed differences between the major lineages identified by the phylogenetic analyses, showing the number of fixed differences is far greater than the expected count of false positives for each comparison.

Lineage 1	Lineage 2	N1	N2	Fixed differences	False positives
D. branchia sp. nov. (P5)	*D. hades* sp. nov. (P8)	45	10	108	28.6
D. branchia sp. nov. (P5)	*D. reticulata* (P3–4, P6)	45	17	311	41.5
D. branchia sp. nov. (P5)	*D. tincta* (P1–2, P7)	45	24	207	67.9
D. hades sp. nov. (P8)	*D. reticulata* (P3–4, P6)	10	17	254	51.4
D. hades sp. nov. (P8)	*D. tincta* (P1–2, P7)	10	24	118	79.7
D. reticulata (P3–4, P6)	*D. tincta* (P1–2, P7)	17	24	72	23.1

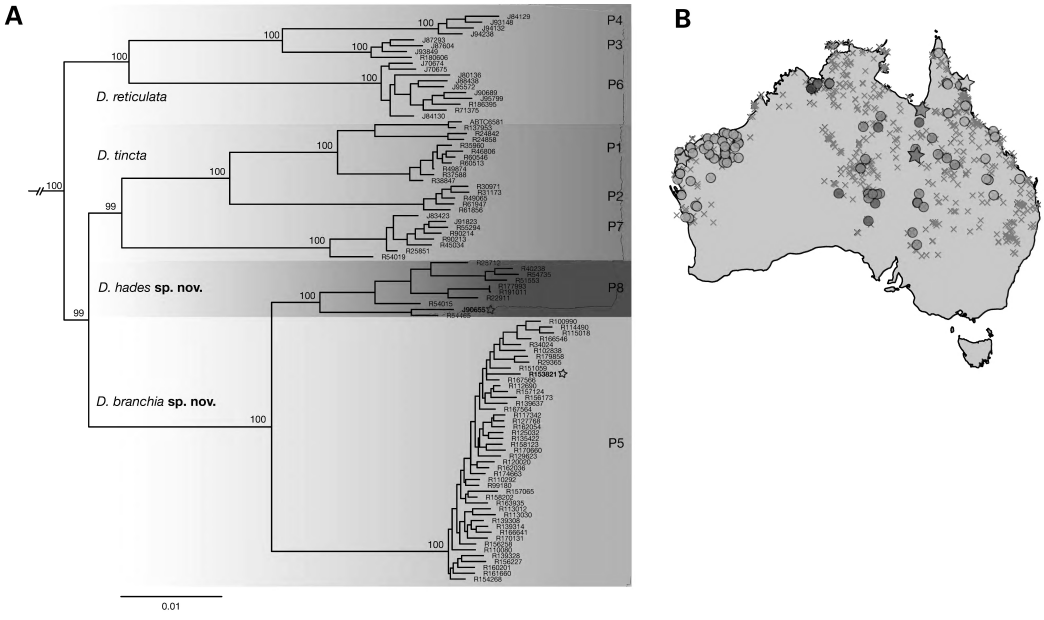

FIGURE 5 Maximum likelihood phylogeny from Figure 4 reflecting the new taxonomy of the *D. tincta* species complex. P1–P8 refer to the populations identified in the sNMF analysis. The map is colour-coded to match the phylogeny, and the stars indicate the location of the holotype or lectotype for each taxon. The grey Xs indicate ALA records for *D. tincta* (*sensu lato*).

species group.

The lectotype for *D. tincta* is from Normanton near the coast of the Gulf of Carpentaria, Qld, where two taxa occur in sympatry. The lack of genetic material for this specimen and the lack of diagnosable characters to definitively assign the lectotype to one of two possible sympatric taxa are problematic. The *D. tincta* lectotype is in poor condition, given its age and state of preservation (Figure 6), and our DFA analysis could not assign this specimen to a lineage. One of our genotyped specimens (SAMA R25851) was collected from within 50 km of Normanton, whereas the closest genotyped specimen from the other lineage was ~200 km away. Here, we have applied the name *D. tincta* (*sensu stricto*) to the genetic lineage with the genotyped specimen that is ~50 km away from Normanton. Although the distribution of each cryptic species ranges for thousands of km across the arid zone, this somewhat arbitrary criterion for designating the name *tincta* to a lineage is at least clear in the absence of other compelling information.

The designation of type specimens to particular species based on genetic proximity to a known reference population carries inherent risks, particularly when geographic sampling is limited. We recognise the downstream implications of misidentifying the type locality and remain cautious in our interpretations, acknowledging the potential for future revisions as additional samples are incorporated.

TAXONOMY

Pygopodidae Boulenger, 1884

Delma Gray, 1831

Type species: *Delma fraseri* Gray, 1831, by monotypy.

DIAGNOSIS

Delma differs from all other pygopod lizard genera in possessing the following combination of characters: head scales, including the parietals, enlarged and symmetrical; anterior nasal scales nearly always in contact; first pair of lower labials in contact behind mental scale; nostril usually bordered by more than two scales (except in some *D. impar*); external ear opening large; 20 or fewer midbody scale rows; dorsal and ventral scales smooth; precloacal pores absent; tail about three times as long as body (Kluge 1974).

Delma tincta species-group vs. *D. tincta* species complex

DIAGNOSIS

Based on the molecular analysis from this study, as well as the published mtDNA and nDNA study of Brennan et al. (2016) and the work of Shea (1991) and Maryan et al. (2007), we redefine a monophyletic '*D. tincta* species-group', comprised of *D. tincta*, *D. borea*, *D. pax*, *D. elegans*, *D. tealei*, *D. desmosa*, *D. reticulata*, *D. branchia* sp. nov. and *D. hades* sp. nov. The original group of Shea (1991), which has been added to by Maryan et al. (2007), is no longer a cohesive entity but rather a morphologically variable group that is supported by genetic data. Morphological characteristics shared by all members of this species-group are: relatively small to moderate size (SVL to 98 mm); one or two pairs of supranasal scales; eye above third or fourth supralabial; 14 to 18 midbody scale rows. Colour is usually brown with shades of olive and orange; banding on the head and neck is prominent on small individuals, but, depending on the species, fades in larger adults.

The '*Delma tincta* species complex' refers to the four species within *D. tincta* (*sensu lato*): *D. tincta*, *D. reticulata*, *D. branchia* sp. nov. and *D. hades* sp. nov. All are redescribed or described as new, below.

Delma tincta De Vis, 1888

Excitable Delma (lineage P1–2, P7)

(Figures 6, 7A)

1888. *Delma tincta* De Vis, Proc. Linn. Soc. N.S.W., 2: 824.

MATERIAL EXAMINED

Lectotype

Australia: *Queensland*: QM J241. Type locality: 'Normanton, Gulf of Carpentaria' [donated by M.

FIGURE 6 Lectotype of *Delma tincta* from Normanton in the Gulf of Carpentaria, Queensland, donated by M. Comley.

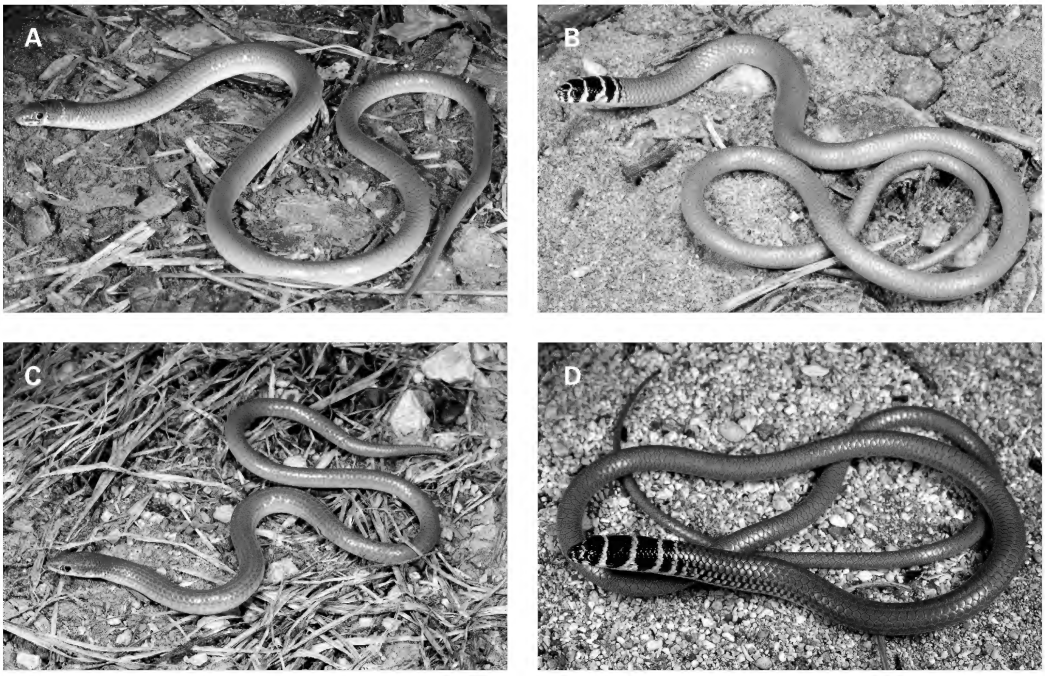

FIGURE 7 Photos of the four *D. tincta* species complex members from near the collection location of the holotypes: A) *D. tincta* (Doomagee, Queensland; photo: S. Macdonald); B) *Delma reticulata* (Laura, Queensland; photo: A. Zimny); C) *D. hades* sp. nov. (Julia Creek, Queensland; photo: A. Zimny); D) *D. branchia* sp. nov. (Bullara Station, Western Australia; photo: B. Maryan).

Comley]. Lectotype designation by Kluge (1974), who also restricted the type locality to Normanton.

Paralectotypes

Australia: ***Queensland:*** specimens lost before the lectotype designation of Kluge (1974) (Covacevich 1971). Collected from 'Springsure, Central Queensland' [donated by M. Comley].

Other material examined

A full list of the material examined is provided in Appendix 4.

DIAGNOSIS

A moderately-sized *Delma* (SVL to 55–96 mm; tail length up to 280 mm long) with one pair of supranasals, third labial below eye and 14 midbody scale rows. Differs from *D. reticulata* by adults lacking a boldly patterned head and neck, where these species come into near-contact in northern Queensland. It differs from *D. branchia* sp. nov. by lacking the series of ventrolateral transverse bars on the neck and posterior edge of ear opening, usually in contact or narrowly separated from the dark nuchal band. If present, pale band separating the crown and nuchal band is twice as wide as the one between the ocular and the crown bands.

Genetically diagnosed from all other members of the *D. tincta* species-group by 11 unique fixed differences (see Appendix 2), and from the sympatric *D. hades* sp. nov. by 118 fixed SNP differences (see Table 2). Appendices 2–3 show the diagnostic positions and sequences for all comparisons and the position on the reference chromosome where it aligns to *Gekko japonicus*.

DESCRIPTION

Snout-vent length 55–96 mm; tail length to 280 mm (up to 300% of SVL). Usually one pair of supranasals. Loreals 1–7. Third upper labial below eye. Midbody scale rows 14.

Head short, narrowing to rounded tip of snout, neck slightly constricted compared to head and forebody; ear opening ovoid, narrowing on either end, ear sloping backwards on a 30° angle bordered above by a narrow scale anteriorly and a large triangular scale posteriorly, and below by more numerous granular scales (~5–12); in profile, snout tapering gradually to rounded tip, gular region flat; body elongate and circular in cross-section but with ventrum flatter; hind flaps small and narrowing to a rounded point, covered by 3–5 scales; tail relatively long (to 300% SVL), tapering gradually to a fine point.

Head scales smooth, non-imbricate and heterogeneous;

top of rostral coming to a point dorsally, wider than long, not in contact with nostril; one pair of supranasals in broad contact; nostril positioned behind anterior extension of supranasal, postnasal and first upper labial; one postnasal, wider than high, angled posteroventrally and in contact with first loreal, excluded from second upper labial; prefrontals in contact; supraloreal 2–3 times as high as wide, in contact ventrally with loreals; 2–3 loreals in contact with supralabials, the anteriormost slightly larger; three supraciliaries; two supraoculars of similar size; two frontals, the anteriormost slightly wider and larger; frontoparietals large and in broad medial contact; two parietals, long with inner edge in contact with interparietal; 3–4 temporals; six upper labials, third widest and positioned below eye; five lower labials; mental width similar to length and coming to a point; first infralabials elongate and in contact; second infralabials elongate and separated by scale. Dorsal and lateral scales smooth, non-imbricate and homogeneous; ventral scales 1.5–2.0 times wider than body scales; three precloacal scales.

Pattern in life: Body typically light brown but with variation including olive hues and grey; head with 2–4 darkish bands: faint loreal band present; dull ocular band through black eyes and continuing as smudge on lower labial; band on crown to upper jaw; if present, nuchal band posterior to ear opening continuing to level of mouth; pale bands on head pale cream; ventrum pale cream. Sides of neck lacking dark markings.

VARIATION

Table 1 presents the individual measurements and meristic counts for all the *D. tincta* examined.

DISTRIBUTION AND SYMPATRY

The following account is based on genotyped specimens. *Delma tincta* occurs across a wide area of central Australia: from the eastern Kimberley, south and east to the Lake Frome region in SA, inland Queensland to near the Gulf of Carpentaria and through the central Northern Territory. Kimberley specimens belong to either *D. tincta* or *D. hades* sp. nov., but not *D. branchia* sp. nov., based on the absence of the diagnostic neck markings in the latter. Genotyping of Top End specimens is necessary to determine whether *D. tincta* occurs there.

Overlaps *D. hades* sp. nov. broadly in central NT and the western edge of inland Queensland. It appears to be allopatric with *D. reticulata* to the east and is entirely allopatric with *D. branchia* sp. nov., which occurs in western WA. Further sequencing of available specimens could result in more precise estimates of distribution and potential sympatry (especially with *D. reticulata*).

HABITAT

Detailed habitat notes are unavailable; however, it is likely to be a terrestrial generalist, sheltering under logs and moving through vegetation to actively hunt prey.

REMARKS

Owing to the lectotype's poor quality, it was not possible to morphologically assign the type to either of the two central lineages recovered in the genetic analyses. Hence, we used the criterion of the closest genotyped individual to the type location of Normanton, which proved to be a choice of ~50 km vs. ~200 km distance. As all species considered here occur over thousands of kilometres, this may or may not indicate the lineage to which the lectotype of *D. tincta* belongs. To resolve the matter, ancient DNA from the lectotype is the best option; a second option is to petition for the type to be set aside and choose a neotype with an available tissue sample, both of which are beyond the scope of this paper. Hence, we regard our allocation of names to the two central lineages as provisional at this stage.

***Delma reticulata* Garman, 1901**

Coastal Queensland Delma (lineage P3–4, P6)

(Figure 7B)

1901. *Delma reticulata* Garman, Bull. Mus. Comp. Zool. Harv., 39: 5, pl. 2, figs. 1-la–f.

MATERIAL EXAMINED

Holotype

Australia: *Queensland*: MCZ 6486 collected from near Cooktown in 1896 by E.A.C. Olive.

Other material examined

A full list of the material examined is provided in Appendix 4.

DIAGNOSIS

A relatively small (to 84 mm SVL) member of the *D. tincta* species-group. In the north of its distribution, it differs from the adjacent two species to the west (where they nearly come into contact) by being boldly patterned on the head whereas *D. tincta* and *D. hades* sp. nov. are plain (however, these taxa may be boldly patterned elsewhere within their distribution). However, in the inland southern part of its distribution, *D. reticulata* is also plain, resembling the plain *D. tincta* and/or *D. hades* sp. nov. It differs from *D. branchia* sp. nov. by lacking the series of ventrolateral transverse bars on the neck and posterior edge of ear opening usually in contact or narrowly separated from the dark nuchal band. Pale band separating the crown and nuchal band narrow (similar thickness to band separating occipital and crown band).

Genetically diagnosed from all other *D. tincta* species complex taxa by 39 unique fixed differences (Appendix 2). Appendix 2 shows the diagnostic positions and sequences for all comparisons as well

as the position on the reference chromosome where it aligns to *Gekko japonicus*.

DESCRIPTION

Snout-vent length 55–84 mm; tail length to 246 mm (up to 293% of SVL). Usually one (occasionally two) pair of supranasals. Loreals 1–7. Third (rarely fourth) upper labial below eye. Midbody scale rows usually 14 (occasionally 13 or 15).

Head short, narrowing to rounded tip of snout, neck is slightly constricted compared to head and forebody; moderately small ear opening ovoid, narrowing on either end, ear sloping backwards on a 30° angle bordered above by a narrow scale anteriorly and a large triangular scale posteriorly, and below by more numerous granular scales (~5–12); in profile, snout tapering gradually to rounded tip, gular region flat; body elongate and circular in cross-section but with ventrum flatter; hind flaps small and narrowing to a rounded point, covered by 3–5 scales; tail relatively long (up to 293% of SVL), tapering gradually to a fine point.

Head scales smooth, non-imbricate and heterogeneous; top of rostral coming to a point dorsally, wider than long, not in contact with nostril; one pair of supranasals in broad contact; nostril positioned behind anterior extension of supranasal and in contact with postnasal and first upper labial; one postnasal, wider than high, angled posteroventrally and in contact with first loreal, excluded from second upper labial; prefrontals in contact; supraloreal 2–3 times as high as wide, in contact ventrally with loreals; 2–3 loreals in contact with supralabials; three supraciliaries; two supraoculars of similar size; two frontals, the anteriormost slightly wider and larger; frontoparietals large and in broad medial contact; two parietals, long and inner edge in contact with interparietal; 3–4 temporals; six upper labials, third the widest and positioned below eye; five lower labials; mental width similar to length and coming to a point; first infralabials elongate and in contact; second infralabials elongate and separated by scale. Dorsal and lateral scales smooth, non-imbricate and homogeneous; ventral scales 1.5–2.0 times wider than body scales; three precloacal scales.

Pattern in life: Body typically light brown to olive brown; head with four prominent dark bands: weakly-defined loreal band continuing as dark smudge on lower labial; ocular band through black eyes and continuing as dark smudge on lower labial; band on crown continuing to lower jaw; nuchal band posterior to ear opening continuing to level of mouth; pale bands on head can range from pale cream to orange; posterior to nuchal band, at most one black mark ventrolaterally; ventrum pale cream. Black banding on head fades in southern inland adults.

VARIATION

Table 1 presents the individual measurements and meristic counts for all the *D. reticulata* examined. In the north, individuals possess prominent dark headbands, whereas in the south, in large adults, these bands fade.

HABITAT AND ECOLOGY

Little known but recorded from dry habitats and is likely a terrestrial generalist.

DISTRIBUTION AND SYMPATRY

Based on genotyped specimens, it occurs in eastern Queensland from the tip of the Cape to Brisbane. It may extend into northern New South Wales. In central Queensland, it comes into near contact with *D. tincta* and/or *D. hades* sp. nov.

REMARKS

This species appears to be largely allopatric to the other three species in the species complex. The Cape York population is deeply diverged genetically from more southern populations of *D. reticulata*, and this area receives far greater annual rainfall as part of the Wet Tropics region.

***Delma hades* sp. nov.**

Hellish Excitable Delma (lineage P8)

(Figures 7C, 8)

urn:lsid:zoobank.org:act:0510C87E-A9F2-47DE-A8EC-72670C19A8BC

MATERIAL EXAMINED

Holotype

Australia: *Queensland*: QM J90655*, collected from Two Rivers Homestead (-22.3964°, 139.9572°) on 22 April 2010 by M. Hutchinson, P. Oliver and D. Rabosky.

Paratypes

Australia: ***Queensland*:** SAMA R54465*, Burke and Wills Roadhouse dump, Queensland (-19.2264°, 140.3481°). ***Northern Territory*:** SAMA R54015*, Barkly Roadhouse, Northern Territory (-19.7114°, 135.8278°).

Other material examined

A full list of the material examined is provided in Appendix 4.

DIAGNOSIS

A moderately-sized (to 95 mm SVL) member of the *D. tincta* species-group. In the eastern part of its distribution, it differs from the geographically adjacent *D. reticulata* by a plain head (vs. boldly patterned); elsewhere, it is indistinguishable from *D. reticulata*. Indistinguishable morphologically from *D. tincta*. It differs from *D. branchia* sp. nov. by lacking the series

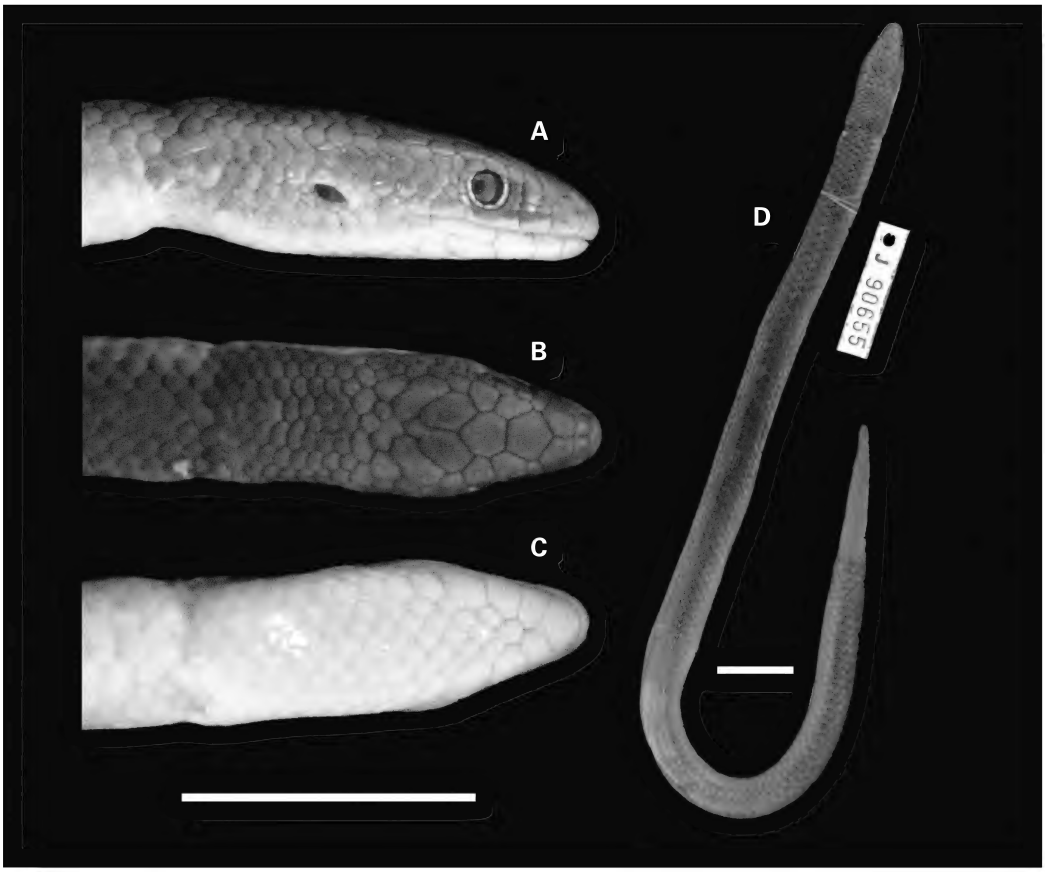

FIGURE 8 *Delma hades* sp. nov. holotype (QM J90655): A) lateral, B) dorsal, and C) ventral views of head, scale = 10 mm; D) whole body, scale = 10 mm.

of ventrolateral transverse bars on the neck.

Genetically diagnosed from all other members of the *D. tincta* species complex by 11 fixed differences (Appendix 2). Appendices 2–3 show the diagnostic positions and sequences for all comparisons as well as the position on the reference chromosome where it aligns to *Gekko japonicus*.

DESCRIPTION

Snout-vent length 55–95 mm; tail length to 292 mm (up to 307% of SVL). Usually, one pair of supranasals. Loreals 1–7. Third upper labial below eye. Midbody scale rows 14.

Head short, narrowing to rounded tip of snout, neck is slightly constricted compared to head and forebody; ear opening ovoid, narrowing on either end, ear sloping backwards on a 30–45° angle bordered above by 2–3 scales, and below by more numerous granular scales (~5–12); in profile, snout tapering gradually to rounded tip, gular region flat; body elongate and circular in cross section but with ventrum flatter; hind flaps small and narrowing to a rounded point, covered by 3–5 scales; tail relatively long (to 307% SVL), tapering gradually to a fine point.

Head scales smooth, non-imbricate and heterogeneous; top of rostral coming to a point dorsally, wider than long, not in contact with nostril; one pair of supranasals in broad contact; nostril positioned behind anterior extension of supranasal, postnasal and first upper labial; one postnasal, wider than high, angled posteroventrally and in contact with first loreal, excluded from second upper labial; prefrontals in contact; supraloreal 2–3 times as high as wide, in contact ventrally with loreals; 2–3 loreals of equal size in contact with supralabials; three supraciliaries; two supraoculars of similar size; two frontals, the anteriormost slightly wider and larger; frontoparietal large and in broad medial contact; two parietals, long and inner edge in contact with interparietal; 3–4 temporals; six upper labials, third the widest and positioned below eye; five lower

labials; mental width similar to length and coming to a point; first infralabials elongate and in contact; second infralabials elongate and separated by scale. Dorsal and lateral scales smooth, non-imbricate and homogeneous; ventral scales 1.5–2.0 times wider than body scales; three precloacal scales.

Pattern in life: Body typically light brown but with variation including olive to orange hues; head with 2–4 dark bands: weakly-defined loreal band continuing as dark smudge on lower labial, ocular band through black eyes and continuing as dark smudge on lower labial, band on crown continuing to lower jaw, nuchal band posterior to ear opening continuing to level of mouth; pale bands on head are pale cream; in large individuals, bands faded with little contrast of dark and light elements; ventrum pale cream.

MEASUREMENTS

Holotype (in mm or counts): SVL 95, HeadD 4.26, HeadL 9.2, HeadW 5.26, SnoutL 3.61, EyeW 1.3, MBS 14, VS 72.

VARIATION

Table 1 presents the individual measurements and meristic counts for all the *D. hades* examined.

HABITAT AND ECOLOGY

Unknown. Likely a habitat generalist.

DISTRIBUTION AND SYMPATRY

The following account is based on genotyped specimens. *Delma hades* sp. nov. occurs across a wide area of central Australia: from the eastern Kimberley, south to central SA, inland Queensland to near the Gulf of Carpentaria and through central NT.

Overlaps *D. tincta* broadly in central NT and the western edge of inland Queensland. Allopatric with *D. reticulata* to the east and allopatric with *D. branchia* sp. nov. in the west. Further sequencing could result in more precise estimates of distribution and potential sympatry (perhaps with *D. reticulata*).

Genotyping of Top End specimens is necessary to determine if *D. hades* sp. nov. occurs there. In the Kimberley, it is unknown if *D. tincta* species complex animals are *D. hades* sp. nov. or *D. tincta* without further genetic information (mtDNA results are equivocal; unpublished data). It may also occur in northern New South Wales.

ETYMOLOGY

The specific name *hades* is derived from the Greek god of the Underworld (or hell), in reference to the distribution of this taxon in broad sympatry, i.e. lying 'underneath', the distribution of *D. tincta* and the 'hellish' difficulty of distinguishing the two taxa in the absence of morphological markers.

REMARKS

As noted above, future work could more firmly establish that this is a newly-named taxon if the lectotype of *D. tincta* can be demonstrated to be a member of the non-*D. hades* lineage through ancient DNA or some other kind of analysis of the type specimen. Field workers and collection managers in museums may simply have to denote non-genotyped individuals as '*D. tincta/hades*' until reliable morphological identifiers are discovered, or the specimen is identified with SNP or other kinds of genetic data.

***Delma branchia* sp. nov.**

Western Excitable Delma (lineage P5)

(Figures 7D, 9)

urn:lsid:zoobank.org:act:32F21DDA-4F0D-4B1C-82CE-E31D08DCE2C1

Holotype

Australia: ***Western Australia*:** WAM R153821*, male, collected from Bullara Station (-22.8091°, 113.9442°) on 10 September 2003 by Brad Maryan and David Algaba.

Paratypes

Australia: ***Western Australia*:** WAM R112690*, 5.5 km SE Onslow (-21.6758°, 115.1450°); WAM R114490*, male, Wicherina Dam (-28.73°, 115.00°); WAM R115018*, Spalding Park, Geraldton (-28.65°, 114.63°); WAM R116545, Depot Hill (-29.13°, 115.35°); WAM R151059*, 10 km E Carnarvon (-24.883°, 113.767°); WAM R162054*, 5.5 km NE Giles Point (-23.214°, 119.202°); WAM R166546* Meka Station, (-27.5797°, 115.8992°).

Other material examined

A full list of the material examined is provided in Appendix 4.

DIAGNOSIS

A small to medium-sized *Delma* (to 93 SVL and 370 mm long) with one pair of supranasals, third labial below eye and 14 midbody scale rows. Pattern differs from other *D. tincta* species-group members by the presence of ventrolateral markings posterior to dark bands of head; anteriorly they resemble a continuation of head banding but fade to checker-like patterns posteriorly on forebody (to 2–3 head lengths down the body). Ear opening not in contact with dark bands on head. Pale band separating the crown and nuchal band thick (twice as wide as band separating occipital and crown band). Large adults do not lose banding on head.

Genetically diagnosed from all other *D. tincta* species complex taxa by 49 fixed differences (Table 2). Appendix 2 shows the diagnostic positions and sequences for all comparisons as well as the position

on the reference chromosome where it aligns to *Gekko japonicus*.

DESCRIPTION

Snout-vent length 55–93 mm; tail length to 260 mm (up to 280% of SVL). Usually one (occasionally two) pair of supranasals. Loreals 1–7. Third (rarely fourth) upper labial below eye. Midbody scale rows usually 14 (occasionally 13 or 15).

Head short, narrowing to rounded tip of snout, neck is slightly constricted compared to head and forebody; ear opening ovoid, narrowing on either end, ear sloping backwards on a 30–45° angle bordered above by a narrow scale anteriorly and a large triangular scale posteriorly, and below by more numerous granular scales (~5–12); in profile, snout tapering gradually to rounded tip, gular region flat; body elongate and circular in cross section but with ventrum flatter; hind flaps small and narrowing to a rounded point, covered by 3–5 scales; tail relatively long (to 280% SVL), tapering gradually to a fine point.

Head scales smooth, non-imbricate and heterogeneous; top of rostral coming to a point dorsally, wider than long, not in contact with nostril; one pair of supranasals in broad contact; nostril positioned behind anterior extension of supranasal and in contact with postnasal and first upper labial; one postnasal, wider than high, angled posteroventrally and in contact with first loreal, excluded from second upper labial; prefrontals in contact; supraloreal 2–3 times as high as wide, in contact ventrally with loreals; 2–3 loreals in contact with supralabials, the anteriormost slightly larger; three supraciliaries; two supraoculars of similar size; two frontals, the anteriormost slightly wider and larger; frontoparietals large and in broad medial contact; two parietals, long and inner edge in contact with interparietal; 3–4 temporals; six upper labials, third the widest and positioned below eye; five lower labials; mental width similar to length and coming to a point; first infralabials elongate and in contact; second infralabials elongate and separated by 1–2 scales. Dorsal and lateral scales smooth, non-imbricate and homogeneous; ventral scales 1.5–2.0 times wider than body scales; three precloacal scales.

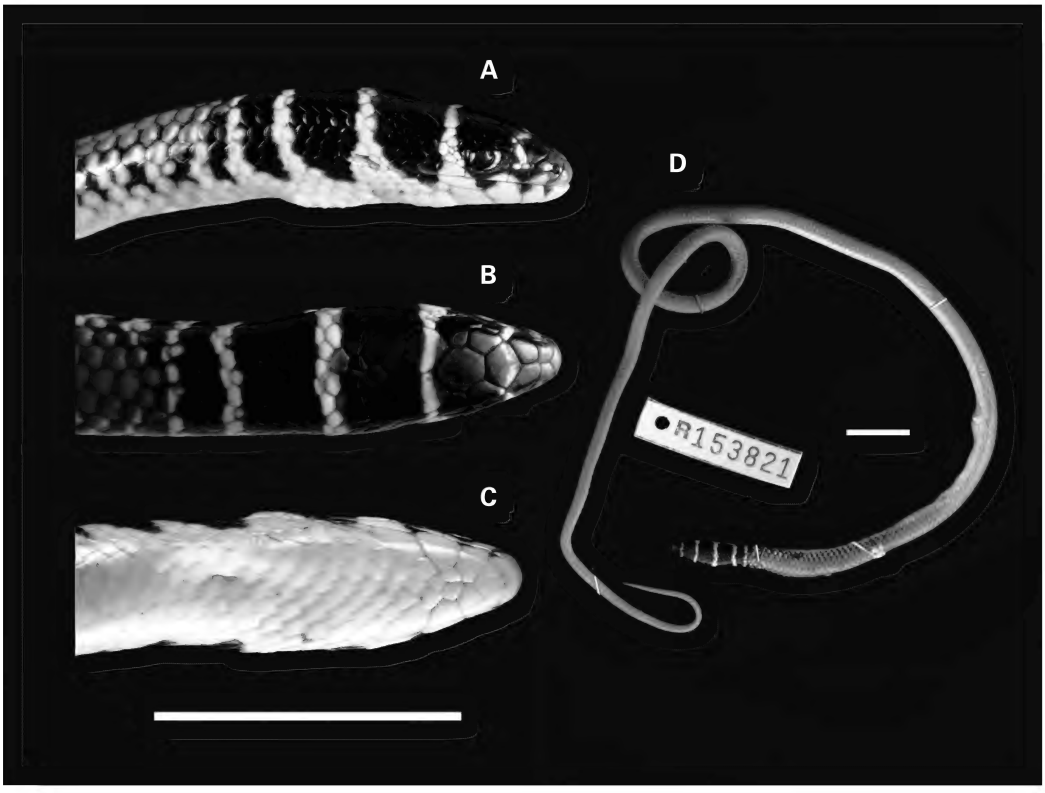

FIGURE 9 *Delma branchia* sp. nov. holotype (WAM R153821): A) lateral, B) dorsal, and C) ventral views of head, scale = 10 mm; D) whole body, scale = 10 mm.

Pattern in life. Body typically light brown but with variation including olive to orange hues; head with four prominent dark bands: weakly-defined loreal band continuing as dark smudge on lower labial; ocular band through black eyes and continuing as dark smudge on lower labial; band on crown continuing to lower jaw; nuchal band posterior to ear opening continuing to level of mouth; pale bands on head can range from pale cream to rich orange; posterior to nuchal band, a ventrolateral series of alternating pale and dark bands that taper and fade 2–3 head lengths along forebody, posteriorly regressing to a checked pattern; ventrum pale cream.

MEASUREMENTS

Holotype (in mm or counts): SVL 64, HeadD 2.87, HeadL 6.94, HeadW 3.78, SnoutL 2.85, EyeW 0.96, MBS 13, VS 72.

VARIATION

Table 1 presents the individual measurements and meristic counts for all the *D. branchia* sp. nov. examined.

ETYMOLOGY

The specific name *branchia* is derived from the Latin noun *branchiae*, meaning gills, alluding to the broken banding and checkered pattern that continues down the side of the neck.

DISTRIBUTION AND SYMPATRY

Delma branchia sp. nov. is distributed throughout the Pilbara and Gascoyne regions, south to near Kalbarri National Park. Scattered records along the western coast and inland (e.g. Ashburton region) indicate it likely occurs throughout these regions as well. Ungenotyped individuals from the Kimberley lack the barring on the neck and are therefore unlikely to belong to this species. *Delma tincta* and/or *D. hades* sp. nov. comes into near sympatry in the Broome region of the Kimberley to the north of this species' distribution.

HABITAT

Mainly heavy red soils including sand, clay and gibber. WAM database habitat notes mention under rocks (limestone and exfoliated granite), inside spinifex clumps and among debris or leaf litter. Several specimens were captured from rubbish tips; one specimen was retrieved from a burrow.

REMARKS

This species adds to the growing list of western endemic reptiles from the Pilbara and Gascoyne regions (McKenzie et al. 2000; Doughty et al. 2008). Owing to the dense survey effort in the Pilbara region, it appears to occur throughout the region, which features a mixture of rocks, clay and sand. Of the four species treated here, *D. branchia* sp. nov. is the easiest to identify and the least likely to be confused with other species owing to its isolation and distinctive patterning on the side of the neck.

DISCUSSION

Our study provides the first range-wide genetic assessment of *Delma tincta* (*sensu lato*). With data from thousands of SNP markers, and a comprehensive assessment of morphological variation, we find evidence for four evolutionarily distinct taxa within this species complex. This brings the number of *Delma* species to 25, making it significantly larger than the next most speciose pygopod genus *Aprasia*, with 15 described species.

A conundrum for field workers and collection managers for the deeply divergent, yet morphologically identical, sympatric species of *D. tincta* and *D. hades* sp. nov., is how to categorise an individual specimen if the essential genetic data are lacking — in this case, only SNP data usefully resolved species identification as mtDNA were insufficient to adjudicate between the two species owing to rampant introgression (unpublished data). There are two options in this case. One is to recognise all such individuals as the originally described name of *D. tincta*. This default option would be straightforward for collection managers with many older specimens that lack tissue samples. In contrast, confidently genotyped *D. hades* sp. nov., would be labelled as such. Another option is to identify the remaining non-genotyped specimens as '*D. tincta/hades*'. Doing so is more conservative in that it is not possible to know the true identity. This leaves open the possibility that future work (genetics, internal morphology) may eventually confidently identify such specimens. This problem is not unique to this group: it will be increasingly common as modern systematic investigations of species groups reveal more and more morphologically cryptic species that are indistinguishable from one another.

The sNMF population structure analysis identified eight populations with very little admixture between them, even in regions of potential contact or broad sympatry. The fixed difference analysis identified significant numbers of fixed allelic differences between all the lineages. Despite this strong evidence of reproductive isolation, we have decided against elevating each to a new species, pending the collection of more genetic data and examining additional material to improve sample sizes. Species tree analysis supports the monophyly of the three central populations (P1–2 and P7) to which we have assigned *D. tincta sensu stricto*, the monophyly of the QLD coastal populations (P3–4 and P6) for which we resurrect the name *D. reticulata*, and the sister relationship of the other central population (P8), which we name *D. hades* sp. nov., and the WA taxon (P5), which we name *D. branchia* sp. nov. The relationships between these major lineages are not strongly supported in this analysis.

Almost all the diversity within the *D. tincta* species

complex is in eastern Australia, with three of the four species (encompassing 7 of the 8 sNMF populations), found almost exclusively in the eastern Australian states (except for a small number of individuals that occur over the WA border in the far north and into Broome). In contrast, the exclusively WA species, *D. branchia* sp. nov., has a broad distribution throughout the Pilbara and the Gascoyne to the south, with little genetic structure across this range. Such contrasting genetic diversity between the eastern and western deserts is seen in several arid zone taxa (i.e. *Geyhra variegata* [Duckett and Stow 2013] and *Centipeda* [Nylinder et al. 2014]) and may relate to the influence of historical hydrological change (discussed in Pepper and Keogh 2021). Increased availability of water due to the large river systems of the eastern arid zone may have enhanced the ability of populations to persist in these deserts following more extreme aridification in the late Miocene. Higher effective population sizes over long periods of time are expected to leave a signature of high nucleotide diversity within populations and species, with relatively constant diversification rates and an overall even topology, a pattern which is typified in the eastern *D. tincta* species complex populations. In contrast, the drier and more arid landscapes in the western deserts may have led to higher rates of extinction, with relatively low effective population sizes and consequently lower levels of nucleotide diversity within populations and species, as seen in the western taxon *D. branchia* sp. nov. A dated phylogenetic analysis from Brennan et al. (2016) of *Delma* and other pygopods suggests the split between *D. borea* and *D. tincta* (*sensu lato*) occurred in the late Miocene (~7 mya) which is consistent with speciation events within the *D. tincta* species complex (and within *Delma* more generally) being late Miocene/Pliocene in age.

Despite a continent-wide distribution, relatively high species richness, deep molecular divergences, and adaptation to a variety of habitat types, the genus *Delma* remains remarkably conservative in morphology, microhabitat and diet (see Brennan et al. 2016). Along with broadly overlapping ranges of closely related species (Jennings et al. 2003) and numerous instances of ancient and recent mitochondrial introgression (Brennan et al. 2016), it is unsurprising that there has been confusion in taxonomy and interspecific relationships within *Delma*. The two closely related *D. tincta* and *D. hades* sp. nov. provide another example of the prevalence of this pattern of closely related sympatric species within *Delma*. Additional finer-scale sampling within central Australia would clarify the degree of sympatry, and fieldwork could determine whether these taxa exist in ecological syntopy. Furthermore, given the taxa in the *D. tincta* species complex are morphologically conservative yet show deep genetic divergence, chemical communication, particularly pheromones, may play an important role in reproductive isolation, as seen in other cryptic lizard species (Zozaya et al. 2019). Pheromone divergence has been shown to drive behavioural isolation in morphologically similar species and may be a key, yet currently unexplored, mechanism facilitating species boundaries in *Delma*.

Despite the overall morphological conservatism across the *D. tincta* species complex in traditional linear measurements and meristic characters, we found significant variation in head colour and pattern within each of the three eastern taxa across their respective distributions (ranging from bold and banded to plain). It has been suggested that the prominent head pattern in other *Delma* (including *D. tincta*) is a characteristic of juveniles and becomes obscure in older individuals (Maryan et al. 2007). However, we have identified many adult-sized individuals that retain the prominent head markings in *D. tincta, D. reticulata* and *D. hades* sp. nov. in some parts of their ranges. In his taxonomic revision of the Pygopodidae, Kluge (1974) referred to individuals of *D. tincta* observed in the lab that were buried in sand or loose gravel and only had their black and white-banded heads projecting above the substrate. Such behaviour was thought to be related to camouflage, as the projecting head was hard to distinguish from small rocks and pebbles. Little is known about the ecology and habitat use of these *D. tincta* species complex members, but the broad habitats occupied by the species vary considerably across each of their ranges. There is a particularly stark contrast between the *Eucalyptus* woodland-dominated landscapes of the coastal Queensland species, *D. reticulata*, and the arid tussock grasslands and mulga habitats of the inland taxa, *D. tincta* and *D. hades* sp. nov. Where these species come into contact between Barcaldine in central QLD and the Gulf of Carpentaria, the morphological disparity is at its greatest, with the heads of *D. reticulata* being highly banded, while those of the neighbouring *D. tincta* and *D. hades* sp. nov. are plain. This morphological distinction will be a useful character for distinguishing between taxa in this part of the continent.

We did not have SNP data from Broome, for which there are specimens with tissues, which are separated from Pilbara *D. branchia* by Dampierland along the Great Sandy Desert and those in the eastern Kimberley (*D. tincta*/*D. hades* sp. nov.). We examined the morphology and colour pattern for a number of individuals from this region, and they do not possess the diagnostic neck pattern of *D. branchia* sp. nov. The closest SNP genotyped individuals from the eastern Kimberley belong to both *D. tincta* and *D. hades,* which are sympatric here and across most of their distribution. Preliminary (unpublished) mtDNA data suggest these Broome individuals are divergent but most closely related to the WA *D. branchia* sp. nov.; however, a more thorough genetic assessment that includes nuclear SNPs is warranted. The same situation is true for *D. tincta* species complex individuals from the remote Top End in the NT, where no genetic material exists.

Compared to other widely distributed *Delma* that show little genetic variation across the continent (i.e. *D. borea*, *D. butleri* and *D. nasuta*; M. Pepper, unpublished data), the multiple and deep lineage divergences within the *D. tincta* species complex, particularly in the arid zone, highlight an evolutionary history characterised by long-term persistence. This geographic pattern of species richness is in line with what is known from geckos more broadly, and pygopods more specifically (Norris et al. 2021). Our discovery of three deeply diverged lineages within the resurrected *D. reticulata* is surprising, given that north Queensland is not recognised as a hotspot of diversity for this group. The distributions of these lineages closely mirror the well-known biogeographic barriers of the Laura Basin and the Burdekin Gap (Bryant and Krosch 2016) and underscore the historical significance of these lowland landscapes in driving and maintaining genetic divergence within and across taxa.

ACKNOWLEDGEMENTS

We acknowledge the Traditional Custodians of the lands across Australia where *Delma tincta* has been collected and studied. We pay our respects to Elders past and present, and recognise their enduring connection to Country and the ongoing significance of their culture and knowledge.

This work could not have been done without support in the form of a research grant from the Australian Biological Resources Study (ABRS) (Activity ID 4-EHPVS3D). An ARC DECRA also supported MP during this project (DE230100014). We thank the herpetology staff at the museums that loaned us material and kindly provided access to vouchers and/or tissue samples. In particular, we are grateful to Andrew Amey and Jessica Worthington-Wilmer from the QM, Sally South, Ralph Foster and Steve Donnellan from SAMA, Gavin Dally from NTM, Dane Trembath and Jodi Rowley from AMS, Joanna Sumner and Jane Melville from Museum Victoria, and Kailah Thorn and Brad Maryan from WAM. Stephen Zozaya and Kailah Thorn generously gave their time to take specimen photos. We thank Ian Brennan for his thoughts and *Delma* expertise the whole way through this project, Bernd Gruber for his help with the population genetics analyses and for proposing the use of fixed genetic differences as diagnostic molecular characters in accordance with ICZN requirements, and Brian Jennings for discussing ideas while carrying out morphological measurements at WAM. We thank Glenn Shea for extensive background information on the provenance of type specimens. Aaron Bauer and Paul Oliver kindly reviewed the manuscript and provided valuable comments that greatly improved the paper. We are grateful for a grant from Bioplatforms Australia as part of the Australian Amphibian and Reptile Genomics project that funded the sequencing costs, and to Sophie Mazzard for facilitating this.

REFERENCES

Ashman, L.G., Bragg, J.G., Doughty, P., Hutchinson, M.N., Bank, S., Matzke, N.J., Oliver, P., Moritz, C. (2018). Diversification across biomes in a continental lizard radiation. *Evolution* **72**(8): 1553–1569. doi: 10.1111/evo.13541

Bickford, D., Lohman, D.J., Sodhi, N.S., Ng, P.K., Meier, R., Winker, K., Ingram, K.K. and Das, I. (2007). Cryptic species as a window on diversity and conservation. *Trends in Ecology & Evolution* **22**(3): 148–155 doi: 10.1016/j.tree.2006.11.004.

Brennan, I.G., Bauer, A.M., and Jackman, T.R. (2016). Mitochondrial introgression via ancient hybridization, and systematics of the Australian endemic pygopodid gecko genus *Delma*. *Molecular Phylogenetics and Evolution* **94**: 577–590. doi: 10.1016/j.ympev.2015.10.005

Bryant, L.M., and Krosch, M.N. (2016). Lines in the land: a review of evidence for eastern Australia's major biogeographical barriers to closed forest taxa. *Biological Journal of the Linnean Society* **119**(2): 238–264.

Byrne, M., Yeates, D.K., Joseph, L., Kearney, M., Bowler, J., Williams, M.A., Cooper, S., Donnellan, S.C., Keogh, J.S., Leys, R., and Melville, J. (2008). Birth of a biome: insights into the assembly and maintenance of the Australian arid zone biota. *Molecular Ecology* **17**(20): 4398–4417. doi: 10.1111/j.1365-294X.2008.03899.x

Chaplin, K., Sumner, J., Hipsley, C.A., and Melville, J. (2019). An integrative approach using phylogenomics and high-resolution X-ray computed tomography for species delimitation in cryptic taxa. *Systematic Biology* **9**: 1049–1114. doi: 10.1093/sysbio/syz048

Chifman, J., and Kubatko, L. (2014). Quartet inference from SNP data under the coalescent model. *Bioinformatics* **30**: 3317–3324. doi: 10.1093/bioinformatics/btu530

Daza, J.D., and Bauer, A.M. (2012). Temporal bones of the Gekkota support molecular relationships within the Pygopodoidea. *Journal of Herpetology* **46**: 381–386. doi: 10.1670/11-183

de Queiroz, K. (2007). Species concepts and species delimitation. *Systematic Biology* **56**: 879–886. doi: 10.1080/10635150701701083

de Queiroz K. (1998) The General Lineage Concept of species, species criteria, and the process of speciation. In Endless forms: species and speciation (ed. D.J.Howard and S.H.Berlocher), pp. 57–75. Oxford University Press, Oxford, United Kingdom.

De Vis, C.W. (1888). A contribution to the herpetology of Queensland. *Proceedings of the Linnean Society of New South Wales* **2**(2): 811–826.

Doughty, P., Bauer, A.M., Pepper, M., and Keogh, J.S. (2018a). Spots before the eyes: revision of the saxicoline geckos of the *Gehyra punctata* (Squamata: Gekkonidae) species complex in the Pilbara region of Western Australia. *Records of the Western Australian Museum* **33**: 1–50. doi: 10.18195/issn.0312-3162.33(1).2018.001-050

Doughty, A.P., Bourke, G., Tedeschi, L.G., Pratt, R.C., Oliver, P.M., Palmer, R.A., and Moritz, C. (2018b). Species delimitation in the *Gehyra nana* (Squamata: Gekkonidae) complex: cryptic and divergent morphological evolution in the Australian Monsoonal Tropics, with the description of four new species. *Zootaxa* **4403**: 201–244. doi: 10.11646/zootaxa.4403.2.1

Doughty, P., Ellis, R.J., and Oliver, P.M. (2016). Many things come in small packages: revision of the clawless geckos (*Crenadactylus*: Diplodactylidae) of Australia. *Zootaxa* **4168**: 239–278. doi: 10.11646/zootaxa.4168.2.2

Duckett, P.E., Stow, A.J. (2013). Higher genetic diversity is associated with stable water refugia for a gecko with a wide distribution in arid Australia. *Diversity and Distributions* **19**: 1072–1083. doi: 10.1111/ddi.12089

Eastwood, J.A., Doughty, P., Hutchinson, M.N., and Pepper, M. (2020). Revision of *Lucasium stenodactylus* (Boulenger, 1896; Squamata: Diplodactylidae), with the resurrection of *L. woodwardi* (Fry, 1914) and the description of a new species from south-central Australia. *Records of the Western Australian Museum* **35**: 63–86. doi: 10.18195/issn.0312-3162.35.2020.063-086

Esquerré, D., Donnellan, S.C., Pavon-Vázquez, C.J., Fenker, J., and Keogh, J.S. (2021). Phylogeography, historical demography and systematics of the world's smallest pythons (Pythonidae, *Antaresia*). *Molecular Phylogenetics and Evolution* **161**: 107181. doi: 10.1016/j.ympev.2021.107181

Frichot, E., and François, O. (2015). LEA: An R package for landscape and ecological association studies. *Methods in Ecology and Evolution* **6**: 925–929. doi: 10.1111/2041-210X.12382

Frichot, E., Mathieu, F., Trouillon, T., Bouchard, G., and François, O. (2014). Fast and efficient estimation of individual ancestry coefficients. *Genetics* **196**: 973–983. doi: 10.1534/genetics.113.160572

Garman, S. (1901). Some reptiles and batrachians from Australasia. *Bulletin of the Museum of Comparative Zoology at Harvard College* **39**: 1–14.

Georges, A., Gruber, B., Pauly, G.B., White, D., Adams, M., Young, M.J., Kilian, A., Zhang, X., Shaffer, H.B., and Unmack, P.J. (2018). Genomewide SNP markers breathe new life into phylogeography and species delimitation for the problematic short-necked turtles (Chelidae: *Emydura*) of eastern Australia. *Molecular Ecology* **27**: 5195–5213. doi: 10.1071/MF18347

Gruber, B., Unmack, P.J., Berry, O.F., and Georges, A. (2018). dartr: An R package to facilitate analysis of SNP data generated from reduced representation genome sequencing. *Molecular Ecology Resources* **18**: 691–699. doi: 10.1111/1755-0998.12745

Georges, A., and Gruber, B. (2020). SNP Analysis Using dartR, Workshop Notes V1.7, Fixed Difference Analysis, The Institute for Applied Ecology, University of Canberra.

Guindon, S., Dufayard, J.F., Lefort, V., Anisimova, M., Hordijk, W., and Gascuel, O. (2010). New algorithms and methods to estimate maximum-likelihood phylogenies: assessing the performance of PhyML 3.0. *Systematic Biology* **59**: 307–321. doi: 10.1093/sysbio/syq010

Han, D., Zhou, K., and Bauer, A.M. (2004). Phylogenetic relationships among gekkotan lizards inferred from C-mos nuclear DNA sequences and a new classification of the Gekkota. *Biological Journal of the Linnean Society* **83**(3): 353–368. doi: 10.1111/j.1095-8312.2004.00393.x

Hutchinson, M.N., Doughty, P., and Oliver, P.M. (2009). Taxonomic revision of the stone geckos (Squamata: Diplodactylidae: *Diplodactylus*) of southern Australia. *Zootaxa* **2167**: 25–46. doi: 10.11646/zootaxa.2167.1.2

Jennings, B., Pianka, E.R., and Donnellan, S.C. (2003). Systematics of the lizard family Pygopodidae with implications for the diversification of Australian temperate biotas. *Systematic Biology* **52**: 757–780. doi: 10.1093/sysbio/52.6.757

Jennings, W.B. (2021). Evolutionary relationships among the snakelike pygopodid lizards: a review of phylogenetic studies of an enigmatic Australian adaptive radiation. *PeerJ* **9**: e11502. doi: 10.7717/peerj.11502

Jörger, K.M. and Schrödl, M. (2013). How to describe a cryptic species? Practical challenges of molecular taxonomy. *Frontiers in Zoology* **10**: 1–27. doi: 10.1186/1742-9994-10-59

Kalyaanamoorthy, S., Minh, B.Q., Wong, T.K.F., von Haeseler, A., and Jermiin, L.S. (2017). ModelFinder: fast model selection for accurate phylogenetic estimates. *Nature Methods* **14**(6): 587–589. doi: 10.1038/nmeth.4285

Kealley, L., Doughty, P., Pepper, M., Keogh, J.S., Hillyer, and M., Huey, J. (2018). Conspicuously concealed: revision of the arid clade of the *Gehyra variegata* (Gekkonidae) group in Western Australia using an integrative molecular and morphological approach, with the description of five cryptic species. *PeerJ* **6**: e5334. doi: 10.7717/peerj.5334

Kilian, A., Wenzl, P., Huttner, E., Carling, J., Xia, L., Blois, H., Caig, V., Heller-Uszynska, K., Jaccoud, D., Hopper, C., Aschenbrenner-Kilian, M., Evers, M., Peng, K., Cayla, C., Hok, P., and Uszynski, G. (2012). Diversity arrays technology: a generic genome profiling technology on open platforms. Data production and analysis in population genomics. Methods in Molecular Biology, Humana Press, Totowa, NJ, pp. 67–89.

Kluge, A.G. (1974). A taxonomic revision of the lizard family Pygopodidae. *Miscellaneous Publications of the Museum of Zoology* University of Michigan **147**: 1–221.

Maddison, W.P., and Whitton, J. (2023). The species as a reproductive community emerging from the past. *Bulletin of the Society of Systematic Biologists* **2**(1): 1–35. doi: 10.18061/bssb.v2i1.9358

McKenzie, N.L., Rolfe, J.K., Aplin, K., Cowan, M. and Smith, L.A. (2000). Herpetofauna of the southern Carnarvon Basin, Western Australia. *Records of the Western Australian Museum* Supplement **61**: 335–360. doi: 10.18195/issn.0313-122x.61.2000.335-360

Melville, J., Haines, M.L., Boysen, K., Hodkinson, L., Kilian, A., Smith Date, K.L., Potvin, D.A., and Parris, K.M. (2017). Identifying hybridization and admixture using SNPs: application of the DArTseq platform in phylogeographic research on vertebrates. *Royal Society Open Science* **4**: 161061. doi: 10.1098/rsos.161061

Melville, J., Chapple, D.G., Keogh, J.S., Sumner, J., Amey, A., Bowles, P., Brennan, I.G., Couper, P., Donnellan, S.C., Doughty, P., and Edwards, D.L. (2021). A return-on-investment approach for prioritization of rigorous taxonomic research needed to inform responses to the biodiversity crisis. *PLoS Biology* **19**(6): e3001210. doi: 10.1371/journal.pbio.3001210

Moritz, C., Fujita, M.K., Rosauer, D., Agudo, R., Bourke, G., Doughty, P., Palmer, R., Pepper, M., Potter, S., Pratt, R., and Scott, M. (2016). Multilocus phylogeography reveals nested endemism in a gecko across the monsoonal tropics of Australia. *Molecular Ecology* **25**(6): 1354–1366. doi: 10.1111/mec.13511

Minh, B.Q., Hahn, M., and Lanfear, R. (2018). New methods to calculate concordance factors for phylogenomic datasets. *bioRxiv* 1–7.

Morton, S.R., and James, C.D. (1988). The diversity and abundance of lizards in arid Australia: a new hypothesis. *The American Naturalist* **132**: 237–256.

Nguyen, L.-T., Schmidt, H.A., von Haeseler, A., and Minh, B.Q. (2015). IQ-TREE: a fast and effective stochastic algorithm for estimating maximum-likelihood phylogenies. *Molecular Biology and Evolution* **32**: 268–274. doi: 10.1093/molbev/msu300

Norris, J., Tingley, R., Meiri, S., and Chapple, D.G. (2021). Environmental correlates of morphological diversity in Australian geckos. *Global Ecology and Biogeography* **30**: 1086–1100. doi: 10.1111/geb.13284

Nylinder, S., Lemey, P., De Bruyn, M., Suchard, M.A., Pfeil, B.E., Walsh, N., and Anderberg, A.A. (2014). On the biogeography of Centipeda: a species-tree diffusion approach. *Systematic Biology* **63**: 178–191. doi: 10.1093/sysbio/syt102

Oliver, P.M., Couper, P.J., and Pepper, M. (2014). Independent transitions between monsoonal and arid biomes revealed by systematic revision of a complex of Australian geckos (*Diplodactylus*; Diplodactylidae). *PLoS One* **9**: e111895. doi: 10.1371/journal.pone.0111895

Oliver, P.M., Donnellan, S.C., and Gunn, B.F. (2022). Plio–Pleistocene vicariance across arid Australia in the 'Spiny Knob-tailed Geckos' (*Nephrurus asper* group), with the description of a new species from western Queensland. *Australian Journal of Zoology* **69**: 216–228. doi: 10.1071/ZO22008

Oliver, P.M., and Doughty, P. (2016). Systematic revision of the marbled velvet geckos (*Oedura marmorata* species complex, Diplodactylidae) from the Australian arid and semi-arid zones. *Zootaxa* **4088**: 151–176. doi: 10.11646/zootaxa.4088.2.1

Oliver, P.M., Prasetya, A.M., Tedeschi, L.G., Fenker, J., Ellis, R.J., Doughty, P., and Moritz, C. (2020). Crypsis and convergence: integrative taxonomic revision of the *Gehyra australis* group (Squamata: Gekkonidae) from northern Australia. *PeerJ* **8**: e7971. doi: 10.7717/peerj.7971

Oliver, P., Keogh, J.S., and Moritz, C. (2014). New approaches to cataloguing and understanding evolutionary diversity: a perspective from Australian herpetology. *Australian Journal of Zoology* **62**(6): 417–430. doi: 10.1071/ZO14091

Oliver, P.M., Adams, M., Lee, M.S., Hutchinson, M.N., and Doughty, P. (2009). Cryptic diversity in vertebrates: molecular data double estimates of species diversity in a radiation of Australian lizards (*Diplodactylus*, Gekkota). *Proceedings of the Royal Society B: Biological Sciences* **276**(1664): 2001–2007. doi: 10.1098/rspb.2008.1881

Oliver, P.M., and Sanders, K.L. (2009). Molecular evidence for Gondwanan origins of multiple lineages within a diverse Australasian gecko radiation. *Journal of Biogeography* **36**: 2044–2055. doi: 10.1111/j.1365-2699.2009.02149.x

Pavón-Vázquez, C.J., Esquerré, D., Fitch, A.J., Maryan, B., Doughty, P., Donnellan, S.C., and Keogh, J.S. (2022). Between a rock and a dry place: phylogenomics, biogeography, and systematics of ridge-tailed monitors (Squamata: Varanidae: *Varanus acanthurus* complex). *Molecular Phylogenetics and Evolution* **173**: 107516. doi: 10.1016/j.ympev.2022.107516

Pepper, M., Doughty, P., Fujita, M.K., Moritz, C., and Keogh, J.S. (2013). Speciation on the rocks: integrated systematics of the *Heteronotia spelea* species complex (Gekkota; Reptilia) from western and central Australia. *PLoS One* **8**: e78110. doi: 10.1371/journal.pone.0078110

Pepper, M., Doughty, P., Hutchinson, M.N., and Keogh, J.S. (2011). Ancient drainages divide cryptic species in Australia's arid zone: morphological and multi-gene evidence for four new species of Beaked Geckos (*Rhynchoedura*). *Molecular Phylogenetics and Evolution* **61**: 810–822. doi: 10.1016/j.ympev.2011.08.012

Pepper, M., and Keogh, J.S. (2021). Life in the "dead heart" of Australia: the geohistory of the Australian deserts and its impact on genetic diversity of arid zone lizards. *Journal of Biogeography* **48**: 716–746. doi: 10.1111/jbi.14063

Pianka, E.R. (1986). Ecology and Natural History of Desert Lizards. Analyses of the Ecological Niche and Community Structure. Princeton University Press, Princeton.

Shea, G.M. (1987). Two new species of *Delma* (Lacertilia: Pygopodidae) from northeastern Queensland and a note on the status of the genus *Aclys*. *Proceedings of the Linnean Society of New South Wales* **109**: 203–212.

Shea, G.M. (1991). Revisionary notes on the genus Delma (Squamata: Pygopodidae) in South Australia and the Northern Territory. *Records of the South Australian Museum* **25**: 71–90.

Storr, G.M., Smith, L.A., and Johnstone, R.E. (1990). Lizards of Western Australia. III. Geckos and pygopods. Western Australian Museum Press, Perth.

Swofford, D.L. (2003). PAUP*. Phylogenetic analysis using parsimony and other methods. Version 4. Sinauer Associates.

Unmack, P.J., Young, M.J., Gruber, B., White, D., Kilian, A., Zhang, X., and Georges, A. (2019). Phylogeography and species delimitation of *Cherax destructor* (Decapoda: Parastacidae) using genome-wide SNPs. *Marine and Freshwater Research* **70**(6): 857–869. doi: 10.1071/MF18347

Webb, J.K., Harlow, P.S., and Pike, D.A. (2014). Australian reptiles and their conservation. In 'Austral Ark: the state of wildlife in Australia and New Zealand'. (Eds A.Stow, N.Maclean, and G.I.Holwell.) pp. 354–381.

Wilson, S.K., and Swan, G. (2021). A complete guide to reptiles of Australia (6th ed.). New Holland Publishers, Chatswood, New South Wales.

Zozaya, S.M., Fenker, J., and Macdonald, S.L. (2019). A new species of rock-dwelling gecko (Gekkonidae: *Gehyra*) from the Mt Surprise region of northern Queensland, Australia. *Zootaxa* **4688**: 503–518. doi: 10.11646/zootaxa.4688.4.3

Zozaya, S.M., Higgie, M., Moritz, C., and Hoskin, C.J. (2019). Are pheromones key to unlocking cryptic lizard diversity? *The American Naturalist* **194**(2): 168–182. doi: 10.1086/704059.

MANUSCRIPT RECEIVED 3 SEPTEMBER 2024; ACCEPTED 3 JULY 2025.

APPENDIX 1 Museum accession numbers and collection localities.

Species	Museum	Tissue No.	Specimen	Population	Latitude	Longitude	State	Locality	Morphology	Genetics
D. branchia sp. nov.	WAM		R179858	P5	-26.4139	114.1728	Western Australia	Hamelin Pool Rd, 4 km N Denham-Hamelin Rd Intersection, road verge	N	Y
D. branchia sp. nov.	SAMA	ABTC52154	R29365	P5	-26.43	114.18	Western Australia	Hamelin Homestead	Y	Y
D. branchia sp. nov.	SAMA	ABTC11679	R34024	P5	-25.05	115.2	Western Australia	Gascoyne Junction	N	Y
D. branchia sp. nov.	SAMA	ABTC104823	R100990	P5	-27.5166	115.75	Western Australia	19 km SE New Forest	N	Y
D. branchia sp. nov.	WAM		R102838	P5	-22.1502	113.9978	Western Australia	Cape Range National Park	Y	Y
D. branchia sp. nov.	WAM		R110080	P5	-20.808	117.073	Western Australia	8 km SW Roebourne	Y	Y
D. branchia sp. nov.	WAM		R110292	P5	-22.7073	119.709	Western Australia	12 km NE Mile Camp	Y	Y
D. branchia sp. nov.	WAM		R112690	P5	-21.6758	115.145	Western Australia	5.5 km SE Onslow	Y	Y
D. branchia sp. nov.	WAM		R113012	P5	-20.2472	118.8472	Western Australia	Lesley Salt Works	Y	Y
D. branchia sp. nov.	WAM		R113030	P5	-20.2472	118.8472	Western Australia	Lesley Salt Works	Y	Y
D. branchia sp. nov.	WAM		R114490	P5	-28.7333	115	Western Australia	Wicherina Dam	Y	Y
D. branchia sp. nov.	WAM		R115018	P5	-28.65	114.6333	Western Australia	Spalding Park, Geralton	Y	Y
D. branchia sp. nov.	WAM		R117342	P5	-22.9458	119.125	Western Australia	Hope Downs	Y	Y
D. branchia sp. nov.	WAM		R120020	P5	-22.4666	117.3	Western Australia	Brockman, 3.5 km NE Mount Brockman	Y	Y
D. branchia sp. nov.	WAM		R125032	P5	-22.7205	118.9906	Western Australia	Yandicoogina	Y	Y
D. branchia sp. nov.	WAM		R127768	P5	-22.7969	117.7889	Western Australia	5 km S Mount Tom Price Mine	Y	Y
D. branchia sp. nov.	WAM		R129623	P5	-22.9166	118.95	Western Australia	120 km NW Newman	Y	Y
D. branchia sp. nov.	WAM		R135422	P5	-22.3105	117.2522	Western Australia	Mount Brockman	Y	Y
D. branchia sp. nov.	WAM		R139308	P5	-21.2447	120.3222	Western Australia	Meentheena	Y	Y
D. branchia sp. nov.	WAM		R139314	P5	-21.2177	120.4556	Western Australia	Meentheena	Y	Y

Species	Museum	Tissue No.	Specimen	Population	Latitude	Longitude	State	Locality	Morphology	Genetics
D. branchia sp. nov.	WAM		R139328	P5	-21.2816	120.4661	Western Australia	Meentheena	Y	Y
D. branchia sp. nov.	WAM		R139637	P5	-22.6891	114.2936	Western Australia	Giralia Station	Y	Y
D. branchia sp. nov.	WAM		R151059	P5	-24.8833	113.7667	Western Australia	10 km E Carnarvon	Y	Y
D. branchia sp. nov. (holotype)	WAM		R153821	P5	-22.8091	113.9442	Western Australia	Bullara Station	Y	Y
D. branchia sp. nov.	WAM		R154268	P5	-22.0675	118.9953	Western Australia	Fortescue Marsh	Y	Y
D. branchia sp. nov.	WAM		R156173	P5	-24.733	117.4186	Western Australia	Waldburg Station	Y	Y
D. branchia sp. nov.	WAM		R156227	P5	-20.6033	120.2642	Western Australia	Cattle Gorge	Y	Y
D. branchia sp. nov.	WAM		R156258	P5	-21.7116	115.1969	Western Australia	Onslow Area	Y	Y
D. branchia sp. nov.	WAM		R157065	P5	-21.9538	118.9958	Western Australia	Fortescue Marsh	Y	Y
D. branchia sp. nov.	WAM		R157124	P5	-23.1991	118.8469	Western Australia	West Angelas	Y	Y
D. branchia sp. nov.	WAM		R158123	P5	-22.3469	119.01	Western Australia	1.5 km NE Cowra Line Camp	Y	Y
D. branchia sp. nov.	WAM		R158202	P5	-22.7419	120.4731	Western Australia	55.2 km W Roy Hill	Y	Y
D. branchia sp. nov.	WAM		R160201	P5	-21.6785	120.088	Western Australia	56.3 km N Nullagine	Y	Y
D. branchia sp. nov.	WAM		R161660	P5	-20.3256	119.211	Western Australia	32.5 km W Goldsworthy	Y	Y
D. branchia sp. nov.	WAM		R162036	P5	-22.2554	115.437	Western Australia	21.5 km NE Mount Mary	Y	Y
D. branchia sp. nov.	WAM		R162054	P5	-23.2136	119.202	Western Australia	5.5 km NE Giles Point	Y	Y
D. branchia sp. nov.	WAM		R163935	P5	-20.3908	119.909	Western Australia	41 km ESE Goldsworthy	Y	Y
D. branchia sp. nov.	WAM		R166546	P5	-27.5797	115.8992	Western Australia	Meka Station	Y	Y
D. branchia sp. nov.	WAM		R166641	P5	-20.8572	117.8342	Western Australia	Mons Cupri Mine	Y	Y
D. branchia sp. nov.	WAM		R167564	P5	-24.2952	114.0442	Western Australia	76 km NE Carnarvon	N	Y
D. branchia sp. nov.	WAM		R167566	P5	-24.2952	114.0444	Western Australia	76 km NE Carnarvon	N	Y
D. branchia sp. nov.	WAM		R170131	P5	-21.0717	118.68	Western Australia	11 km N Wodgina	Y	Y
D. branchia sp. nov.	WAM		R170660	P5	-21.8397	116.683	Western Australia	11.5 km W Mount Elvire	Y	Y
D. branchia sp. nov.	WAM		R174663	P5	-21.47673	117.14898	Western Australia	Millstream National Park	Y	Y

Species	Museum	Tissue No.	Specimen	Population	Latitude	Longitude	State	Locality	Morphology	Genetics
D. branchia sp. nov.	WAM		R99180	P5	-21.6097	118.9622	Western Australia	Woodstock Station	Y	Y
D. tincta	WAM		R137953	P1	-15.5888	128.9833	Western Australia	35 km NNE Kununurra	N	Y
D. tincta	SAMA		R37588	P1	-22.860833	134.418167	Northern Territory	Alcoota Station	N	Y
D. tincta	SAMA	ABTC441	R35960	P1	-26.3	136.02	South Australia	Alka Seltzer Bore	Y	Y
D. tincta	SAMA	ABTC6581	ABTC6581	P1	-15.7905	128.7661	Western Australia	Kununurra	N	Y
D. tincta	SAMA	ABTC67965	R24842	P1	-15.320667	130.457333	Northern Territory	Bradshaw Station	N	Y
D. tincta	SAMA	ABTC67988	R24858	P1	-15.320667	130.457333	Northern Territory	Bradshaw Station	N	Y
D. tincta	SAMA	ABTC12058	R38847	P1	-23.77	133.88	Northern Territory	Camel Farm, Ross River Hwy, Alice Springs	Y	Y
D. tincta	SAMA	ABTC36156	R46806	P1	-26.3575	135.7075	South Australia	0.2 km W Anvil Hole Native Well, Witjira	Y	Y
D. tincta	SAMA	ABTC58700	R49874	P1	-26.2869	134.7244	South Australia	Eringa Waterhole	Y	Y
D. tincta	SAMA	ABTC88012	R60513	P1	-26.7511	134.7622	South Australia	31.5 km W Hamilton Homestead	Y	Y
D. tincta	SAMA	ABTC88082	R60546	P1	-26.3181	135.2008	South Australia	Witjira National Park	Y	Y
D. tincta	SAMA	ABTC23937	R30971	P2	-27.18	140.15	South Australia	Coongie	Y	Y
D. tincta	SAMA	ABTC51994	R31173	P2	-27.2	140.13	South Australia	Cooper Creek area	Y	Y
D. tincta	SAMA	ABTC37312	R49065	P2	-27.6325	140.8294	South Australia	7.2 km SW Table Hill, Innamincka Area	Y	Y
D. tincta	SAMA	ABTC132053	R61856	P2	-31.4014	140.0886	South Australia	3.5 km NE Billeroo West Homestead	Y	Y
D. tincta	SAMA	ABTC132086	R61947	P2	-30.1825	139.6033	South Australia	29.6 km ENE Arkaroola Village	Y	Y
D. tincta	SAMA	ABTC6492	R90213	P7	-22.375	142.412	Queensland	63km W Winton	N	Y
D. tincta	SAMA	ABTC6493	R90214	P7	-22.764	143.391	Queensland	55km SE Winton	N	Y
D. tincta	SAMA	ABTC70822	R25851	P7	-18	140.55	Queensland	Road junction, Inverleigh Station	N	Y

Species	Museum	Tissue No.	Specimen	Population	Latitude	Longitude	State	Locality	Morphology	Genetics
D. tincta	SAMA	A009149	J91823	P7	-20.7681	141.7417	Queensland	12 km S Julia Creek	Y	Y
D. tincta	SAMA	A001706	J83423	P7	-23.4318	144.2511	Queensland	Gin Creek, Longreach	Y	Y
D. tincta	SAMA	ABTC34964	R45034	P7	-26.3181	140.3361	South Australia	6.2 km SSE Elbow Well	Y	Y
D. tincta	SAMA	ABTC72712	R54019	P7	-18.5922	136.0894	Northern Territory	Brunette Downs Racecourse	Y	Y
D. tincta	SAMA	ABTC82403	R55294	P7	-21.8769	139.9456	Queensland	Phosphate Hill, Grassland Site	Y	Y
D. tincta (lectotype)	QM		J241	-			Queensland	Normanton, Gulf of Carpentaria	Y	N
D. reticulata	QM	A013415	J94238	P3	-15.4242	143.4947	Queensland	Killarney Station Homestead	Y	Y
D. reticulata	QM		J93148	P3	-12.293889	142.444167	Queensland	Steve Irwin Wildlife Reserve	N	Y
D. reticulata	QM	A013311	J94132	P3	-15.3000	143.4000	Queensland	Olkola area	N	Y
D. reticulata	AMS		R180606	P4	-17.53	145.42	Queensland	1 km S Kaban	Y	Y
D. reticulata	QM	A005376	J87604	P4	-15.5652	145.2511	Queensland	Killarney, 15 km S Cooktown	N	Y
D. reticulata	QM	A012124	J93849	P4	-15.5014	144.8497	Queensland	Kings Plains Station	Y	Y
D. reticulata	QM	A005047	J87293	P4	-15.4297	145.1189	Queensland	Jensen's Crossing Via Cooktown	Y	Y
D. reticulata	QM	A002121	J70675	P6	-24.9450	147.9606	Queensland	Carnarvon National Park, Mount Moffatt Section, near Marlong Creek	Y	Y
D. reticulata	QM	A002120	J70674	P6	-24.9450	147.9606	Queensland	Carnarvon National Park, Mount Moffatt Section, near Marlong Creek	Y	Y
D. reticulata	AMS		R186395	P6	-20.082243	148.489181	Queensland	Hydeaway Bay	N	Y
D. reticulata	QM	A000261	J80136	P6	-26.4658	148.5433	Queensland	Donnybrook Rd, 15.6 km NW Warrego Hwy	Y	Y
D. reticulata	QM	A007889	J90689	P6	-18.2900	143.5489	Queensland	Georgetown	Y	Y
D. reticulata	QM	A006522	J88438	P6	-22.8243	147.6411	Queensland	Clermont, Herschel Street	Y	Y
D. reticulata	QM	A014574	J95572	P6	-24.8431	151.3969	Queensland	Goondicum, Near Monto	Y	Y

Species	Museum	Tissue No.	Specimen	Population	Latitude	Longitude	State	Locality	Morphology	Genetics
D. reticulata	QM	A003140	J84130	P6	-24.8464	147.7408	Queensland	Carnarvon	Y	Y
D. reticulata	QM	A014749	J95799	P6	-19.1206	145.3350	Queensland	Christmas Creek Station	Y	Y
D. reticulata	WAM	ABTC149823	R71375	P6	-20.61817	148.6658	Queensland	Laguna Quays Driveway	Y	Y
D. reticulata	QM		J56465	-	-16.5333	145.1333	Queensland	Mount Carbine, town area	Y	N
D. reticulata	QM		J57250	-	-16.8167	145.6833	Queensland	Cairns	Y	N
D. reticulata	QM		J75298	-	-20.1667	149.0833	Queensland	Whitsundays	Y	N
D. reticulata	QM		J77978	-	-21.1925	147.9433	Queensland	Newlands Coal Mine	Y	N
D. reticulata	QM		J78002	-	-21.1914	147.9025	Queensland	Newlands Coal Mine	Y	N
D. reticulata	QM		J81285	-	-19.0833	146.4167	Queensland	Toomulla Beach Rd, Clemant State Forest, 3 km WNW Bruce Hwy	Y	N
D. reticulata	QM		J88170	-	-15.5652	145.2511	Queensland	Kallarney Station, 15 km S Cooktown	Y	N
D. hades sp. nov.	WAM		R191011	P8	-15.832345	128.46196	Western Australia	34.6 km W Kununurra, Victoria Highway	Y	Y
D. hades sp. nov.	SAMA	ABTC30108	R22911	P8	-15.3461	129.1514	Northern Territory	Spirit Hills, Keep River	N	Y
D. hades sp. nov.	SAMA	ABTC70681	R25712	P8	-19.652	134.184	Northern Territory	Tennant Creek	N	Y
D. hades sp. nov. (holotype)	SAMA	ABTC113677	J90655	P8	-22.3964	139.9572	Queensland	8.5 km SW Two Rivers Homestead	Y	Y
D. hades sp. nov.	SAMA	ABTC35520	R40238	P8	-27.27	135.5	South Australia	14 km WSW Macumba Homestead	Y	Y
D. hades sp. nov.	SAMA	ABTC42381	R51553	P8	-26.27	131.4767	South Australia	36 km ESE Amata	Y	Y
D. hades sp. nov.	SAMA	ABTC72709	R54015	P8	-19.7114	135.8278	Northern Territory	Barkly Roadhouse	Y	Y
D. hades sp. nov.	SAMA	ABTC72877	R54465	P8	-19.2264	140.3481	Queensland	Burke and Wills Roadhouse Dump	Y	Y
D. hades sp. nov.	SAMA	ABTC73397	R54735	P8	-29.02	134.75	South Australia	Coober Pedy	Y	Y
D. hades sp. nov.	WAM		R177993	P8	-15.832	128.462	Western Australia	Victoria Highway	Y	Y

APPENDIX 2 The sequences of diagnostic fixed differences between the four taxa in the *D. tincta* species complex with the SNP in [bold] and corresponding coordinates provided for the reference genome (*Gekko japonicus* v1.1) where alignments were possible.

Sequence	Length	SNP alleles	Diag. allele	SNP pos	RefChrom	Chrom pos
***D. hades* sp. nov. vs rest**						
TGCAGTTAGAGTGACCAACTGTCCCAGTTTGCCC**[A]**GGAGAGTCCCAGATTGAAGGGTGGTTGTCCTGCA	69	G>A	A	35		
TGCAGAAATA**[A]**GGCAGGTGAAGTTTTCCTGGTTAAGAAACCTGCACCTGACACACAACAGCTCTTAAAC	69	A>G	A	11		
TGCAGGCAACACCATTTGGCAGCCA**[T]**TAATATATTCCTTCTGACTTCTTTTTCTGCATG	59	C>T	T	26	NW_015170280.1_scaffold203	1324869
TGCAGCTATTTTGCAAG**[C]**ACAGGGAAATGCATG	33	T>C	C	18		
TGCAGGCACGGGAAAC**[T]**TTGGTTTAGGCCCAAGGCATG	38	T>C	T	17		
TGCAGTGTCTGCACAGCGTGCTAATCAAAATATGCACCAATTCCCAAATACAACATTTTTAAA**[C]**CCATT	69	C>T	C	64		
TGCAGGGAGTTGGACTAGATGATCCTTGTGGTCCCTTCCAGCTCTAATATTCTATGATTC**[G]**TTGATGCT	69	G>T	G	61	NW_015170918.1_scaffold929	169621
TGCAGTGTGTAATCAGCAAAGGAAGAAGGAAAAGTCTTTAGGTAGCTCCCTG**[G]**ACAACAAAATGGAAAG	69	G>T	G	53		
TGCAGT**[T]**CCTGACCATTTGTTCTGCATG	28	C>T	T	7		
TGCAGCATA**[A]**CCCTGTGCATGAGCGGTTCAGCAGGAATGCCGAGACCGATCTCGTATGCCGTCTTCTGC	69	G>A	A	10		
TGCAGATAGGCAGGTGTTCTGTGTAGGTATGGCTATATAAAGCTTTCA**[A]**AGCAGCAGTTCTAAAAAGAG	69	G>A	A	49		
***D. branchia* sp. nov. vs rest**						
TGCAGGGCTGCAAGACAGTGAGACTAGCAAGATTTGCCCTTGTCTGG**[C]**TGTAATCTTTTATCAGCATGA	69	T>C	C	48	NW_015176056.1_scaffold2651	33328
TGCAGATTTGCCCT**[T]**ACTTAGTTTAAGGCATG	32	G>T	T	15		
TGCAGGTATGAAGGATTTGTATGTAATAG**[G]**ACCTTGAACTGTGGCCAATAAATGATGAGCAACCAATGG	69	G>T	G	30		
TGCAGGT**[T]**ACTATCCTACCACCCTATTGCATG	32	T>G	T	8		
TGCAGC**[T]**TTGCTTTGAGAGTCAAAATGGATAGTAGCCCCTGATCTCTTCTAGAAGATTGTTCCAGAGGC	69	T>C	T	7		
TGCAGTAGGGGTGTGTGCA**[T]**TCAGAATGTGGATTTCTGCATG	42	T>C	T	20		
TGCAGATTTGCCACCAGCATATTGGAGAGGCTGGTTGTTACAGAACTGA**[C]**ATATGAAACTGGTTGGCAG	69	A>C	C	50		

Sequence	Length	SNP alleles	Diag. allele	SNP pos	RefChrom	Chrom pos
TGCAGAA**[C]**AGTTACACACATATTCAGGAGAATCAGTGGAGTGGTTCCTTCATTCTTAATCTCTTTTATC	69	T>C	C	8		
TGCAGATTTCCTGTCA**[C]**TGCATATTGTTTGAACCCTAAGCTTGATGGTGAAACATGGACTTGCATGAGC	69	T>C	C	17		
TGCAGTGCTTCAAGCAGTGTACGAGAGTCATAATGTGAGGGTTGTCCCTTTGTAGTTG**[A]**TAATGACTCT	69	T>A	A	59		
TGCAGGTTTGAGCTAGAAAGCAGAACATGAGGCAAGGAAACAGAGAATATCAACTTTTAAAGA**[T]**ATTTA	69	G>T	T	64		
TGCAGGATCACAGCACTATC**[A]**CAATTGCTGTTGGTGCCACTATGGCCCACGAAATGGGCCATAACTTTG	69	G>A	A	21		
TGCAGAGCCTGCAAAGTTAAACTATTCTGTTGAGCTTT**[T]**AGTACTTGAACTGGGACAGCTTGGCCAAAC	69	C>T	T	39		
TGCAGTCTACCCTTCCCTTTCAGTTA**[T]**CCCCTGGCACACCATTTGCATG	49	T>C	T	27		
TGCAG**[A]**AAAACCATCTAATAGATCTGTTACATAATTCATGATGGGGCTTGTAGTTTTAAAACTCTACCA	69	G>A	A	6		
TGCAGTGAGATGAGAGCACCCTGCCATCACTGGCATAAAAGGA**[A]**TTGCTACTGCAAATGCATG	63	G>A	A	44	NW_015159712.1_scaffold84	1219696
TGCAGGCCCCACAGCAAGGTCAAGGGG**[A]**TGCCGCCCGCCAATGGGGGGCCCTTGCATG	58	A>C	A	28		
TGCAGGTCAAATTTGTTGGCTAGTTTGT**[G]**TTGTCCTCTGAAGTGCTAAAAGAAGCGTAGCATG	63	A>G	G	29		
TGCAGACCA**[A]**GTGTTCCCATTCTCTGTCTGCATTGGCATG	40	T>A	A	10		
TGCAGTCTGTGCCTATTCTGG**[C]**GCATG	27	A>C	C	22		
TGCAGAGCTGTGGTAGGCATGAGGCTGGGAG**[T]**GGGCATG	39	T>G	T	32		
TGCAGACCTTAAATAACTTGTGTTCAGAGTATCCAAAAGACTTT**[A]**TCTGCATATATAAATATCCTCAGG	69	C>A	A	45		
TGCAGGATGGATGTTTTCTTGGAAATGGGAGGAGGTGGATTTAGATTGCTTCCATGATCAAAC**[A]**TAATG	69	A>G	A	64		
TGCAGTTAGTTTTTATTCAT**[G]**TGAGTAGTTCTATTGAACCTAGAGAGCCTCTTACATTGCAAAAGCATC	69	A>G	G	21		
TGCAG**[A]**GGATGGGATCCAGCATCCTGCCTGTAGCATG	37	A>G	A	6		
TGCAGTCCA**[G]**TTAATGAACTTTGTTTAAGGTTTACTATTTGTGTTCTCTGAGCCTTTTTGCATG	64	G>A	G	10		
TGCAGAAACATTTCTTGTGAATTTGACAGGCA**[A]**TCATGTTGCATG	45	A>G	A	33		
TGCAGC**[C]**GTAACTTAAATGTTCAACAGAAACCCCACAGAGGTTGGCTTGGTGGATTTCCTAAAGCACTT	69	C>A	C	7		
TGCAGGTGGAG**[A]**TTGCAGTGGCATG	25	A>C	A	12		
TGCAGGCCCTCCTCAGCCACAGGGTCTGGAAA**[A]**AAATCCAGCAGACAACCTTCAAGCCATGGCTCTGAG	69	C>A	A	33		
TGCAGACCCAAGAAAGATTTGATTTGCCAGGGTAAGTCTTGACCTTAGATTT**[A]**GCATG	58	A>G	A	53		

Sequence	Length	SNP alleles	Diag. allele	SNP pos	RefChrom	Chrom pos
TGCAGAAAAGTGGCATATGATCCTGCCATGGAAATAATAAATTAA**[T]**CCTTAATGGCTAAACCAAGCCTC	69	T>C	T	46		
TGCAGGAATCTTGGCTTTCAAAGTTTCAGAATTTGATGTA**[T]**CTTATTTGTAAAGCATG	58	C>T	T	41		
TGCAGGGCAAAAAAACAGACCATTTTGGCATGA**[A]**ATCAGCATG	43	A>G	A	34		
TGCAGAGGTATCTTTCCAAAGTATGCATGAAAACCTAAGTGATAAGGGAATCTCCTGTGCAT**[A]**GGGACA	69	G>A	A	63		
TGCAGTCAGCTAACACGTCACAGAAATGACTGAAACCCTTGGTGTAATCCATCATA**[G]**GACAAAAACCTT	69	G>C	G	57		
TGCAGTCTAAACTTTGAGAACTAT**[G]**AAATAGTCTTGCAGGTATGCAATGCTGCATG	56	G>A	G	25		
TGCAGT**[A]**TTGTTGCTTGGCATGTTGCATATGTGTGCATG	39	A>G	A	7		
TGCAGAATTCAATAAAA**[C]**TCTTACCTTTGGTGCATG	36	C>T	C	18		
TGCAGTGTCAGGGTTCTTTCTC**[T]**TCCTCCTTTTGTCCTCAACACCATCTCTGCATG	56	T>A	T	23		
TGCAGATGAATAGGTGCCTT**[T]**CAGATTCAGCAGTTCCCACCAGCCACTCTTGCCTAACCAGGAGTGAGT	69	G>T	T	21		
TGCAGGC**[T]**CCTCTAACCAATAAAGGCATG	29	T>C	T	8		
TGCAGTCAATAGGCATAAGGGGGACTCTCTGTGGTGAGTTAATGCCTGAAAAGTGCATGACATCAGAA**[T]**	69	C>T	T	69		
TGCAGAATGACTTGCTCTAGAAACAGGTTTTAAAGTCCAC**[A]**AAATCAACACACAGATACATATATTTTC	69	A>T	A	41		
TGCAGGCTGCATCACAC**[A]**GGTCGGTCGTTTATAGCTCAGCACCCAATCAGCTGAGCATG	59	G>A	A	18		
TGCAGCTCTCCACCCACAT**[T]**GCTTGGATTGGCTCGCATG	39	T>G	T	20		
TGCAGTTTATGGGATTACATCCTTTTCAAAGTGCCTGT**[T]**AGTTAATAACTACCTGTGAGTGGGGAAAGT	69	T>G	T	39		
TGCAGGTGGAACAG**[A]**TGCTTGATGCGCCCTGGGGGCACTTGCATG	45	A>G	A	15		
TGCAGTAACTCTGCATACAACACTACTGTTAAA**[A]**TGACCTGGAGCATCATCTGCATGATTTCTGTGCAT	69	A>C	A	34		
***D. reticulata* vs rest**						
TGCAGTGGGGATTCAGAACAGTCTTTCTGAGCCAGTGGGTGGGGTGGGGTGGGCA**[C]**ATTCTAGTGTGGT	69	C>T	C	56		
TGCAGTCA**[T]**CTGCCTTTTCAGTTTGTGTTCTGTTTAGACAGTGTAGGTTTAACATAGATCTCTATTGGC	69	T>G	T	9		
TGCAGCAATGGCTGTGAGGCATCCTTGCGGCTCAGGGGAAATAT**[T]**ATGTGACACTGGCATG	61	T>G	T	45		
TGCAGC**[A]**AGAAATGCTTCCAGCATG	25	G>A	A	7		

Sequence	Length	SNP alleles	Diag. allele	SNP pos	RefChrom	Chrom pos
TGCAGAAAAAATG**[C]**TCAGAAAATTGTCTCTCAGGAATTAAATTGGGATCGGTCAAATGCTAAGAATTAG	69	A>C	C	14		
TGCAGCTGGCA**[T]**GACAGCACTGCTTGACTGAAAGTAACCTGTGTGTATGCAAAAATATGTTTTGAAATA	69	C>T	T	12		
TGCAGTTTAGCTATTACTGAGAGCTACATG**[G]**GGCATG	37	T>G	G	31		
TGCAGTCTTAAAA**[T]**GGCTACATTTCACAATCGTCAGAGCAGCAGGTAGCAAAGTCGCCCACACATGATG	69	T>A	T	14		
TGCAGCCTAC**[G]**ATATTGGAATATGGCATG	29	A>G	G	11		
TGCAGGTTCTCAGGAGGAGCCAATGGAACTGAGGATGAAAATAT**[G]**ATTTTGTTTTATTCTAAAAGCCTT	69	G>T	G	45		
TGCAGCCTGGGGCATGGGATGGGTGGGGCC**[A]**CAGCATG	38	A>C	A	31		
TGCAGGTTAAGAGGATTTTCCAGGAAAAACTCAGATGAAGTACCACATGG**[T]**GCATG	56	T>C	T	51		
TGCAGTGGATTCAAGGAAGACACAAGGG**[C]**AATGTGTAGTAGAAATTTACAAGGTATATATGTATGGCAT	69	C>T	C	29		
TGCAGG**[A]**GACAGGGAGAAGTGCTGTGTGCCTTTGGCATG	39	A>G	A	7		
TGCAGGT**[G]**CCCATACCGCGATGAAAGCACTGATGGAAGAAAGACTTCCTCATTCTGACACGCATG	65	G>A	G	8		
TGCAGGGACAGCTCAGCTT**[T]**AGACACTTCAAAGAACTTAGAAGGGATACACAAAACACTCAATCTCTTT	69	T>C	T	20		
TGCAGTAATGCACTCTGTGTAGGTCTCC**[T]**CTTGAAATCTGTTCTGACTCCAGTTGGTACTGTCTGGTGG	69	T>C	T	29		
TGCAGAAGCTTAT**[T]**TCACTTGGTCATCTGAGACAATCCACTTGGGAAGTCTAATGGGGAGTAAATAGAA	69	T>C	T	14		
TGCAG**[T]**GCTTGTTTCAGAAAACTCATGTGAAGGAGTGTTTCATGCATGTAGGTTTCCAGGTTTCTACAT	69	T>A	T	6		
TGCAGATAATGCGAGTTCTGAATCTGCT**[A]**GCTGTGTCTCTGGCTTTCTTTTAGGTTTTCTGCCCCCACG	69	G>A	A	29		
TGCAGCCAACACTTGATCATGGGACACACTTAAAAAC**[T]**CCTTTTCCATCAGAATATAAACAGCATGAGC	69	T>C	T	38		
TGCAGAGCCCACCCCTCCCCTTGC**[T]**TCCTGCATG	34	C>T	T	25		
TGCAGCTAGACAATAACTTTGAGGTTTGTGCTTACCTCTCTTGCCCC**[G]**TCTTTATTGCAGGTTCTTCCC	69	G>A	G	48		
TGCAGTGTATGAGAACTGAGACTGTGGTGGAATTGGGTGTGGTTCTTCCCCCTCTGAA**[C]**ATTTGCAGTG	69	T>C	C	59		
TGCAGTAAGTGACAATCCTGATC**[A]**GAGCTCTTGAATAAAAGGTCAGTGCAGCCAAGGATGAGGCTGCAT	69	A>G	A	24		
TGCAGACAGACACAAGCTAATTTATTAC**[A]**GTTTTGCATTGCAATGTTTTATCTAAGAGACTGAGCACAG	69	T>A	A	29		
TGCAGCATGGATAAGGGCTCATTGAAGTTAACCTGGGGGCAAAAGCAGCAAGTTACAGCCAGAAGA**[T]**CT	69	C>T	T	67	NW_015171552.1_scaffold1660	412461
TGCAGTTAAAGCTGG**[C]**ACACAAGAATGTCCACAAAAAAGCATG	43	G>C	C	16		

Sequence	Length	SNP alleles	Diag. allele	SNP pos	RefChrom	Chrom pos
TGCAGCTCACCTCCTTCACTTGGGTGTGAAGGATACTCTTGGTCTGGGTT**[A]**CAAGGAGAAGCCCACATG	69	A>C	A	51		
TGCAGA**[G]**ACATGGTCATACAGTTTGGATCATTTCAATGCATG	42	A>G	G	7		
TGCAGCCTTTCTTGGGCAGAAAAGATC**[T]**GGTCAATGTGGTGCATG	45	T>A	T	28	NW_015165318.1_scaffold2512	191827
TGCAGGTT**[C]**AGCACATTCCCACCTGCATG	29	T>C	C	9		
TGCAGAAACTTGAAACCAAGCGTCATCTGAACAAAGC**[T]**TAAGAATTAAATTTGACAATGCAGAGCATGA	69	T>A	T	38		
TGCAGGTTTAAGGCCATCCTGACTTC**[T]**CCTCCCAGAGGGAAGCACTGATTATCCCAGGAAACAGATATC	69	T>C	T	27		
TGCAGCATTTTGGACTAATTGAAGATTATGAACACTTTTCAAGAGCAGCCTTTCATAGTGTTTTG**[A]**AGT	69	A>G	A	66		
TGCAGAGCAGAAAA**[T]**AGTAAACCAATTCTTGCATTTTTCTAGGACCAGTCATGAGAGCAGTGTGCGGGA	69	T>C	T	15	NW_015163115.1_scaffold956	268489
TGCAGTCCCAAAGACAACACATATT**[T]**AGCATG	32	C>T	T	26		
TGCAGATGCCATGGTCTGAACCTA**[C]**GACCTTCTGCATG	38	C>G	C	25		
TGCAGAGGACAGATACTGAGGAGAAA**[A]**GCCTGGTCTCTCCTGAGCATG	48	A>G	A	27		
***D. tincta* vs rest**						
TGCAGAGGCAGGGGAAGAAGATGGATGAGATGGTCAAAAGT**[G]**GATCAGGAAATGCATG	58	G>A	G	42		
TGCAGCTCTCCTGGCA**[C]**AGGTCTTTCCCATCCCTGCCACCATAGATTCTTTCTTCAATTGGCAAGGCAA	69	C>G	C	17		
TGCAGATTGGTTTTTAACTCTGGGAGATCTCCAGGTACCACCTGGAACTTGGCAAGCCTAG**[C]**TCATGGG	69	C>T	C	62		
TGCAGTTAACACCACCTTCTTGCCTGCCTTAATTCTCAGCTG**[A]**TATTTATTGGTGGTGGTGGAATCTGC	69	A>T	A	43		
TGCAGGACATAA**[A]**GCTTTGGTGTTATGCATG	31	T>A	A	13		
TGCAGAGGGGGTACCTACT**[A]**CCTAATGCATG	31	A>G	A	20		
TGCAGACCACATAAAAGAGTTTTTGGAAATCGGTTAG**[T]**TATTTAACACCTGTCATAAGTTTCACAGAAA	69	C>T	T	38		
TGCAGTGCTTTGCACAACACGTGCATTGACAGGAATGTAAGTTGAGCAAAATGGTTCTGTG**[G]**TCCAGCA	69	A>G	G	62		
TGCAGCTTTGA**[C]**GTACAGGCATGAGCGGTTCAGCAGGAATGCCGAGACCGATCTCGTATGCCGTCTTCT	69	T>C	C	12		
TGCAGGCTCTGCACTCCTGACCCTTCATTGCTACTGCTTTACTGGA**[T]**CTTAAACCATGTAATGCACTGT	69	T>G	T	47		
TGCAGCACTATTTTCCTGACCTGGGAAAGGGTGCCATTTGACCCACAGTAACTCAGCAGT**[T]**TTTATGCA	69	T>G	T	61		

APPENDIX 3 The sequences of diagnostic fixed differences between the sympatric *D. tincta* and *D. hades* sp. nov., with corresponding coordinates provided for the reference genome (*Gekko japonicus* v1.1) where alignments were possible.

Sequence	Length	SNP alleles	Diag. allele	SNP pos	Ref Chrom	Chrom pos
D. hades* sp. nov. vs *D. tincta						
TGCAGAGGCAGGGGAAGAAGATGGATGAGATGGTCAAAAGT**[A]**GATCAGGAAATGCATG	58	G>A	A	42		
TGCAGATTTTTCACATGATTATGT**[C]**TACTTTCTTGTGTGTATGTGGCATG	50	C>T	C	25		
TGCAGCAGGTGCTGCTGACTAGTGCACCTTTCCTTGAAGCCTCAC**[C]**TGGCTACAGAAGACAGAGGCGAT	69	T>C	C	46		
TGCAGCCCAGAA**[A]**TGTATCCCCCATCCAGTATGCATG	37	G>A	A	13	NW_015170301.1_scaffold882	395551
TGCAGCCTCAAGACACTGT**[T]**TGCTTGTGCATG	32	C>T	T	20		
TGCAGATTCATGCTGCACAGAAAGTGTGATAAAAAG**[C]**AAAATTGGAAAGATGGAAAGATTCAGGCATAC	69	T>C	C	37		
TGCAGTTAGAGTGACCAACTGTCCCAGTTTGCCC**[A]**GGAGAGTCCCAGATTGAAGGGTGGTTGTCCTGCA	69	G>A	A	35		
TGCAGCCCTACTGCTACTA**[A]**GAAATAGGTAGAGCATG	37	A>G	A	20		
TGCAGCAGCTCTAATTTTTCC**[G]**CAAGGGTATGGCCCCAGTATGATCAGAACACCAGCATG	60	G>A	G	22		
TGCAGTTTCTGGGGGCTTTTTGCATACATGGGGAACAAGAGTTGACCTCACTAATGAGGAATGCGCTT**[C]**	69	C>T	C	69	NW_015165830.1_scaffold15	131044
TGCAGATAACACAAAATTGGAGGGCCTGGCTAACACCCAGGTTGACAGAAGGAAA**[A]**TGCCTCAACAGGT	69	G>A	A	56		
TGCAGGAGTCCCACCC**[G]**CAAAATGCCTCTCAGATCCATGTGAAACGGGAAGAGCTTGTTGCAAACTGGG	69	G>T	G	17		
TGCAG**[T]**GGCATTTGGAGCATGAGCGGTTCAGCAGGAATGCCGAGACCGATCTCGTATGCCGTCTTCTGC	69	C>T	T	6		
TGCAGACTGTCATCTC**[T]**GACAGCATG	26	A>T	T	17		
TGCAGTGCAC**[A]**TGTTTCCTTATTCCCTCTGGACAGAAAATAGGAGCATAGAATCTCTGCTGGCCATGTG	69	A>G	A	11		
TGCAGATTCTGCTACTAAGACTAATGCACGTAGGAG**[G]**AGCATGGAAATAAAGCTAGAAATAAAAGCAGC	69	G>C	G	37		
TGCAGTGATGGATCACAGATGTACTGATTTGTTCTGGACATGCCCCTACTGCAACC**[A]**AGCATG	63	A>G	A	57		
TGCAGCTGTCAGAAACTTTATTTATCAGTT**[A]**CTAGCAAAACCACCATCATTATCCAGGGAGAGATGGCC	69	A>T	A	31	NW_015166440.1_scaffold634	539315
TGCAGCATTCCAATTTAGGCAGTCATCTG**[C]**CTGGCAAGTCCACCCTGCTCACAGGCATG	59	C>T	C	30		
TGCAGAAAGGAAAGG**[A]**AAAAATCCTGTAGAAAGGGAGAGAGGGAGATAGGTAAGTAAGTAATGTGGTTC	69	T>A	A	16		
TGCAGAACAC**[G]**GCCGGAAGACATGGGGACAACCTACGCAACATCAGGCAGGAGATTCAAGAGCTGACCA	69	G>A	G	11		
TGCAGGGTAGAGCATAGAGAGGGAGGTGATCCCTCAG**[A]**TATGAAGGACCAAGTCTATGAAAGGCTTTGT	69	G>A	A	38		
TGCAGGAAGTGGTGCATC**[T]**AAACTATTGGTGGTGGTCAGGGGTAAGGGGATTGGAACAAACACTAATTG	69	C>T	T	19		

Sequence	Length	SNP alleles	Diag. allele	SNP pos	Ref Chrom	Chrom pos
TGCAGCTCTCCTGGCA**[G]**AGGTCTTTCCCATCCCTGCCACCATAGATTCTTTCTTCAATTGGCAAGGCAA	69	C>G	G	17		
TGCAGTCTT**[A]**TATAGGGAGTTTCCCTACAGGGGCTACTGGGTTCCAAGCTAGGTTCTTCTTCTTAAGAT	69	G>A	A	10		
TGCAGGTGC**[T]**AGGGATTGAACCTGGGACCTCTGGCATG	38	T>C	T	10		
TGCAGTTCAGGCAC**[G]**GCCATCAAAACAAATATATTCTTTGGCATTCTTGAAAACTGTGGGAAAGCAGGG	69	A>G	G	15	NW_015172036.1_scaffold1095	224085
TGCAGGCTGAGCAGGAAACTGTTGGTCAT**[A]**TTTTCAGTGAAAGGGTAGACATTCCTGATGGTGTCAATT	69	G>A	A	30		
TGCAGGCACTTCTTCCTAGGCTAATATTCT**[T]**CTCTGAATAAGAATATAACTAAATTTAAAGGTGCATAA	69	C>T	T	31		
TGCAGCCATTTTACCTC**[C]**TCAAAAGGCATAGTTTTGTGCATG	42	A>C	C	18		
TGCAGACTAAT**[A]**ATACCCAGTGTGAGGCCACCCTCTGAGTAACCAAGTCCACTATATGGTTTTGCAGAA	69	A>G	A	12		
TGCAGAAATA**[A]**GGCAGGTGAAGTTTTCCTGGTTAAGAAACCTGCACCTGACACACAACAGCTCTTAAAC	69	A>G	A	11		
TGCAGGCAGAGAG**[A]**TAAAGGCAGAGATAGATCTCGGAGGAATCACTGTATCACTGCACCAGAACTCTCT	69	T>A	A	14		
TGCAGCAGGAGACAGAGAAAGTCAGGCTAAATGTTACAGCTTGGCAGCCCACA**[G]**TTTCCCTCCTGCTGA	69	G>A	G	54		
TGCAGA**[G]**TATGTGTCTGTTTATAGCATG	28	A>G	G	7		
TGCAGTCAGGAGGGTGTGCCAGGAGGGACATCATAGACAAATTGCTGATAAGTG**[C]**CCTTGACATTTGCA	69	C>T	C	55		
TGCAGACAGGGAAGGATCAGGATCAGCTCCTGAGCTGGG**[T]**GGAACGGGCATG	52	C>T	T	40		
TGCAGTGC**[G]**CCAGGACCAGGCAACATCTCTGGTCGCATG	39	A>G	G	9		
TGCAGTATAGTTTTGTTATAACAGACTATGATTGCTGGGTAAAGTGTTTCTTTTTAGA**[T]**AATTTTATAA	69	C>T	T	59		
TGCAGATTGGTTTTTAACTCTGGGAGATCTCCAGGTACCACCTGGAACTTGGCAAGCCTAG**[T]**TCATGGG	69	C>T	T	62		
TGCAGCT**[T]**TAACCACACATTAAGTGCACTAGGTTGACTCCATTGTGCATG	50	A>T	T	8		
TGCAG**[G]**CGCTGTAACCTTTGGCTCTCCAAATACAGACTGATGAACCATGCTCATGTGCTCATAAACTAT	69	A>G	G	6	NW_015175360.1_scaffold153	367239
TGCAGTGGGAGGAAA**[T]**GCATGAGCGGTTCAGCAGGAATGCCGAGACCGATCTCGTATGCCGTCTTCTGC	69	G>T	T	16		
TGCAGTTTGT**[C]**ATCTTATCTCTATACCTTGGCATG	35	C>T	C	11		
TGCAGACAGATAATGAAACTTTTGAAAAA**[C]**TAAGCATTCTGTAGGATACAGTGCTTCATAAAAATGTTT	69	C>A	C	30		
TGCAGAAACAAAAATAAATCACTTTTAAAT**[T]**ATTGCATG	39	G>T	T	31		
TGCAGCCTGC**[G]**GCAGGGCAGCTTTGTTTGGATTTCCCAGCATG	43	G>A	G	11		
TGCAGTGGAGTGAGTTATGTGCTGTTGTATGTGCCCACCTAATGAA**[C]**AGATTGTATTGTTCACTTTCAA	69	T>C	C	47		
TGCAGCTTGCTCATCCCTTGCTTCTGA**[G]**CTTCCACATGCATG	42	G>A	G	28		

Sequence	Length	SNP alleles	Diag. allele	SNP pos	Ref Chrom	Chrom pos
TGCAGACTTTTCTCTTTTCTCTACATTTCTCTGCACACT**[G]**TCTTCAGAGCAGAAGGCAGCAGCAGTCAG	69	G>A	G	40		
TGCAG**[G]**TACTGTCAGAAGCCAGATGGTGCATG	32	G>C	G	6		
TGCAGATTCTGGACTTCTGCTCCAGTCTTGCCATGTTCTGTGCCTCTGTGGCTAC**[A]**GTGGTCAAACTCA	69	G>A	A	56		
TGCAGGTATCTCTGTAGATGGCACCAAGGA**[G]**AGCATG	37	A>G	G	31		
TGCAGTTTCCC**[A]**GGTTGTCATCCTTCCCTTTTTTGAAGATTGGGATAACATTCTTCCTCCGTCAGTATT	69	A>G	A	12		
TGCAGCAGAACTATAACAATATTTTAAAGCATTGCTTTTGAAGTTATCTTATTCTAAAT**[A]**AAAAAGCAT	69	C>A	A	60		
TGCAGTTAACACCACCTTCTTGCCTGCCTTAATTCTCAGCTG**[T]**TATTTATTGGTGGTGGTGGAATCTGC	69	A>T	T	43		
TGCAGGG**[T]**ATGTATTTTGTCTCTTCAGTACTTCTGATTCGGATGAGCATG	50	T>G	T	8	NW_015161459.1_scaffold1869	41294
TGCAGGACATAA**[T]**GCTTTGGTGTTATGCATG	31	T>A	T	13		
TGCAGCTAGTTTGTTG**[A]**AGAAGCATG	26	A>G	A	17		
TGCAGTGGCCATGGTGGGTGCATCCTTGTCCAGTTGCAG**[G]**AGCAGCTATGGCTCCACAGGGGCTAAGGA	69	G>C	G	40		
TGCAGCTT**[A]**ATGTTAAAACCCATGTGTTGCATG	33	A>T	A	9		
TGCAGTGAGGTATGATACATGTATATGGAAGTGCAGAGGAG**[A]**AGCACTGTCTTGTAGGCAGCAGCAACA	69	G>A	A	42		
TGCAGGCAACACCATTTGGCAGCCA**[T]**TAATATATTCCTTCTGACTTCTTTTTCTGCATG	59	C>T	T	26	NW_015170280.1_scaffold203	1324869
TGCAGAGGGGGTACCTACT**[G]**CCTAATGCATG	31	A>G	G	20		
TGCAGTCATGGCACAACAAACCCTATGGCTGAGGACCTG**[A]**CAGGCCAACTTCCATTTGAGGGCCATCCT	69	G>A	A	40		
TGCAGTTGACC**[C]**GGCAGATGAAATAGTAGATGTGTATATGATTCTAGGCATG	52	C>T	C	12		
TGCAGACCACATAAAAGAGTTTTTGGAAATCGGTTAG**[C]**TATTTAACACCTGTCATAAGTTTCACAGAAA	69	C>T	C	38		
TGCAGAGATAACTCAAAGCAAGTTTGCATTTTAACTGTCTTTTTATGCAACTGT**[G]**ACCATTTGATTTTA	69	T>G	G	55		
TGCAGTGCTTTGCACAACACGTGCATTGACAGGAATGTAAGTTGAGCAAAATGGTTCTGTG**[A]**TCCAGCA	69	A>G	A	62		
TGCAGCTATTTTGCAAG**[C]**ACAGGGAAATGCATG	33	T>C	C	18		
TGCAGCC**[A]**CAATTAAACAGGTTGCTTACCTGTAACTGTTGTTCTCAAGTGGTCATTTGTGCACTTACAT	69	A>C	A	8	NW_015173673.1_scaffold34	1086238
TGCAGTGCATGAATTCAGT**[C]**TTGTATTGCATG	32	C>G	C	20		
TGCAGAATCTTCCTTGGTGGCCTCCCATGCAAGGACTGA**[T]**CCTGCTTAGCTTCTGAGATCTGACAAGAT	69	T>C	T	40	NW_015177026.1_scaffold612	249092
TGCAGCCAGACAG**[T]**CCTCTCCAATCGTTTTCTTGAGCTGCAATCATCTGATCACAACCAAATAGCTTGA	69	C>T	T	14	NW_015166447.1_scaffold825	529383
TGCAGG**[A]**CTGAGAAAGATCTTGGCTTAAGGTTTAAGAGAACTGCTTTCAAGTAGAATAAAGGCATGAGC	69	A>G	A	7		

Sequence	Length	SNP alleles	Diag. allele	SNP pos	Ref Chrom	Chrom pos
TGCAGCCTAATGAAGGACTTTTCTCATCTGTTACAG**[C]**TTTATCAAGAAAGCCAGGAACATGCAAGTGCA	69	T>C	C	37	NW_015165873.1_scaffold1783	18546
TGCAGCAGAGTTGCCCACATA**[T]**GCTGCAACCAGCACTCAGCATG	44	T>C	T	22		
TGCAGATCCA**[G]**TTTGTGAAGAAAAGATGCATG	32	A>G	G	11	NW_015169778.1_scaffold39	1181212
TGCAGGCACGGGAAAC**[T]**TTGGTTTAGGCCCAAGGCATG	38	T>C	T	17		
TGCAGAACTAGAAG**[C]**TGGGGGCATG	25	C>T	C	15		
TGCAGAAGCCTATGACACTTGTACAGGAGCTAGAAAATTCTCAAAGCTCACAG**[T]**TGCTTGAGCATATTA	69	T>C	T	54		
TGCAGTGTCTGCACAGCGTGCTAATCAAAATATGCACCAATTCCCAAATACAACATTTTTAAA**[C]**CCATT	69	C>T	C	64		
TGCAGGTGTCATAGCTGAAATTGCCCTGCTTCAGAATGTACTC**[A]**TTTTGCTTCTGCACATGCCCAGAGC	69	G>A	A	44	NW_015175365.1_scaffold337	121076
TGCAGGGGCATTCTGTATGTAGTTGCA**[C]**AGATCAGTGTAGAACTTGCTCTTTTCTTCAGGATTTGCTTG	69	C>T	C	28		
TGCAGCTTTGA**[T]**GTACAGGCATGAGCGGTTCAGCAGGAATGCCGAGACCGATCTCGTATGCCGTCTTCT	69	T>C	T	12		
TGCAGGGAGTTGGACTAGATGATCCTTGTGGTCCCTTCCAGCTCTAATATTCTATGATTC**[G]**TTGATGCT	69	G>T	G	61	NW_015170918.1_scaffold929	169621
TGCAGTAGCTCATTTAATTTTGTTTCCAGATGCCCCATCAGTCA**[T]**GGCACAAAGACTGAAGCCTTTCAA	69	G>T	T	45		
TGCAGAATTCCTGTTCTGCTAAGAGCAACTCCA**[C]**GGTAGCATG	43	T>C	C	34		
TGCAGAACTGCTTGTCAAAAATAGAAAGGGGGTAGGTTCATGTAAGCTCTTCTCACCTCTAG**[C]**TCCCAT	69	C>A	C	63		
TGCAGACA**[T]**AAGTGGTGAGAATCAAGGCAAACCACAAAATGTGAATAAATCATAAATTTTATAGGCATT	69	G>T	T	9		
TGCAGGCTCTGCACTCCTGACCCTTCATTGCTACTGCTTTACTGGA**[G]**CTTAAACCATGTAATGCACTGT	69	T>G	G	47		
TGCAGCAGGTTGGAGTATCAGCAAAAATCACATTCTC**[C]**TTGCATG	45	C>T	C	38		
TGCAGGAAAATTTACT**[C]**TTTTCTCACTATGGATTTGGGTGCATG	44	C>G	C	17		
TGCAGAATGGAAGTGATGTTACCCTAGTGGCTTGGGGCAC**[T]**CAGGTTAGTATGACTGTTGTGAGATACC	69	A>T	T	41		
TGCAGTGTGTAATCAGCAAAGGAAGAAGGAAAAGTCTTTAGGTAGCTCCCTG**[G]**ACAACAAAATGGAAAG	69	G>T	G	53		
TGCAGGTGACCCATGTTCTGAGGAC**[G]**AAAGATGCATG	37	A>G	G	26		
TGCAGCAGGGTATGTTAGAGCACATAGCTCCTGCTAGCACACATGG**[T]**AGCTTCCTCAACAATGTGTTTC	69	G>T	T	47		
TGCAGTTGTGTTCTAAGTCAGATTTGGCAC**[C]**ATAATAAAGTCTCAAAGCCAACAGCAGGGTCAAAAGTC	69	T>C	C	31		
TGCAGA**[C]**CTGGAGGAGGTGGTGAGCAGCATG	31	C>G	C	7		
TGCAGT**[G]**CCGACTTTGATCTTCATGCAATCTGACAGAAGCATG	43	A>G	G	7		
TGCAGTTTCTCTTTGTCTAGTGCTCTGTTCTGCATCCTCCTGTGGAGAC**[C]**TGGTGATTTTCTGTGAACT	69	C>T	C	50		

Sequence	Length	SNP alleles	Diag. allele	SNP pos	Ref Chrom	Chrom pos
TGCAGCACTATTTTCCTGACCTGGGAAAGGGTGCCATTTGACCCACAGTAACTCAGCAGT**[G]**TTTATGCA	69	T>G	G	61		
TGCAGAACAGGTCAGAAGAAAAACAGGAAGAGAGGGTAGAAAGTAATGCAATGTAGTAGGTT**[A]**ACAGAG	69	G>A	A	63		
TGCAGT**[T]**CCTGACCATTTGTTCTGCATG	28	C>T	T	7		
TGCAGTTTAAGAAATAAATAAGA**[G]**TGGTGATTGATGAATGTGGATGTGAACAGCATCTGTTTTATTTCT	69	T>G	G	24		
TGCAGTG**[T]**GCTTGCTCATTCCTTCTGACAACATAAGATGCTTGTATGCACCTTACAGTCAGCAACCCAC	69	C>T	T	8		
TGCAGACAAGTCAGATGCTATGATGAGGTAACA**[C]**TGTGGTATGGAGTGCTATGAAACATCCAAAAATAT	69	G>C	C	34	NW_015170309.1_scaffold1106	373447
TGCAGTTTCATAAAACTTCCAGCTGTCGACCAAAGGATTTGTAGCTGAATTAATCACCTGCCATTTAG**[T]**	69	T>C	T	69		
TGCAGTATTGTGTACCGTTCTGGAGACCTTGCTTCAAAAAG**[A]**ATGTGGGCAAATCAGTACCATTGTTAG	69	G>A	A	42		
TGCAGAGCTAGGAACCTCAGGACAAA**[A]**AACAGCCAAGGCATG	42	A>G	A	27		
TGCAGGAACTAAA**[T]**CCACGTGCATG	25	T>A	T	14		
TGCAGCATA**[A]**CCCTGTGCATGAGCGGTTCAGCAGGAATGCCGAGACCGATCTCGTATGCCGTCTTCTGC	69	G>A	A	10		
TGCAGACCTGCCAAACACAGTGATAACAGAATTGTCACACAGAAACTTCCAAG**[A]**GTCAGATCTAGGTAC	69	A>G	A	54		
TGCAGATAGGCAGGTGTTCTGTGTAGGTATGGCTATATAAAGCTTTCA**[A]**AGCAGCAGTTCTAAAAAGAG	69	G>A	A	49		
TGCAGGGG**[C]**AGAACATCTTCTTGGCATG	28	C>T	C	9		
***D. tincta* sp. nov. vs *D. hades* sp. nov.**						
TGCAGAGGCAGGGGAAGAAGATGGATGAGATGGTCAAAAGT**[G]**GATCAGGAAATGCATG	58	G>A	G	42		
TGCAGATTTTTCACATGATTATGT**[T]**TACTTTCTTGTGTGTATGTGGCATG	50	C>T	T	25		
TGCAGCAGGTGCTGCTGACTAGTGCACCTTTCCTTGAAGCCTCAC**[T]**TGGCTACAGAAGACAGAGGCGAT	69	T>C	T	46		
TGCAGCCCAGAA**[G]**TGTATCCCCCATCCAGTATGCATG	37	G>A	G	13	NW_015170301.1_scaffold882	395551
TGCAGCCTCAAGACACTGT**[C]**TGCTTGTGCATG	32	C>T	C	20		
TGCAGATTCATGCTGCACAGAAAGTGTGATAAAAAG**[T]**AAAATTGGAAAGATGGAAAGATTCAGGCATAC	69	T>C	T	37		
TGCAGTTAGAGTGACCAACTGTCCCAGTTTGCCC**[G]**GGAGAGTCCCAGATTGAAGGGTGGTTGTCCTGCA	69	G>A	G	35		
TGCAGCCCTACTGCTACTA**[G]**GAAATAGGTAGAGCATG	37	A>G	G	20		
TGCAGCAGCTCTAATTTTTCC**[A]**CAAGGGTATGGCCCCAGTATGATCAGAACACCAGCATG	60	G>A	A	22		
TGCAGTTTCTGGGGGCTTTTTGCATACATGGGGAACAAGAGTTGACCTCACTAATGAGGAATGCGCTT**[T]**	69	C>T	T	69	NW_015165830.1_scaffold15	131044
TGCAGATAACACAAAATTGGAGGGCCTGGCTAACACCCAGGTTGACAGAAGGAAA**[G]**TGCCTCAACAGGT	69	G>A	G	56		

Sequence	Length	SNP alleles	Diag. allele	SNP pos	Ref Chrom	Chrom pos
TGCAGGAGTCCCACCC**[T]**CAAAATGCCTCTCAGATCCATGTGAAACGGGAAGAGCTTGTTGCAAACTGGG	69	G>T	T	17		
TGCAG**[C]**GGCATTTGGAGCATGAGCGGTTCAGCAGGAATGCCGAGACCGATCTCGTATGCCGTCTTCTGC	69	C>T	C	6		
TGCAGACTGTCATCTC**[A]**GACAGCATG	26	A>T	A	17		
TGCAGTGCAC**[G]**TGTTTCCTTATTCCCTCTGGACAGAAAATAGGAGCATAGAATCTCTGCTGGCCATGTG	69	A>G	G	11		
TGCAGATTCTGCTACTAAGACTAATGCACGTAGGAG**[C]**AGCATGGAAATAAAGCTAGAAATAAAAGCAGC	69	G>C	C	37		
TGCAGTGATGGATCACAGATGTACTGATTTGTTCTGGACATGCCCCTACTGCAACC**[G]**AGCATG	63	A>G	G	57		
TGCAGCTGTCAGAAACTTTATTTATCAGTT**[T]**CTAGCAAAACCACCATCATTATCCAGGGAGAGATGGCC	69	A>T	T	31	NW_015166440.1_scaffold634	539315
TGCAGCATTCCAATTTAGGCAGTCATCTG**[T]**CTGGCAAGTCCACCCTGCTCACAGGCATG	59	C>T	T	30		
TGCAGAAAGGAAAGG**[T]**AAAAATCCTGTAGAAAGGGAGAGAGGGAGATAGGTAAGTAAGTAATGTGGTTC	69	T>A	T	16		
TGCAGAACAC**[A]**GCCGGAAGACATGGGGACAACCTACGCAACATCAGGCAGGAGATTCAAGAGCTGACCA	69	G>A	A	11		
TGCAGGGTAGAGCATAGAGAGGGAGGTGATCCCTCAG**[G]**TATGAAGGACCAAGTCTATGAAAGGCTTTGT	69	G>A	G	38		
TGCAGGAAGTGGTGCATC**[C]**AAACTATTGGTGGTGGTCAGGGGTAAGGGGATTGGAACAAACACTAATTG	69	C>T	C	19		
TGCAGCTCTCCTGGCA**[C]**AGGTCTTTCCCATCCCTGCCACCATAGATTCTTTCTTCAATTGGCAAGGCAA	69	C>G	C	17		
TGCAGTCTT**[G]**TATAGGGAGTTTCCCTACAGGGGCTACTGGGTTCCAAGCTAGGTTCTTCTTCTTAAGAT	69	G>A	G	10		
TGCAGGTGC**[C]**AGGGATTGAACCTGGGACCTCTGGCATG	38	T>C	C	10		
TGCAGTTCAGGCAC**[A]**GCCATCAAAACAAATATATTCTTTGGCATTCTTGAAAACTGTGGGAAAGCAGGG	69	A>G	A	15	NW_015172036.1_scaffold1095	224085
TGCAGGCTGAGCAGGAAACTGTTGGTCAT**[G]**TTTTCAGTGAAAGGGTAGACATTCCTGATGGTGTCAATT	69	G>A	G	30		
TGCAGGCACTTCTTCCTAGGCTAATATTCT**[C]**CTCTGAATAAGAATATAACTAAATTTAAAGGTGCATAA	69	C>T	C	31		
TGCAGCCATTTTACCTC**[A]**TCAAAAGGCATAGTTTTGTGCATG	42	A>C	A	18		
TGCAGACTAAT**[G]**ATACCCAGTGTGAGGCCACCCTCTGAGTAACCAAGTCCACTATATGGTTTTGCAGAA	69	A>G	G	12		
TGCAGAAATA**[G]**GGCAGGTGAAGTTTTCCTGGTTAAGAAACCTGCACCTGACACACAACAGCTCTTAAAC	69	A>G	G	11		
TGCAGGCAGAGAG**[T]**TAAAGGCAGAGATAGATCTCGGAGGAATCACTGTATCACTGCACCAGAACTCTCT	69	T>A	T	14		
TGCAGCAGGAGACAGAGAAAGTCAGGCTAAATGTTACAGCTTGGCAGCCCACA**[A]**TTTCCCTCCTGCTGA	69	G>A	A	54		
TGCAGA**[A]**TATGTGTCTGTTTATAGCATG	28	A>G	A	7		
TGCAGTCAGGAGGGTGTGCCAGGAGGGACATCATAGACAAATTGCTGATAAGTG**[T]**CCTTGACATTTGCA	69	C>T	T	55		
TGCAGACAGGGAAGGATCAGGATCAGCTCCTGAGCTGGG**[C]**GGAACGGGCATG	52	C>T	C	40		

Sequence	Length	SNP alleles	Diag. allele	SNP pos	Ref Chrom	Chrom pos
TGCAGTGC**[A]**CCAGGACCAGGCAACATCTCTGGTCGCATG	39	A>G	A	9		
TGCAGTATAGTTTTGTTATAACAGACTATGATTGCTGGGTAAAGTGTTTCTTTTTAGA**[C]**AATTTTATAA	69	C>T	C	59		
TGCAGATTGGTTTTTAACTCTGGGAGATCTCCAGGTACCACCTGGAACTTGGCAAGCCTAG**[C]**TCATGGG	69	C>T	C	62		
TGCAGCT**[A]**TAACCACACATTAAGTGCACTAGGTTGACTCCATTGTGCATG	50	A>T	A	8		
TGCAG**[A]**CGCTGTAACCTTTGGCTCTCCAAATACAGACTGATGAACCATGCTCATGTGCTCATAAACTAT	69	A>G	A	6	NW_015175360.1_scaffold153	367239
TGCAGTGGGAGGAAA**[G]**GCATGAGCGGTTCAGCAGGAATGCCGAGACCGATCTCGTATGCCGTCTTCTGC	69	G>T	G	16		
TGCAGTTTGT**[T]**ATCTTATCTCTATACCTTGGCATG	35	C>T	T	11		
TGCAGACAGATAATGAAACTTTTGAAAAA**[A]**TAAGCATTCTGTAGGATACAGTGCTTCATAAAAATGTTT	69	C>A	A	30		
TGCAGAAACAAAAATAAATCACTTTTAAAT**[G]**ATTGCATG	39	G>T	G	31		
TGCAGCCTGC**[A]**GCAGGGCAGCTTTGTTTGGATTTCCCAGCATG	43	G>A	A	11		
TGCAGTGGAGTGAGTTATGTGCTGTTGTATGTGCCCACCTAATGAA**[T]**AGATTGTATTGTTCACTTTCAA	69	T>C	T	47		
TGCAGCTTGCTCATCCCTTGCTTCTGA**[A]**CTTCCACATGCATG	42	G>A	A	28		
TGCAGACTTTTCTCTTTTCTCTACATTTCTCTGCACACT**[A]**TCTTCAGAGCAGAAGGCAGCAGCAGTCAG	69	G>A	A	40		
TGCAG**[C]**TACTGTCAGAAGCCAGATGGTGCATG	32	G>C	C	6		
TGCAGATTCTGGACTTCTGCTCCAGTCTTGCCATGTTCTGTGCCTCTGTGGCTAC**[G]**GTGGTCAAACTCA	69	G>A	G	56		
TGCAGGTATCTCTGTAGATGGCACCAAGGA**[A]**AGCATG	37	A>G	A	31		
TGCAGTTTCCC**[G]**GGTTGTCATCCTTCCCTTTTTTGAAGATTGGGATAACATTCTTCCTCCGTCAGTATT	69	A>G	G	12		
TGCAGCAGAACTATAACAATATTTTAAAGCATTGCTTTTGAAGTTATCTTATTCTAAAT**[C]**AAAAAGCAT	69	C>A	C	60		
TGCAGTTAACACCACCTTCTTGCCTGCCTTAATTCTCAGCTG**[A]**TATTTATTGGTGGTGGTGGAATCTGC	69	A>T	A	43		
TGCAGGG**[G]**ATGTATTTTGTCTCTTCAGTACTTCTGATTCGGATGAGCATG	50	T>G	G	8	NW_015161459.1_scaffold1869	41294
TGCAGGACATAA**[A]**GCTTTGGTGTTATGCATG	31	T>A	A	13		
TGCAGCTAGTTTGTTG**[G]**AGAAGCATG	26	A>G	G	17		
TGCAGTGGCCATGGTGGGTGCATCCTTGTCCAGTTGCAG**[C]**AGCAGCTATGGCTCCACAGGGGCTAAGGA	69	G>C	C	40		
TGCAGCTT**[T]**ATGTTAAAACCCATGTGTTGCATG	33	A>T	T	9		
TGCAGTGAGGTATGATACATGTATATGGAAGTGCAGAGGAG**[G]**AGCACTGTCTTGTAGGCAGCAGCAACA	69	G>A	G	42		
TGCAGGCAACACCATTTGGCAGCCA**[C]**TAATATATTCCTTCTGACTTCTTTTTCTGCATG	59	C>T	C	26	NW_015170280.1_scaffold203	1324869

Sequence	Length	SNP alleles	Diag. allele	SNP pos	Ref Chrom	Chrom pos
TGCAGAGGGGGTACCTACT**[A]**CCTAATGCATG	31	A>G	A	20		
TGCAGTCATGGCACAACAAACCCTATGGCTGAGGACCTG**[G]**CAGGCCAACTTCCATTTGAGGGCCATCCT	69	G>A	G	40		
TGCAGTTGACC**[T]**GGCAGATGAAATAGTAGATGTGTATATGATTCTAGGCATG	52	C>T	T	12		
TGCAGACCACATAAAAGAGTTTTTGGAAATCGGTTAG**[T]**TATTTAACACCTGTCATAAGTTTCACAGAAA	69	C>T	T	38		
TGCAGAGATAACTCAAAGCAAGTTTGCATTTTAACTGTCTTTTTATGCAACTGT**[T]**ACCATTTGATTTTA	69	T>G	T	55		
TGCAGTGCTTTGCACAACACGTGCATTGACAGGAATGTAAGTTGAGCAAAATGGTTCTGTG**[G]**TCCAGCA	69	A>G	G	62		
TGCAGCTATTTTGCAAG**[T]**ACAGGGAAATGCATG	33	T>C	T	18		
TGCAGCC**[C]**CAATTAAACAGGTTGCTTACCTGTAACTGTTGTTCTCAAGTGGTCATTTGTGCACTTACAT	69	A>C	C	8	NW_015173673.1_scaffold34	1086238
TGCAGTGCATGAATTCAGT**[G]**TTGTATTGCATG	32	C>G	G	20		
TGCAGAATCTTCCTTGGTGGCCTCCCATGCAAGGACTGA**[C]**CCTGCTTAGCTTCTGAGATCTGACAAGAT	69	T>C	C	40	NW_015177026.1_scaffold612	249092
TGCAGCCAGACAG**[C]**CCTCTCCAATCGTTTTCTTGAGCTGCAATCATCTGATCACAACCAAATAGCTTGA	69	C>T	C	14	NW_015166447.1_scaffold825	529383
TGCAGG**[G]**CTGAGAAAGATCTTGGCTTAAGGTTTAAGAGAACTGCTTTCAAGTAGAATAAAGGCATGAGC	69	A>G	G	7		
TGCAGCCTAATGAAGGACTTTTCTCATCTGTTACAG**[T]**TTTATCAAGAAAGCCAGGAACATGCAAGTGCA	69	T>C	T	37	NW_015165873.1_scaffold1783	18546
TGCAGCAGAGTTGCCCACATA**[C]**GCTGCAACCAGCACTCAGCATG	44	T>C	C	22		
TGCAGATCCA**[A]**TTTGTGAAGAAAAGATGCATG	32	A>G	A	11	NW_015169778.1_scaffold39	1181212
TGCAGGCACGGGAAAC**[C]**TTGGTTTAGGCCCAAGGCATG	38	T>C	C	17		
TGCAGAACTAGAAG**[T]**TGGGGGCATG	25	C>T	T	15		
TGCAGAAGCCTATGACACTTGTACAGGAGCTAGAAAATTCTCAAAGCTCACAG**[C]**TGCTTGAGCATATTA	69	T>C	C	54		
TGCAGTGTCTGCACAGCGTGCTAATCAAAATATGCACCAATTCCCAAATACAACATTTTTAAA**[T]**CCATT	69	C>T	T	64		
TGCAGGTGTCATAGCTGAAATTGCCCTGCTTCAGAATGTACTC**[G]**TTTTGCTTCTGCACATGCCCAGAGC	69	G>A	G	44	NW_015175365.1_scaffold337	121076
TGCAGGGGCATTCTGTATGTAGTTGCA**[T]**AGATCAGTGTAGAACTTGCTCTTTTCTTCAGGATTTGCTTG	69	C>T	T	28		
TGCAGCTTTGA**[C]**GTACAGGCATGAGCGGTTCAGCAGGAATGCCGAGACCGATCTCGTATGCCGTCTTCT	69	T>C	C	12		
TGCAGGGAGTTGGACTAGATGATCCTTGTGGTCCCTTCCAGCTCTAATATTCTATGATTC**[T]**TTGATGCT	69	G>T	T	61	NW_015170918.1_scaffold929	169621
TGCAGTAGCTCATTTAATTTTGTTTCCAGATGCCCCATCAGTCA**[G]**GGCACAAAGACTGAAGCCTTTCAA	69	G>T	G	45		
TGCAGAATTCCTGTTCTGCTAAGAGCAACTCCA**[T]**GGTAGCATG	43	T>C	T	34		
TGCAGAACTGCTTGTCAAAAATAGAAAGGGGGTAGGTTCATGTAAGCTCTTCTCACCTCTAG**[A]**TCCCAT	69	C>A	A	63		

Sequence	Length	SNP alleles	Diag. allele	SNP pos	Ref Chrom	Chrom pos
TGCAGACA**[G]**AAGTGGTGAGAATCAAGGCAAACCACAAAATGTGAATAAATCATAAATTTTATAGGCATT	69	G>T	G	9		
TGCAGGCTCTGCACTCCTGACCCTTCATTGCTACTGCTTTACTGGA**[T]**CTTAAACCATGTAATGCACTGT	69	T>G	T	47		
TGCAGCAGGTTGGAGTATCAGCAAAAATCACATTCTC**[T]**TTGCATG	45	C>T	T	38		
TGCAGGAAAATTTACT**[G]**TTTTCTCACTATGGATTTGGGTGCATG	44	C>G	G	17		
TGCAGAATGGAAGTGATGTTACCCTAGTGGCTTGGGGCAC**[A]**CAGGTTAGTATGACTGTTGTGAGATACC	69	A>T	A	41		
TGCAGTGTGTAATCAGCAAAGGAAGAAGGAAAAGTCTTTAGGTAGCTCCCTG**[T]**ACAACAAAATGGAAAG	69	G>T	T	53		
TGCAGGTGACCCATGTTCTGAGGAC**[A]**AAAGATGCATG	37	A>G	A	26		
TGCAGCAGGGTATGTTAGAGCACATAGCTCCTGCTAGCACACATGG**[G]**AGCTTCCTCAACAATGTGTTTC	69	G>T	G	47		
TGCAGTTGTGTTCTAAGTCAGATTTGGCAC**[T]**ATAATAAAGTCTCAAAGCCAACAGCAGGGTCAAAAGTC	69	T>C	T	31		
TGCAGA**[G]**CTGGAGGAGGTGGTGAGCAGCATG	31	C>G	G	7		
TGCAGT**[A]**CCGACTTTGATCTTCATGCAATCTGACAGAAGCATG	43	A>G	A	7		
TGCAGTTTCTCTTTGTCTAGTGCTCTGTTCTGCATCCTCCTGTGGAGAC**[T]**TGGTGATTTTCTGTGAACT	69	C>T	T	50		
TGCAGCACTATTTTCCTGACCTGGGAAAGGGTGCCATTTGACCCACAGTAACTCAGCAGT**[T]**TTTATGCA	69	T>G	T	61		
TGCAGAACAGGTCAGAAGAAAAACAGGAAGAGAGGGTAGAAAGTAATGCAATGTAGTAGGTT**[G]**ACAGAG	69	G>A	G	63		
TGCAGT**[C]**CCTGACCATTTGTTCTGCATG	28	C>T	C	7		
TGCAGTTTAAGAAATAAATAAGA**[T]**TGGTGATTGATGAATGTGGATGTGAACAGCATCTGTTTTATTTCT	69	T>G	T	24		
TGCAGTG**[C]**GCTTGCTCATTCCTTCTGACAACATAAGATGCTTGTATGCACCTTACAGTCAGCAACCCAC	69	C>T	C	8		
TGCAGACAAGTCAGATGCTATGATGAGGTAACA**[G]**TGTGGTATGGAGTGCTATGAAACATCCAAAAATAT	69	G>C	G	34	NW_015170309.1_scaffold1106	373447
TGCAGTTTCATAAAACTTCCAGCTGTCGACCAAAGGATTTGTAGCTGAATTAATCACCTGCCATTTAG**[C]**	69	T>C	C	69		
TGCAGTATTGTGTACCGTTCTGGAGACCTTGCTTCAAAAAG**[G]**ATGTGGGCAAATCAGTACCATTGTTAG	69	G>A	G	42		
TGCAGAGCTAGGAACCTCAGGACAAA**[G]**AACAGCCAAGGCATG	42	A>G	G	27		
TGCAGGAACTAAA**[A]**CCACGTGCATG	25	T>A	A	14		
TGCAGCATA**[G]**CCCTGTGCATGAGCGGTTCAGCAGGAATGCCGAGACCGATCTCGTATGCCGTCTTCTGC	69	G>A	G	10		
TGCAGACCTGCCAAACACAGTGATAACAGAATTGTCACACAGAAACTTCCAAG**[G]**GTCAGATCTAGGTAC	69	A>G	G	54		
TGCAGATAGGCAGGTGTTCTGTGTAGGTATGGCTATATAAAGCTTTCA**[G]**AGCAGCAGTTCTAAAAAGAG	69	G>A	G	49		
TGCAGGGG**[T]**AGAACATCTTCTTGGCATG	28	C>T	T	9		

APPENDIX 4 Morphological measurements taken for all specimens in this study. See text for abbreviations of characters used.

Museum	Specimen	Species	Population	SVL	HeadD	HeadL	HeadW	SnoutL	EyeW	VS	MBS	TL	HLS (R)	Supralabial scales (R)	Infralabial scales (R)	Supralabial scales (L)	Infralabial scales (L)	sex
SAMA	42945	not genotyped		70	3.58	7.66	4.51	3.16	1.18	67	14	108	3	6	5	6	5	
SAMA	67717	not genotyped		80	3.89	8.40	5.18	3.47	1.29	68	14	126	3	6	5	6	5	
QM	J80509	not genotyped		48	1.90	3.86	3.45	2.05	0.92	74	14	84	-	5	4	5	5	juv
SAMA	10377	not genotyped		81	5.07	8.86	6.08	3.65	1.37	66	14	-	3	6	5	6	5	
SAMA	14498	not genotyped		75	3.94	8.01	4.94	3.77	1.20	64	14	174	3	6	5	6	5	
SAMA	15189	not genotyped		70	4.75	8.37	5.08	3.52	1.08	-	-	249	3	6	5	6	5	
SAMA	18254	not genotyped		75	3.54	8.09	5.05	3.46	1.21	66	14	134	3	6	5	6	5	m
SAMA	32453	not genotyped		79	4.26	8.22	5.29	3.32	1.21	67	14	129	3	6	5	6	5	
SAMA	34447	not genotyped		71	3.48	7.90	4.87	3.04	0.91	65	14	183	3	6	5	6	5	
SAMA	42946	not genotyped		75	3.90	8.02	4.63	3.07	1.20	67	14	231	3	6	4	6	5	
SAMA	44804	not genotyped		64	2.71	7.06	3.91	2.70	1.11	69	14	-	3	6	5	6	5	
SAMA	45033	not genotyped		51	3.08	6.32	3.09	2.58	0.99	66	14	-	2	5	5	6	5	juv
SAMA	57467	not genotyped		43	2.40	5.88	3.45	2.26	1.04	67	14	77	2	6	5	6	5	juv
SAMA	60966	not genotyped		86	4.20	8.16	5.23	3.62	1.40	72	14	155	4	6	5	6	6	
SAMA	72368	not genotyped		79	4.11	8.03	4.80	3.11	1.06	69	14	109	4	6	5	6	5	
SAMA	72376	not genotyped		74	4.00	7.77	4.17	2.95	1.10	69	14	234	4	6	5	6	5	
SAMA	72372	not genotyped		90	4.13	8.22	5.24	3.44	1.16	68	14	126	4	6	5	6	5	
QM	J241	not genotyped		63	3.38	6.75	4.06	2.84	0.97	66	14	-	3	6	5	6	5	
SAMA	7875	not genotyped		66	4.75	7.98	5.15	3.36	1.07	68	14	-	3	6	5	6	5	
SAMA	18571	not genotyped		77	4.70	8.40	5.28	3.32	1.18	70	14	175	3	6	5	6	5	
WAM	93701	not genotyped		44	2.36	5.43	3.11	2.28	0.84	71	14	-	3	6	4	6	5	
WAM	114391	not genotyped		69	3.06	7.66	4.37	2.96	1.13	69	14	96	3	6	5	6	5	

Museum	Specimen	Species	Population	SVL	HeadD	HeadL	HeadW	SnoutL	EyeW	VS	MBS	TL	HLS (R)	Supralabial scales (R)	Infralabial scales (R)	Supralabial scales (L)	Infralabial scales (L)	sex
WAM	114392	not genotyped		67	3.44	7.89	4.31	3.17	1.14	65	14	238	3	6	5	6	5	m
WAM	116439	not genotyped		76	2.71	7.39	4.04	2.94	0.92	72	14	105	3	6	5	6	5	
WAM	146890	not genotyped		80	3.41	8.94	4.86	3.40	1.05	73	15	284	3	6	5	6	5	
WAM	146957	not genotyped		82	2.50	8.34	4.51	3.42	1.21	72	14	93	3	6	5			
WAM	168506	not genotyped		54	2.69	6.40	3.29	2.32	1.06	65	14	178	3	6	5	6	5	
WAM	168507	not genotyped		70	3.28	7.54	4.23	2.96	1.15	70	14	126	3	7	5	6	5	
WAM	168520	not genotyped		70	3.09	7.90	4.33	3.14	1.17	69	15	160	3	6	5	6	5	
WAM	168521	not genotyped		46	2.16	6.11	2.82	2.41	0.89	66	14	-	3	6	5	6	5	
WAM	176401	not genotyped		77	3.80	8.26	5.09	3.41	1.16	71	14	282	3	6	5	6	5	
WAM	180214	not genotyped		84	4.02	8.58	4.89	3.57	1.24	74	14	305	3	6	4	6	4	
SAMA	4978	not genotyped		75	4.30	8.34	5.38	3.39	1.13	70	14	241	-	-	-	-	-	
QM	21786	not genotyped		75	3.84	7.69	4.38	2.93	1.25	69	14	217	3	6	5	6	5	
QM	51530	not genotyped		53	3.26	6.98	4.19	2.60	0.97	71	14	-	-	6	5	6	5	
QM	54476	not genotyped		70	2.69	6.92	3.86	2.76	0.88	72	14	200	-	6	5	6	5	
QM	59911	not genotyped		81	3.59	8.70	4.57	3.39	1.17	69	14	-	3	6	5	6	5	
QM	70487	not genotyped		75	3.44	7.06	4.40	2.72	0.99	67	14	235	3	6	5	6	5	
QM	81877	not genotyped		81	4.49	8.36	5.32	3.41	1.24	69	14	-	-	6	5	6	5	
QM	82226	not genotyped		74	2.91	7.10	4.25	2.66	1.13	73	14	-	3	6	5	6	5	
QM	83469	not genotyped		87	4.02	8.47	5.29	3.36	1.38	74	15	218	3	6	5	6	5	
QM	84099	not genotyped		67	4.08	7.25	4.44	2.93	1.21	66	14	-	4	6	5	6	5	
QM	86155	not genotyped		65	2.85	6.46	2.91	2.76	0.88	72	14	-	3	6	5	6	5	
QM	97651	not genotyped		78	3.81	8.06	5.56	3.09	1.36	70	16	195	3	6	5	6	6	
QM	97653	not genotyped		74	3.76	7.97	4.92	3.26	1.39	64	14	-	3	6	5	6	5	
WAM	117215	not genotyped		74	3.29	7.99	4.74	3.11	1.18	69	14	-	3	6	4	6	4	

Museum	Specimen	Species	Population	SVL	HeadD	HeadL	HeadW	SnoutL	EyeW	VS	MBS	TL	HLS (R)	Supralabial scales (R)	Infralabial scales (R)	Supralabial scales (L)	Infralabial scales (L)	sex
WAM	157704	not genotyped		70	3.25	7.28	4.34	2.9	1.19	70	14	197	3	6	5	6	5	m
QM	46687	not genotyped		74	3.11	7.23	3.56	2.84	1.17	74	14	118	3	6	5	6	5	
QM	56465	not genotyped		77	3.34	8.00	5.36	3.23	1.03	63	14	98	-	6	5	6	5	
QM	57250	not genotyped		56	3.41	6.35	3.85	2.54	0.94	63	14	155	3	6	5	6	5	
QM	69324	not genotyped		60	3.04	6.72	4.10	2.37	0.93	63	14	-	3	6	5	6	5	
QM	75298	not genotyped		74	3.59	7.87	5.62	3.14	1.17	67	14	132	3	6	5	6	5	
QM	76459	not genotyped		67	4.07	6.81	4.03	2.98	1.05	61	14	104	3	6	5	6	5	
QM	77978	not genotyped		64	3.55	6.65	4.85	2.51	1.17	66	14	186	3	5	6	6	5	
QM	78002	not genotyped		78	3.81	7.69	4.69	3.17	1.25	68	14	-	3	6	5	6	5	
QM	81285	not genotyped		57	3.31	6.72	4.11	2.80	1.21	62	15	187	3	6	5	7	5	
QM	83188	not genotyped		63	3.41	6.87	4.03	2.71	1.13	64	14	176	3	6	5	6	5	
QM	88170	not genotyped		78	3.41	8.10	5.22	3.09	1.17	66	14	-	-	-	-	6	5	
QM	97844	not genotyped		75	3.47	7.63	4.42	3.13	1.22	68	14	-	3	6	5	6	5	
SAMA	35960	*D. tincta*	P1	65	3.44	7.80	4.86	3.19	1.16	66	14	-	3	6	5	6	4	
SAMA	38847	*D. tincta*	P1	87	3.57	8.55	6.02	3.22	1.3	74	14	237	3	6	5	6	5	
SAMA	46806	*D. tincta*	P1	80	4.24	8.23	5.77	3.39	1.23	68	14	248	4	6	5	6	5	
SAMA	49874	*D. tincta*	P1	83	4.36	8.79	5.89	3.44	1.35	70	14	158	4	6	5	6	5	
SAMA	60513	*D. tincta*	P1	41	2.10	5.57	2.81	1.97	0.94	64	14	101	3	6	4	6	4	juv
SAMA	60546	*D. tincta*	P1	56	2.97	6.90	4.05	2.73	1.04	64	14	84	2	6	5	6	5	
WAM	137953	*D. tincta*	P1	80	3.73	8.35	4.25	3.32	1.12	73	-	-	-	6	5	6	5	m
SAMA	30971	*D. tincta*	P2	75	3.40	7.60	4.67	2.87	1.07	67	14	182	3	6	5	6	5	
SAMA	31173	*D. tincta*	P2	64	2.81	7.22	4.65	2.97	1.12	63	14	135	3	6	5	6	5	
SAMA	49065	*D. tincta*	P2	74	3.57	8.33	4.94	3.10	1.25	65	14	151	4	6	5	6	5	
SAMA	61947	*D. tincta*	P2	96	3.76	8.71	5.28	3.54	1.3	71	14	143	4	6	5	6	5	

Museum	Specimen	Species	Population	SVL	HeadD	HeadL	HeadW	SnoutL	EyeW	VS	MBS	TL	HLS (R)	Supralabial scales (R)	Infralabial scales (R)	Supralabial scales (L)	Infralabial scales (L)	sex
SAMA	61856	*D. tincta*	P2	85	3.56	8.60	5.29	3.28	1.05	71	14	125	4	5	4	6	5	
SAMA	45034	*D. tincta*	P7	69	3.19	7.10	3.53	2.61	1.11	70	14	151	3	6	4	6	5	
SAMA	54019	*D. tincta*	P7	93	3.81	8.25	4.55	3.15	1.18	78	14	280	3	6	5	6	5	
SAMA	55294	*D. tincta*	P7	89	3.01	7.57	4.19	2.91	1.01	77	14	237	3	6	5	6	5	
QM	90118	*D. tincta*	P7	59	2.63	6.35	3.44	2.45	1.12	70	14	156	3	6	5	6	5	
QM	J83423	*D. tincta*	P7	71	3.34	7.11	3.97	3.08	0.95	70	14	-	3	6	5	6	5	
QM	J91823	*D. tincta*	P7	71	3.17	7.11	4.61	2.67	1.08	68	14	146	3	6	5	6	5	
SAMA	40238	*D. hades*	P8	76	4.55	8.67	4.92	3.64	1.19	67	14	-	2	6	5	6	5	
SAMA	51553	*D. hades*	P8	90	4.44	9.03	5.44	3.58	1.24	66	14	-	3	6	5	6	5	
SAMA	54015	*D. hades*	P8	79	4.10	8.70	5.53	3.40	1.18	69	14	292	3	6	5	6	4	
SAMA	54465	*D. hades*	P8	76	4.12	8.29	4.79	3.41	1.06	63	14	263	3	6	5	6	5	
SAMA	54735	*D. hades*	P8	85	3.79	8.89	5.09	3.50	1.15	71	14	145	3	6	5	6	5	
QM	90655	*D. hades*	P8	95	4.26	9.20	5.26	3.61	1.30	72	14	-	3	6	5	6	5	
WAM	177993	*D. hades*	P8	56	2.62	6.59	3.74	2.67	1.05	68	14	190	3	6	5	6	5	
WAM	99180	*D. branchia*	P5	67	3.49	7.32	4.25	2.89	1.14	13	-	107	3	6	5	6	5	
WAM	102838	*D. branchia*	P5	61	3.21	6.74	4.07	2.60	1.10	66	14	205	3	6	5	6	5	
WAM	110080	*D. branchia*	P5	78	3.80	7.76	4.72	3.04	1.25	73	14	174	3	6	5	6	5	
WAM	110292	*D. branchia*	P5	75	3.41	7.60	4.13	3.08	1.13	61	13		3	6	5	6	5	
WAM	112690	*D. branchia*	P5	55	2.96	6.34	3.81	2.49	1.13	69	14	182	3	6	5	6	5	
WAM	113012	*D. branchia*	P5	72	3.84	8.04	5.15	3.25	1.21	67	14	211	3	6	5	6	6	
WAM	113030	*D. branchia*	P5	78	3.13	7.92	4.90	3.14	1.07	69	14	123	3	6	5	6	5	m
WAM	114490	*D. branchia*	P5	71	2.92	7.87	4.55	2.98	1.18	68	13	183	3	6	4	6	4	m
WAM	115018	*D. branchia*	P5	68	3.11	7.27	4.53	2.90	1.23	70	14	155	3	6	5	6	5	m
WAM	116545	*D. branchia*	P5	85	3.41	8.33	4.63	3.35	1.19	70	14	221	3	6	5	6	5	

Museum	Specimen	Species	Population	SVL	HeadD	HeadL	HeadW	SnoutL	EyeW	VS	MBS	TL	HLS (R)	Supralabial scales (R)	Infralabial scales (R)	Supralabial scales (L)	Infralabial scales (L)	sex
WAM	117342	*D. branchia*	P5	61	2.56	6.63	3.69	2.60	1.00	68	14	155	3	6	4	6	5	
WAM	120020	*D. branchia*	P5	75	3.16	7.45	4.19	3.24	1.19	67	14	188	3	6	4	6	5	
WAM	125032	*D. branchia*	P5	65	3.02	7.31	4.09	2.70	1.10	70	13	130	3	6	4	6	5	
WAM	127768	*D. branchia*	P5	58	2.96	6.45	3.51	2.67	1.04	71	14	153	3	6	5	6	5	
WAM	129623	*D. branchia*	P5	70	3.44	7.78	4.00	2.94	1.12	72	14	219	3	5	4	6	5	
WAM	135422	*D. branchia*	P5	70	3.21	7.43	4.34	2.89	1.27	68	13	166	3	6	5	6	5	
WAM	138078	*D. branchia*	P5	93	4.34	8.84	5.62	3.52	1.28	73	14	274	3	6	4	6	5	
WAM	139308	*D. branchia*	P5	44	2.19	5.89	3.05	2.45	1.06	65	14	122	3	6	5	6	5	
WAM	139314	*D. branchia*	P5	75	3.73	8.13	4.97	3.31	1.29	69	14	191	3	6	5	6	5	
WAM	139328	*D. branchia*	P5	71	3.37	7.77	4.55	3.05	1.36	64	14	126	3	6	5	6	5	
WAM	139637	*D. branchia*	P5	57	3.62	6.96	3.97	2.97	1.04	62	14	210	3	6	5	6	5	
WAM	141273	*D. branchia*	P5	66	3.21	7.32	4.04	2.73	1.00	75	15	236	3	6	5	6	5	
WAM	151059	*D. branchia*	P5	72	2.95	8.06	4.80	3.10	1.22	68	14	212	3	6	4	6	5	
WAM	151060	*D. branchia*	P5	72	3.56	8.44	4.60	3.47	1.22	68	14	107	3	6	5	6	5	m
WAM	153821	*D. branchia*	P5	64	2.87	6.94	3.78	2.85	0.96	72	13	220	3	6	5	6	5	m
WAM	154268	*D. branchia*	P5	67	2.94	7.63	4.30	2.84	1.19	68	14	92	3	6	5	6	5	
WAM	156173	*D. branchia*	P5	75	2.99	7.90	4.78	3.26	1.25	68	14	260	3	6	5	6	4	
WAM	156227	*D. branchia*	P5	65	3.72	7.08	4.49	3.05	1.20	69	14	172	3	6	5	6	5	m
WAM	156258	*D. branchia*	P5	71	3.10	7.19	4.15	2.82	1.16	70	14	136	3	6	5	6	5	
WAM	157065	*D. branchia*	P5	58	2.99	6.44	3.30	2.13	1.07	66	14	176	3	6	5	6	5	
WAM	157124	*D. branchia*	P5	64	3.29	6.59	3.45	2.58	1.02	72	14	180	3	6	4	6	5	
WAM	158123	*D. branchia*	P5	63	3.04	6.90	4.02	2.65	1.05	68	14	-	3	6	4	6	4	
WAM	158202	*D. branchia*	P5	79	3.42	7.75	4.32	2.87	1.24	75	14	-	3	7	5	6	5	
WAM	160201	*D. branchia*	P5	62	2.95	6.95	3.94	2.55	1.12	68	14	166	3	6	4	6	5	

Museum	Specimen	Species	Population	SVL	HeadD	HeadL	HeadW	SnoutL	EyeW	VS	MBS	TL	HLS (R)	Supralabial scales (R)	Infralabial scales (R)	Supralabial scales (L)	Infralabial scales (L)	sex
WAM	161660	*D. branchia*	P5	63	3.11	7.23	4.36	2.84	1.11	66	14	176	3	6	5	6	5	
WAM	162036	*D. branchia*	P5	70	3.16	7.93	4.35	3.03	1.10	68	14	130	3	6	5	6	5	
WAM	162054	*D. branchia*	P5	74	3.30	7.29	4.63	2.94	1.08	69	13	230	3	6	5	6	5	
WAM	163935	*D. branchia*	P5	70	2.95	7.38	4.23	2.82	1.15	71	14	232	3	6	5	6	5	
WAM	166546	*D. branchia*	P5	75	4.06	8.22	5.10	3.22	1.18	67	14	257	3	6	5	6	5	
WAM	166641	*D. branchia*	P5	75	3.78	8.02	4.51	3.21	1.19	69	14	185	3	6	5	6	5	
WAM	170131	*D. branchia*	P5	76	3.28	8.40	4.46	3.29	1.21	66	14	146	3	6	5	6	5	
WAM	170660	*D. branchia*	P5	77	3.47	7.80	4.27	3.07	1.22	71	14	134	3	6	5	6	5	
WAM	174663	*D. branchia*	P5	51	2.53	6.48	3.13	2.37	1.07	67	14	151	3	6	5	6	4	
SAMA	29365	*D. branchia*	P5	67	2.79	7.578	4.48	3.20	0.95	70	14	-	3	6	5	6	5	
SAMA	71375	*D. reticulata*	P6	51	2.66	5.95	4.17	2.20	0.84	63	14	76	3	6	5	6	5	
QM	90689	*D. reticulata*	P6	45	2.57	6.11	3.30	2.99	1.00	65	14	-	-	6	5	6	5	
QM	95572	*D. reticulata*	P6	49	2.26	5.76	3.62	2.31	-	66	14	-	-	-	-	-	-	
QM	J70674	*D. reticulata*	P6	84	4.08	7.89	4.81	3.19	1.21	67	14	199	3	5	4	5	4	
QM	J70675	*D. reticulata*	P6	70	3.81	7.16	4.21	2.75	1.04	63	15	125	3	6	5	6	5	
QM	J80136	*D. reticulata*	P6	51	2.50	6.02	3.42	2.30	0.98	63	15	123	3	6	5	6	5	
QM	J84130	*D. reticulata*	P6	54	3.02	6.15	3.21	2.26	-	66	14	-	3	6	5	6	5	
QM	J88438	*D. reticulata*	P6	52	2.44	6.55	3.81	2.44	1.16	73	14	146	3	6	5	6	5	
QM	J95799	*D. reticulata*	P6	80	3.58	8.13	5.34	3.14	1.36	63	14	246	3	6	4	6	5	
QM	84129	*D. reticulata*	P4	56	2.64	6.01	3.29	2.30	1.23	65	14	-	-	-	-	-	-	
QM	J94238	*D. reticulata*	P4	55	2.69	6.43	3.79	2.63	0.97	69	14	168	3	6	5	6	5	
QM	93849	*D. reticulata*	P3	33	2.34	4.99	2.62	1.99	0.97	62	14	-	-	5	5	5	4	juv
QM	J58918	*D. reticulata*	P3	66	3.37	7.26	4.05	2.80	1.34	61	14	213	3	6	5	6	5	
QM	J87293	*D. reticulata*	P3	48	2.83	6.89	3.38	2.68	1.15	62	14	-	-	5	4	5	4	

RECORDS OF THE WESTERN AUSTRALIAN MUSEUM 40 047–078 (2025) DOI: 10.18195/issn.0312-3162.40.2025.047-078

The mammalian fauna of Madura Cave, Western Australia. Part IX, the placental mammals

Ernest L. Lundelius Jr[1], William D. Turnbull[2]† and Steven R. May[1*]

[1] Jackson School Museum of Earth History, The University of Texas at Austin, Austin, Texas 78758, United States of America.

[2] Department of Geology, Field Museum of Natural History, Chicago, Illinois 60605, United States of America.

† Deceased

* Corresponding author: srmay@utexas.edu

ABSTRACT – Placental mammals, recovered in 1955 and 1964 from Madura Cave, N-62, on the Roe Plain in Western Australia, are described here. This material is late Pleistocene and early Holocene in age, based on C14 dates from bone and is part of a much larger fauna previously reported elsewhere. Rodents are the most abundant and diverse group of placental mammals within the Madura Cave fauna, represented by seven taxa including *Leporillus conditor*, *L. apicalis*, *Pseudomys bolami*, *P. gouldii*, *P. australis*, *Pseudomys* sp. cf. *desertor*, and *Notomys* sp. indet. Only two of these taxa are known from the Nullarbor region today and *Leporillus apicalis* is extinct. Bats are also present in the Madura Cave fauna with at least two taxa represented, including *Chalinolobus* sp. cf. *morio*. All specimens are dissociated and fragmentary, probably being derived from disintegrated owl pellets that were originally deposited near the mouth of the cave and then redeposited in the cave sediments during storms. The dingo *Canis familiaris* and rabbit *Oryctolagus cuniculus* are represented by single specimens found on the cave floor. The most significant change in composition of the entire mammalian fauna is recorded between the early Holocene and present day. Although increasing aridity from the late Pleistocene to early Holocene might have been a contributing factor, the dramatic decrease in mammal diversity in the Madura Cave fauna is most probably a result of European settlement and introduced predators.

KEYWORDS: Pleistocene, Holocene, rodents, bats, cave, Western Australia

INTRODUCTION

This report deals with specimens of placental mammals recovered from stratified deposits in Madura Cave, N-62, in Western Australia (Figure 1). Initial work in 1955, resulted in a brief description of the cave and demonstrated its potential for providing a detailed record of late Pleistocene through early Holocene faunal remains (Lundelius 1963). At that time, two stratigraphic units were recognised based on two excavated trenches (1 and 2). The extinct kangaroo, *Sthenurus,* was found in the oldest stratigraphic units in both trenches. Seven additional publications in this series, described the marsupial fossils collected in 1955 and 1964 (Lundelius and Turnbull 1973, 1975, 1978, 1981, 1982, 1984, and 1989). These papers documented 38 taxa representing 10 families of marsupials. The rodent *Leporillus* was reported separately (Lundelius and Turnbull 1999). An additional two genera of rodents, two taxa of bats, a single canid and a single lagomorph are reported here bringing the final mammalian faunal list from Madura Cave to 49 taxa.

Madura Cave is located on the Roe Plain (Figure 1), part of the Nullarbor physiographic region south of the Hampton Tableland. The boundary between the Hampton Tableland of the Nullarbor and the Roe Plain is a series of paleo-sea cliffs known as the Hampton Range (James et al. 2006). The Nullarbor region is an arid to semiarid scrubland with calcareous loamy soils. It averages approximately 200–250 mm of annual rainfall increasing southward toward the coast (Waddell et al. 2010).

Madura Cave formed by dissolution of Neogene limestone. The Northern Tunnel contains at least 2.75 metres of complexly stratified deposits primarily associated with roof collapse and ephemeral run-off into the cave from the main entrance (Lundelius and Turnbull 1973) (Figure 2). In addition to the main entrance, there is at least one sink-hole that connects the cave to the surface near Trench 4, but there is no debris cone underneath it. Lundelius excavated Trench 1 and 2 in 1955 and reported the results in Lundelius (1963). Trenches 3–5 were excavated in 1964. Neither murids nor bats were recovered from Trench 5, but *Leporillus conditor* was found in the upper units of that trench and discussed in Lundeliius and Turnbull (1999). The highest concentrations of murid and bat remains were in Trenches 3, 1, and 4 which are closest to the main entrance (Figure 3).

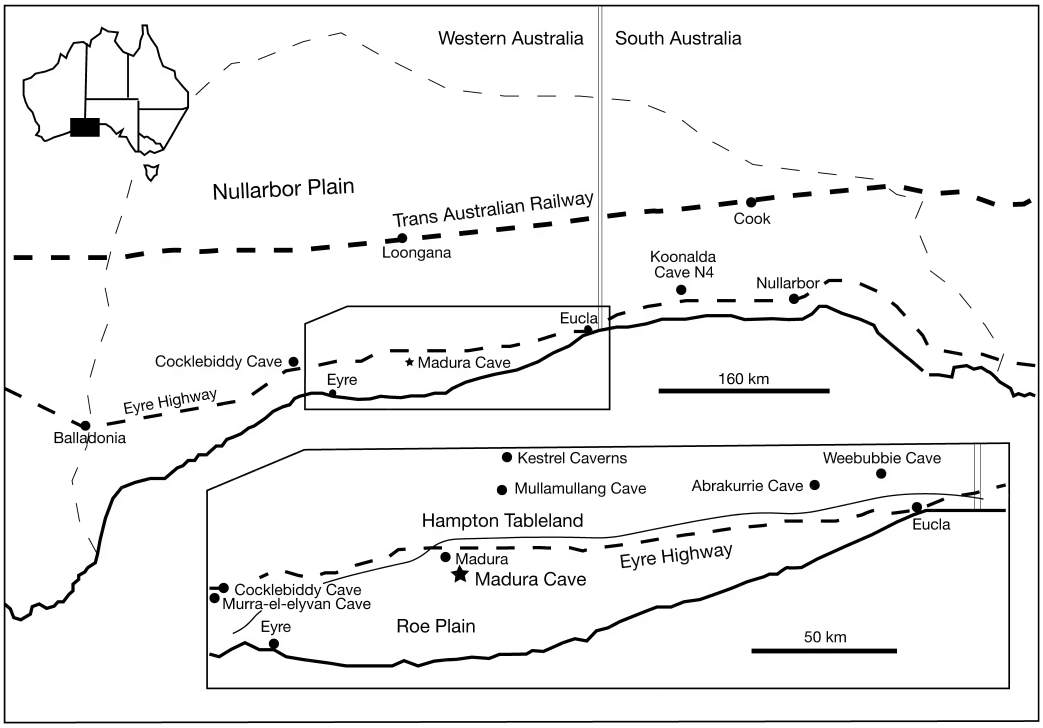

FIGURE 1 Map of the Eucla Basin in Western Australia and South Australia, with detail of the area showing location of the Madura Cave (star) and other caves nearby on the Hampton Tableland (adapted from Lundellius and Turnbull 1973).

This paper represents the final chapter by Lundelius and Turnbull on the fossil mammals from Madura Cave, Western Australia. Much of the field work, and most of the Madura Cave papers, represent the collaborative efforts of Lundelius and Turnbull with assistance, as documented in their previously published acknowledgements as well as this paper. William Turnbull died in 2011 before the work could be completed. Seven papers, published by Lundelius and Turnbull between 1973 and 1989, appeared in Fieldiana, while an eighth paper on the murid *Leporillus* was published in 1999 in the Proceedings of the Linnean Society of New South Wales. The other murids and the bats remained unpublished until now.

Access to specimens, notebooks of descriptions and measurements, and early versions of the manuscript allowed May to collaborate with Lundelius to finish this paper. Many hours were shared in discussion during 2024–25 about questions concerning taxonomy, stratigraphy, and philosophy. At age 97, Prof. Lundelius remained heartily engaged and provided the inspiration to complete this paper. Initial identifications and descriptions of *Pseudomys*, *Chalinolobus*, *Canis* and *Oryctolagus* had been completed by Lundelius and Turnbull, supported by a number of SEM images and

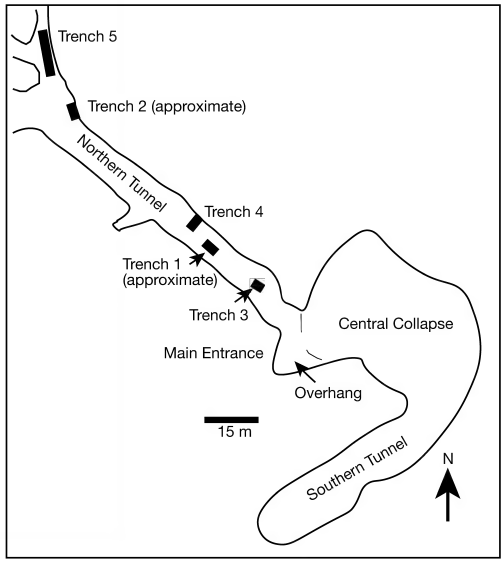

FIGURE 2 Map of Madura Cave with trench locations. Simplified from Lundellius and Turnbull (1973).

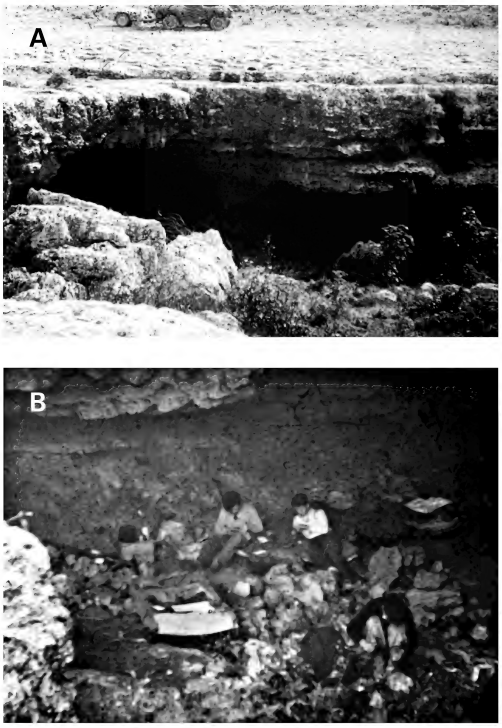

FIGURE 3 A) Main entrance to Madura Cave, 1955. Vehicle and trailer in background for scale; B) Working inside Madura Cave, 1955.

conventional photography. May continued the work on *Notomys* that had been largely absent from draft versions of the manuscript. He revisited the identifications and descriptions of *Pseudomys*, added images from micro-CT, reviewed the bats, and summarised the complete Madura Cave faunal list.

MATERIAL AND METHODS

Material was excavated from Trenches 3–5 in approximately 15 cm intervals within each stratigraphic unit. All matrix was dry sieved in the field and all concentrate, larger than 0.5 mm, was kept. The better specimens were picked in the field and treated with shellac to minimize breakage and loss of teeth. The term 'Madura Cave fauna' is used here to designate the assemblage of all fossil vertebrates recovered from sedimentary units of the cave, including those found on the cave floor at the time of excavation.

For this paper, Trench 1 through Trench 5 are referred to as proper names of localities within Madura Cave. Similarly, units within the stratigraphy are referred to as Units 1–7, as used in previous papers in this series.

Measurements, abbreviations, statistical and dental terminology are either those in standard use or are defined where used. Specimen numbers beginning with 'PM' indicate Field Museum of Natural History, Chicago specimens. Specimen numbers beginning 'TMM 41106-' indicate specimens in the Texas Vertebrate Paleontology Collections at the University of Texas at Austin (TxVP). Dental measurements, for specimens of *Pseudomys* were made using a microscope reticle and/or with calipers. Measurements for *Notomys* were made with a Dino-Lite digital scope and DinoXscope software. Measurements on the bats were based on Scanning Electron Microscope photos and direct caliper measurements.

Abbreviations include: C/c – canine, I/i – incisor, P/p – premolar, M/m – molar (upper and lower as per upper and lower case), L – left, R – right, l – length, w – width, TRL – tooth row length upper, trl – tooth row length lower, CT – computed tomography, SEM – scanning electron microscope, and C14 – Carbon 14.

All CT imaging was performed at The University of Texas at Austin High-Resolution X-ray CT Facility using the following parameters: Zeiss, Flat panel, 80kV, 10W, 0.06s acquisition time, 5 samples per view, detector 210.4 mm, source -28.8 mm, camera bin 1, angles ±180, 4501 views, LE3 filter, dithering, sample drift correction. Single reference. Reconstructed with centre shift -0.949, beam hardening 0.45, theta 0, byte scaling [-0.01, 0.28], binning 1, recon filter smooth (kernel size = 0.7). Total slices = 1,302. Scans are archived at www.morphosource.org. The CT data were visualised and analysed using 3D Slicer version 5.8.1.

REVIEW OF THE STRATIGRAPHY AND RADIOCARBON GEOCHRONOLOGY

The first comprehensive account of the stratigraphy of Madura Cave was presented in Lundelius and Turnbull (1973). The stratigraphic units, lithologies, and C14 dates for each of the trenches are summarised in Figure 4. A more detailed description of these data can be found in Lundelius and Turnbull (1973). None of the trenches sampled the full thickness of the cave stratigraphy. Seven C14 dates were obtained on fossil bone scrap (primarily long bones of small mammals with dense cortical bone) from a number of stratigraphic units in Trenches 3 and 4 (Lundelius and Turnbull 1973). The age range of the cave sediments, based on the C14 geochronology, extends from approximately 38,000 BP to 7,500 BP. The distribution of radiometric ages is stratigraphically consistent within each trench. The accuracy of these dates is uncertain, given the relative antiquity of the analytical work, although they have not been superseded by more recent geochronology. C14 dates were reported from the Southern Tunnel of Madura Cave in an unpublished dissertation by Marun (1972). The dates were from charcoal and included values of 7,880 ± 390 BP from 330 cm and 4,260 ± 130 BP from 195 cm. It is unclear how the stratigraphy sampled by Marun (1972) in the Southern Tunnel correlates with that

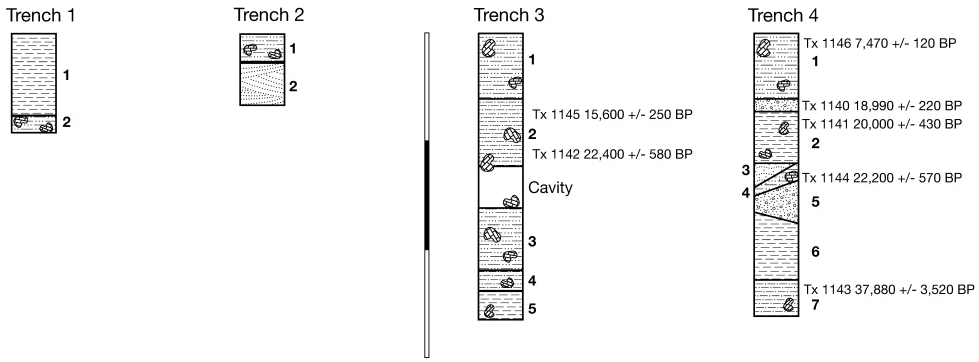

FIGURE 4 Summary of stratigraphic and geochronologic data from Trenches 1–4 in Madura Cave Northern Tunnel. Trench locations shown in Figure 2. Unit numbers are shown adjacent to each column (scale: 1 m).

Trench 1: 1 brown silt, 2 red sandy–silt; Trench 2: 1 red sandy–silt, 2 white cross–bedded sand and dark silt; Trench 3: 1 grey–brown silt, 2 red clay and silt, 3 brownish-red silt, 4 white sandy–silt, 5 red clay. Trench 4: 1 grey–brown silt, 2 red clay with gravel at top, 3 yellow–orange silty sand, 4 dark red clayey–silt, 5 red–grey sand and gravel, 6 white–orange silt and clay, 7 red–orange silty–clay. Trench 5: 1 brownish–grey sandy–silt, 2 orange–red sand and gravel, 3 reddish–brown silt, 4 brown silt and whitish clay, 5 reddish–brown silt, 6 reddish–orange clayey silt. Descriptions of Trenches 1–2 are from Lundelius (1963). Trenches 3–4 are summarised from previous descriptions and figures in Lundelius and Turnbull (1973). The stratigraphic position of radiometric dates designated Tx 1140–1146 are taken from Lundelius and Turnbull (1973).

of Lundelius and Turnbull (1973) in the Northern Tunnel. More recent accelerator mass spectrometry (AMS) dates, obtained directly from dingo bones originally collected by Marun (1972) within the top metre of Madura Cave Southern Tunnel sediments, yielded an age estimate of approximately 3,250 BP (Balme et al. 2018). The majority of rodent and bat fossils reported here are from stratigraphic units associated with C14 ages of approximately 22,000 to 7,500 BP, although a few specimens are from sediments with dates as old as 38,000 BP (Trench 4, Unit 7).

SYSTEMATIC PALAEONTOLOGY

Taxonomic names are based on The Australian Mammal Taxonomy Consortium Australian Mammal Species List AMTC (2024).

Class Mammalia Linnaeus, 1758

Order Rodentia Bowdich, 1821

Family Muridae Illiger, 1811

Subfamily Murinae Illiger, 1811

Rodents are the most common of the placental mammals in the Madura Cave sediments. Cheek tooth terminology is modified from Musser et al. (2005) with upper molar cusps labeled T1–T9 and lower molar morphology designated with standard terms inferring homology (Figure 5).

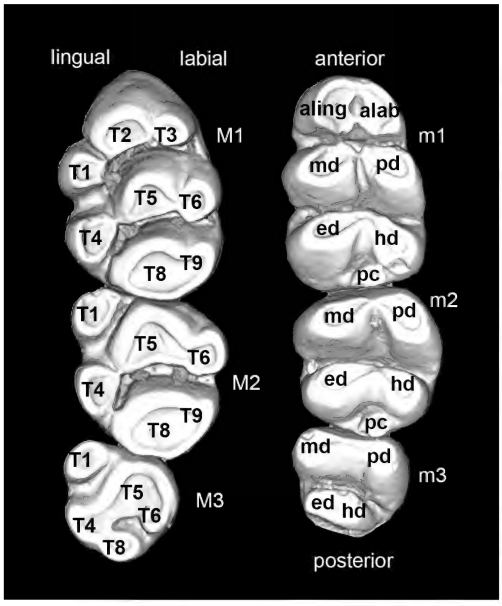

FIGURE 5 Occlusal views of upper (left) and lower (right) cheek teeth of *Notomys* [sp. indet. from Madura Cave] illustrating terminology used for dental descriptions modified from Musser et al. (2005). Abbreviations for lower cheek teeth m1–3: alab, anterolabial cuspid; aling, anterolingual cuspid; ed, entoconid; hd, hypoconid; md, metaconid; pc, posterior cuspid; pd, protoconid.

Genus *Pseudomys* Gray, 1832

The *Pseudomys* group belongs to the tribe Hydromyini within the subfamily Murinae and includes 22 extant species (AMTC 2024). Phylogenetic relationships have been well documented through molecular analysis, but the living species are poorly characterised with respect to those skeletal features that are preserved in the Madura Cave fossils. Species assigned to *Pseudomys* differ from *Leporillus* in their smaller size and more brachyodont cheek teeth. Most *Pseudomys* taxa differ from *Notomys* in lacking the anteriorly projecting zygomatic spine and the broadening of the dorsal part of the zygomatic arch. The zygomatic spine in those species of *Pseudomys* that possess it, is smaller and less prominent than in *Notomys*.

Based primarily on size and morphology of the upper cheek-teeth, four species of *Pseudomys* can be identified in the Madura Cave fauna. These identifications are supported by earlier analysis by A. Baynes (pers. comm.) and by dental descriptions provided by J. Cramb (pers. comm.). One of the species is a very small form of *Pseudomys,* while three fall in the medium size range for the genus. *Pseudomys bolami* is very small with an anterolingual accessory cusp on M1. The cusps of the labial row (T3, T6, T9) are distinct but smaller than the lingual cusps. T2 and T3 are close together and form a loph transverse to the long axis of the tooth, while T1 is on the lingual edge of the tooth and is located well posterior of T2. Three additional species are middle size forms with M1 (l x w) dimensions of 2.3–2.9 mm x 1.5–1.9 mm. The three mid-size species have been identified on the basis of M1 morphology. *Pseudomys australis* lacks an anterolingual accessory cusp on M1 as well as an anterior cingulum. T1 and T2 are approximately aligned, T3 is absent, T6 is small, and T9 is smaller. *Pseudomys gouldii* has a well developed anterolingual accessory cusp and an anterior cingulum, T1 and T4 are posteriorly placed, T3 and T6 are small, but present. *Pseudomys* sp. cf. *desertor* has straight lophs with T1 and T4 placed more anteriorly than in other species. In addition M1 has a well-developed anterior cingulum, but an anterolingual accessory cusp is rare.

Pseudomys bolami Troughton, 1932

(Figures 6–9, Tables 1–4)

MATERIAL EXAMINED

72 specimens (see Appendix 1).

DESCRIPTION

The smallest species of *Pseudomys* from Madura Cave is also the most common. Cheek tooth measurements are within the range of *P. bolami*, one of the smallest extant species of the genus. The incomplete skull (PM 6079, Figure 6) allows for a partial comparison with other small species of *Pseudomys*. The specimen agrees with the description of *P. bolami* given by Kitchener et al. (1984) in the following ways. The nasal bones extend anteriorly slightly beyond the premaxillae. The posterior end of the anterior palatal foramen is broad, rounded, and extends to the level of the first loph of M1, stated by Kitchener et al. (1984) to be characteristic of *P. bolami*. The anterior half of the median palatal septum is inflated. The premaxilla-maxilla septal suture is located near the midpoint of the septum. The anterior margin of the zygomatic plate of the maxillar is slightly concave. There is no anteriorly projecting spine, nor is the dorsal part of the zygomatic arch broadened, as in *Notomys*.

Two specimens (PM 6079, PM 6080) from Trench 1, Unit 1 of Madura Cave preserve the premaxilla and palate (Figure 6). The length of the palate of the Madura Cave specimens falls at the small end of the distribution of *Pseudomys bolami*, *P. hermannsburgensis* and *P. chapmani*. One specimen (PM 6079) allows comparison of the relative lengths of the palate (10.73 mm) and the anterior palatal foramen (4.93 mm) with specimens from other localities. It differs from the Kitchener et al. **(**1984**)** description of *P. bolami* in both average length of the anterior palatal foramen and in the ratio of the anterior palatal foramen length to the palatal length. Specimens of *P. bolami* in the TxVP collection from the Nullarbor region from the surface of Gurneys Cave (TMM 41232) and Jennings Cave (TMM 42121) have shorter palatal lengths than the Madura Cave specimens, but similar lengths of the anterior palatal foramina. The significance of this variability is uncertain, but does not warrant exclusion of the Madura Cave material from *P. bolami*.

The M1 is oval in outline with the cusps inclined posteriorly (Figure 7). Cusps of the labial row (T3, T6, T9) are distinct but smaller than the lingual cusps (T1, T4). Cusps T2 and T3 are close together and form a loph transverse to the long axis of the tooth. Cusp T1 is on the lingual edge of the tooth and is located posterior of T2. When worn, T1, T2 and T3, form a loph that turns abruptly posteriorly at the lingual end. This is in contrast to the very similar *P. hermannsburgensis* in which the longest axes of the cusps T2 and T1 are more closely aligned (A. Baynes pers. comm. 1988) because of the more anterior placement of cusp T1.

Cusp T4 of M1 bears the same relationship to T5 and T6 as does T1 to T2 and T3. Its posterior position results in a posteriorly angled second loph. An accessory cusp is present on the anterolingual corner of the tooth. This is consistent with the description of *P. bolami* by Kitchener et al. (1984). The anterolingual accessory cusp is not as tall as T2.

The large T1 cusp, on the anterolingual corner of M2, is as large as cusp T5. Cusp T6 is the smallest of these and is closely appressed to T5. Cusp T4 lies posterior to

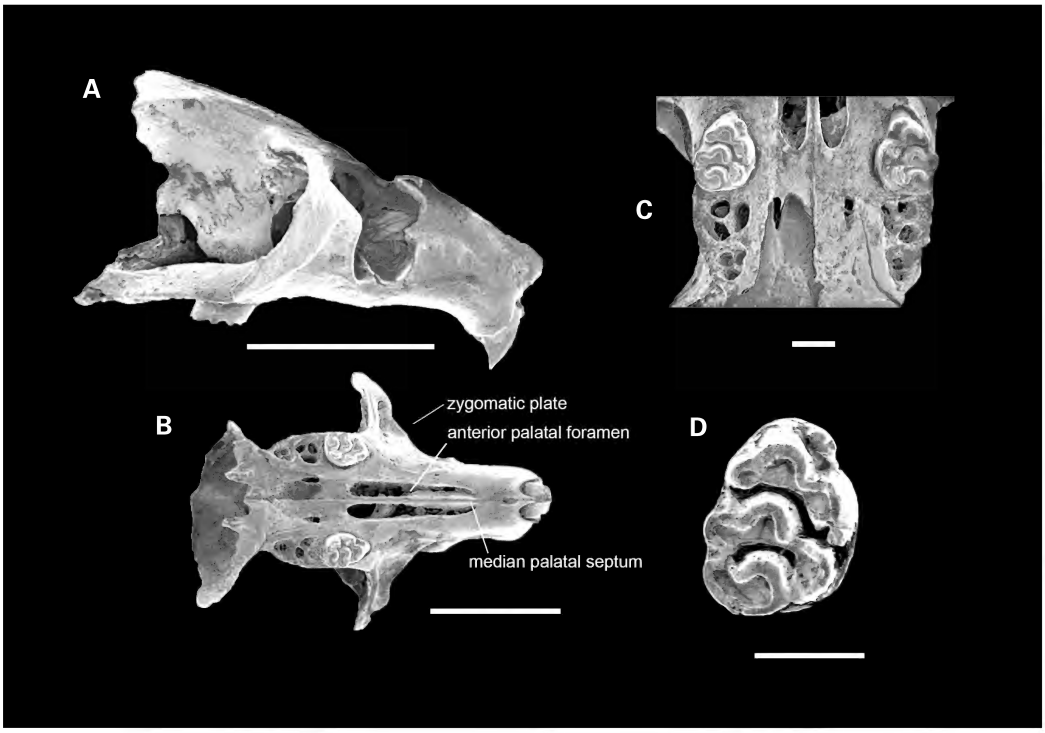

FIGURE 6 *Pseudomys bolami* (PM 6079), Trench 1, Unit 1, partial skull: A) lateral view from right side, anterior to right, scale = 5 mm; B) palatal view, anterior to right, scale = 5 mm; C) palatal view, anterior up, scale = 1 mm; D) R M1, anterior up, scale = 1 mm. (SEM images.)

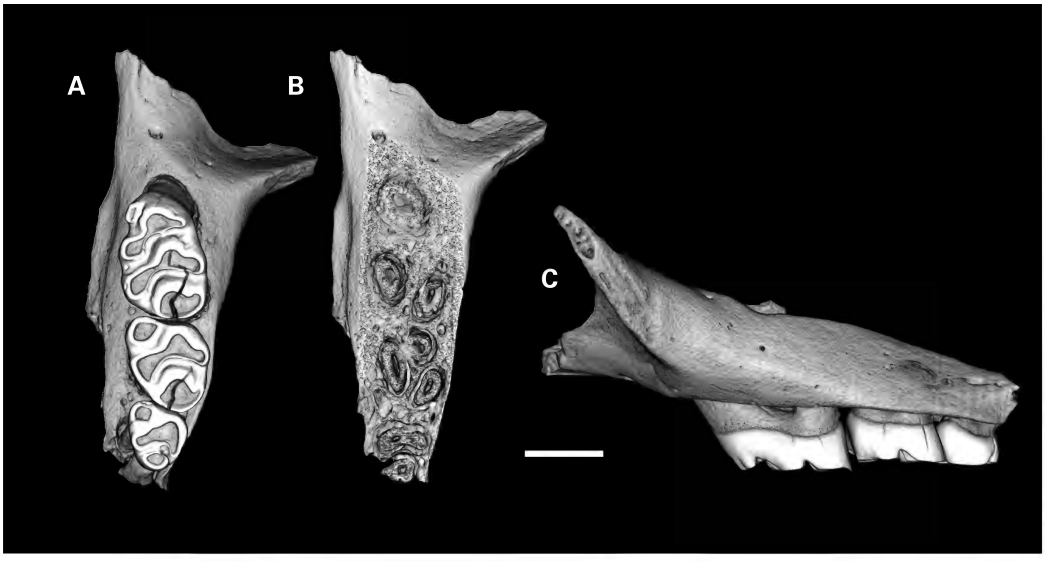

FIGURE 7 *Pseudomys bolami* (TMM 41106-3520), Trench 4, Unit 1, partial L maxilla with M1–3: A) occlusal view, anterior up; B) arbitrary slice through occlusal view showing roots of M1–3; C) labial view. Scale = 1 mm. (Micro-CT images.)

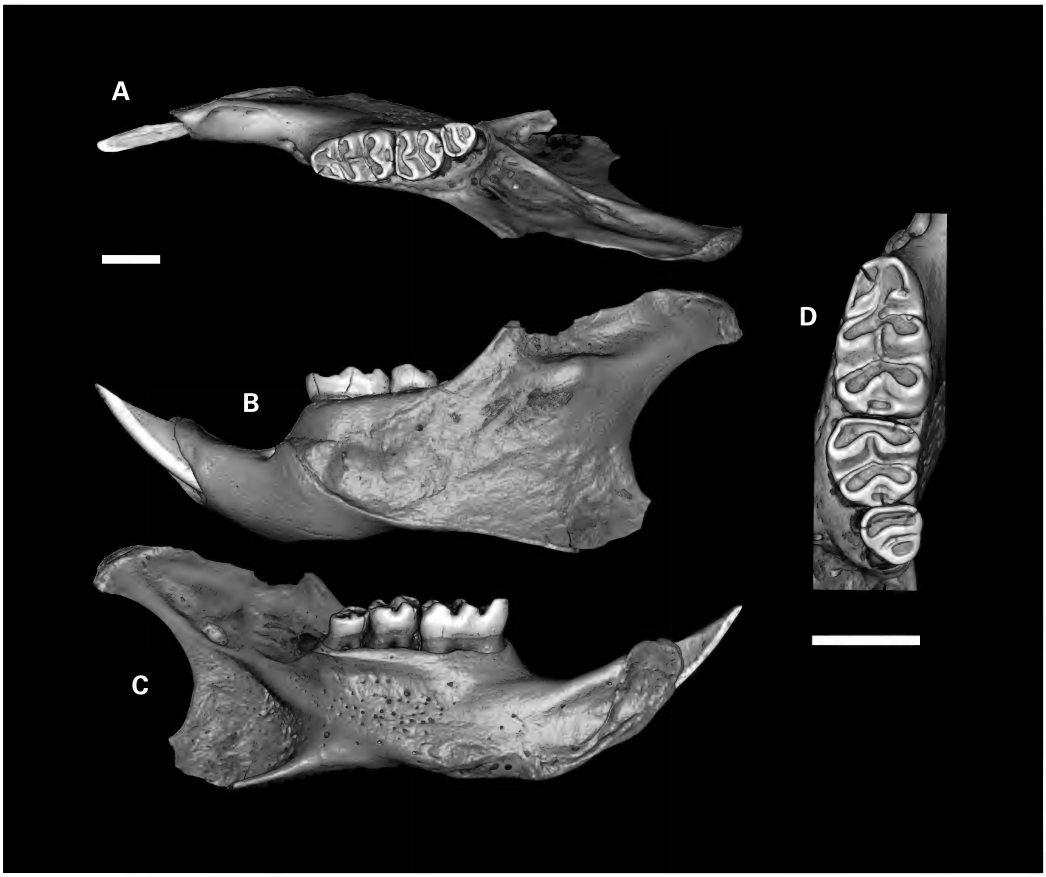

FIGURE 8 *Pseudomys bolami* (TMM 41106-3514), Trench 4, Unit 1, L dentary with i, m1–3: A) dorsal view, anterior to the left, scale = 1 mm; B) labial view, anterior to the left, scale = 1 mm; C) lingual view, anterior to the right, scale = 1 mm; D) occlusal view of m1–3, scale = 1 mm. (Micro-CT images.)

T5 and is joined to it by a ridge. The posterior loph is composed of the central cusp, T8, and is relatively large and oval.

The M3 has a large T1 on the anterolingual corner and a large T5 on the labial side of the median loph. T5 is connected to a posteriorly located T4 to form a loph oriented about 30° to the long axis of the tooth. T6 is very small and is close to T5. The posterior end of the tooth has a small cusp T8.

Specimens assigned to *P. bolami* are similar in size to measurements provided in Kitchener et al. (1984), as well as those conducted as part of this study on specimens from the Western Australian Museum (WAM) and data provided by J. Cramb (pers. comm. 2024) (Tables 1–3). M1 dimensions for the Madura Cave specimens, lie near the centre of a series of measurements for *P. bolami*. Five specimens from WAM have a mean length for M1 of 1.75 ± 0.11 mm and width of 1.13 ± 0.06 mm. The observed range in these specimens, of 1.59–1.85 mm x 1.07–1.22 mm, is very similar to the Madura Cave sample. Although the mean length of M1 decreases up section in the Madura Cave stratigraphy, this variation is not statistically significant.

The dentary is somewhat variable in shape as reported by Kitchener et al. (1984). A well developed masseteric scar terminates anteriorly above the mental foramen that is located about one third of the distance between the m1 and the incisor on the dorsolateral edge of the diastema (Figure 8). The capsule for the lower incisor forms a bulge on the labial side of the dentary just below and behind the coronoid process. The coronoid process is short and slender, and is turned sharply posteriorly (missing in Figure 8).

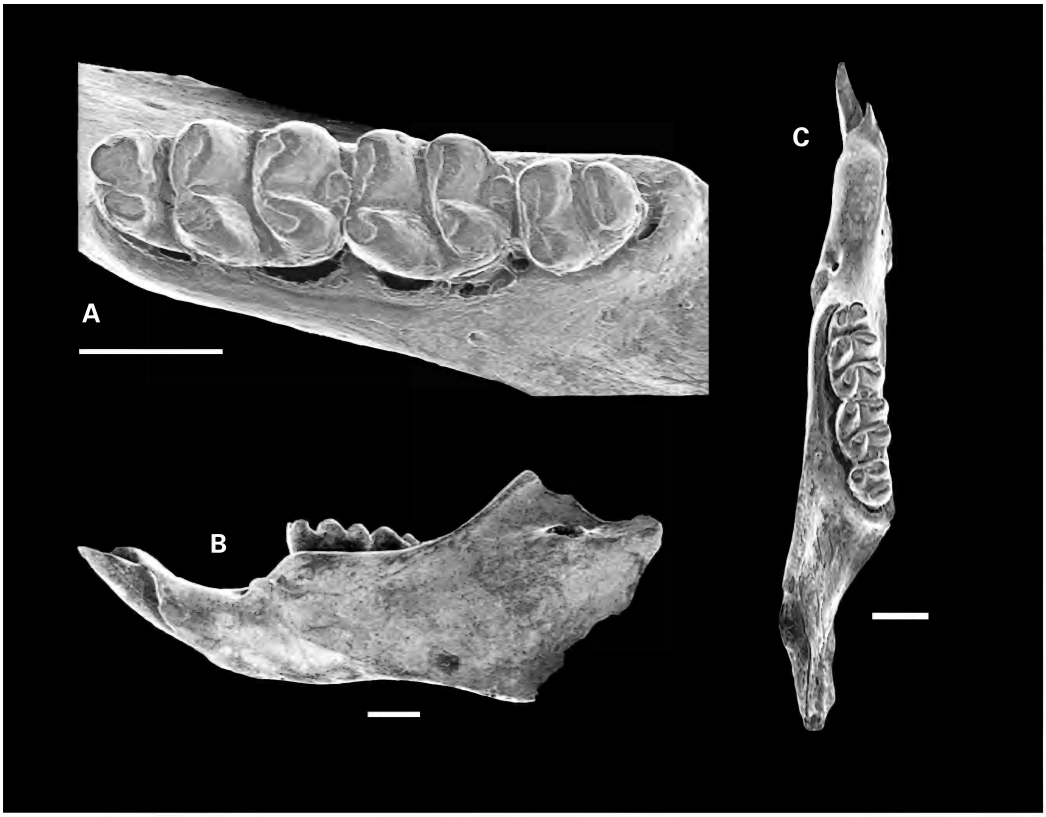

FIGURE 9 *Pseudomys bolami* (TMM 41106-2992), Trench 4, Unit 2, left dentary with i and m1–3; A) occlusal view of m1–3, anterior to the left, scale = 1 mm; B) labial view, anterior to the left, scale = 1 mm; C) occlusal view, anterior up, scale = 1 mm. (SEM images.)

The m1 has two anterior cuspids (alab and aling) that are separate, with the labial cuspid being significantly smaller than the lingual (Figures 8–9). A deep valley separates the anterior cuspids from the protoconid and metaconid. The protoconid is smaller than the metaconid and both second and third lophids are arcuate in occlusal view. The hypoconid and entoconid are subequal in size. There is a small posterior cuspid at the posterior end of the tooth. The protoconid and hypoconid are sub-oval on m2, while the metaconid and entoconid are elongate. As in m1, there is a small posterior cuspid at the posterior end of the tooth. The m3 is small and sub-triangular in shape. The hypoconid and entoconid are merged into a single posterior lophid (Figure 9). The mean m1–3 trl of 3.25 mm (Table 4) is small for species of *Pseudomys*.

DISCUSSION

Pseudomys bolami is the most abundant species of *Pseudomys* in the Madura Cave fauna and specimens are found throughout the stratigraphic section. Those from Unit 7 of Trench 4 represent some of the oldest murids known from the cave, possibly as old as ~38,000 BP based on C14 ages. Mean dimensions of upper cheek teeth suggest a minor decrease in the size of *P. bolami* with decreasing age in the cave stratigraphy, but this variation is not statistically significant. *Pseudomys bolami* is one of the smaller *Pseudomys* species, however, there are as many as ten species of small *Pseudomys* recognised in Australia (Watts and Aslin 1981). Small *Pseudomys* specimens from the Nullarbor Plain were assigned to *P. bolami* by Baynes (1987). The Madura Cave specimens are comparable to those of *P. bolami* in the morphology of M1, especially the shape of the first loph. A single partial skull agrees with the description of *P. bolami* given by Kitchener et al. (1984) in the following ways: 1) the nasal bones extend anteriorly slightly beyond the premaxillae; 2) the posterior end of the anterior palatal foramen extends to the level of the first loph of M1. Measured lengths of the anterior palatal foramen of the Madura Cave specimens are slightly longer than *P. bolami* provided by Kitchener et al. (1984).

TABLE 1 Measurments for upper dentition of *Pseudomys bolami*, Trench 4, Unit 1.

	Mean (mm)	SD	Range (mm)	N
M1–3 l	3.59	0.148	3.23–3.83	22
M1 l	1.82	0.112	1.58–1.99	37
M1 w	1.17	0.053	1.07–1.29	37
M2 l	1.06	0.056	0.97–1.18	33
M2 w	1.07	0.058	0.95–1.19	33
M3 l	0.73	0.070	0.64–0.89	23
M3 w	0.76	0.048	0.69–0.89	24

TABLE 2 Measurments for upper dentition of *Pseudomys bolami*, Trench 3, Unit 2.

	Mean (mm)	Range (mm)	N
M1–3 l	3.61	3.46–3.80	3
M1 l	1.84	1.73–1.96	3
M1 w	1.18	1.13–1.19	3
M2 l	1.05	0.96–1.13	3
M2 w	1.08	1.05–1.13	3
M3 l	0.71	0.69–1.73	3
M3 w	0.82	0.68–0.97	3

TABLE 3 Measurments for *Pseudomys bolami*, Trench 4, Unit 7.

	Mean (mm)	SD	Range (mm)	N
M 1 l	1.89	0.13	1.73–2.06	10
M 1 w	1.23	0.05	1.13–1.29	10

TABLE 4 Measurments for lower dentition of *Pseudomys bolami*, Trench 3, Unit 2.

	Mean (mm)	SD	Range (mm)	N
m1–3 l	3.25	-	3.09–3.41	2
m1 l	1.70	0.08	1.59–1.88	14
m1 w	1.05	0.03	1.00–1.10	14
m2 l	1.04	0.05	0.97–1.10	10
m2 w	1.04	0.04	0.97–1.10	10
m3 l	0.76	-	0.71–0.81	2
m3 w	0.81	-	0.81–0.81	2

The Madura Cave material was originally called *Leggadina hermannsburgensis* by Lundelius (1963). *Pseudomys bolami* was later recognised as distinct from *P. hernannsburgensis* by the more posterior placement of cusp T1 on M1 resulting in an anterior loph that is angled posteriorly, as well as an elongated accessory cusp. When worn, T1, T2, and T3 form a loph whose lingual end turns abruptly posteriorly, in contrast to the situation in *P. hermannsburgensis*.

The Madura Cave specimens differ from *P. chapmani* in the geometry of the anterior palatal foramen relative to the length of the palate. The specimens differ from most other small *Pseudomys* by having an accessory cusp on the anterolingual margin of M1. While *P. delicatulus* and *P. novaehollandiae* have an accessory cusp on the anterior edge of the M1 in some specimens, those taxa do not exhibit the distinct posterior angulation of the first loph of M1. With the exception of *P. delicatulus*, the lengths of the palate of these species are longer than in the Madura Cave specimens, based on measurements made by E.L.L. at WAM.

Specimens of this taxon were reported by Baynes (1987) from numerous caves along the southern margin of the Nullarbor Plain as well as across the central Nullarbor and Carlisle Plain. The present day distribution map for *P. bolami* includes much of the southern parts of South Australia and Western Australia including the Nullarbor Plain (Baker and Gynther 2023).

Pseudomys australis Gray, 1832

(Figure 10, Table 5)

MATERIAL EXAMINED

21 specimens (see Appendix 1).

DESCRIPTION

This material represents a medium sized species of *Pseudomys* with M1 dimensions of approximately 2.5 x 1.7 mm (Table 5). The anterior palatal foramen is narrow and terminates posteriorly in a relatively sharp point. M1 lacks an anterolingual accessory cusp and has no anterior cingulum. T1 is approximately aligned with T2 rather than being posteriorly displaced (Figure 10). T3 is very reduced, or absent, on M1; T6 is small and T9 is smaller. M3 is sub-triangular in outline with a well-developed T1.

DISCUSSION

Pseudomys australis is represented by 6 specimens from Trench 1, Unit 1, and 15 specimens from Trench 3, Unit 2. It is not recognised in sediments older than about 22,000 BP from Madura Cave. Only a single dentary with m1 has been tentatively assigned to this

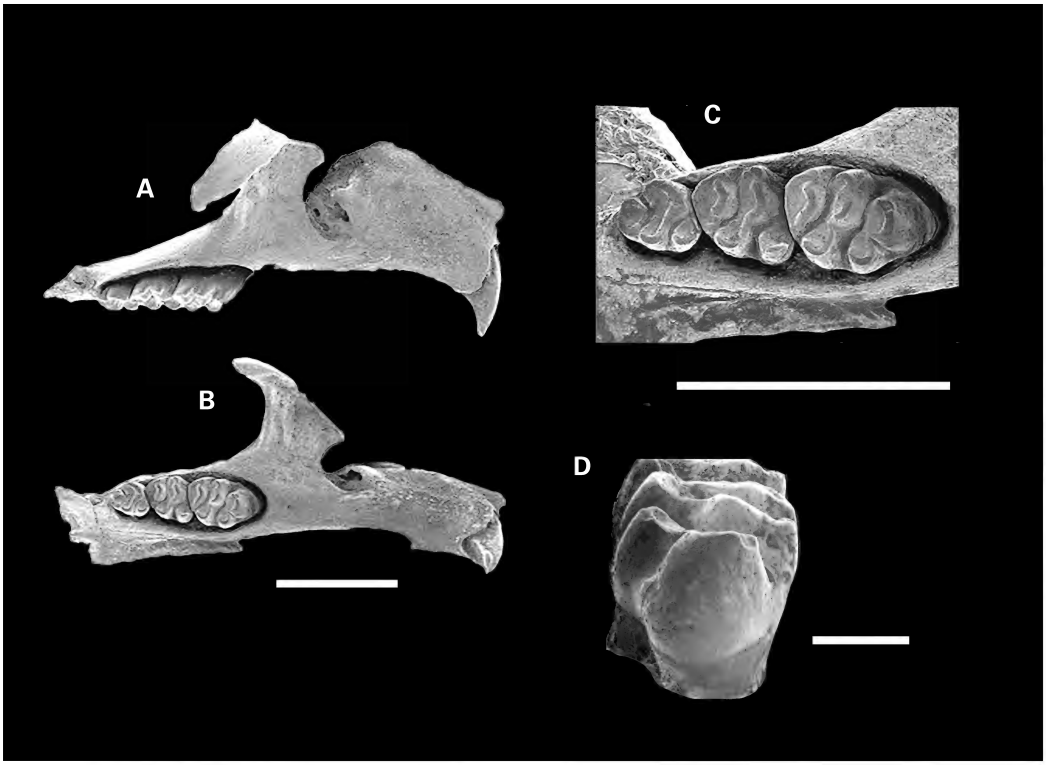

FIGURE 10 *Pseudomys australis* (PM 6110), R maxilla and premaxilla with I, M1–3; A) labial view, anterior to the right, scale = 5 mm; B) occlusal view, anterior to the right, scale = 5 mm; C) occlusal view of M1–3, anterior to the right, scale = 5 mm; D) anterior view of M1, lingual to the left, scale = 1 mm. (SEM images.)

taxon, so the description and identification is largely based on the size and morphology of M1. Although morphologically similar to specimens from other populations of *P. australis* and *P. shortridgei*, the average M1 dimensions of 2.49 mm ± 0.17 mm by 1.71 mm ± 0.1 mm are relatively small and significantly smaller than *P. shortridgei*. Measurements of M1 for *P. australis* compiled by J. Cramb (pers. comm. 2024) exhibit the largest size range of any species of *Pseudomys*. Distinguishing features of M1 on *P. australis* include the lack of an anterolingual accessory cusp with no anterior cingulum, the alignment of T1 and T2 and the highly reduced, or absent, T3 with a small T6. The Madura Cave material is morphologically similar to *P. shortridgei* in the alignment of T1 and T2. However, it lacks the anterior cingulum seen in the latter and T1 on M3 is larger. It is identified as *P. australis* based on M1 morphology, but is smaller than *P. australis* from other localities. The pointed shape of the posterior end of the anterior palatal foramen is also consistent with *P. australis* (A. Baynes pers. comm. 2025). The present day range of *P. australis* is restricted to central and eastern South Australia, western New South Wales and southern Northern Territory, although its prior range included the Nullarbor Plain (Baker and Gynther 2023).

TABLE 5 Upper cheek tooth dimensions for *Pseudomys australis* from Trench 1, Unit 1 and Trench 3, Unit 2.

	Mean (mm)	SD	Range (mm)	N
M1 l	2.49	0.17	2.28–2.85	15
M1 w	1.71	0.10	1.52–1.87	15
M2 l	1.50	0.08	1.38–1.62	12
M2 w	1.54	0.08	1.40–1.66	12
M3 l	1.16	0.14	0.92–1.29	7
M3 w	1.20	0.07	1.13–1.32	7

Pseudomys gouldii (Waterhouse, 1839)

(Figure 11, Table 6)

MATERIAL EXAMINED

9 specimens (see Appendix 1).

DESCRIPTION

The upper cheek teeth are relatively brachyodont with cusps that slope posteriorly. The sizes of the upper cheek teeth are similar to *Pseudomys australis* and other mid-sized *Pseudomys* (Table 6). A well developed accessory cusp is present on the anterolingual corner of M1 along with an anterior cingulum (Figure 11). The accessory cusp has been noted as a characteristic feature of *P. gouldii* (e.g. Watts and Aslin 1981), but careful examination of the original figure of this taxon by Waterhouse (1839) shows no such cusp (*Mus gouldii*, plate 34, figure 18a). T1 and T4 are posteriorly placed while T3 and T6 are small but present on M1. There is also a small anterolabial accessory cusp on M2 of the Madura Cave specimens. The posterior end of the anterior palatal foramen is rounded. The anterior edge of the zygomatic plate is concave and there is a spine at the top as in *Notomys*. However, the zygomatic arch is not broadened as in *Notomys* (Figure 11). *Pseudomys gouldii* differs from the other medium sized taxa of *Pseudomys* primarily in M1 morphology.

DISCUSSION

Pseudomys gouldii is relatively rare in the Madura Cave fauna (9 specimens), but is recognised on the basis of size, M1 morphology, and the narrow, rounded shape of the posterior end of the anterior palatal foramen (A. Baynes pers. comm. 2025). *Pseudomys fieldi* is now considered a junior synonym of *P. gouldii* (Roycroft et al. 2021). Suggestions that *P. gouldii* had become extinct are superseded by the occurrence of a population on Bernier Island in Shark Bay, Western Australia previously assigned to *P. fieldi.* While *P. gouldii* was once widespread across the southern half of Australia, its natural range is now restricted to this single island (Roycroft et al. 2021). The presence of *P. gouldii* in Madura Cave shows that in the late Pleistocene and early Holocene, this range included the Nullarbor Plain.

TABLE 6 Measurements of upper cheek teeth of *Pseudomys gouldii* from Madura Cave.

	Mean (mm)	SD	Range (mm)	N
M1 l	2.46	0.14	2.32–2.60	3
M1 w	1.63	0.04	1.60–1.67	3
M2 l	1.41	0.09	1.50–1.52	4
M2 w	1.51	0.01	1.50–1.52	4
M3 l	1.12	0.07	1.05–1.19	3
M3 w	1.16	0.06	1.11–1.23	3

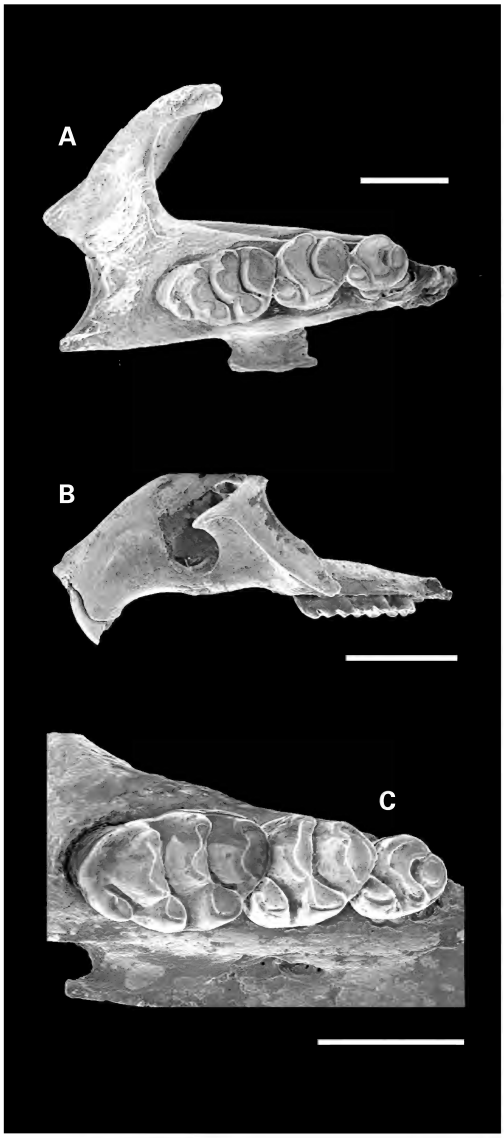

FIGURE 11 *Pseudomys gouldii* (TMM 41106-1992): A) L maxilla with M1–3, occlusal view anterior up, scale = 2 mm. *Pseudomys gouldii* (PM 6114): B) partial skull with M1–3 lateral view, anterior to the left, scale = 5 mm; C) occlusal view of M1–3, anterior to the left, scale = 2 mm. (SEM images.)

Pseudomys sp. cf. *desertor* Troughton, 1932

(Figure 12, Table 7)

MATERIAL EXAMINED

60 specimens (see Appendix 1).

DESCRIPTION

A medium sized mouse, larger than *Pseudomys gouldii*, with brachydont M1 and posteriorly angled cusps (Table 7). The lophs on M1 are straight, as T1 and T4 are not displaced posteriorly as in many other species of *Pseudomys* (Figure 12). An anterior cingulum is usually present on M1, while the anterolingual accessory cusp is usually absent. A few specimens (TMM 41106-3956, TMM 41106-3930, Figure 12B), have a small accessory cusp on the anterior margin. The shape of M1 in the Madura Cave sample is variable, but the cusp morphology compares well with specimens of *P. desertor*, including those at WAM examined by E.L.L. The length of M1 is consistent with measurements compiled by J. Cramb (pers. comm. 2024) although the mean width is greater.

TABLE 7 M1 dimensions for *Pseudomys* sp. cf. *desertor*, Trench 4, Units 4–5.

	Mean (mm)	SD	Range (mm)	N
M1 l	2.57	0.167	2.22–2.81	37
M1 w	1.75	0.001	1.64–1.87	36

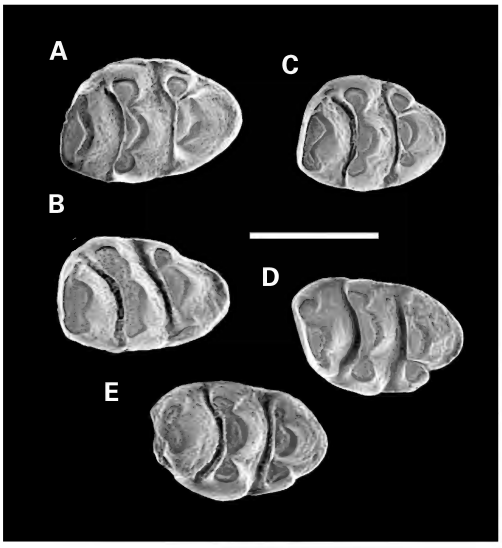

FIGURE 12 *Pseudomys* sp. cf. *desertor*, anterior to the right: A) TMM 41106-4046, L M1; B) TMM 41106-3930, L M1; C) TMM 41106-3922, L M1; D) TMM 41106-4044, R M1; E) TMM 41106-3950, R M1. Scale = 2mm. (SEM images.)

DISCUSSION

Nearly all of the specimens assigned to *Pseudomys* sp. cf. *desertor* are isolated upper first molars. Whereas this may reflect an anatomy prone to separation of the teeth from the maxilla after death, the observation of differential preservation of maxilla with teeth vs isolated teeth is fully addressed by Baynes et al. (2019). M1 is the diagnostic tooth for this taxon, so lacking associated upper cheek teeth in maxillae, and associated maxillae with dentaries, assignment of additional cheek teeth to this taxon is uncertain. *Pseudomys* sp. cf. *desertor* is recognised by the presence of relatively straight lophs on M1 and the presence of a well-developed anterior cingulum. In addition, this taxon usually lacks an anterolingual accessory cusp on M1. *Pseudomys desertor* is widespread across the arid and semi-arid environments of central Australia.

Genus *Notomys* Lesson, 1842

Notomys sp. indet.

(Figures 13–21, Tables 8–10)

Rodents of the genus *Notomys* are most easily distinguished, from other similarly sized rodents in Australia, by having the anterior edge of the zygomatic plate deeply concave with a prominent anterior zygomatic spine at its dorsal end. The radius of curvature of the anterior edge of the zygomatic plate increases ventrally (A. Baynes pers. comm. 2025). The dorsal part of the zygomatic arch is very broad and is abruptly constricted about half way along its length. The interorbital area is relatively broad. *Pseudomys* sometimes exhibits an anterior zygomatic spine (e.g. *P. nanus*, *P. australis)*, but it is never as well developed as in *Notomys* and these taxa lack the assymetric concavity of the anterior edge of the zygomatic plate and the dorsal broadening of the zygomatic arch.

MATERIAL EXAMINED

126 specimens (see Appendix 1). Approximately 1100 specimens from Madura Cave have been tentatively identified as *Notomys*. A full listing of these specimens can be viewed via an online search at https://specify-portal.tacc.utexas.edu/vpl/ using 'advanced search', filtered with 'Catalog Number contains' 41106, and 'Genus =' *Notomys*. A subset of specimens listed in Appendix 1 are those measured and studied for this paper. Specimens were selected based on condition,

completeness, state of wear, and stratigraphic location. The sample includes specimens from Trench 3, Units 1–2 and Trench 4, Units 1–5, with an age range of approximately 22,000 BP to 7,500 BP based on previously published C14 dates. Considering size and dental morphology, all of the specimens of *Notomys* are considered to represent a single species. A complete analysis of all 1,100 specimens would result in a better understanding of intraspecific variability and potentially morphological variation over time.

DESCRIPTION

Notomys is recognised on the basis of the morphology of the zygomatic arch and the well developed anterior zygomatic spine. The dentary exhibits a masseteric scar that terminates on the posterolabial margin of the diastema above a well-developed mental foramen. Dorsal and ventral ridges of the scar form a narrow angle. Detailed dental morphology is described below, however, individual cheek teeth, or even partial maxillae and dentaries, can be difficult to separate from *Pseudomys*.

Dental measurements are provided in Tables 8–9 and plotted in Figure 13. These data suggest that *Notomys* is represented by a single species in the Madura Cave sediments. Some variability in the length of M1 is almost certainly attributable to the shape of the tooth with a posteriorly sloping anterior edge. This causes length measurements to vary slightly with state of wear. Regardless, the dimensions of all cheek teeth cluster tightly and statistical analysis indicates approximately normal distributions. Based on specimens with complete M1–3, the mean TRL (M1–3) of the Madura Cave *Notomys* (4.68 mm ± 0.19 mm, N = 39) is smaller than all extant species of *Notomys.* Mean upper TRLs of the smallest species range from 5.0 mm (*N. fuscus*, *N. aquilo*) to 5.2 mm (*N. cervinus, N. mitchellii*) (Vakil et al. 2023). The largest specimens from Madura Cave overlap with smaller specimens of this group. The Madura Cave *Notomys* is smaller than *N. longicaudatus* and *N. amplus*. It is also smaller than *N. robustus* from South Australia, as well as *N. magnus* from northeastern Queensland (Mahoney et al. 2008; Vakil et al. 2023). Based on specimens with a complete m1–3, the mean trl for *Notomys* from Madura Cave is 4.90 mm ± 0.40 mm, N = 13.

There are no consistent trends in size vs. stratigraphic position. The mean length of M1 varies from 2.12 ± 0.15 mm (Unit 4) to 2.08 ± 0.16 mm (Unit 2) in Trench 4, and from 2.16 ± 0.07 mm (Unit 2) to 2.19 ± 0.10 mm (Unit 1) in Trench 3. Neither were any stratigraphic trends in morphologic variation observed. Therefore, all specimens of *Notomys* are interpreted as a single species.

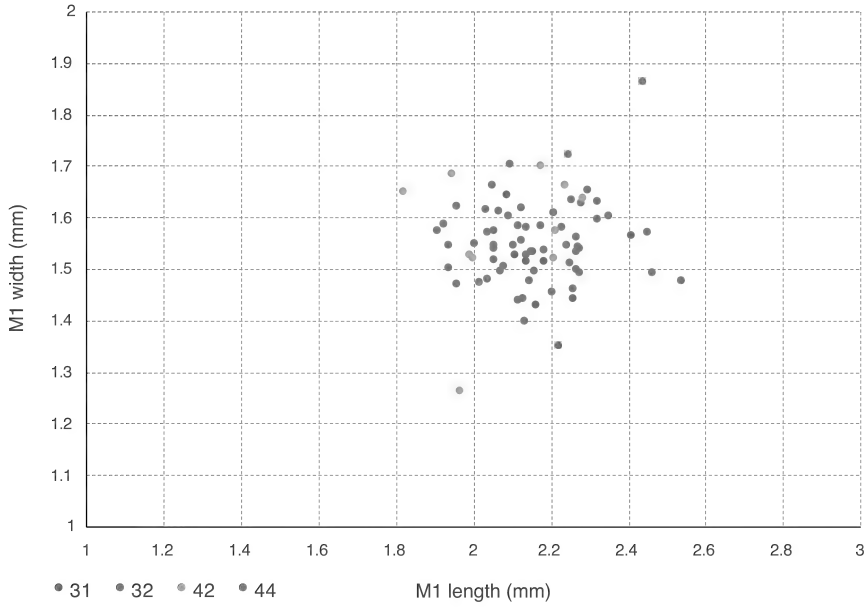

FIGURE 13 Graph of M1, l x w for *Notomys* sp. indet. Blue = Trench 3, Unit 1; Orange = Trench 3, Unit 2; Grey = Trench 4, Unit 2; Yellow = Trench 4, Unit 4.

The most complete cranial specimens from Madura Cave are TMM 41106-341 and TMM 41106-342, both from Trench 3, Unit 2. The anterior palatal foramina are long and taper slightly toward the anterior (Figure 14). The posterior termination is approximately aligned with the T1–3 loph on M1. The ratio of foramen to diastema length is approximately 0.71. The premaxilla-maxilla suture occurs just anterior to the midpoint of the anterior palatal foramina. The posterior palatal foramina are relatively large and elongate and are located at the anterior edge of the palatine (Table 10). The anterior portion of the zygomatic arch is broad with a concave zygomatic plate and a well-developed anterior zygomatic spine (Figures 14–19).

A series of images shown in Figures 16–20 illustrates maxillae of *Notomys* sp. indet. with variable cheek tooth wear. Arbitrary slices, through some of the CT volumes, clearly illustrate three roots on M1, three roots on M2, and three roots on M3, although the anterior two roots on the last are fused together. The concave anterior edge of the zygomatic plate and the anterior zygomatic spine, imaged in these figures, are characteristic of *Notomys*. The M1 is oval in shape with T1 and T4 displaced posteriorly. The lingual cusps (T1, T4) are distinct and larger than the labial (T3, T6). The posterior loph (T8–T9) is wide and inflated antero-posteriorly. There is no evidence for an anterior cingulum or accessory cusps. The posterior loph of M3 is relatively small and oval in shape and connects to the medial loph with wear. It is most similar to the small posterior loph in *N. mitchellii* but narrower than in both *N. longicaudatus* and *N. alexis*.

The dentary and lower cheek teeth of *Notomys* sp. indet. are illustrated in Figure 21. The first two lophs on m1 are separated by a deep valley and not joined by a low cristid as in *N. cervinus*. The m1 and m2 have very distinct posterior cuspids as in *N. cervinus* and *N. mitchellii*. This cuspid is absent, or very weakly developed, in *N. longicaudatus* and *N. alexis*. The lower cheek teeth have two roots each. The dorsal and ventral crests of the masseteric scar form a relatively acute angle terminating in a rugose tip above the mental foramen. The mental foramen is located on the posterolabial portion of the diastema. The average length of the diastema is 3.71 mm (SD = 0.43, N = 11).

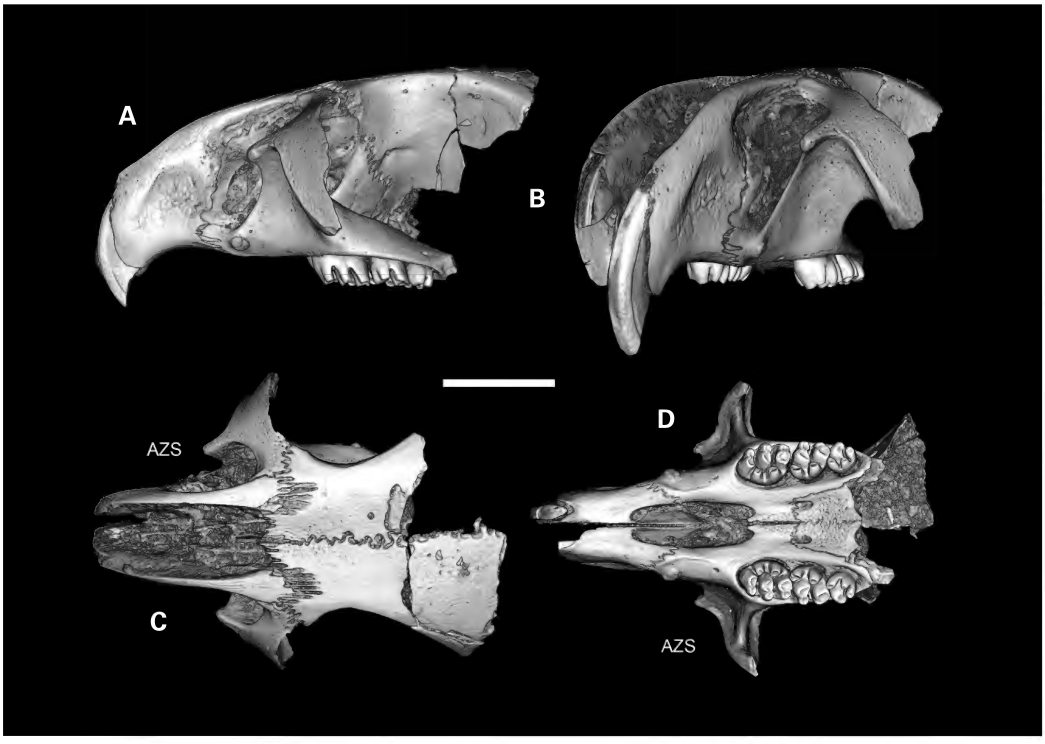

FIGURE 14 *Notomys* sp. indet. (TMM 41106-342), Trench 3, Unit 2, partial skull with slightly worn L and R M1–3, L I and partial R I: A) lateral view, anterior to the left; B) oblique anterior view showing anterior zygomatic spine and broad concave zygomatic plate, medial groove on anterior margin of incisor; C) dorsal view, anterior to the left; D) palatal view, anterior to the left, showing anterior and posterior palatal foramina. AZS: anterior zygomatic spine. Scale = 5 mm. (Micro-CT images.)

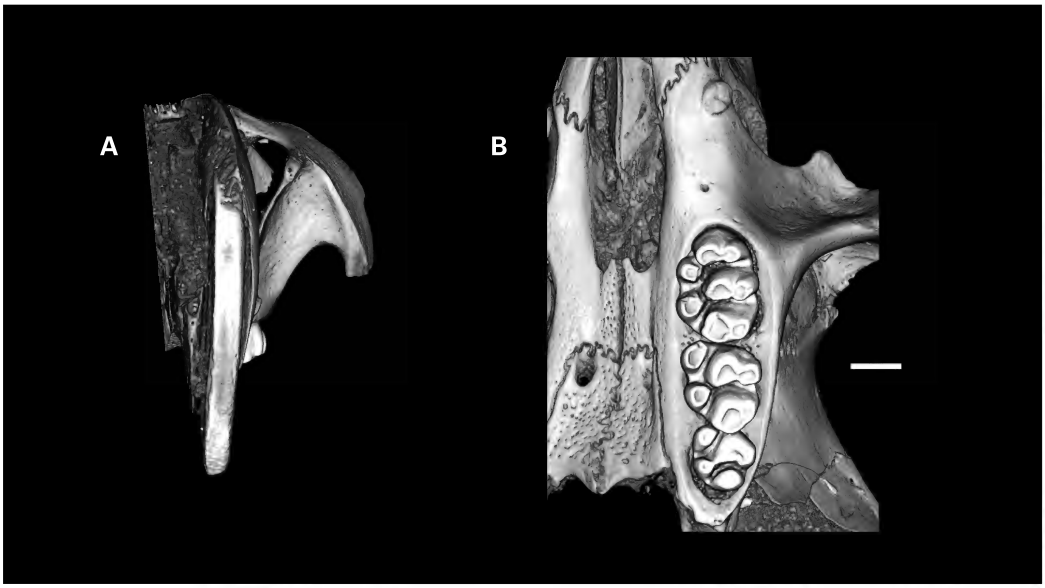

FIGURE 15 *Notomys* sp. indet. (TMM 41106-342): A) anterior view showing shallow groove along anterior margin of left incisor; B) occlusal view showing morphology of L M1–3, anterior up. Scale = 1 mm. (Micro-CT images.)

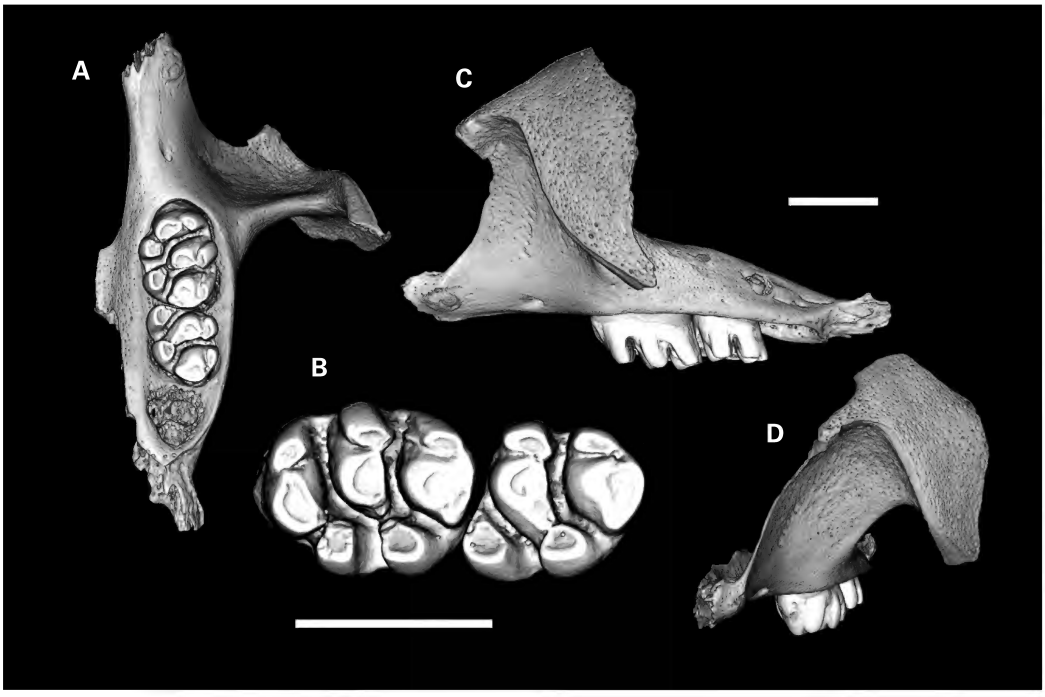

FIGURE 16 *Notomys* sp. indet. (TMM 41106-2008), Trench 3, Unit 2, L maxilla with slightly worn M1–2; A) occlusal view, anterior up, showing zygomatic spine and broad zygomatic plate, scale = 2 mm; B) close up of M1–2, anterior to left, scale = 2 mm; C) labial view, anterior to left, scale = 2 mm; D) anterior view showing zygomatic spine and concave zygomatic plate, scale = 2 mm. (Micro-CT images.)

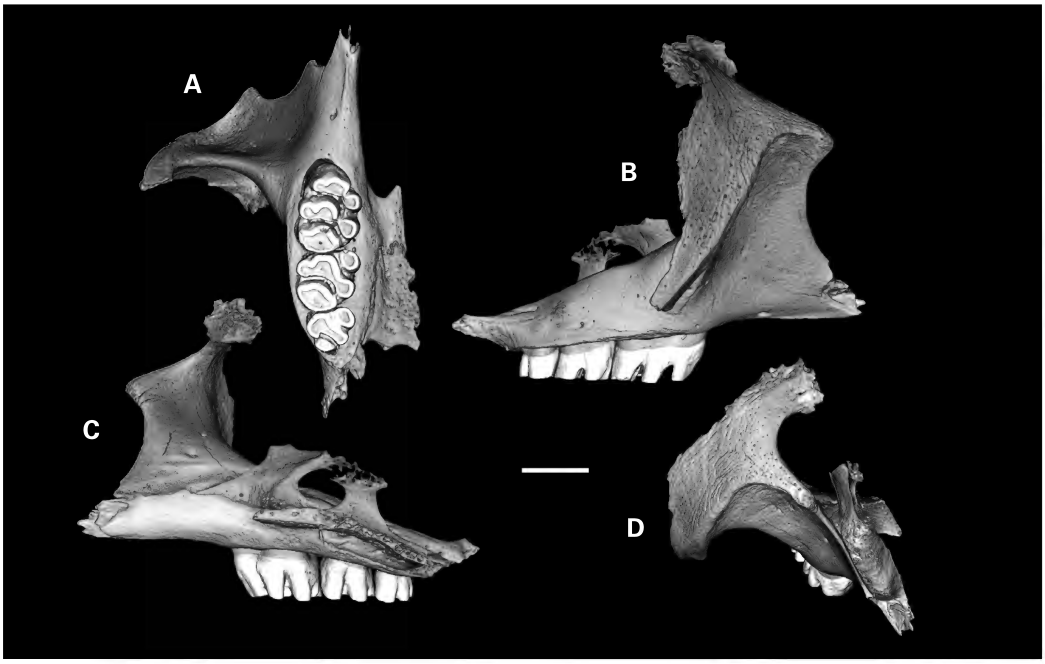

FIGURE 17 *Notomys* sp. indet. (TMM 41106-3717), Trench 1, top 30 cm, R maxilla with moderately worn M1-3: A) occlusal view, anterior up, showing zygomatic spine and broad zygomatic plate; B) labial view, anterior to right; C) lingual view, anterior to left; D) anterior view showing zygomatic spine and concave zygomatic plate. Scale = 2 mm. (Micro-CT images.)

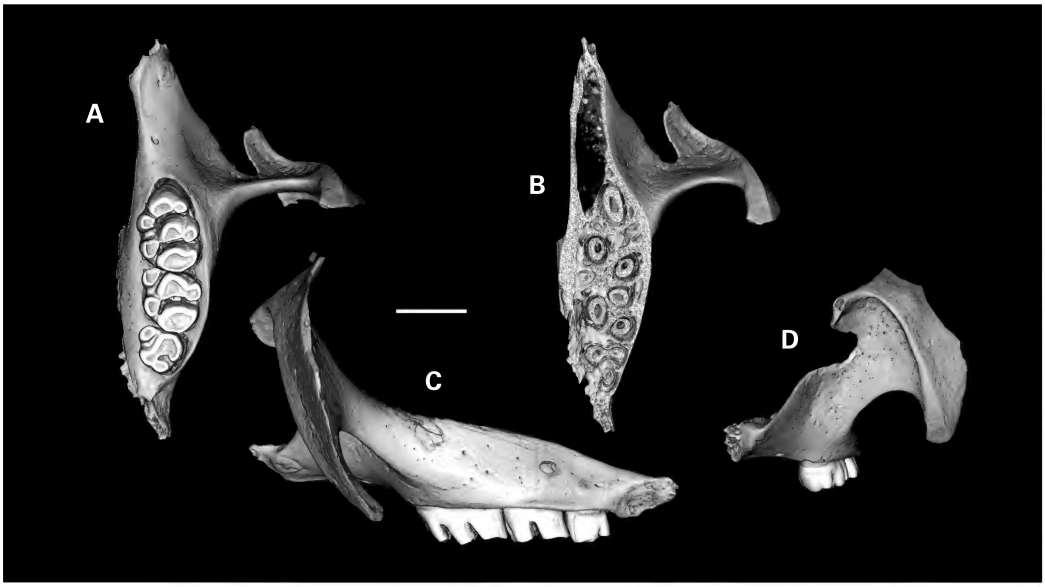

FIGURE 18 *Notomys* sp. indet. (TMM 41106-2012), Trench 3, Unit 2, L maxilla with moderately worn M1–3; A) occlusal view, anterior up; B) arbitrary slice through occlusal view showing three roots for each of M1–3, anterior roots of M3 are fused; C) labial view, anterior to left; D) anterior view showing broken zygomatic spine and zygomatic plate. Scale = 2 mm. (Micro-CT images.)

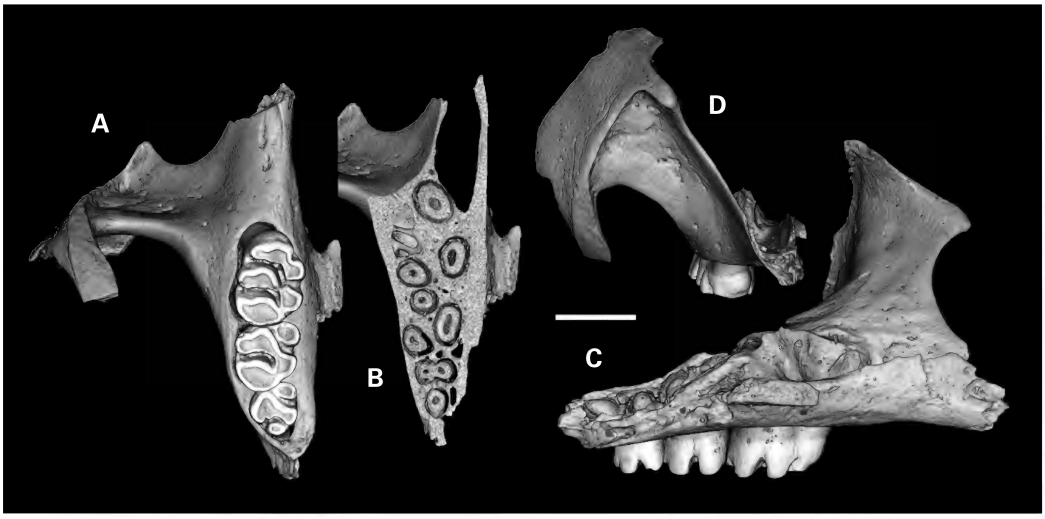

FIGURE 19 *Notomys* sp. indet. (TMM 41106-5657), Trench 3, Unit 2, R maxilla with worn M1–3: A) occlusal view, anterior up, showing zygomatic spine and broad zygomatic plate; B) arbitrary slice through occlusal view showing three roots for each of M1–3, anterior roots of M3 are fused; C) lingual view, anterior to right; D) anterior view showing zygomatic spine and zygomatic plate. Scale = 2 mm. (Micro-CT images.)

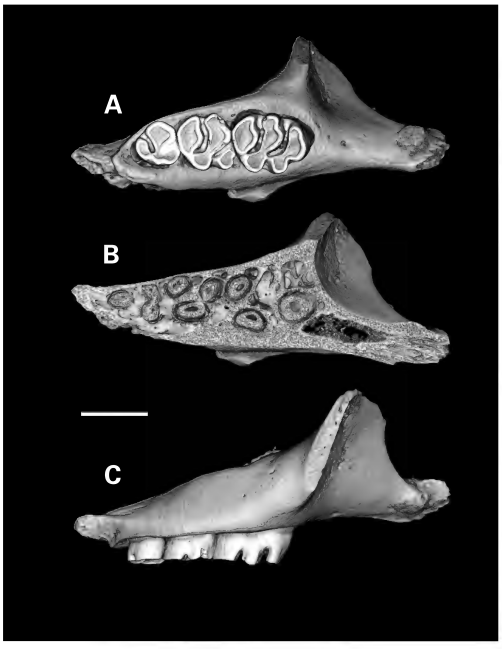

FIGURE 20 *Notomys* sp. indet. (TMM 41106-2183), Trench 3, Unit 2, R maxilla with well-worn M1–3: A) occlusal view, anterior to right; B) arbitrary slice through occlusal view showing three roots for each of M1–3 (note the anterior roots of M3 are fused at this level); C) labial view, anterior to right. Scale = 2 mm. (Micro-CT images.)

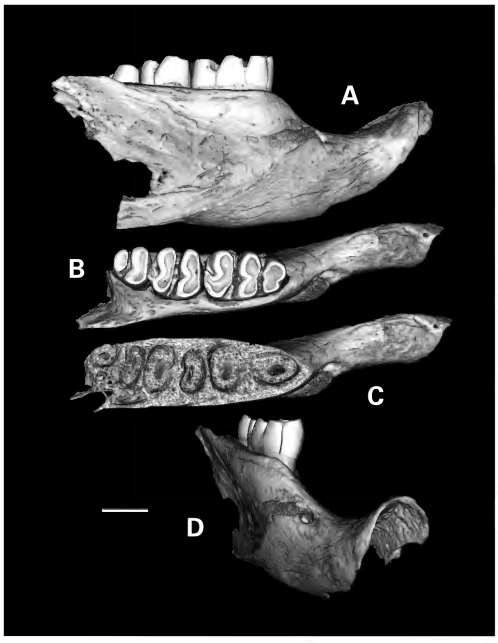

FIGURE 21 *Notomys* sp. indet. (TMM 41106-1204), Trench 3, Unit 2, R dentary: A) labial view, anterior to right; B) occlusal view, anterior to right; C) arbitrary slice through occlusal view showing two roots for m1–3, anterior to right; D) oblique anterolabial view showing anterior termination of the masseteric scar above mental foramen. Scale = 2 mm. (Micro-CT images.)

TABLE 8 Dimensions of *Notomys* sp. indet. cheek teeth from Madura Cave, all units.

	Mean (mm)	SD	Range (mm)	N
M1 l	2.15	0.14	1.82–2.54	87
M1 w	1.54	0.09	1.26–1.86	87
M2 l	1.51	0.12	1.24–1.88	71
M2 w	1.42	0.10	1.18–1.71	71
M3 l	1.07	0.07	0.95–1.28	51
M3 w	1.10	0.07	0.93–1.25	51
m1 l	2.17	0.30	1.51–2.50	41
m1 w	1.34	0.21	0.87–1.58	41
m2 l	1.33	0.23	0.85–1.64	22
m2 w	1.32	0.24	0.88–1.62	21
m3 l	1.14	0.17	0.97–1.53	11
m3 w	1.11	0.10	0.95–1.22	11

TABLE 9 M1 length statistics for *Notomys* sp. indet. from Madura Cave by trench and stratigraphic unit.

Trench/Unit	3/1	3/2	4/2	4/4–5
Mean (mm)	2.19	2.16	2.08	2.12
Median (mm)	2.16	2.14	2.09	2.02
SD	0.10	0.07	0.16	0.15
N	9	64	10	5

TABLE 10 Skull dimensions in mm for *Notomys* sp. indet. as defined by Musser et al. 2005.

Length of the rostrum	10.83
Width of the rostrum	4.42
Interorbital width	6.34
Width between zygomatic spines	8.06
Width across the nasals	3.23
Length of the nasals	9.54
Length of the anterior palatal foramina	5.69
Max. width of the anterior palatal foramina	2.22
Length of diastema	7.95
Length of bony palate	4.78
Width between posterior palatal foramina	1.58
Width of zygomatic plate	3.96
TRL (M1–3)	4.85

DISCUSSION

Based on size and dental morphology, *Notomys* sp. indet. compares most closely with *N. fuscus*, *N. cervinus* and *N. mitchellii.* However, in addition to being smaller than these taxa, it differs in details of dental morphology. *Notomys* sp. indet. differs from *N. cervinus* in the separation of the anterolabial and anterolingual cuspids from the protoconid and metaconid on m1. T1 is more strongly connected to T2, and T9 is less distinct on M1. The T4–T6 loph is better developed on M3, but T8 is much smaller than in *N. cervinus*. However, like *N. cervinus*, the Madura Cave *Notomys* exhibits a shallow groove on the anterior margin of the upper incisors (Figures 14–15) (Watts and Aslin 1981). The anterior groove on the upper incisor was considered diagnostic of *N. cervinus* and *N. macrotis* by Watts and Aslin (1981). The latter taxon is not well known, but appears to have a larger skull with anterior palatal foramina that broaden posteriorly. M1 measurements for *N. macrotis* in Mahoney (1975) are 2.8 x 1.9 mm with a TRL of 5.5 mm and trl of 5.5 mm. This is significantly larger than *Notomys* sp. indet. from Madura Cave (2.15 mm x 1.54 mm, TRL = 4.90, trl = 4.68). *Notomys* sp. indet. is distinct from both *N. cervinus* and *N. macrotis* even though it exhibits an anterior groove on the upper incisor.

Notomys sp. indet. from the Madura Cave fauna differs from *N. mitchellii* in having a more distinct T6 on M1 and a broader T8–T9 posterior loph. T8–T9 is also broader on M2 than in *N. mitchellii*. The M3 of these two taxa is similar with a very small posterior loph (T8). The posterior cuspids on m1 and m2 are better developed than in *N. mitchellii* and the anterolabial and anterolingual cuspids on m1 are more equal in size. *Notomys* sp. indet. differs from *N. fuscus* in having a much larger T3 on M1 and in lacking the accessory cusp adjacent to T6. T6 on M2 is relatively larger than in *N. fuscus* and T8 on M3 is rounder in occlusal view. *Notomys fuscus* appears to lack the posterior cuspids on m1 and m2 as seen in *Notomys* sp. indet. and the posterior lophid (entoconid-hypoconid) on m3 is more reduced, relative to the anterior lophid.

A single species of *Notomys* is present and very abundant in the Madura Cave fauna. Fossils of this taxon range in age from approximately 22,000–7,500 BP based on the available C14 data. On the basis of size and dental morphology, *Notomys* sp. indet. can be distinguished from all other species of the genus and perhaps deserves a separate name. Among the rodents in the Madura Cave fauna, *Notomys* sp. indet. is the second most abundant species behind *Leporillus conditor* (Lundelius and Turnbull 1999). Several species of *Notomys* are extant on the Nullarbor Plain and adjacent areas (Boscacci et al. 1987). *Notomys mitchellii* is known from southern Western Australia, southern South Australia, and north-western Victoria. *Notomys alexis* is known from the arid zone in central Australia. *Notomys fuscus* was previously recorded on the Nullarbor, but is now

restricted to eastern South Australia (Baker and Gynther 2023). *Notomys longicaudatus*, although now probably extinct, was previously widespread across the central arid zone north of the Nullarbor Plain. *Notomys cervinus* was identified from Horseshoe Cave on the Hampton Tableland northeast of Madura by Archer (1974) while the range is now restricted to the Lake Eyre Basin of South Australia and south-western Queensland (Baker and Gynther 2023).

Genus *Leporillus* Thomas 1906

Specimens of the genus *Leporillus* are abundant. *Leporillus conditor* is represented by ~1,800 specimens from all stratigraphic units, including Unit 7, and all trenches, including Trench 5. *Leporillus apicalis* is much less abundant and is only known from Units 1–2 in Trenches 1–4. The *Leporillus* material has been described in an earlier publication (Lundelius and Turnbull 1999) and is not repeated here.

Order Lagomorpha Brandt, 1855

Genus *Oryctolagus* Lilljeborg, 1871

Oryctolagus cuniculus (Linnaeus,1758)

MATERIAL EXAMINED

TMM 41106-29, partial left dentary p3–4. This specimen was recovered from the surface of the cave floor.

DISCUSSION

TMM 41106-29 demonstrates that at least some of the surface material is 'recent' in age. Following the introduction from Europe, rabbits spread across the Nullarbor Plain in the 19th century. They were reported at Eucla in 1894 (Long 1974) and at Eyre on the Roe Plain in 1896 (Mason 1897; Brooker 1977).

Order Carnivora Bowdich, 1821

Family Canidae Fischer de Waldheim, 1817

Genus *Canis* Linnaeus, 1758

Canis familiaris Linnaeus, 1758

(Figure 22)

MATERIAL EXAMINED

TMM 41106-21, R dentary c, p1–4, m1–2, alveoli for m3 and i1–3. Collected from the floor surface in Madura Cave.

DESCRIPTION

The dentary is elongate, deepest beneath m1 and has the usual form of a long jawed canid (Figure 22). There is a pronounced masseteric fossa that extends posteriorly, from beneath the m3 to the condyle. The pit shallows gently in an arc-shaped bend, about at the level of the condyle. The coronoid process is rounded, and extends above the condyle for about the same distance as the condyle is above the bottom of the angular process. The angular process is stout and extends posteriorly for about one cm to end just beneath the condyle. There is a thin, sharp ridge along its ventral edge. A shallow smooth fossa lies on its dorso-lingual surface. This fossa is bounded by a ridge that forms the lower part of the angular notch. It is bounded lingually by a sharp ridge that extends from the posterior end of the process to the lingual surface of the dentary below and behind the mandibular foramen. The mandibular foramen is slit-like. The mental foramen is oval, and is situated midway to the ventral edge of the dentary beneath p1 and p2.

The teeth of this adult show moderate wear. Alveolar length from the front of p1 to the rear of the alveolus of m3 is 73 mm. Other dental measurements include: c = 10.0 mm (l), 7.6 mm (w); p1= 4.1 mm (l); p2 = 8.8 mm (l); p3 = 9.6 mm (l); p4 = 11.9 mm (l); m1= 21.0 mm (l); m2 = 9.5 mm (l).

On the lingual side of the dentary, the symphysis provided a ligamentous attachment for its counterpart and extends back to the level of the rear of p2. The coronoid process is thickest anteriorly and thins posteriorly. It is gently recurved, and its hooked posterior end reaches back to the front of the condyle. The angular process is deflected lingually and there is a distinct scar for the internal pterygoid muscle. The deep temporalis attachment scar covers the medial face of the coronoid process to its base at the level of the alveolar margin, and extends nearly to the anteromedian edge of the condyle.

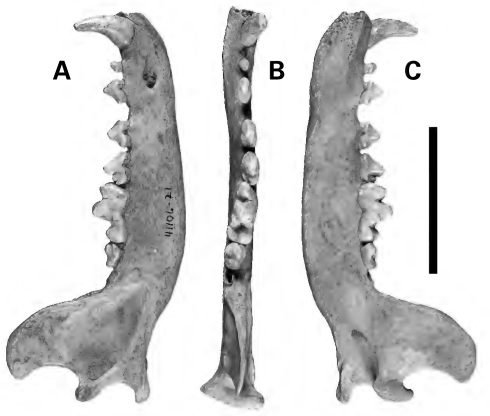

FIGURE 22 *Canis familiaris* (TMM 41106-21), R dentary with c, p1–4, m1–2, alveoli for m3 and i1–3; A) labial view; B) occlusal view; C) lingual view. Anterior up. Scale = 50 mm.

There are four small diastemae: between p2 and p3 is the largest, followed in descending size by c and p1, then p1 and p2, and by a minute one between p3 and p4.

DISCUSSION

The differentiation of dingo from domestic dogs is difficult and the subject of some debate. Eleven skull characters have been used to separate the two canids (Macintosh 1975). The depth of the medial fossa of the angular process and the diastema between the p2 and p3 are from the dentary. The diastema between p2 and p3 was present in all dingoes examined by Macintosh (1975) and was absent in all domestic dogs examined by him. A survey of 15 domestic dog skulls in the TxVP collection showed that 4 had a p2–p3 diastema, but not as well developed as in the Madura Cave specimen. The depth of the medial fossa of the angular process in the TxVP sample of domestic dogs was variable.

In summary the Madura Cave specimen has a very well-developed diastema between the p2 and p3. The medial fossa on the angular process is distinct but, since Macintosh (1975) did not describe criteria for scoring its development, it cannot be reliably compared. The mandibular foramen is slit–shaped in TMM 41106-21, differing from the TxVP sample of dogs. In view of these characters, we conclude that the Madura Cave specimen is a dingo. Additional dingo specimens from within the stratigraphic section in the Southern Tunnel of Madura Cave (see Figure 2), are the oldest known record of dingos from Australia based on C14 (AMS) dates (Balme et al. 2018).

Order Chiroptera Blumenbach, 1779

A small number of specimens, identified as bats, were found in the excavations in Madura Cave. Based on size, all of the material is identified as Yangochiroptera. Six specimens include partial skulls, maxillae and upper dentitions with a sufficient suite of morphological characters to permit identification. Size and morphology suggest that all of the upper dentitions are from a single species. A group of dentaries and lower dentitions is associated with this taxon based on size, although no uppers and lowers were found in clear association. At least one additional taxon is significantly larger, but represented only by dentaries and lower dentitions of unremarkable character. Fossil bats were recovered from multiple trenches, and are most common in stratigraphic Units 1 and 2. Two isolated teeth of Yangochiroptera indet. were recovered from Trench 4, Unit 4–5. Dental terminology follows Martinez (2010). Dental measurements for the Madura Cave bats were made with an reticle for single teeth and with calipers for multi-tooth dimensions.

Suborder Yangochiroptera Springer et al. 2001

Family Vespertilionidae Gray, 1821

Genus *Chalinolobus* Peters,1866

Chalinolobus sp. cf. *morio* (Gray, 1841)

(Figures 23–25, Tables 11–12)

MATERIAL EXAMINED

12 specimens (see Appendix 1).

DESCRIPTION

Specimens of a small bat are characterised by having a single, small alveolus for P2 situated lingually between C and P4. P1 and P3 are absent. The hypocone is reduced and the metacone is large especially on M1. M3 is relatively large (Figure 23). Lower molars are myotodont (hypoconulid isolated from postcristid). The mental foramen is located on the labial side of the dentary beneath the canine and p3.

TABLE 11 Dimensions in mm of upper cheek teeth for *Chalinolobus* sp. cf. *morio*. Estimates based on alveoli designated with 'a'.

Specimen	P4 l	P4 w	M1–3	M1 l	M1 w	M2 l	M2 w	M3 l	M3 w
PM 6076 L	0.82	1.18	-	1.41	1.39	-	-	-	-
PM 6076 R	0.87	1.02	3.19	1.26	1.21	1.22	1.36	1.26	1.41
TMM 41106-485	0.80	1.14	3.13a	1.30a	1.34a	1.36	1.55	1.40	1.62
PM 61077 L	1.04	1.13	3.11a	-	-	1.34	1.36	1.34	1.40
PM 61077 R	0.85	1.10	3.11	1.32	1.27	1.29	1.44	1.32	1.41
PM 61054	0.932	1.18	3.33	1.46	1.36	1.40	1.55	1.29	1.49
Mean	0.89	1.13	3.21	1.36	1.31	1.32	1.45	1.32	1.47
SD	0.09	0.06	0.11	0.09	0.08	0.07	0.10	0.05	0.09

TABLE 12 Dimensions in mm of lower cheek teeth for *Chalinolobus* sp. cf. *morio*. Estimates based on alveoli designated with 'a'.

Specimen	m1–3 l	m1 l	m2 l	m3 l
TMM 41106-484	3.55	1.35	1.24	1.26
PM 61032	3.11a	0.98a	1.23	-
PM 61033	3.10a	1.10a	1.18	0.82a
PM 61034	3.19a	1.16a	1.20	0.98a
PM 61035	3.07a	0.95a	1.01a	0.88a
PM 61046	3.12a	1.03a	1.03a	0.89a

DISCUSSION

A small bat from the Madura Cave fauna is represented by 12 specimens, including both upper and lower dentitions. P2 is has fallen out in all specimens, but is represented by a single, small alveolus positioned lingually between C and P4. This character is observed in vespertilionid bats belonging to the genera *Chalinolobus*, *Pipistrellus* and *Falsistrellus*. Other Microchiropoterans are known to have reduced P2, such as *Tadarida*, *Chaerephon*, *Emballonura*, *Hipposideros, Rhinolophus* and *Rhinonicteris.* All specimens of these taxa, that we examined, have the P2 situated labially rather than lingually.

Additional characters of the upper molars, and the size of these specimens, compare well with

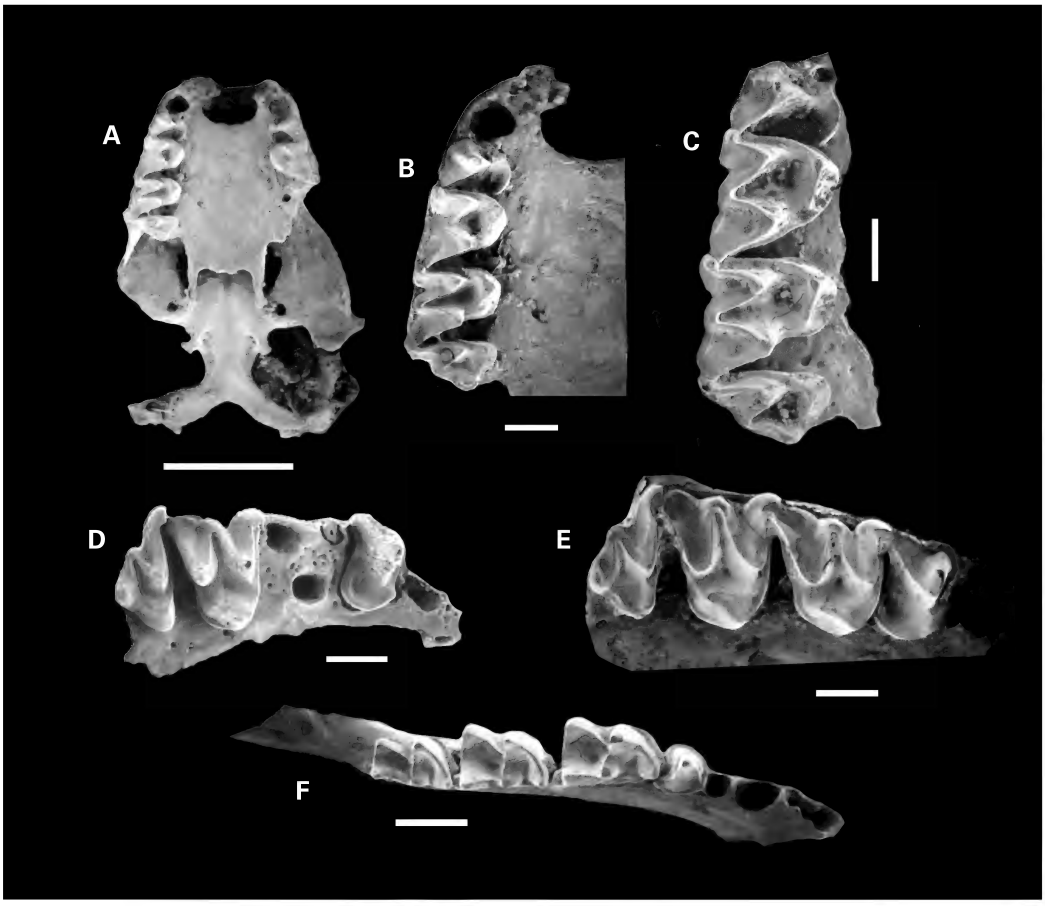

FIGURE 23 *Chalinolobus* sp. cf. *morio*: A) PM 6076, Trench 1, Unit 1, partial skull, palatal view, anterior to top (scale: 5 mm); B) PM 6076, occlusal view right P4–M3, anterior to the top, scale= 1 mm; C) PM 61054, Trench 4, Unit 2, R maxilla with alveolus for P2, P4–M3, anterior to the top, scale= 1 mm; D) TMM 41106-485, right maxilla with P4, M2–3, anterior to the right, scale= 1 mm; E) PM 61077, Trench 1, Unit 1, partial right maxilla with occlusal view of P4–M3, anterior to the right, scale= 1 mm; F) TMM 41106-484, Trench 2, Unit 1, L dentary with p4–m3, anterior to the right, scale = 1 mm. (SEM images).

Chalinolobus morio. The size is also similar to *C. picatus*, but the palate of *C. picatus* has broad transverse grooves and ridges while the palate of *C. morio* and *C. gouldii* are smooth. The Madura Cave specimens have smooth palates (Figure 23). *Chalinolobus morio* is smaller than *C. gouldii* and both M1 and M2 are more triangular, due to the smaller hypocone. *Chalinolobus* was described by Miller (1907) as lacking a hypocone, however, the hypocone is variably developed in extant species and its presence was noted in *C. gouldii*, *C. dwyeri*, and *C. morio* by Martinez (2010). The Madura Cave specimens fall in the M1 length range of *C. morio* and *C. dwyeri*, but are longer than *C. picatus* (Figure 24). The l x w trend is different from the modern species of *Chalinolobus,* with the M1 being narrower relative to length. *Chalinolobus dwyeri* is only distinguished dentally from *C. morio* and *C. picatus* by size (Martinez, 2010). The dimensions of the lower cheek teeth of *Chalinolobus* sp. cf. *morio* are similar to *C. morio* and *C. picatus* (Figure 25).

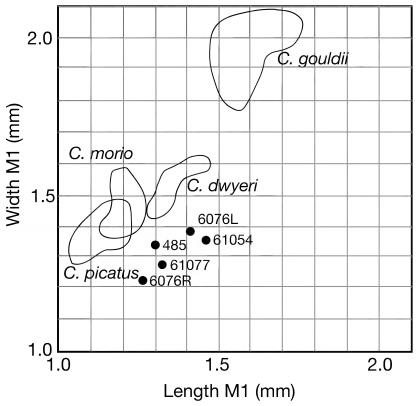

FIGURE 24 Measurements for M1 of *Chalinolobus* sp. cf. *morio* from Madura Cave (dots with specimen numbers). Enclosed regions illustrate the range of M1 dimensions for species of *Chalinolobus* from Martinez (2010).

Boscacci et al. (1987) recorded eight species of bats on the Nullarbor Plain including *Chalinolobus morio* and *Chalinolobus gouldii*. The current range of *Chalinolobus morio* includes southern Western Australia, south-eastern Australia, Tasmania, and isolated areas through the central part of the country. The current range of *Chalinolobus dwyeri* includes south-eastern Queensland and north-eastern New South Wales. It was recognised in the Pleistocene Mount Etna fauna of eastern-central Queensland (Martinez 2010).

***Yangochiroptera* sp. indet.**

(Figure 26, Table 13)

MATERIAL EXAMINED

Four specimens (see Appendix 1).

DESCRIPTION

Four dentaries, with partial lower dentitions, loosely cluster in a size range significantly larger than *Chalinolabus morio* (Figure 25, Table 13). All lower molars are myotodont with no outstanding characters. The mental foramen is located on the labial side of the dentary beneath the canine and p3. The most complete specimen is PM 6078, which has a sub-cylindrical articular condyle that tapers slightly medially (Figure 26).

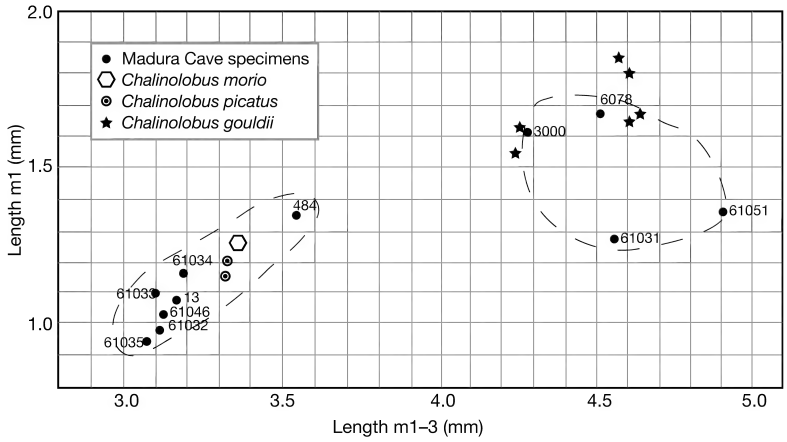

FIGURE 25 Bivariate plot of m1 length vs m1–3 length for bats from Madura Cave. Madura Cave specimens are numbered and shown by solid dots. Values for specimens of *Chalinolobus morio, Chalinolobus picatus,* and *Chalinolobus goudii* as per embedded legend.

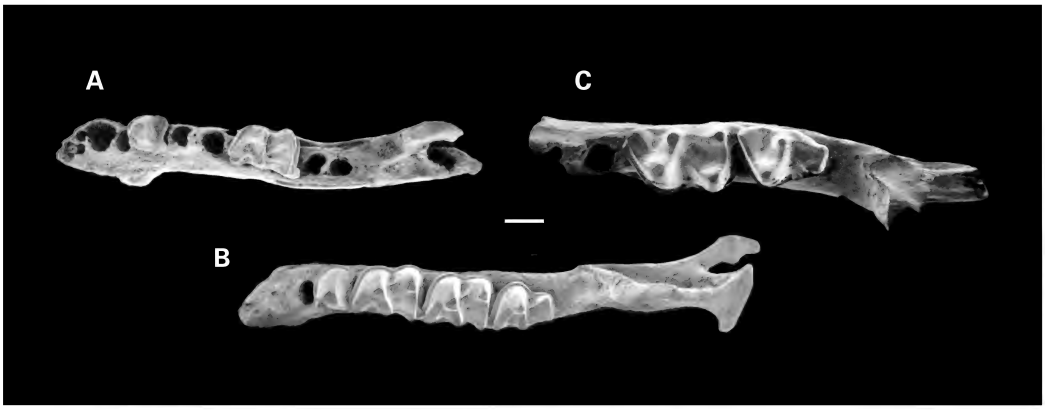

FIGURE 26 *Yangochiroptera* sp. indet., dentaries and lower dentitions: A) PM 61031, R dentary with p4 and m2; B) PM 6078, R dentary with p4–m3; C) PM 61051, partial L dentary with m2–3. Anterior to the left in all. Scale = 1 mm. (SEM images).

DISCUSSION

At least two taxa of yangochiropteran bats were present in the Madura Cave fauna from about 22,000 to 7,500 BP. *Chalinolobus morio* is still found in the area (Boscacci et al. 1987). A second taxon, represented only by lower dentitions, partially overlaps the size range of *C. gouldii*, but, lacking associated upper dentitions, we offer no identification. There is a significant range in size of these lower dentitions, as shown in Figure 26. Based on comparison of Figure 26 with specimens in the collection at WAM, N.L. McKenzie (pers. comm. 2025) has suggested that PM 6078 and PM 61031 represent two different species of *Nyctophilus*, while PM 61051 is an example of the molossid *Austronomus*.

TABLE 13 Measurements in mm for *Yangochiroptera* sp. indet. Estimates based on alveoli designated with 'a'.

Specimen	m1–3 l	m1 l	m2 l	m3 l
PM 6078	4.51	1.66	1.65	1.47
PM 61051	5.10a	1.35a	1.95	1.51
PM 61031	4.55a	1.27a	1.82	1.23a
TMM 41106-3000	4.29	1.61	1.46	1.36

GENERAL DISCUSSION

Sedimentary strata in the Northern Tunnel of Madura Cave span at least the last 38,000 years. The limestone floor of the cave was never reached during excavations. The stratigraphy is complex and lithostratigraphic correlation between nearby trenches is difficult. The sedimentary strata within the cave were deposited through a combination of ephemeral stream deposits and cave collapse. Our trenches did not encounter material dated between 7,500 BP and the present time, other than the surface specimens. The post-7,500 BP gap may be partly represented by archaeological excavations in the Southern Tunnel (Milham and Thompson 1976). Most of the taxa, mentioned from the Southern Tunnel, are the same as those identified from the Northern Tunnel, with the addition of the macropodid *Osphranter rufus* ('*Megaleia rufa*'). The rabbit and dingo specimens were found on the present floor of the cave. Additional work, on other dingo material from shallow deposits in the Southern Tunnel of Madura Cave, yielded age estimates based on C14 (AMS) of approximately 3,250 BP (Balme et. al. 2018).

The Madura Cave strata contain remains of vertebrates that provide a record of the fauna living on the Roe Plain during the late Pleistocene and early Holocene. The marsupials and one genus of rodent were reported earlier and we now add the remaining placental record. Included are five additional species of rodents, two of bats, one each of *Oryctolagus* and *Canis*. Most of the rodents and bats, were recovered from Units 1 and 2 (Holocene and Pleistocene). The record of *Notomys* sp. indet. continues back to Unit 4–5. *Pseudomys desertor* is apparently absent from Unit 1, but present in Units 2–7 extending back to ~38,000 BP.

As the final chapter of our work on the Madura Cave fauna, it is useful to review the entire faunal list. The marsupials were summarised by Lundelius and Turnbull (1989). The faunal list (Table 14) has been updated for taxonomic changes that have occurred in the past 35 years. It also includes the placental mammals bringing the total number of taxa to 49.

TABLE 14 Fossil mammal fauna from the Northern Tunnel of Madura Cave, Western Australia. R: recent fauna of the Nullarbor Plain; Unit 1: Holocene (~7,500 BP); Units 2–3: ~5,000–22,000 BP; Units 4–5: ~22,000–30,000 BP; Units 6–7: ~38,000 BP.

[1] *Antechinomys spenceri* in Lundelius and Turnbull (1975).
[2] *Dasyuroides byrnei* in Lundelius and Turnbull (1978) according to Newman-Martin et al. (2023),
[3] *Isoodon obesulus* in Lundelius and Turnbull (1981) according to Travouillon and Phillips (2018),
[4] *Caloprymnus campestris* in Lundelius and Turnbull (1984) according to McNamara (1997),
[5] *Bettongia penicillata* in Lundelius and Turnbull (1984) according to Haouchar et al. (2016),
[6] *Macropus robustus* in Lundelius and Turnbull (1989),
[7] *Megaleia rufa* in Milham and Thompson (1976).

Order	Family	Taxon	R	1	2–3	4–5	6–7
Dasyuromorphia	Dasyuridae	cf. *Planigale* sp.			●	●	●
		Sminthopsis crassicaudata	●	●	●	●	●
		Sminthopsis murina group		●	●	●	●
		Antechinomys laniger[1]		●	●	●	●
		Antechinus flavipes			●	●	●
		Phascogale calura		●	●	●	
		Phascogale tapoatafa		●	●		
		cf. *Parantechinus apicalis*		●			
		Dasycercus cristicauda		●	●	●	●
		Dasycercus archeri[2]		●	●	●	●
		Dasyurus geoffroii		●	●	●	●
		Sarcophilus harrisii		●	●		
	Thylacinidae	*Thylacinus cynocephalus*			●		
	Myrmecobiidae	*Myrmecobius fasciatus*		●			
Peramelemorphia	Peramelidae	*Perameles* sp. indet.	●	●	●	●	●
		Isoodon fusciventer[3]		●	●	●	●
	Chaeropodidae	*Chaeropus ecaudatus*		●	●	●	●
	Thylacomyidae	*Macrotis lagotis*		●	●	●	●
Diprotodontia	Thylacoleonidae	*Thylacoleo* sp.		●			
	Vombatidae	*Lasiorhinus* sp. cf. *latifrons*	●		●	●	●
	Phascolarctidae	*Phascolarctos cinereus*		●			
	Phalangeridae	*Trichosurus vulpecula*			●		
	Pseudocheiridae	*Pseudocheirus peregrinus*			●		
	Burramyidae	*Cercartetus concinnus*	●		●	●	●
	Potoroidae	*Potorous platyops*		●	●	●	●
		Bettongia pusilla[4]		●	●	●	●
		Bettongia lesueur		●	●		
		Bettongia penicillata Clade I[5]		●	●	●	
	Macropodidae	*Sthenurus* sp. indet.			●	●	
		Lagorchestes hirsutus		●	●	●	
		Lagostrophus fasciatus		●	●		
		Onychogalea lunata		●	●		
		Protemnodon sp. indet.			●		
		Petrogale sp. indet.		●	●		
		Macropus fuliginosus	●	●			
		Macropus titan			●	●	●
		Osphranter robustus[6]	●		●	●	
		Osphranter rufus[7]	●	●			

Order	Family	Taxon	R	1	2–3	4–5	6–7
Rodentia	Muridae	*Leporillus conditor*		●	●	●	●
		Leporillys apicalis		●	●		
		Pseudomys bolami	●	●	●		
		Pseudomys gouldii		●	●		
		Pseudomys australis		●	●		
		Pseudomys sp. cf. *desertor*			●	●	●
		Notomys sp. indet.		●	●	●	
Chiroptera	Vespertilionidae	*Chalinolobus* sp. cf. *morio*	●	●	●		
		Yangochiroptera sp. indet.		●	●	●	
Carnivora	Canidae	*Canis familiaris*	●				
Lagomorpha	Leporidae	*Oryctolagus cuniculus*	●				

Based on analysis of the marsupial fauna, Lundelius and Turnbull (1989) interpreted the major change in faunal composition to have occurred between the Pleistocene (Units 2–7) and Holocene (Unit 1). Much of the change was interpreted to predate environmental perturbations associated with European settlement. However, Simpson Similarity Indices (Simpson 1960) have now been calculated for the same stratigraphic groupings defined in Lundelius and Turnbull (1989) utilising the entire Madura Cave faunal list (except for the rabbit and dingo).

The Simpson Similarity Indices for faunal comparison between Units 6–7 vs Units 4–5, and between Units 4–5 vs Units 2–3 are very high (100%). The similarity index between Unit 1 and Unit 2–3 is 83%, indicating significant change, but a high degree of similarity between the Pleistocene and Holocene faunas. Taxa present in the Pleistocene, but apparently absent from the early Holocene, include cf. *Planigale, Antechinus flavipes*, *Thylacinus cynocephalus*, *Myrmecobius fasciatus*, *Lasiorhinus* sp. cf. *latifrons*, *Cercartetus concinnus, Sthenurus* sp., *Protemnodon* sp., *Osphranter robustus,* and *Pseudomys* sp. cf. *desertor*. Three of these taxa are known from the present Nullarbor Plain fauna suggesting that their absence in Unit 1 may have been a preservation/sampling issue. In that case, the faunal change from Units 2–3 to Unit 1, would be even less dramatic. Based on the entire faunal list, faunal change had begun during the transition from the Pleistocene to Holocene. However, the most significant change in the Madura Cave area occurred between the early Holocene and present faunas. A Simpson Similarity Index of ~43% is calculated between Unit 1 and the present fauna of the Nullarbor Plain based on restricting the present taxon count to current known ranges (Boscacci et al. 1987; Baker and Gynther 2023).

Mammalian diversity within the Madura Cave fauna was much higher than in the present fauna of the Nullarbor Plain. Approximately 20% of the taxa known from the Madura Cave sedimentary units are now extinct. Forty percent are threatened, according to the IUCN 3.1 classification, and have limited ranges that do not include the Nullarbor Plain. Boscacci et al. (1987) noted minor differences in faunal composition between the Nullarbor Plain and the Roe Plain.

The placental mammals contribute little to our understanding of factors influencing faunal evolution in the Madura Cave area. *Chalinolobus morio* is known through large parts of Australia and roosts in trees as well as caves (Baker and Gynther 2023). The species of *Notomys* recovered from Madura Cave cannot be confidently identified as any of the extant species. The current range of *Pseudomys bolami* includes the arid lands of the Nullarbor Plain, however, *P. desertor* is now restricted to the arid and semi-arid central parts of Australia and north into the dry-tropical savannas (Baker and Gynther 2023). The absence of *P. desertor* from Unit 1 may indicate a change in local environment near the Pleistocene – Holocene boundary. However, *P. desertor* is very rare in the Madura Cave fauna and may never have been present in significant numbers. *Pseudomys gouldii*, although once widespread across southern Australia, is now found naturally on a single island in Shark Bay, Western Australia (Roycroft et al. 2021). The current range of *P. australis* is restricted primarily to the eastern half of South Australia, although records indicate a prior distribution along coastal areas of the Great Australian Bight (Baker and Gynther 2023). Abundance and distribution of *P. australis* has been correlated with changes in food resources associated with rainfall events, as well as predation by feral cats and red foxes (Pavey et al. 2014). There is no consistent, climate-change related pattern reflected in the geographic ranges of fossil placental mammals from Madura Cave. Higher aridity in the late Pleistocene – early Holocene may be consistent with the relatively small sizes of some of the Madura Cave rodents (e.g. *Pseudomys australis*, *Notomys* sp. indet.) and the presence of *Pseudomys* sp. cf. *desertor*. The climate of the Nullarbor Plain was more arid in the late Pleistocene compared to the late Holocene, based on interpretation of mammals from Allen's Cave by Baynes (1994).

The rodent ranges have almost certainly been influenced by habitat destruction imposed by European settlement, agriculture, and introduced predators (Baynes 1979; Burbidge and McKenzie 1989; Vakil et al. 2023). The rapid loss of mammal diversity documented at Madura Cave between the early Holocene and present day is similar to other records from southern Australia (Bilney et al. 2010; McDowell and Medlin 2010, Start et al. 2011; Fusco et al. 2016).

ACKNOWLEDGEMENTS

We gratefully acknowledge the encouragement, support, and collecting assistance given by J. Lundelius and P. Turnbull; without their help the work could not have been completed. J. Lundelius Welch provided much appreciated assistance in surveying Madura Cave. The original fieldwork was supported in part by a grant from the National Science Foundation (GB975), and others from the Geological Foundation, University of Texas, and from Field Museum. The Foundation further supported Lundelius on a study trip to Field Museum. We thank A. Baynes of the Western Australian Museum for assistance in help identifying species of *Pseudomys*, for allowing access to material, and for information on the distribution of Australian rodents. J. Cramb provided valuable assistance to May regarding identification of *Pseudomys* and *Notomys*. M. McDowell helped with additional information on Australian rodents. J. Maissano produced the CT volumes at the University of Texas High Resolution X-ray CT Facility in the Jackson School of Geoscience. B. Strack operated the Scanning Electron Micrscope at the Unviersity of Chicago, L. Grove assisted with art work, M. Widhalm assissted with photography and L. Kannelos helped with data analysis. A. Thompson helped with developing specimen figures. C. Sagebiel helped with access to specimens at the Texas Vertebrate Paleontology Collections. M. Brown helped with access to archival material.

The manuscript has been significantly improved by reviews from A. Baynes, J. Cramb, D. Fusco, M. May, and M. McDowell. A. Baynes provided much appreciated guidance in the preparation of the manuscript.

REFERENCES

AMTC (2024). The Australian Mammal Taxonomy Consortium Australian Mammal Species List (Version 4.2). [accessed November 2024]. https://australianmammals.org.au/publications/amtc-species-list

Archer, M. (1974). New information about the Quaternary distribution of the thylacine (Marsupialia, Thylacinidae) in Australia. *Journal of the Royal Society of Western Australia* **57**: 43–51.

Baker, A.M. and Gynther, I.C. (eds) (2023). *Strahan's mammals of Australia*. Fourth edition. Bloomsbury Publishing: London, United Kingdom, 848 pp.

Balme, J, O'Connor, S., and Fallon, S. (2018). New dates on dingo bones from Madura Cave provide oldest firm evidence for arrival of the species in Australia. *Scientific Reports* **8**: 9933. doi: 10.1038/s41598-018-28324-x

Baynes, A. (1979). The Analysis of a Late Quaternary mammal fauna from Hastings Cave, Jurien. Unpublished PhD thesis, University of Western Australia: Perth.

Baynes, A. (1987). The original mammal fauna of the Nullarbor and southern peripheral regions: evidence from skeletal remains in superficial deposits. In: McKenzie N.L. and Robinson A.C. (eds), *A biological survey of the Nullarbor Region South and Western Australia in 1984*. South Australian Department of Environment and Planning, Western Australian Department of Conservation and Land Management, Australian National Parks. pp: 139–152.

Baynes, A. (1994). A concise report on the analysis of mammal material from the E4 excavation in Allen's Cave. Appendix I. In: Walshe, K.A. (ed.), *A taphonomic analysis of the vertebrate assemblage from Allen's Cave: implications for Australian arid zone archaeology*. Unpublished Ph.D. thesis. Australian National University: Canberra, ACT.

Baynes, A., Piper, C.J., and Thorn, K.M. (2019). An experimental investigation of differential recovery of native rodent remains from Australian palaeontological and archaeological deposits. *Records of the Western Australian Museum* **34**(1): 1–30. doi: 10.18195/issn.0312-3162.34(1).2019.001-030

Bilney, R.J., Cooke, R., and White, J.G. (2010). Underestimated and severe: small mammal decline from the forests of south-eastern Australia since European settlement, as revealed by a top-order predator. *Biological Conservation* **143**(1): 52–59. doi: 10.1016/j.biocon.2009.09.002

Blumenbach, J.F. (1779). *Handbuch der Naturgeschichte*. J.C. Dieterich: Göttingen, Germany. 559 pp.

Boscacci, L.J., McKenzie, N.L., and Kemper, C.M. (1987). Mammals. In: McKenzie, N.L. and Robinson, A.C. (eds), *A biological survey of the Nullarbor Region South and Western Australia in 1984*. South Australian Department of Environment and Planning, Western Australian Department of Conservation and Land Management, and Australian National Parks and Wildlife Service. Adelaide: South Australia. pp: 103–137.

Bowdich, T.E. (1821). *An analysis of the natural classifications of Mammalia, for the use of students and travelers*. J. Smith: Paris, France. 115 pp.

Brandt, J.F. (1855). Untersuchungen €uber die craniologischen Entwicklungsstufen und Classification der Nager der Jetzwelt. *Memoires de l'Acad emie imp eriale des sciences de St Petersbourg* **6**: 1–365.

Brooker, M.G. (1977). Some notes on the mammalian fauna of the western Nullarbor Plain, Western Australia. *The West Australian Naturalist* **14**(1): 2–15.

Burbidge, A.A. and McKenzie, N.L. (1989). Patterns in the modern decline of Western Australia's vertebrate fauna: causes and conservation implications. *Biological Conservation* **50**: 143–198.

Fischer de Waldheim, G. (1817). Adversaria zoological. *Memoir Societe Naturelle (Moscow)* **5**: 368–428.

Fusco, D.A., McDowell, M.C., and Prideaux, G.J. (2016). Late-Holocene mammal fauna from southern Australia reveals rapid species declines post-European settlement: Implications for conservation biology. *The Holocene* **26**: 699–708. doi: 10.1177/0959683615618261

Gray, J.E. (1821). On the natural arrangement of vertebrose animals. *London Medical Repository* **15**(1): 296–310.

Haouchar, D., Pacioni, C., Haile, J., McDowell, M.C., Baynes, A., Phillips, M.J., Austin, J.J., Pope, L.C., and Bunce, M. (2016). Ancient DNA reveals complexity in the evolutionary history and taxonomy of the endangered Australian brush-tailed bettongs (*Bettongia*: Marsupialia: Macropodidae: Potoroinae). *Biodiversity and Conservation* **25**: 2907–2927. doi: 10.1007/s10531-016-1210-y

Illiger, J.K.W. (1811). *Prodomus Systematis Mammalium et Avium Additis Terminis Zoographicis Utriusque Classis, Eorumque Versione Germanica. Sumptibus C.* Salfeld: Berolini [Berlin], Prussia. 327 pp.

James, N.P., Bone, Y., Carter, R.M. and Murray-Wallace, C.V. (2006). Origin of the Late Neogene Roe Plains and their calcarenite veneer: implications for sedimentology and tectonics in the Great Australian Bight. *Australian Journal of Earth Sciences* **53**: 407–419. doi: 10.1080/08120090500499289

Kitchener, D.J., Adams, M., and Baverstock, P. (1984). Redescription of *Pseudomys bolami* Troughton, 1932 (Rodentia: Muridae). *Australian Mammalogy* **7**: 149–159.

Lilljeborg, W. (1873). *Sveriges Og Norges Ryggradsdjur. 1: Däggdjuren*. Upsala: Berling, Sweden. pp: 417.

Linnaeus, C. (1758). *Systema naturae per regna tria naturae: secundum classes, ordines, genera, species, cum characteribus, differentiis, synonymis, locis. Volume 1.* Laurentii Salvii: Holmiae, Sweden. pp: 42.

Long, J.L. (1974). 'Introduced birds and mammals in Western Australia.' Technical Series 1. Agricultural Protection Board of Western Australia. Perth.

Lundelius, E.L. (1963). Vertebrate remains from the Nullarbor caves. *Journal of the Royal Society of Western Australia* **46**: 75–80.

Lundelius, E.L. and Turnbull, W.D. (1973). The mammalian fauna of Madura Cave, Western Australia. Part I. *Fieldiana: Geology* **31**(1): 1–35.

Lundelius, E.L. and Turnbull, W.D. (1975). The mammalian fauna of Madura Cave, Western Australia. Part II. *Fieldiana: Geology* **31**(2): 37–117.

Lundelius, E.L. and Turnbull, W.D. (1978). The mammalian fauna of Madura Cave, Western Australia. Part III. *Fieldiana: Geology* **38**(1): 1–120.

Lundelius, E.L. and Turnbull, W.D. (1981). The mammalian fauna of Madura Cave, Western Australia. Part IV. *Fieldiana: Geology, New Series* **6**: 1–72.

Lundelius, E.L. and Turnbull, W.D. (1982). The mammalian fauna of Madura Cave, Western Australia. Part V: Diprotodonta (Part). *Fieldiana: Geology, New Series* **11**: 1–32.

Lundelius, E.L. and Turnbull, W.D. (1984). The mammalian fauna of Madura Cave, Western Australia. Part VI, Macropodidae: Potoroinae. *Fieldiana: Geology, New Series* **14**: 1–63.

Lundelius, E.L. and Turnbull, W.D. (1989). The mammalian fauna of Madura Cave, Western Australia. Part VII, Macropodidae: Sthenurinae, Macropodinae, with a review of the marsupial portion of the fauna. *Fieldiana: Geology, New Series* **17**: 1–71.

Lundelius, E.L. and Turnbull, W.D. (1999). *Leporillus* (Rodentia: Muridae) from Madura Cave, Western Australia. *Proceedings of the Linnean Society of New South Wales* **121**: 129–146.

McNamara, J.A. (1997). Some smaller macropod fossils of South Australia. *Proceedings of the Linnean Society of New South Wales* **117**: 97–105.

Macintosh, N.W.G. (1975). The origin of the dingo: an enigma. In: Fox, M.W. (ed), *The wild canids. Their systematics, behavioral ecology and evolution*. Van Nostrand Reinhold Co. Behavioral Science Series. pp: 87–106.

Mahoney, J.A. (1975). *Notomys macrotis* Thomas, 1921, a poorly known Australian hopping mouse (Rodentia: Muridae). *Australian Mammalogy* **1**: 367–374.

Mahoney, J.A., Smith, M.J., and Medlin, G.C. (2008). A new species of hopping-mouse, *Notomys robustus* sp. nov. (Rodentia: Muridae), from cave deposits in the Flinders and Davenport Ranges, South Australia. *Australian Mammalogy* **29**: 117–135. doi: 10.1071/AM07017

Martinez, S. (2010). 'Palaeoecology of the Mount Etna bat fauna, coastal eastern Queensland.' Unpublished Ph.D. dissertation, Queensland University of Technology, Brisbane. 339 pp.

Marun, L.H. (1972). 'The Mirning and their predecessors on the coastal Nullarbor Plain.' Unpublished Ph.D. thesis, University of Sydney, New South Wales.

Mason, A. (1897). 'Report of an expedition in the south-eastern portion of Western Australia, to inquire into a reported incursion of rabbits.' Western Australian Government, Perth.

McDowell, M.C., and Medlin, G.C. (2010). Natural Resource Management implications of the pre-European non-volant mammal fauna of the southern tip of Eyre Peninsula, South Australia. *Australian Mammalogy* **32**: 87–93. doi: 10.1071/AM09020

Miller, G.S. (1907). The families and genera of bats. *United States National Museum Bulletin* **57**: 1–282.

Milham, P. and Thompson, P. (1976). Relative antiquity of human occupation and extinct fauna at Madura Cave, southeastern Western Australia. *Mankind* **10**(3): 175–180.

Musser, G.G., Smith, A.L., Robinson, M.F., and Lunde, D.P. (2005). Description of a new genus and species of rodent (Murinae, Muridae, Rodentia) from the Khammouan Limestone National Biodiversity Conservation Area in Lao PDR. *American Museum Novitates* **3497**: 31 pp.

Newman-Martin, J., Travouillon, K.J., Warburton, N., Barham, M., and Blyth, A.J. (2023). Taxonomic review of the genus *Dasycercus* (Dasyuromorphia: Dasyuridae) using modern and subfossil material; and the description of three new species, *Alcheringa: An Australasian Journal of Palaeontology* **47**: 624–661. doi: 10.1080/03115518.2023.2262083

Pavey, C.R., Cole, J.R., McDonald, P.J., and Nano, C. (2014). Population dynamics and spatial ecology of a declining desert rodent, *Pseudomys australis*: the importance of refuges for persistence. *Journal of Mammalogy* **95**(3): 615–625. doi: 10.1644/13-MAMM-A-183

Peters, W. (1866). Über neue oder ungengend bekannte Flederthiere (Vampyrops, Uroderma, Chiroderma, Ametrida, Tylostoma, Vespertilio, Vesperugo) und Nager (Tylomys, Lasiomys). *Monatsberichte der Königlich Preussischen Akademie der Wissenschaften zu Berlin* **1867**: 392–411.

Roycroft, E., MacDonald, A.J., Moritz, C., Moussalli, A., Portela Miguez, R., and Rowe, K.C. (2021). Museum genomics reveals the rapid decline and extinction of Australian rodents since European settlement. *Proceedings of the National Academy of Sciences of the United States of America* **118**(27): 1–8. doi: 10.1073/pnas.2021390118

Simpson, G.G. (1960). Notes on the measurement of faunal resemblance. *American Journal of Science* **258**(A): 300–311.

Springer, M.S., Teeling, E.C., Madsen, O., Stanhope, M.J., and de Jong, W.W. (2001). Integrated fossil and molecular data reconstruct bat echolocation. *Proceedings of the National Academy of Sciences of the United States of America* **98**: 6241–6246. doi: 10.1073/pnas.111551998

Start, A.N., Burbidge, A.A., McDowell, M.C., and McKenzie, N.L. (2011). The status of non-volant mammals along a rainfall gradient in the south-west Kimberley, Western Australia. *Australian Mammalogy* **34**(1): 36–48. doi: 10.1071/AM10026

Thomas, O. (1906). On the generic arrangement of the Australian rats hitherto referred to *Conilurus*, with remarks on the structure and evolution of their molar cusps. *The Annals and Magazine of Natural History, Series 7,* **17**: 81–85.

Travouillon, K.J. and Phillips, M.J. (2018). Total evidence analysis of the phylogenetic relationships of bandicoots and bilbies (Marsupialia: Peramelemorphia): reassessment of two species and description of a new species. *Zootaxa* **4378(**2): 224–256. doi: 10.11646/zootaxa.4378.2.3

Troughton, E. le G. (1932). On five new rats of the genus *Pseudomys*. *Records of the Australian Museum* **18**: 18–23.

Vakil, V., Cramb, J., Price, G., Webb, G., and Louys, J. (2023). Conservation implications of a new fossil species of hopping-mouse, *Notomys magnus* sp. nov. (Rodentia: Muridae), from the Broken River Region, northeastern Queensland, *Alcheringa: An Australasian Journal of Palaeontology* **47**(4): 590–601. doi: 10.1080/03115518.2023.2210192

Waddell, P.A., Gardner, A.K., and Hennig, P. (2010). 'An inventory and condition survey of the Western Australian part of the Nullarbor region.' Department of Primary Industries and Regional Development, Western Australia, Perth. Technical Bulletin No. 97.

Waterhouse, G. (1839). *The zoology of the voyage of the H.M.S. Beagle under the command of Captain Fitzroy, R.N., during the years 1823 to 1836. Part II, Mammalia*. Smith, Elder and Co.: London, United Kingdom.

Watts, C. and Aslin, H. (1981). *The Rodents of Australia*. Angus and Robertson: Sydney. 321pp.

MANUSCRIPT RECEIVED 22 JULY 2025; ACCEPTED 13 AUGUST 2025.

APPENDIX 1 Specimens examined in this study.

Specimen	Material examined
Pseudomys bolami	
Trench 1, top 30 cm	
PM 6079	partial skull L, R M1
PM 6080	R maxilla and premaxilla I, M1–3
PM 6081	R maxilla and premaxilla I, M1–3
PM 6082	R maxilla M1–3
PM 6083	R maxilla M1–3
PM 6084	L maxilla M1–3
PM 6085	L maxilla M1–3
PM 6086	L maxilla M1–3
PM 6087	L maxilla M1–3
PM 6088	R maxilla M1–3
PM 6089	L maxilla M1–3
Trench 3, Unit 1	
TMM 41106-450	L edentulous maxilla
TMM 41106-455	L maxilla M3
TMM 41106-466	R maxilla M1
Trench 3, Unit 2, Level 1	
TMM 41106-3790	L maxilla M1–3
Trench 3, Unit 2, Level 2	
TMM 41106-1785	L dentary m1–2
TMM 41106-1786,	L dentary m1
TMM 41106-1788	L dentary i, m1–2
TMM 41106-1789	L dentary m1–2
TMM 41106-1791	L dentary m1–2
TMM 41106-1792	L dentary i, m1
Trench 4, Unit 1, Level 1, top 30 cm	
TMM 41106-3501	L dentary m1
TMM 41106-3502	R dentary m1
TMM 41106-3503	R dentary i, m1–2
TMM 41106-3504	R dentary i, m1–3
TMM 41106-3505	R dentary m1–2
TMM 41106-3507	R dentary i, m1–2
TMM 41106-3508	R dentary i, m1
TMM 41106-3509	L dentary m1
TMM 41106-3510	R dentary m1
TMM 41106-3511	R dentary m1
TMM 41106-3513	L dentary m1–2
TMM 41106-3514	L dentary i, m1–3
TMM 41106-3515	L dentary i
TMM 41106-3516	R dentary m1
TMM 41106-3517	R edentulous maxilla
TMM 41106-3518	R edentulous maxilla
TMM 41106-3519	R maxilla M2
TMM 41106-3520	L maxilla M1–3
Trench 4, Unit 1	
TMM 41106-451	L maxilla M1
TMM 41106-452	L maxilla M1–3
TMM 41106-453	L maxilla M1–2
TMM 41106-454	L maxilla M1–3
TMM 41106-455	L maxilla M3
TMM 41106-456	L maxilla M2
TMM 41106-457	L maxilla M1
TMM 41106-458	L maxilla M1–3
TMM 41106-459	L maxilla M1–2
TMM 41106-460	R maxilla M1–3
TMM 41106-461	L maxilla M1–3
TMM 41106-463	L maxilla M1–3
TMM 41106-464	L maxilla M2
TMM 41106-466	R maxilla M1
TMM 41106-467	R maxilla M1–2
TMM 41106-468	R maxilla M1–2
TMM 41106-469	R maxilla M2
TMM 41106-470	R maxilla M2
TMM 41106-471	R maxilla M2
TMM 41106-472	R maxilla M2
TMM 41106-473	R maxilla M2
TMM 41106-474	R maxilla M2
Trench 4, Unit 2, top 30 cm	
TMM 41106-2995	L dentary i, m1
TMM 41106-2996	R dentary i, m1–3
TMM 41106-2997	R dentary i, m1–2
TMM 41106-2998	L dentary m1–2
TMM 41106-2999	R dentary m1–3
TMM 41106-3521	L maxilla M1–2
Trench 4, Unit 2	
TMM 41106-2990	R dentary i, m1
TMM 41106-2991	R dentary i, m1–2
TMM 41106-2992	L dentary i, m1–3
TMM 41106-2993	L dentary i, m1–3
TMM 41106-2994	R dentary i, m1–3
Pseudomys australis	
Trench 1, Unit 1	
PM 6110	R maxilla and premaxilla I, M1–3
PM 6112	R maxilla M1–2
PM 6113	L maxilla and premaxilla M1–2
PM 6115	L maxilla M1–3
PM 6116	R maxilla M1–2
PM 25364	R maxilla M1–2
TMM 41106-3815	R dentary m1

Specimen	Material examined
Trench 3, Unit 2	
TMM 41106-3543	L maxilla M1
TMM 41106-3545	L maxilla M1
TMM 41106-3546	L maxilla M2–3
TMM 41106-3547	L maxilla M2–3
TMM 41106-3548	L maxilla M3
TMM 41106-3553	L maxilla M1
TMM 41106-3554	L maxilla M1
TMM 41106-3555	L maxilla M1
TMM 41106-3556	L maxilla M1
TMM 41106-3557	L maxilla M2
TMM 41106-3558	L maxilla M1
TMM 41106-3559	L maxilla M1–2
TMM 41106-3560	L maxilla M2
TMM 41106-3561	L maxilla M1
Pseudomys gouldii	
Trench 1, top 30 cm	
PM 6114	L premaxilla and maxilla M1–3
PM 25365	R premaxilla and maxilla I, M3
Trench 1, top 76 cm	
PM 26178	L dentary m1
Trench 3, Unit 1, Level 1	
TMM 41106-1555	R maxilla M1–3
TMM 41106-1556	R maxilla M2–3
TMM 41106-1560	R maxilla M2–3
Trench 3, Unit 2	
TMM 41106-1984	L maxilla M2
TMM 41106-1992	L maxilla M1–2
TMM 41106-3547	L maxilla M2–3
Pseudomys* sp. cf. *desertor	
Trench 3, Unit 2, Level 1	
TMM 41106-2071	R maxilla M2–3
Trench 3, Unit 2, Level 2	
TMM 41106-3551	L edentulous maxilla
Trench 4, Unit 2, top 30 cm	
TMM 41106-3528	L maxilla
TMM 41106-4060	R M1
Trench 4, Unit 2, Level 2	
TMM 41106-4069	R M1
TMM 41106-4072	R M1
TMM 41106-4073	L M1
TMM 41106-4074	L M1

Specimen	Material examined
Trench 4, Unit 3	
TMM 41106-3974	L M1
TMM 41106-3979	R M1
TMM 41106-3984	L M1
Trench 4, Units 4–5	
TMM 41106-3911	R M1
TMM 41106-3912	L M1
TMM 41106-3913	R M1
TMM 41106-3914	R M1
TMM 41106-3915	R M1
TMM 41106-3919	L M1
TMM 41106-3920	L M1
TMM 41106-3922	L M1
TMM 41106-3928	R M1
TMM 41106-3930	L M1
TMM 41106-3933	R M1
TMM 41106-3935	R M1
TMM 41106-3939	L M1
TMM 41106-3940	R M1
TMM 41106-3945	R M1
TMM 41106-3947	R M1
TMM 41106-3948	L M1
TMM 41106-3950	L M1
TMM 41106-3953	R M1
TMM 41106-3956	L M1
TMM 41106-3962	R M1
TMM 41106-3964	L M1
TMM 41106-3965	R M1
TMM 41106-3968	L M2
TMM 41106-4018	L M1
TMM 41106-4019	L M1
TMM 41106-4021	R M1
TMM 41106-4029	R M1
TMM 41106-4030	L M1
TMM 41106-4031	R M1
TMM 41106-4033	L M1
TMM 41106-4035	L M1
TMM 41106-4037	L M1
TMM 41106-4040	L M1
TMM 41106-4041	R M1
TMM 41106-4044	R M1
TMM 41106-4045	L M1
TMM 41106-4046	L M1
TMM 41106-4050	R M1
TMM 41106-4051	R M1
TMM 41106-4057	R M1
Trench 4, Unit 7, Level 2	
TMM 41106-3907	L M1

Specimen	Material examined
***Notomys* sp. indet.**	
Trench 1, top 30 cm	
TMM 41106-3717	R maxilla M1–3
Trench 3, Unit 1	
TMM 41106-442	L dentary m1–2
TMM 41106-443	L dentary m1–3
TMM 41106-444	L dentary m1–2
TMM 41106-445	L dentary m1–3
TMM 41106-449	L dentary m1
TMM 41106-1557	R maxilla M1–3
TMM 41106-1558	R maxilla M1–3
TMM 41106-1559	R maxilla M1–2
TMM 41106-1561	R maxilla M1–3
TMM 41106-1566	R maxilla M1–2
TMM 41106-1569	R maxilla M1–3
TMM 41106-1570	R maxilla M1–3
TMM 41106-1571	R maxilla M1–2
TMM 41106-1578	R maxilla M1–2
TMM 41106-1614	L maxilla M2
Trench 3, Unit 2	
TMM 41106-341	partial skull L and R M1–3
TMM 41106-342	partial skull L and R M1–3
TMM 41106-360	L maxilla M1–3
TMM 41106-1996	L maxilla M3
TMM 41106-1997	L maxilla M2–3
TMM 41106-1998	L maxilla M1–3
TMM 41106-2000	L maxilla M1–3
TMM 41106-2001	L maxilla M3
TMM 41106-2002	L maxilla M1–3
TMM 41106-2003	L maxilla M2–3
TMM 41106-2004	L maxilla M1–3
TMM 41106-2005	L maxilla M1–3
TMM 41106-2006	L maxilla M1–3
TMM 41106-2008	L maxilla M1–2
TMM 41106-2011	L maxilla M1–3
TMM 41106-2012	L maxilla M1–3
TMM 41106-2013	L maxilla M1–2
TMM 41106-2014	L maxilla M1–3
TMM 41106-2015	L maxilla M1–3
TMM 41106-2110	L maxilla M1–3
TMM 41106-2111	L maxilla M1–2
TMM 41106-2112	L maxilla M1–3
TMM 41106-2115	L maxilla M1–3
TMM 41106-2119	L maxilla M1–3
TMM 41106-2120	L maxilla M1–3
TMM 41106-2122	L maxilla M1–3
TMM 41106-2125	L maxilla M1–3
TMM 41106-2179	R maxilla M1–2
TMM 41106-2181	R maxilla M1–2
TMM 41106-2182	R maxilla M2–3
TMM 41106-2183	L maxilla M1–3
TMM 41106-2184	L maxilla M1–3
TMM 41106-2185	R maxilla M1–3
TMM 41106-2187	R maxilla M1–2
TMM 41106-2188	R maxilla M1–3
TMM 41106-2189	R maxilla M1
TMM 41106-2190	R maxilla M1–2
TMM 41106-2191	L maxilla M1 and 3
TMM 41106-2193	R maxilla M1–2
TMM 41106-2196	R maxilla M1–2
TMM 41106-2197	R maxilla M1–3
TMM 41106-3553	L maxilla M1
TMM 41106-3554	L maxilla M2
TMM 41106-3555	L maxilla M1
TMM 41106-3556	L maxilla M1
TMM 41106-3557	L maxilla M2
TMM 41106-3559	L maxilla M1–2
TMM 41106-3560	L maxilla M2
TMM 41106-3561	L maxilla M1
TMM 41106-3622	R maxilla M3
TMM 41106-3625	R maxilla M1
TMM 41106-3627	R maxilla M1
TMM 41106-3628	R maxilla M1
TMM 41106-3630	R maxilla M1
TMM 41106-3631	R maxilla M1
TMM 41106-3632	R maxilla M1
TMM 41106-3633	R maxilla M1
TMM 41106-3634	R maxilla M1
TMM 41106-3635	R maxilla M1
TMM 41106-3636	R maxilla M1
TMM 41106-3637	R maxilla M1
TMM 41106-3639	R maxilla M1
TMM 41106-3640	R maxilla M2–3
TMM 41106-3641	R maxilla M2–3
TMM 41106-3642	R maxilla M2–3
TMM 41106-3643	R maxilla M2–3
TMM 41106-3662	L dentary i, m1–3
TMM 41106-3663	L dentary i, m1–3
TMM 41106-3664	R dentary i, m1–3
TMM 41106-3666	L dentary i, m1–3
TMM 41106-3667	R dentary i, m1–3
TMM 41106-3674	R dentary i, m1–3
TMM 41106-3684	R dentary i, m1–2
TMM 41106-3686	R dentary m1
TMM 41106-3687	R dentary i, m1–2
TMM 41106-3705	L dentary m1
TMM 41106-3707	L dentary m1
TMM 41106-5657	R maxilla M1–3
TMM 41106-5657.2	R maxilla M1–3
TMM 411106-3558	L maxilla M1

Specimen	Material examined
Trench 4, Unit 2	
TMM 41106-994	L maxilla M1–3
TMM 41106-998	L maxilla M1–2
TMM 41106-1000	L maxilla M1
TMM 41106-1001	L maxilla M1–2
TMM 41106-1041	L dentary m2
TMM 41106-1045	L dentary m1
TMM 41106-1046	L dentary m1
TMM 41106-1047	L dentary m1
TMM 41106-1049	L dentary m1
TMM 41106-1051	L dentary m1
TMM 41106-1173	R maxilla M1
TMM 41106-1174	R edentulous maxilla
TMM 41106-1175	R maxilla M1
TMM 41106-1176	R maxilla M1–3
TMM 41106-1182	L dentary i, m1–2
TMM 41106-1183	L dentary m1
TMM 41106-1196	L maxilla M1
TMM 41106-2903	M1
TMM 41106-2904	M1
Trench 4, Unit 3	
TMM 41106-1185	L dentary i, m1
Trench 4, Unit 4–5	
TMM 41106-1204	R dentary m1–3
TMM 41106-1205	R dentary m1
TMM 41106-1215	R dentary m1
TMM 41106-1223	R dentary m1
TMM 41106-1242	R maxilla M1–2
TMM 41106-1243	R maxilla M1
TMM 41106-1244	R maxilla M1
TMM 41106-1245	R maxilla M1–2
TMM 41106-1246	R maxilla M2
TMM 41106-1247	R maxilla M1–2

Specimen	Material examined
Chalinolobus* sp. cf. *morio	
Trench 1, Unit 1	
PM 6076	partial skull L P4–M1, R P4–M3
PM 6077	partial skull L P4, M2-3, R P4–M3
PM 26165	partial skull L M2–3
PM 61043	R dentary fragment m2–3
PM 61077	L maxilla P4–M3
Trench 2, Unit 1	
TMM 41106-484	L dentary p4–m3
TMM 41106-485	partial skull R P4, M1–3, L P4, M2–3
PM 61032	R dentary p4, m2–3
PM 61033	L dentary m2
PM 61034	R dentary m2
PM 61035	L dentary p4
Trench 4, Unit 2	
PM 61054	R maxilla P4–M3
***Yangochiroptera* sp. indet.**	
Trench 1, Unit 1	
PM 6078	R dentary p4–m3
PM 61031	R dentary p4 and m2
Trench 3, Unit 2	
TMM 41106-3000	R dentary p4–m3
PM 61051	L dentary m2–3
Trench 4, Unit 4–5	
PM 26282	R m2
PM 26283	R m2

RECORDS OF THE WESTERN AUSTRALIAN MUSEUM 40 079–098 (2025) DOI: 10.18195/issn.0312-3162.40.2025.079-098

The subfossil fauna of Goat Cave and Prostate Pit Cave, Mundrabilla Station, Nullarbor Plain, Western Australia

Kenny J. Travouillon[1,2], Kailah M. Thorn[1], Shelby C. Middleton[1,3], Corey S. Whisson[1], Lucy I. Stokes[1,2], Arianna Urso[1] and Alexander Baynes[1]

[1] Collections and Research, Western Australian Museum, 49 Kew Street, Welshpool, Western Australia 6106, Australia.

[2] School of Molecular and Life Sciences, Curtin University, Bentley, Western Australia 6102, Australia.

[3] School of Science, Edith Cowan University, Joondalup, Western Australia 6027, Australia.

Corresponding author: kenny.travouillon@museum.wa.gov.au

ABSTRACT – The Nullarbor Plain of southern Australia contains a vast karst system, with thousands of caves recording remains of the original fauna before European modification of the Australian landscape and biota. The Nullarbor region records the highest rate of mammal extinction in Australia. We report the results of an expedition to the Nullarbor Plain, with surface collections from Goat and Prostate Pit caves. Goat Cave preserved 25 mammal, six bird, six reptile and three snail taxa and had incredibly well preserved, fully furred, mummified Common Brush-tailed Possums and a Chuditch. Prostate Pit Cave preserved 20 mammal, one bird, seven reptile and four snail taxa. Accumulation of remains in Goat Cave was predominantly due to predation from Australian Masked Owls, while remains in Prostate Pit Cave were accumulated mainly by Dingoes and pitfall trapping. We also report cave use by brushtail possums and Dingoes, and a collection, transport, and preservation methodology for fragile soft-bodied, furred, cave mummies.

KEYWORDS: mammals, birds, reptiles, snails, owl roost, Dingo den

INTRODUCTION

The Nullarbor Plain is a vast plain in southern Australia, extending across the southern border of South Australia and Western Australia. It is the world's largest exposed karst terrain, with a vast system of shallow caves beneath the arid surface (Woodhead et al. 2019). The Nullarbor caves have been accumulating faunal remains since the middle Pleistocene, when the Nullarbor Plain was covered in open woodland with records of arboreal species, including tree kangaroos (Prideaux et al. 2007; Prideaux and Warburton 2008, 2009). By the late Pleistocene the woodland had retreated, and the fauna changed over many climatic cycles (Lundelius 1963; Lundelius and Turnbull 1973, 1975, 1978, 1981, 1982, 1984, 1989, 1999; Lundelius et al. 2025).

A biological survey of the Nullarbor region in 1984 showed that the diversity of fauna had been declining, with several species becoming extinct in the last 100 years (Boscacci et al. 1987). This was also shown by a review of the subfossil record accumulated in caves in the region, demonstrating that many species recorded from the cave floors were no longer extant on the Nullarbor Plain (Baynes 1987). The decline is attributed to two major events. First by diseases in the late 19th century claiming some species, including brushtail possums, possibly one of them being toxoplasmosis spread by feral Cats (*Felis catus*; Richards and Short 1996). The other reason is the arrival of foxes in 1917 that predated many medium-sized species such as the bilby, bandicoots, bettongs (Richards and Short 1996). Both exotic species were aided by the establishment of bores to provide water for the Transcontinental Railway.

Goat Cave (6N-0745) is located on Mundrabilla Station on the Nullarbor Plain, on Mirning Country (Figure 1). It was first surveyed and mapped by Max Meth, Ray Gibbons and Ken Boland in 1996, with only the entrance chamber and some side passages known at the time (MacLucas 1996). In 2023, a party of cavers, including Alan Pryke, Megan Pryke, Bert De Waele and Brett Wiltshire, made a significant discovery (De Waele et al. 2023). They found multiple mammal remains beyond the entrance series of chambers, of brushtail possums that were fully furred. While this part of the cave was slowly uncovered over multiple

trips over multiple years (2021–25) by multiple teams of people, the 2023 discovery was the one that identified Goat Cave as a significant site (De Waele et al. 2023). The discovery was reported to the Western Australian Museum (WAM), which after seeing the incredible preservation of the brushtail possums, decided to undertake an expedition to the Nullarbor Plain to recover those specimens.

Prostate Pit Cave (6N-1369), also on Mundrabilla Station (Figure 1), was first recorded by Plane Caving members David 'Max' Hall, Judy Shaw and Phil McGuigan in April 1995 (Poulter 2020). It was named by the late Lindsay Hatcher to honour a friend who was suffering from prostate problems at the time. Some specimens were collected by Lindsay Hatcher from the cave, including skulls of Tasmanian Devil (*Sarcophilus harrisii*), Southern Hairy-nosed Wombat (*Lasiorhinus latifrons*) and Western Grey Kangaroo (*Macropus fuliginosus*), which were donated to WAM after his passing. The cave is well-known to cavers who visit it to see stegamites, gypsum and halite columns, and calcite decorations. It also contains unique invertebrates, including cave spiders in the genus *Troglodiplura* (Poulter 2020). Nothing has been reported to date of its vertebrate remains.

Herein we report the findings of the 2025 expedition to Goat Cave and Prostate Pit Cave on the Nullarbor Plain. We present the collection of terrestrial vertebrate and mollusc specimens, some interpretation of how the caves were used by animals in the area, and what species were there until extirpation after the arrival of Europeans in Australia.

MATERIALS AND METHODS

FIELDWORK

Fieldwork to recover vertebrate remains was undertaken between the 20th and 28th of April 2025. Three days of works was undertaken at Goat Cave, and two days at Prostate Pit Cave. Opportunistic collection of live fauna (invertebrates and reptiles) was also conducted in the cave dolines and surrounding area with the assistance of a cultural monitor.

RECOVERY OF MUMMIFIED SPECIMENS

The mummified remains were photographed on a previous expedition, but their structural integrity was unknown to the collection team as they were not touched or moved by the cavers. Each mummified

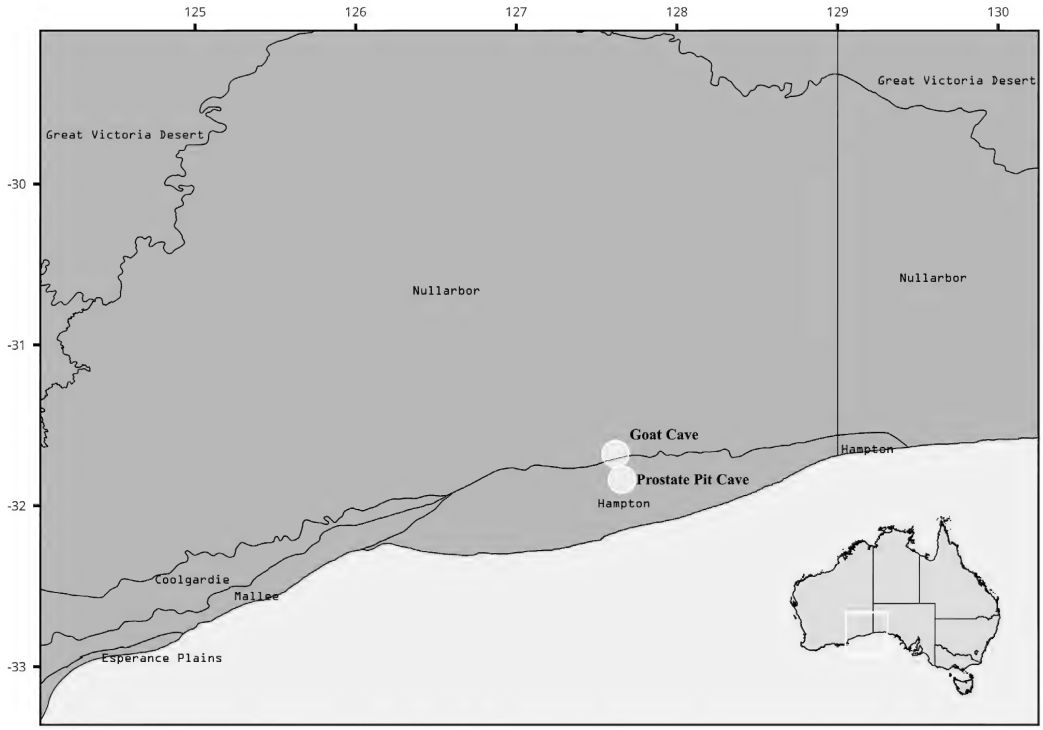

FIGURE 1 General location of Goat and Prostate Pit caves on the Nullarbor Plain, Mirning Country, Western Australia.

FIGURE 2 Recovery of the mummified specimens.

animal was mapped to the nearest cave survey marker, photographed, measured, and probed for overall preservation integrity and pliability on day one in Goat Cave. External measurements for the specimens marked for retrieval were used to precut rectangular pieces of 3 mm white foam board for mounting. Each mounting board also had corner braces and a lid, and two pieces of 10 mm dowel rod, flat-packed into a labelled, 150 µm thick, clear polyethylene 'mining sample' bag, for final assembly with cloth tape in the cave (Figure 2). Flat packing allowed for easier transport of materials into the cave. Each mummy was slid onto the flat mounting board and pinned into place with fine stainless steel entomological pins to prevent movement in any direction. After pinning, the corner braces and lid were added to the mounting board to prevent compression, and the wooden dowel rods positioned diagonally across the lid and base to prevent twisting. The mining bag was slid over the 'boxed' mummy and taped shut, with corners folded, flattened, and taped to prevent snagging. The bag prevented dust incursion and fluctuations in humidity as the specimen was transported through the cave. A cloth tape handle was added to the lid of the box for passing the package one-handed through cave crevices.

All mummified remains in their sealed packages were then packed into a padded Pelicase in the entrance cavern of Goat Cave which was filled with packing peanuts to minimise movement during transport back to the vehicle and during return to Perth.

COLLECTION OF SUBFOSSILS

Collection of subfossil material was only from the cave floor surface, by hand, with natural and LED headtorch light. Surface density of subfossil material was localised to patches within the entrance chamber of both caves, positioned beneath suitable owl roost location or within the range of pitfall trappings. As all collections were made by hand, the smallest vertebrate remains (disarticulated anurans, passerines, geckos and small skinks) are likely to be under-represented.

IDENTIFICATION OF SUBFOSSILS

Taxonomy follows the WAM Taxonomic Checklist (https://visit.museum.wa.gov.au/collections/terrestrial-zoology/checklist-terrestrial-vertebrate-fauna-WA). All subfossils were first sorted into major taxonomic groups: mammals, birds, reptiles and molluscs. Then they were identified to order or family. Using WAM collections, comparative specimens were used to identify to the lowest taxonomic rank possible, subspecies for some of them (e.g. *Chaeropus ecaudatus occidentalis*), or morphotype for osteologically cryptic taxa (e.g. Agamidae morphotype 1). Examples of each taxon identified are shown in Figures 3–10.

The mummified specimens of *Amphibolurus norrisi* and *Pseudonaja affinis* were identified using preserved external morphological characters reported by Storr et al. (1983), Storr et al. (2002) and Cogger (2018).

RESULTS

GOAT CAVE

Entrance chamber

Subfossils collected in the entrance chamber consisted of 25 mammal, six bird, five reptile and three snail taxa (Table 1). The number of identified specimens (NISP) of mammals is 422. The bulk of the bones are likely prey remains accumulated by predators such as Australian Masked Owl (*Tyto novaehollandiae*), Dingo (*Canis familiaris*), Red Fox (*Vulpes vulpes*) and feral Cat, all of which have remains also collected in the cave. One intact, mummified, Mallee Dragon Lizard (*Amphibolurus norrisi*) was found underneath a ledge outside of the reach of sunlight suggesting the individual may have been unable to climb out of the cave once cold, effectively pit-trapped within a few metres of the cave opening.

The absence of diplodactylid or gekkonid geckos in the surface material is unexpected, but most likely due to size biases as they are smaller vertebrates than others collected (snout-vent lengths usually <50 mm).

A specimen of Nullarbor Marbled Gecko (*Christinus alexanderi*, WAM R182378) was collected from within 50 m of the mouth of Goat Cave during this expedition, and a Tree Dtella (*Gehyra variegata*, WAM R182379) vouchered from the camp site ~800 m from the cave. Carphodactylid gecko material attributed to Southern Barking Gecko (*Underwoodisaurus milii*) was relatively abundant in the entrance chambers of both Prostate Pit and Goat caves and a live specimen was found basking on a rock pile outside Goat Cave (WAM R182377). Most of the fossils attributed to the family Agamidae could not be further refined due to a lack of comparative osteological material and the lack of morphological variation between species detectable from isolated or incomplete elements (see Ramm et al. 2024).

Snake and Possum Chamber

One chamber contains both a snake skeleton and a possum skeleton (hence the name of the chamber). The snake skeleton namesake for this chamber is a partially mummified adult Dugite (*Pseudonaja affinis*). The head was found wedged between loose limestone boulders and collected for identification purposes. The mummified body remains in-situ to preserve the context of the chamber name and as a landmark for cavers.

Beyond the entrance series

Deep into the cave tunnels, remains of nine brushtail possums were found on the cave floor surface. Some were incredibly well preserved, being fully furred and one having a blood-stained nose (Figure 11A), while others were completely skeletonised on a thin cushion or ring of fur. All specimens were identified as juveniles, due to their small size, and their teeth showing deciduous premolars still present or the M4/m4 not erupted. Scent trails (urine stains) and possum scats were found on the path in multiple areas of the cave, showing that possums were regularly using the cave. A very small Chuditch (*Dasyurus geoffroii*) approximately 32 cm in length from head to tail tip and 12 cm in width, was also found mummified (Figure 11B), with only the right forepaw fully skeletonised. A mummified microbat was also mapped and photographed, then left in place as it was too fragile to move.

PROSTATE PIT CAVE

Entrance chamber

Subfossils collected in the entrance chamber consisted of 18 mammal, one bird, seven reptile and four snail taxa (Table 1). The number of identified specimens (NISP) of mammals is 72. Skeletal remains of Tasmanian Devils and Southern Hairy-nosed Wombats had previously been recovered from this cave, but it is not clear if they were collected from the entrance or further inside the cave. Possum urine on one of the devil skulls suggests that it was collected further into the cave. There was no evidence of Australian Masked Owl in the cave, and the prey size was biased toward larger animals, lacking the usual abundance of small rodents and small dasyurids which are typical of owl diets. As a result, the accumulation of bones is likely from mammalian predators such as Dingo and Red Fox whose remains were found in the cave.

Dingo den

A set of chambers with a very low ceiling, named the 'ossuary' by cavers, was littered with large macropod bones (Figure 12A). There were fewer remains from other mammals such as Rabbit (*Oryctolagus cuniculus*), bandicoots and brushtail possums, and only one reptile represented by one large agamid dentary. The prey species and the way bones were broken suggest that this area of the cave was used by Dingoes to feed (the prey size rules out foxes as the main contributor). Several locations in the chamber had an accumulation of bones in front of depressions in the cave floor, that appeared to be dug by Dingoes to rest in. We believe this is the first time this behaviour is reported. Along the back walls of the chambers, brushtail possum scats were found in stacks (Figure 12B). This suggests that possums would come into the chamber and follow the edge of the chamber, rather than going through the middle, perhaps to avoid becoming a Dingo meal. They would likely feed from carcasses left by Dingoes or perhaps steal some of the carcasses (see section on brushtail possum den). No Dingo scat was found within the Dingo den chambers. However, immediately outside the Dingo den chambers, there was a large raised platform with several Dingo scats on it, which we suspect was used as a latrine.

Brushtail possum den

In a chamber that was topographically higher than the Dingo den, the floor was covered in brushtail possum scats, with a few small carcasses, mostly Rabbit remains, present amongst the scats (Figure 13A). This chamber is interpreted as being a brushtail possum den, with scavenged remains that they potentially stole from other predators (proximity suggests the Dingo den). This chamber is connected to another much larger room by a tunnel with trails of possum scats, this room had multiple trails of scats going in various directions within it (Figure 13B). It is interpreted here that the scats were used as scent trails in the dark for the possums to find their way to various resting spots within the chamber. One resting spot was a large speleothem covered in possum urine (Figure 13C). These two chambers and the Dingo den were the only place in the Prostate Pit Cave that large amounts of possum scats were found, suggesting that brushtail possums fed in the same area that they also used as latrines (contrary to the Dingoes).

TABLE 1 Species and specimen list of the subfossils recovered from Goat Cave and Prostate Pit Cave with Western Australian Museum registration numbers. † † = extinct; † = locally extinct.

Taxon	Goat Cave	Prostate Pit Cave
MAMMALIA		
Order: Monotremata		
Tachyglossus aculeatus (Short-beaked Echidna)	-	M65630
Order: Dasyuromorphia		
Antechinomys sp. † (kultarr)	M65640	M65639
Dasycercus archeri † † (Southern Mulgara)	M65638	-
Dasycercus cristicauda † † (Crest-tailed Mulgara)	M65636	-
Dasyurus geoffroii † (Western Quoll/Chuditch)	M65637, M65692	M65632
Sarcophilus harrisii † (Tasmanian Devil)	-	04.2.403-404, 2024.3.1
Sminthopsis dolichura (Little Long-tailed Dunnart)	M65635	M65634
Order: Peramelemorphia		
Chaeropus ecaudatus occidentalis † † (Pig-footed Bandicoot)	M65612, M65613	-
Macrotis lagotis † (Greater Bilby)	M65614	-
Perameles myosuros † † (Marl)	M65610	M65625
Perameles papillon † † (Nullarbor Barred Bandicoot)	M65609	M65627
Order: Diprotodontia		
Bettongia haoucharae † †	-	M65633
Bettongia lesueur † (Burrowing Bettong/Boodie)	M65615	M65621
Lagorchestes hirsutus hirsutus † (Rufous Hare-wallaby)	-	M65626
Lasiorhinus latifrons (Southern Hairy-nosed Wombat)	M65607	04.2.405-406,
Macropus fuliginosus melanops (Western Grey Kangaroo)	M65605	M65618, 04.2.407-410, 2024.3.2-3, M65643
Onychogalea lunata † † (Crescent Nail-tailed Wallaby)	M65616	M65628
Osphranter rufus (Red Kangaroo)	-	M65622
Trichosurus vulpecula † (Common Brush-tailed Possum)	M65611, M65690, M65691	M65620, M65623, M65624
Order: Rodentia		
Leporillus apicalis † † (Lesser Stick-nest Rat)	M65647	M65644
Leporillus conditor † (Greater Stick-nest Rat)	M65646	-
Notomys sp. indet. (Hopping mouse)	M65648	-
Pseudomys australis † (Plains Mouse)	M65649	-
Pseudomys bolami (Bolam's Mouse)	M65650	M65645
Rattus villosissimus † (Long-haired Rat)	M65651	-
Order: Lagomorpha		
Oryctolagus cuniculus (Rabbit)	M65606	M65631
Order: Chiroptera		
Chalinolobus gouldii (Gould's Wattled Bat)	-	Observed live
Chalinolobus morio (Chocolate Wattled Bat)	M65617	-

Taxon	Goat Cave	Prostate Pit Cave
Order: Carnivora		
Canis familiaris (Dingo)	M65604	M65629
Felis catus (domestic/feral Cat)	M65641	-
Vulpes vulpes (Red Fox)	M65608	M65619, M65642
Mammal species total	**25**	**20**
AVES		
Order: Strigiformes		
Tyto novaehollandiae (Australian Masked Owl)	A52933	-
Order: Passeriformes		
Hirundo neoxena (Welcome Swallow)	A52952, A52953	A52934
Artamus cinereus (Black-faced Woodswallow)	A52978	-
Cinclosoma alisteri (Nullarbor Quail-thrush)	A52979	-
Gavicalis virescens (Singing Honeyeater)	A52980	-
Melanodryas cucullata (Hooded Robin)	A52981	-
Bird species total	**6**	**1**
REPTILIA		
Order: Squamata		
Family: Agamidae		
Amphibolurus norrisi (Mallee Dragon Lizard)	R182390	-
Agamidae indet.	R182399	R182397
Agamidae morphotype 1	-	R182396
Agamidae morphotype 2	-	R182395
Family: Carphodactylidae		
Underwoodisaurus milii (Southern Barking Gecko)	R181028	R182394
Family: Scincidae		
Liopholis sp. (skink)	R181030	-
Tiliqua rugosa (Bobtail)	R181029	R181031
Family: Elapidae		
Pseudonaja affinis (Dugite)	R160413	-
Family: Pythonidae		
cf. *Morelia* sp. indet. (python)	-	R152532
Family: Varanidae		
Varanus sp. indet. (goanna)	-	R182393
Reptile species total	**6**	**7**
MOLLUSCA		
Order: Stylommatophora		
Bothriembryon barretti	S27695	S27690
Basedowena elfina	S27696	S27691
Sinumelon nullarboricum	S27694	-
Westralaoma sp. indet.	-	S27693
Pupoides adelaidae	-	S27692
Snail species total	**3**	**4**

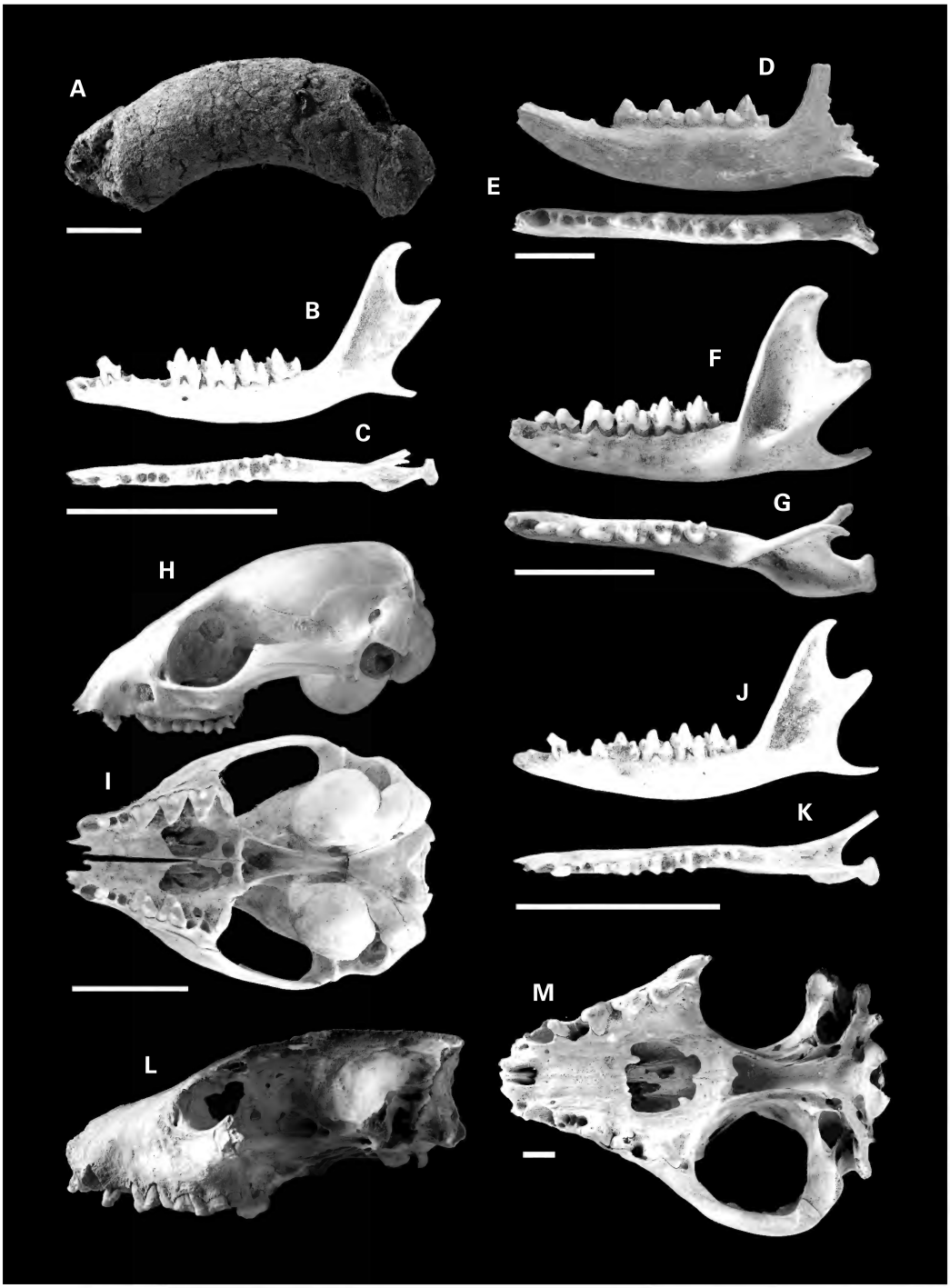

FIGURE 3 Monotreme and dasyurid specimens identified in Goat and Prostate Pit caves: A) *Tachyglossus aculeatus* (M65630), scat; B–C) *Antechinomys* sp. (M65640), left dentary; D–E) *Dasyurus geoffroii* (M65632), right dentary; F–G) *Dasycercus archeri* (M65638), left dentary; H–I) *Dasycercus cristicauda* (M65636), skull; J–K) *Sminthopsis dolichura* (M65635), left dentary; L–M) *Sarcophilus harrisii* (04.2.404), skull. Scale = 10 mm.

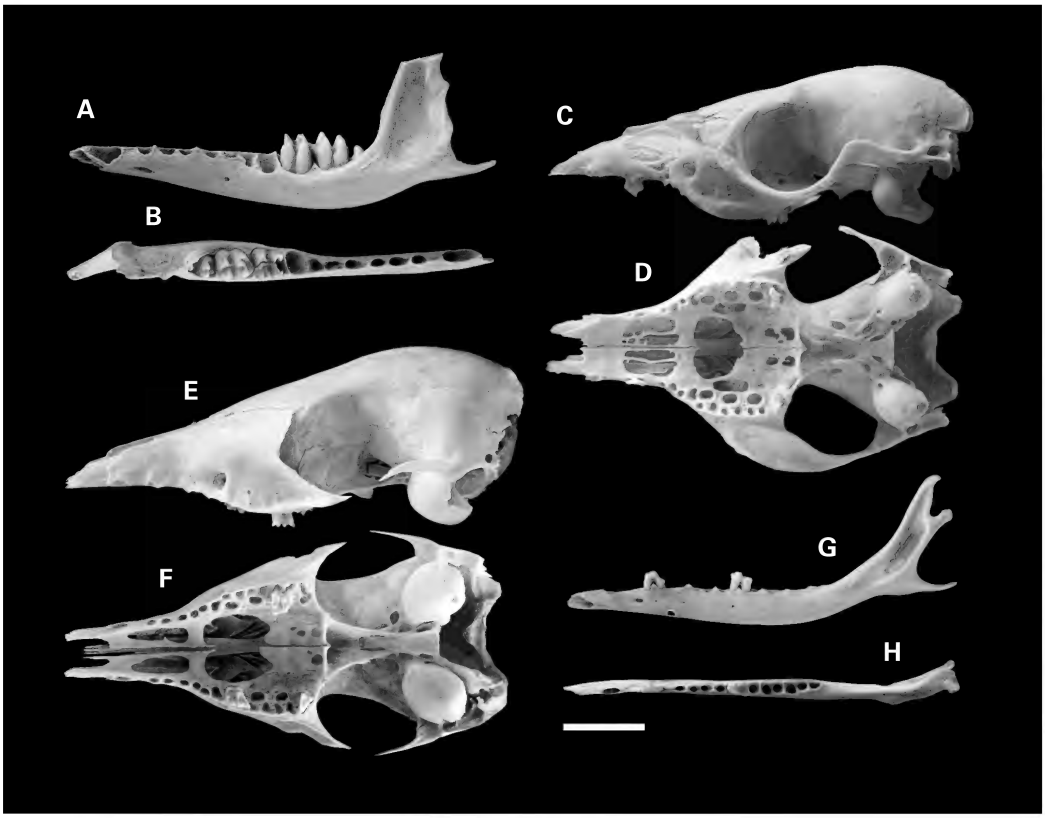

FIGURE 4 Peramelemorphian specimens identified in Goat and Prostate Pit caves: A–B) *Macrotis lagotis* (M65614), left dentary; C–D) *Chaeropus ecaudatus occidentalis* (M65612), skull; E–F) *Perameles papillon* (M65609), skull; G–H) *Perameles myosuros* (M65610), left dentary. Scale = 10 mm.

DISCUSSION

FAUNAL DIVERSITY IN GOAT AND PROSTATE PIT CAVE

Considering how little time was spent collecting subfossil remains from the cave floors, the diversity recorded in both caves is high, with 39 taxa recorded from Goat Cave (Goat Cave NISP = 422) and 32 taxa recorded from Prostate Pit Cave (Prostate Pit Cave NISP = 72) (Table 1). While the bird and reptile faunas are very much an under-representation of the diversity that exists outside the cave today, the mammal fauna is close to that reported previously (Boscacci et al., 1987; Baynes 1987). Of the original native mammals (~54 species; Boscacci et al. 1987; Baynes 1987), 15 taxa, previously reported as part of the original fauna, are missing from our dataset: four dasyurids (*Phascogale calura, Sminthopis gilberti, S. ooldea, S. crassicaudata*), one pygmy possum (*Cercartetus concinnus*), one bandicoot (*Isoodon fusciventer*), four rodents (*Pseudomys desertor, P. gouldii, Notomys mitchellii, N. alexis*) and five bats (*Austronomus australis, Nyctophilus major tor, N. geoffroyi, Scotorepens balstoni, Vespadelus regulus*). All of these are small taxa that could have been easily missed during the collection of bones but some of those might not occur at all locally as both caves are near the escarpment where the vegetation is more wooded, and some of those taxa would only occur in the more arid parts of the Nullarbor Plain further north (e.g. both *S. ooldea* and *N. alexis* are desert species and unlikely to have occurred near these caves) or in the more forested vegetation further south. Also, note that we do have *Notomys* on our list (Table 1), but the species could not be identified. Of the introduced mammals, the House Mouse (*Mus musculus*) was not detected, perhaps for similar reasons to the small native mammals. Mundrabilla station is currently a cattle station, so *Bos primigenius taurus* is still present, but other domestic mammals such as Goats (*Capra aegagrus hircus*), Sheep (*Ovis aries*) and Horses (*Equus ferus caballus*) are no longer kept on the property. Feral Camels (*Camelus dromedarius*) still occur in the northern part of the station.

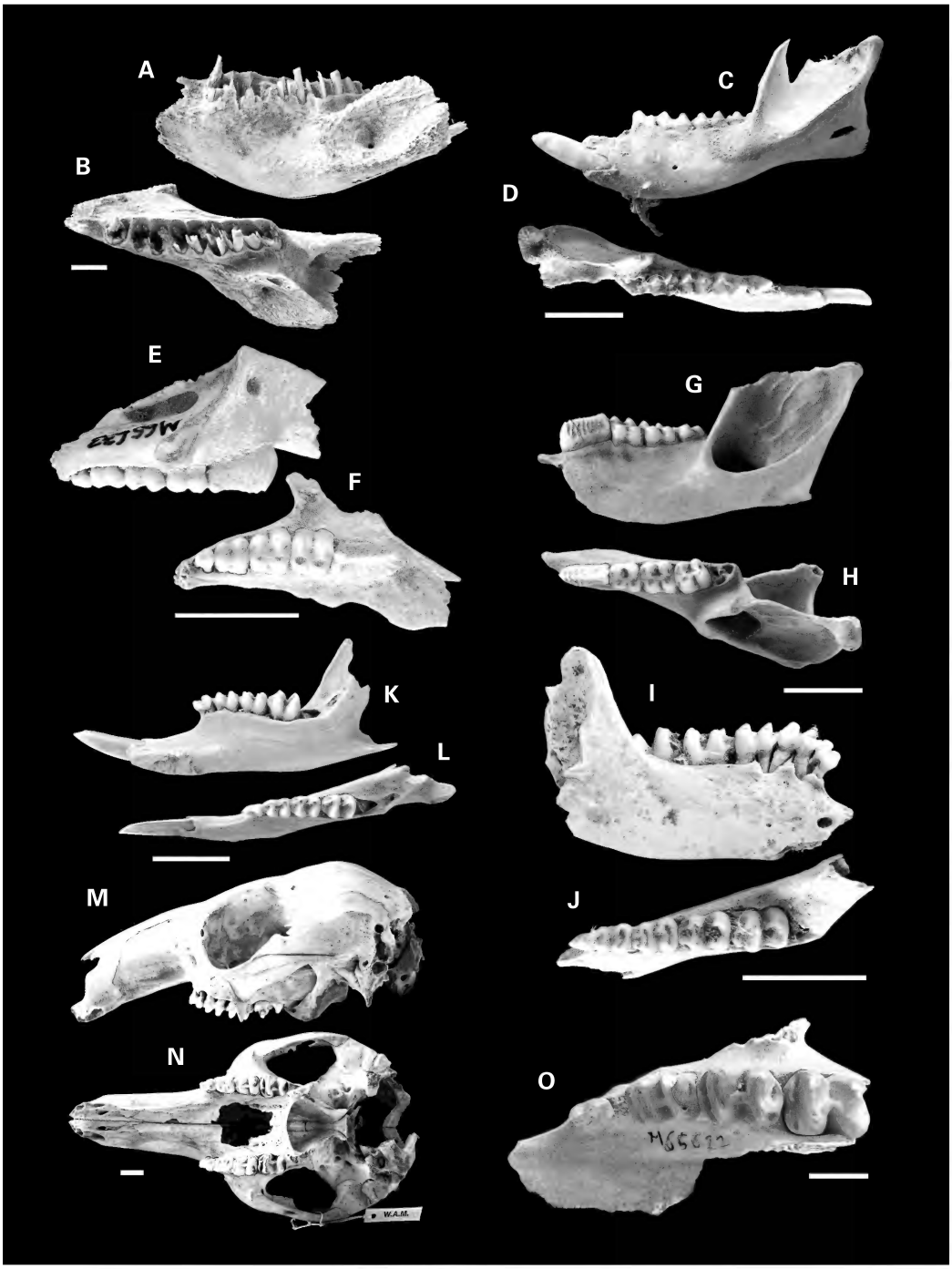

FIGURE 5 Diprotodontian specimens identified in Goat and Prostate Pit caves: A–B) *Lasiorhinus latifrons* (M65607), left dentary; C–D) *Trichosurus vulpecula* (M65623), left dentary; E–F) *Bettongia haoucharae* (M65633), right maxilla; G–H) *Bettongia lesueur* (M65621), left dentary; I–J) *Onychogalea lunata* (M65616), right dentary; K–L) *Lagorchestes hirsutus hirsutus* (M65626), right dentary; M–N) *Macropus fuliginosus melanops* (M65618), skull; O) *Osphranter rufus* (M65622), left maxilla. Scale = 10 mm.

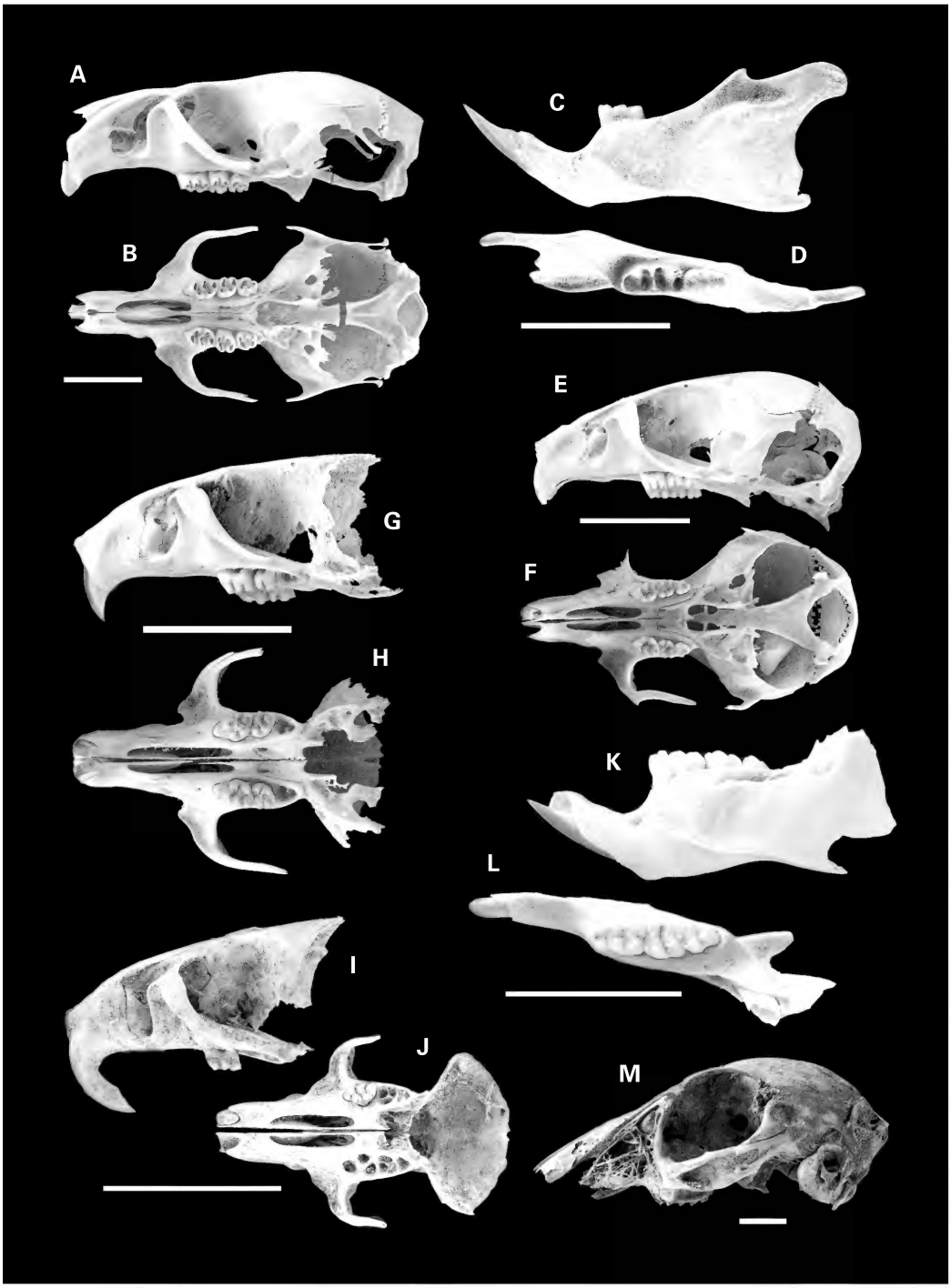

FIGURE 6 Rodent and lagomorph specimens identified in Goat and Prostate Pit caves: A–B) *Leporillus conditor* (M65646), skull; C–D) *Leporillus apicalis* (M65644), right dentary; E–F) *Notomys* sp. indet. (M65648), skull; G–H) *Pseudomys australis* (M65649), skull; I–J) *Pseudomys bolami* (M65650), skull; K–L) *Rattus villosissimus* (M65651), left dentary; M) *Oryctolagus cuniculus* (M65606), skull. Scale = 10 mm.

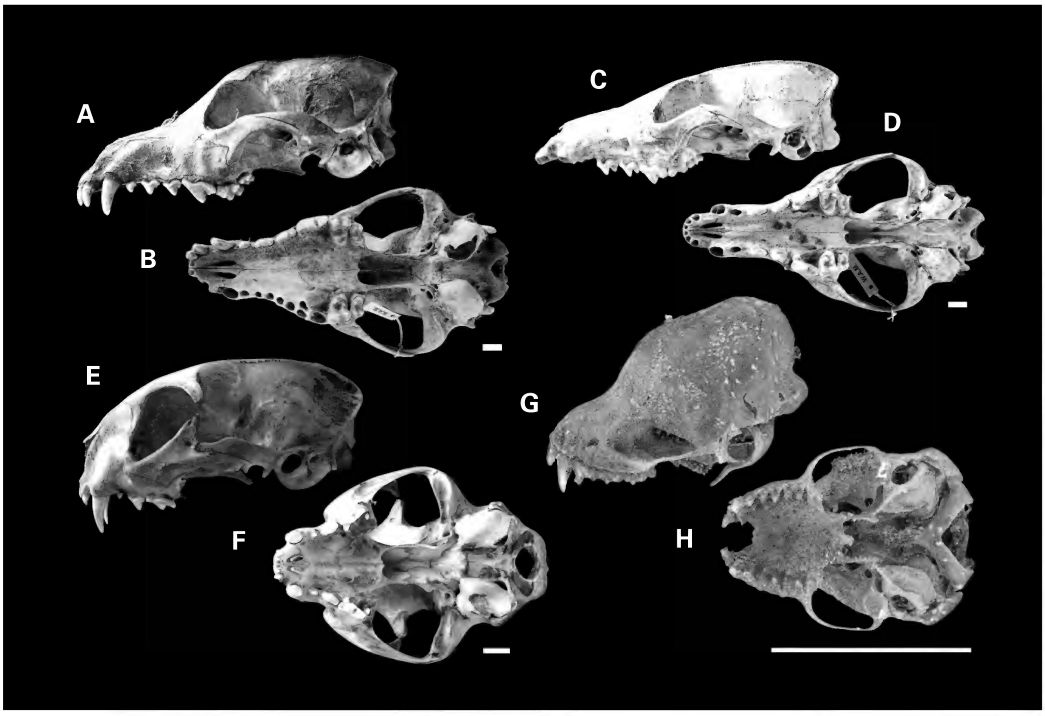

FIGURE 7 Carnivoran and chiropteran specimens identified in Goat and Prostate Pit caves: A–B) *Canis familiaris* (M65606), skull; C–D) *Vulpes vulpes* (M65619), skull; E—F) *Felis catus* (M65641), skull; G–H) *Chalinolobus morio* (M65617), skull. Scale = 10 mm.

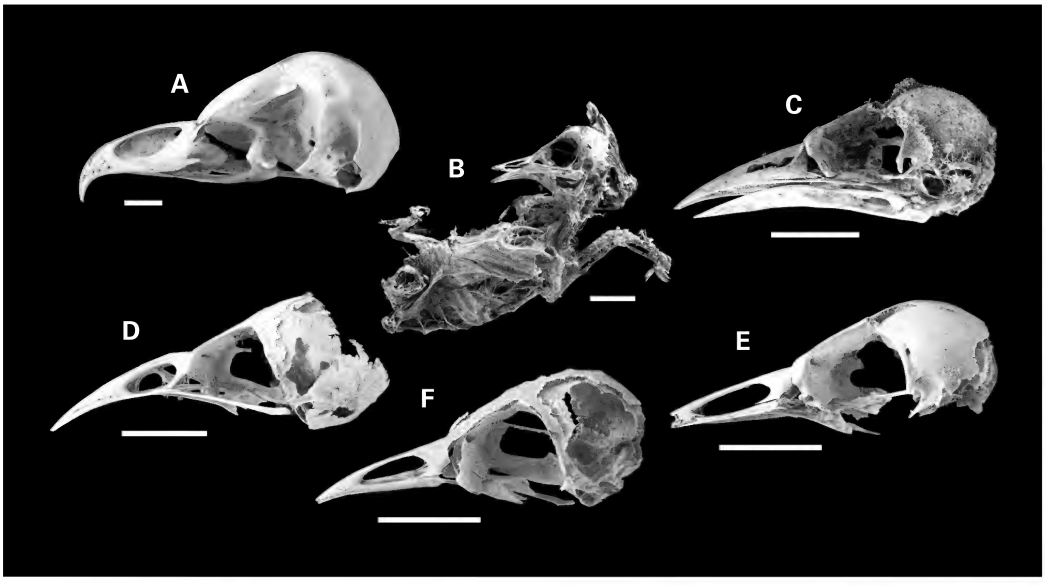

FIGURE 8 Bird specimens identified in Goat and Prostate Pit caves: A) *Tyto novaehollandiae* (A52933), skull; B) *Hirundo neoxena* (A52953), mummified specimen; C) *Artamus cinereus* (A52978), skull; D) *Cinclosoma alisteri* (A52979), skull; E) *Gavicalis virescens* (A52980), skull; F) *Melanodryas cucullata* (A52981), skull. Scale = 10 mm.

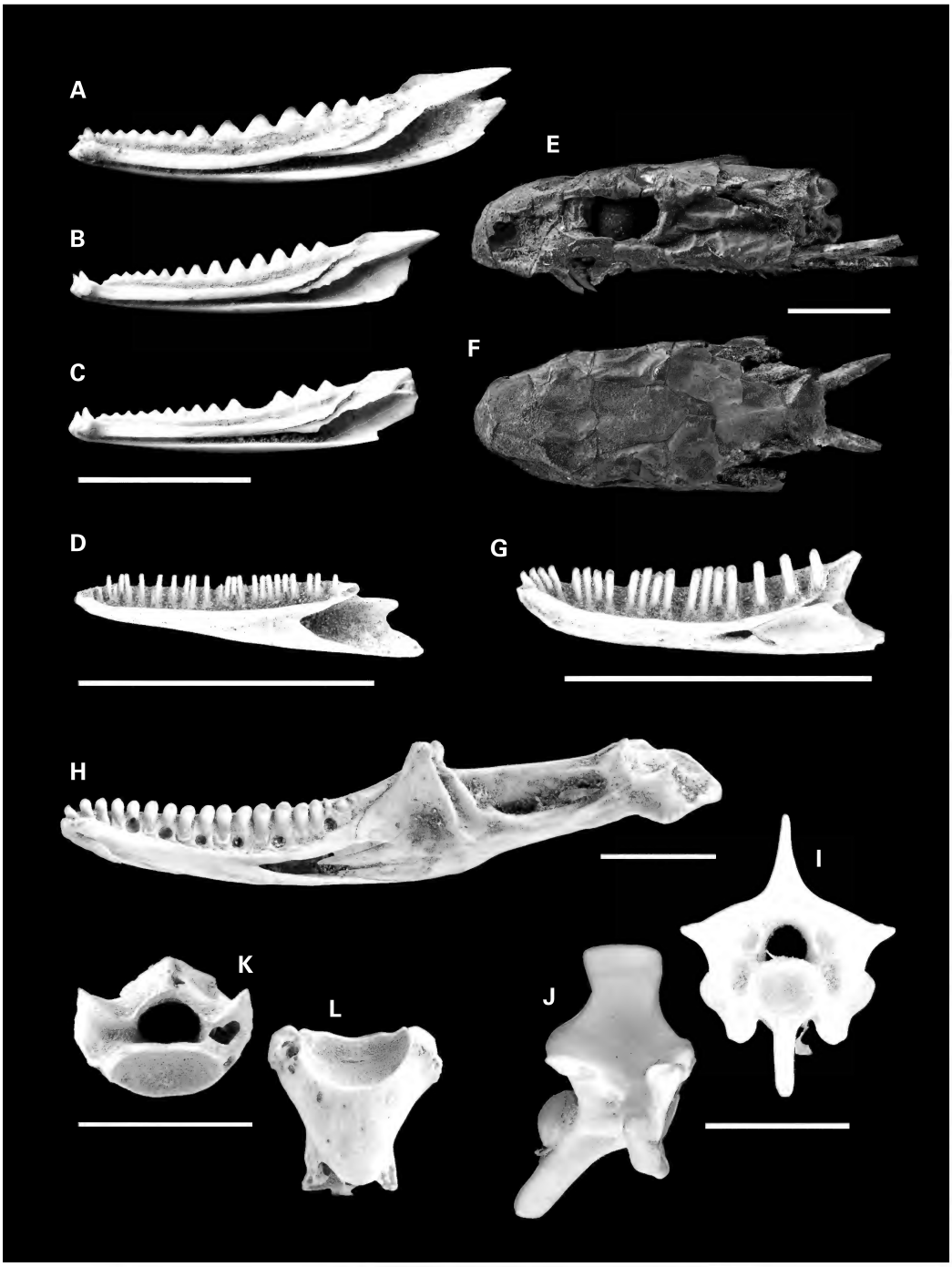

FIGURE 9 Reptile morphotype specimens identified in Goat and Prostate Pit caves; A) Agamidae indet. (R182399), right dentary; B) Agamidae morphotype 1 (R182396), right dentary; C) Agamidae morphotype 2 (R182395), right dentary; D) *Underwoodisaurus milii* (R181028), right dentary; E–F) *Pseudonaja affinis* (R160413), mummified skull; G) *Liopholis* sp. (R181030), right dentary; H) *Tiliqua rugosa* (R181029), right mandible; I–J) cf. *Morelia* sp. (R152532), vertebra; K–L) *Varanus* sp. (R182393), vertebra. Scale = 10 mm (except G–H = 5 mm).

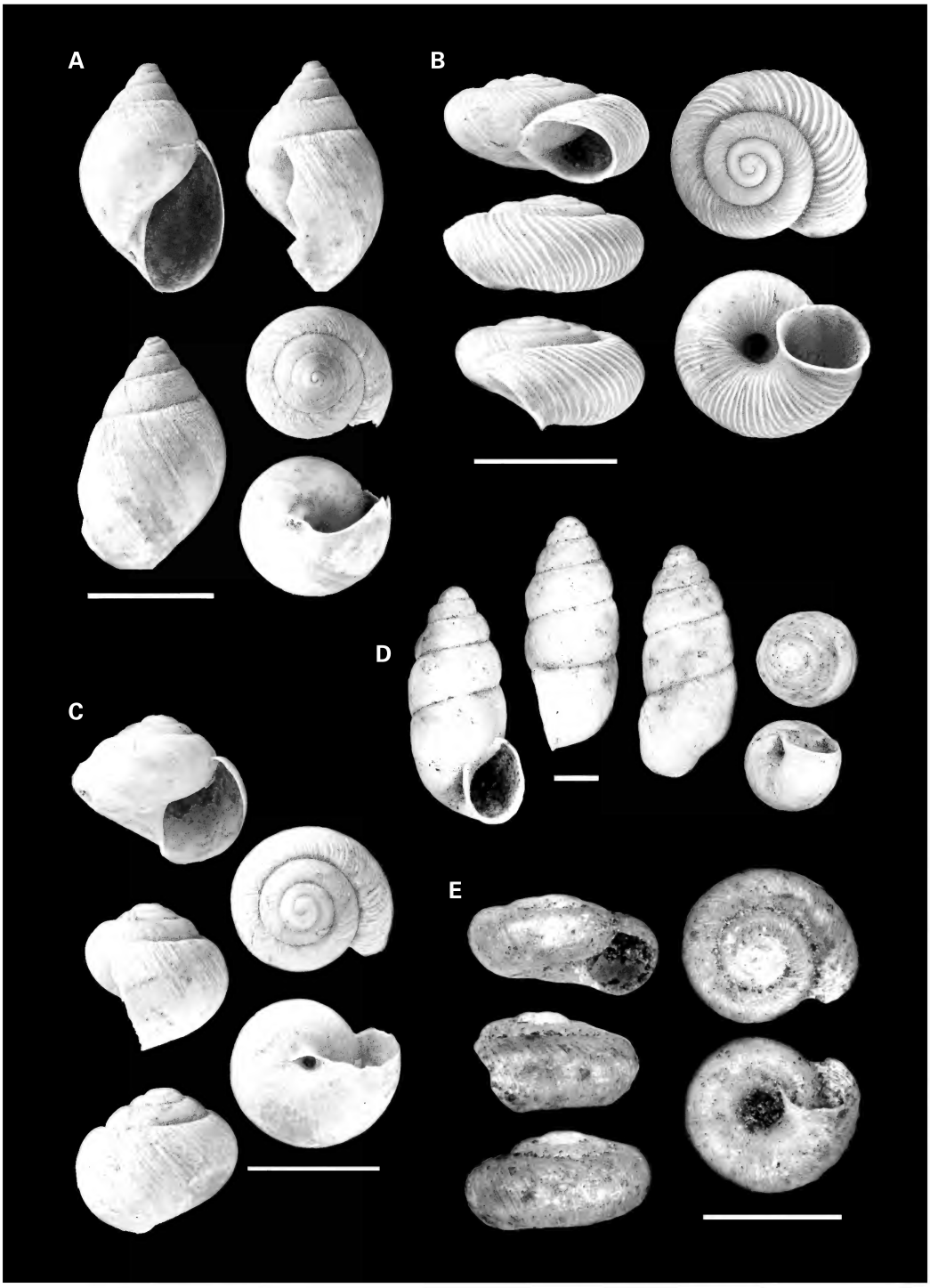

FIGURE 10 Gastropod mollusc specimens identified in Goat and Prostate Pit caves: A) *Bothriembryon barretti* (S27690); B) *Basedowena elfina* (S27691); C) *Sinumelon nullarboricum* (S27694); D) *Pupoides adelaidae* (S27692); E) *Westralaoma* sp. (S27693);. Scale = 10 mm (except D–E = 1 mm).

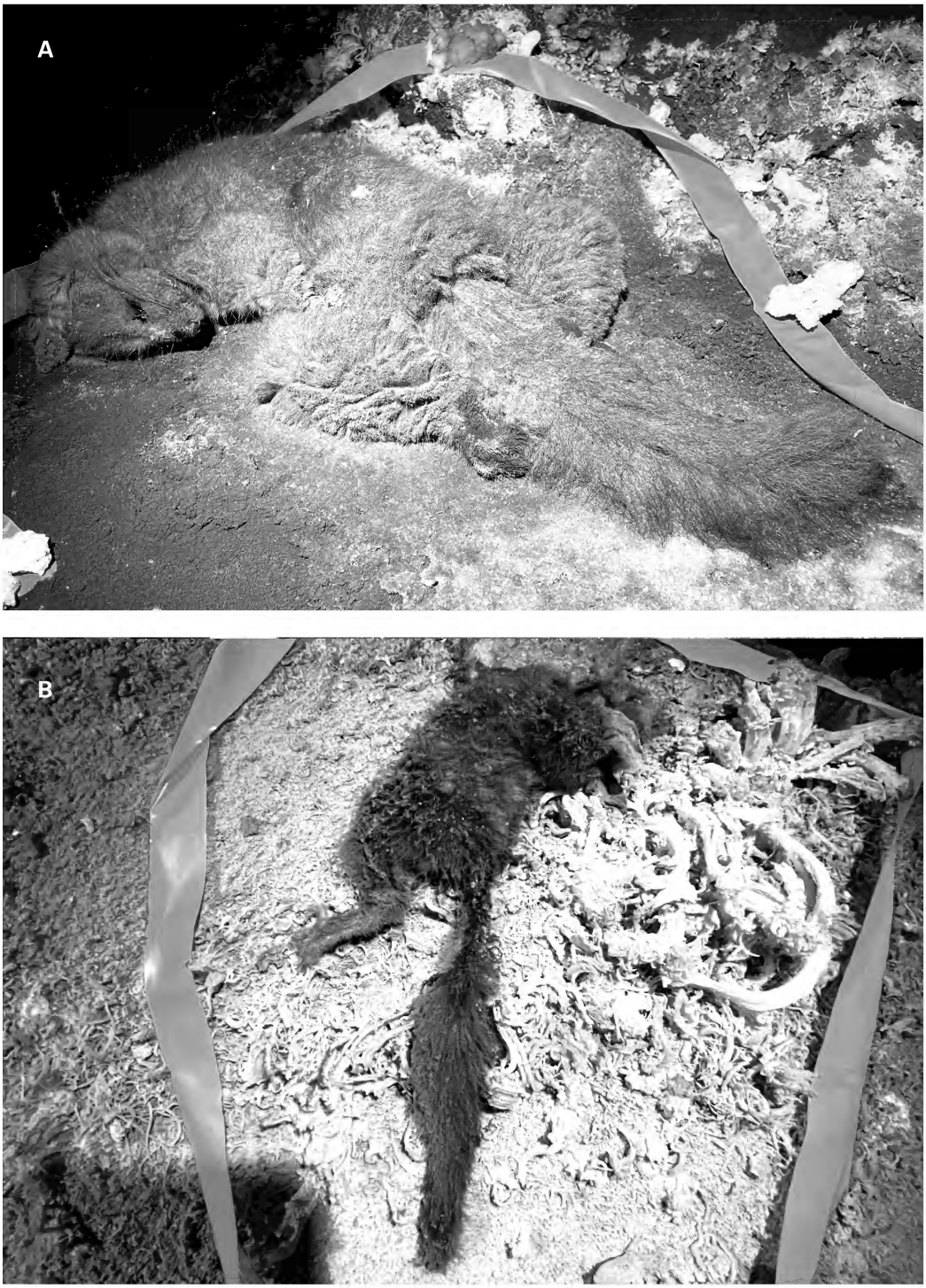

FIGURE 11 Mummified specimens found in the deep tunnels of Goat Cave: A) Common Brush-tailed Possum (*Trichosurus vulpecula*); B) Chuditch (*Dasyurus geoffroii*).

FIGURE 12 Dingo den in Prostate Pit Cave: A) main chamber showing macropod bone remains in stacks on cave floor; B) possum scats located on the outer edges of the Dingo den.

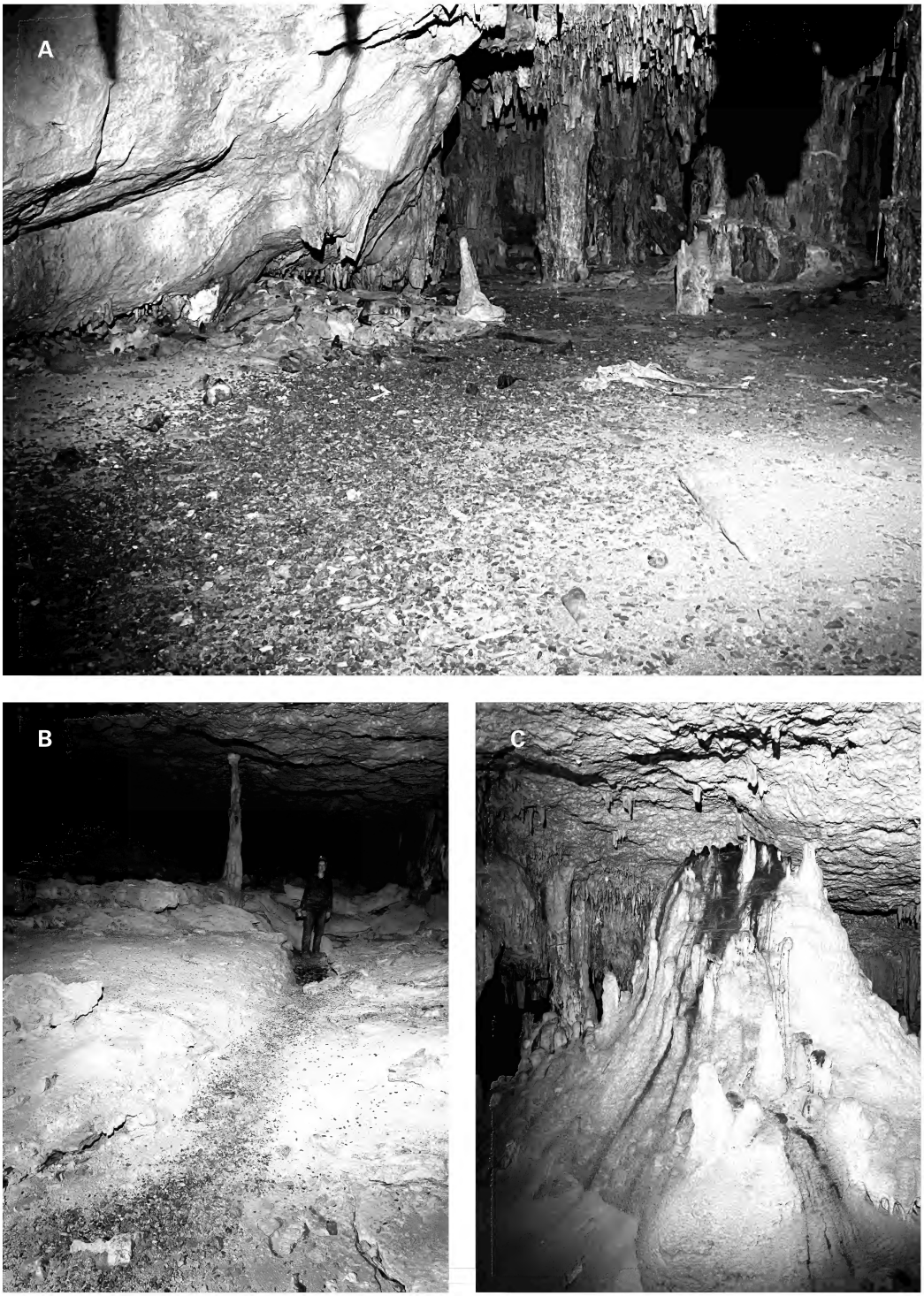

FIGURE 13 Brushtail possum den in Prostate Pit Cave: A) first small chamber showing thousands of possum scats on cave floor and carcasses; B) possum scats trail in second larger chamber; C) possum urine staining cave decoration.

We have recorded a total of 8 extinct and 9 locally extinct mammal species (Table 1). Some of the extinct species have been revised since the original survey (Boscacci et al. 1987; Baynes 1987; McKenzie et al. 1987). In the order Peramelemorphia, the Nullarbor Barred Bandicoot *Perameles papillon* (previously *Perameles bougainville notina* in Boscacci et al. 1987) and the Marl *Perameles myosuros* (previously *Perameles bougainville* in Boscacci et al. 1987) were both revised by Travouillon and Phillips (2018) and identified as distinct taxa. The Pig-footed Bandicoot subspecies *Chaeropus ecaudatus occidentalis* was also reinstated by Travouillon et al. (2019). In the order Dasyuromorphia, a new mulgara was recognised by Newman-Martin et al. (2023), *Dasycercus archeri,* which was previously misidentified by Lundelius and Turnbull (1978) as *Dasyuroides.* Also, the kultarr, *Antechinomys laniger*, has been revised and no longer occurs in Western Australia. Instead, the newly described *Antechinomys auritus* occurs in the arid zone of WA, and there is another undescribed *Antechinomys* that occurs in the wheatbelt and on the Nullarbor of WA (Dodd et al. 2025). In the order Diprotodontia, a new bettong *Bettongia haoucharae* (referred to as *B. penicillata* by Baynes 1987) has also recently been described by Newman-Martin et al. (2025).

We recorded a total of 10 reptile taxa from Goat Cave and Prostrate Pit Cave. Prior to 1900 only two reptiles (*Varanus gouldi* and *Rhinoplocephalus bicolor*) were collected by Australian museums from the Nullarbor Plain (Atlas of Living Australia 2025). Very little was known of the herpetofauna until 1914 when W.B. Alexander made small collections from stations along Eyre Highway, and until the 1950s museums were only receiving specimens collected ad hoc by members of the public (Storr et al. 1981). Evidently, the original herpetofauna of this part of Australia was not well-documented before the impact of introduced predators, Rabbits, or extensive sheep and cattle grazing.

Surface collecting of skeletal remains from natural pitfall traps and predator accumulations might be the only means by which we can determine the pre-European reptile fauna from this remote region of Australia. Mead et al. (2008) reported three *Pygopus* dentaries in mid-Holocene deposits from Webbs Cave (6N-132; 5,200 to 4,160 cal. BP) and Wombat Cave (5N-264; undated) on the Nullarbor. Two species of legless geckos (*Pygopus)* are known from the extant fauna of the Nullarbor IBRA region, the Common Scaly-Foot (*Pygopus lepidopodus)* and Western Hooded Scaly-Foot (*P. nigriceps*; McKenzie et al. 1987; Atlas of Living Australia 2025). The absence of pygopodid remains from this investigation is not unexpected, as only the three dentaries were recorded from the large sample of thousands of reptile bones sorted by Mead et al. (2008). Present knowledge of reptile osteology prevents identification of most groups to species-level determinations, but with the expanding application of ancient DNA (see Scarsbrook et al. 2023), the remains collected from caves can be further refined in years to come.

Identification of the mummified remains allow for direct comparisons of the herpetofaunal subfossil record to modern survey efforts. Harold and Hanlon's survey (Storr et al. 1981) of the herpetofauna of the Great Australian Bite in 1979 referred to both Mallee Heath Dragons and Dugites as relatively common in coastal areas with mallee or heath. McKenzie et al. (1987) recorded Dugites, Western Brown Snakes (*P. nuchalis*, now *P. mengdeni*) and Peninsula Brown Snake (*P. textilis* now *P. inframaculata*) along the southern escarpment of the Nullarbor and on Roe Plain in 1984 (figure 56, p. 182). Goat Cave is located approximately midway between their southern records of *P. affinis* at Madura and *P. mengdeni* at Eucla. The same survey also records *Amphibolurus norrisi* (previously *A. muricatus*) in the same region.

Dugites are moderately large elapids with broad habitat preferences and a large distribution spanning south-western Australia and the Great Australian Bight to the Eyre Peninsula. While they are expected to occur in Holocene deposits throughout this range, no published record of their fossil occurrence is known. Holocene agamid material from Kangaroo Island was referred to *Amphibolurus norrisi* (Gray et al. 2017), and WAM R182390 from Goat Cave represents the only other fossil record for this species to date. Overall, the reptile diversity of the Nullarbor Plain is underrepresented in the surface deposits, as records within 10 km of the cave locations include at least 15 species while the IBRA region has 115 species listed (Atlas of Living Australia, 2025).

Six species of birds were recorded in total. Welcome Swallows (*Hirundo neoxena*) were the only species present in both caves, as they were actively using the cave entrances to nest. The Australian Masked Owl was likely the main accumulator of bones in Goat Cave. All other birds found were small local birds that may have been predated, as they are all similar in size.

All five taxa of snail recorded during this survey are semi-arid taxa with widespread distributions (Stanisic et al. 2018) and represent a high percentage of extant surface taxa found in the region. Most of the recorded species live at or near the surface among leaf litter, except for the rock-dwelling *Basedowena.* Cave entrances and near surface systems would be a refuge for Nullarbor snails during hot, dry periods, providing dependable shade, moisture and litter.

TAPHONOMY

In both caves, bones would have been accumulated by a mixture of pitfall trapping and accumulation from bones left by predators and owl pellets. There is a

noticeable difference in fauna between the two caves, with Prostate Pit Cave missing many small mammals (e.g. fewer rodents) and small birds, due to a difference in the predator presence between caves. The shape of the entrance of Prostate Pit Cave, with a low flat roof with very few places to perch doesn't encourage owls to use the cave. As a result, the fauna represented is composed of larger species, as it would have been biased by the prey size preference of mammalian predators, such as Dingoes. Goat Cave doesn't seem to have any size bias in its fauna, which includes taxa of all sizes. The entrance of Goat Cave is very large with a domed roof and many large boulders that owls could use to perch. Two species of owl, Barn Owl (*Tyto javanica*) and Australian Masked Owl (McAllan 1997) may live in the region. Both species could have used the caves at some point in time, but we only recovered bones from Australian Masked Owls, providing evidence that at least this species was present in the cave and contributing to the accumulation of bones of the smaller taxa.

The herpetofauna recorded from the opportunistic collecting of surface material is biased towards groups that have remains large enough to be noticed by the naked eye when disarticulated. This excludes many of the smaller skinks, smallest geckos (most gekkonids, and diplodactylids), pygopodids, and blind snakes. Owls as accumulators prefer mammalian prey, resorting to small crepuscular/nocturnal lizards only in times of drought (McDowell and Medlin 2009). Therefore, geckos are typically under-represented in owl roost deposits if small mammalian prey are in abundance. Diurnal predators such as small raptors (kestrels, kites) are more likely to collect reptiles that are active and exposed in the hottest parts of the day – dragons and small monitor lizards. Typically, when larger lizards (*Pogona*, *Varanus*, or *Tiliqua*) are taken by predatory birds the animal is 'unzipped' ventrally and the brain accessed from beneath the chin (KMT pers. obvs.), leaving the body mostly intact and in-situ rather than being transported, partially digested and pelletised. Therefore, the presence of these animals in cave deposits is most likely to be from pit trapping or mammalian accumulators.

CAVE USE, NESTING AND DEN BEHAVIOUR

Upon entering both Goat and Prostate Pit caves, it was very apparent that Welcome Swallows use the cave entrance, as they constantly flew in and out of the caves and were seen tending to their nests built in the cave roof. It is well known that this species uses caves in that manner (Tarburton 1986). As mentioned previously, Australian Masked Owls did occupy Goat Cave at some point in the past but have likely gone locally extinct as a result of fewer prey species available, with many mammalian species now extinct on the Nullarbor Plain (McKenzie et al. 2023).

Denning behaviour in Dingoes is poorly understood, with very few studies in existence (Smith and Vague 2016). Dingoes using caves to den has been reported anecdotally, without a detailed study of behaviour and use within caves (Corbett 2025). Here, we recorded in Prostate Pit Cave, how Dingoes used particular cave chambers to feed, through the accumulation of large prey attributed to Dingoes. The same chamber was used to rest, evidenced by shallow depressions without bones thought to be excavated by Dingoes to lie in, with piles of bones accumulated next to them. We also reported that Dingoes used an adjacent cave chamber as a latrine, evidenced by several Dingo scats found near each other in one area of the cave. Skulls of Tasmanian Devils were also found in the Prostate Pit Cave. As they were collected previously by cavers, we do not know where exactly in the cave they were collected. As a result, it is not possible to understand if Tasmanian Devils also used the cave as a den before going extinct locally, or if they were prey of Dingoes.

Both Goat Cave and Prostate Pit Cave showed evidence of brushtail possum use, although this was far more pronounced in Prostate Pit Cave. In both caves, scent trails and scats were present, suggesting that they may have served as shelters for brushtail possums after the loss of trees on the Nullarbor reduced the availability of shelter. While brushtail possums primarily shelter in tree hollows, they are known to use alternative shelters where trees are absent, including rock crevices and caves (Butler 1970).

In Prostate Pit Cave, evidence suggested that brushtail possums were scavenging carcasses, likely sourced from the nearby Dingo den, and transporting them back to their own den area. Brushtail possums are omnivorous and have been documented to opportunistically feed on carrion (Cruz et al. 2012). The presence of Rabbit remains in both the brushtail possum and Dingo dens further indicates that brushtail possums persisted in this region of the Nullarbor after European settlement, when Rabbits were first introduced.

FUTURE WORK

We have collected samples from seven brushtail possum specimens and the single Chuditch found in the deep tunnels of Goat Cave with the aim to undertake sequencing of their DNA in an ancient DNA lab at Curtin University. This should help resolve the genetic affinity of the Nullarbor Brushtail Possum and Chuditch (Middleton et al. 2025). The same samples will be subsampled and sent to ANSTO for radiocarbon dating, to understand the timing of the death of the specimens in the cave, perhaps helping to understand when and why they died the way they did. Invertebrates other than snails were also collected in the cave, mainly insects and arachnids, which will be studied by colleagues at Adelaide University and the WA Museum.

ACKNOWLEDGEMENTS

We acknowledge the Traditional Custodians of the Country from which these subfossils originate, the Mirning nation, and the Custodians of the lands where we live and work on Whadjuk Noongar Boodja. We acknowledge elders past and present. We thank the Foundation for the Western Australian Museum for providing a Minderoo grant to undertake this fieldwork. We would like to also thank the Western Australian Speleological Group for their help getting into the caves. We thank Osprey International for providing logistic support during the field work.

REFERENCES

Atlas of Living Australia website [accessed 5 August 2025]. http://www.ala.org.au

Baynes, A. (1987). The original mammal fauna of the Nullarbor and southern peripheral regions: evidence from skeletal remains in superficial deposits. In: McKenzie N.L. and Robinson A.C. (eds), *A biological survey of the Nullarbor Region South and Western Australia in 1984*. South Australian Department of Environment and Planning, Western Australian Department of Conservation and Land Management, Australian National Parks. pp: 139–152.

Boscacci, L.J., McKenzie, N.L., and Kemper, C.M. (1987). Mammals. In: McKenzie, N.L. and Robinson, A.C. (eds), *A biological survey of the Nullarbor Region South and Western Australia in 1984*. South Australian Department of Environment and Planning, Western Australian Department of Conservation and Land Management, and Australian National Parks and Wildlife Service. Adelaide: South Australia. pp: 103–137.

Butler, W.H. (1970). A summary of the vertebrate fauna of Barrow Island, W.A. *The Western Australian Naturalist* **11**(7): 149–160.

Cogger, H.G. (2018) *Reptiles & Amphibians of Australia*. Updated Seventh Edition. CSIRO Publishing, Clayton South, Victoria, Australia.

Corbett, L. (2025). *The Dingo Hunter.* Austin Macauley Publishers Ltd, London.

Cruz, J., Sutherland, D.R., Martin, G.R., and Leung, L.K.P. (2012). Are smaller subspecies of common brushtail possums more omnivorous than larger ones? *Austral Ecology* **37**(8): 893–902. doi: 10.1111/j.1442-9993.2011.02346.x

De Waele, B., Wiltshire, B. and Pryke, A. (2023). Six incredible days in Goat Cave – uncovering a secret on the Nullarbor. *The Western Caver* **63**: 82–86.

Dodd, C.S., Catullo, R.A., Travouillon, K.J., Baker, A.M., Westerman, M., and Umbrello, L.S. (2025). Cryptic Kultarr: integrative taxonomy reveals unrecognized species of carnivorous marsupial (Dasyuridae: *Antechinomys*) in arid Australia. *Ecology and Evolution* **15**(7): e71618. doi: 10.1002/ece3.71618

Gray, J.A., McDowell, M.C., Hutchinson, M.N., and Jones, M.E.H. (2017). Geometric morphometrics provides an alternative approach for interpreting the affinity of fossil lizard jaws. *Journal of Herpetology* **51**(3): 375–382. doi: 10.1670/16-145

Lundelius, E.L. (1963). Vertebrate remains from the Nullarbor caves, Western Australia. *Journal of the Royal Society of Western Australia* **46**: 75–80.

Lundelius, E.L., and Turnbull, W.D. (1973). The mammalian fauna of Madura Cave, Western Australia. Part I. *Fieldiana: Geology* **31**(1): 1–35.

Lundelius, E.L., and Turnbull, W.D. (1975). The mammalian fauna of Madura Cave, Western Australia. Part II. *Fieldiana: Geology* **31**(2): 37–117.

Lundelius, E.L., and Turnbull, W.D. (1978). The mammalian fauna of Madura Cave, Western Australia. Part III. *Fieldiana: Geology* **38**(1): 1–120.

Lundelius, E.L., and Turnbull, W.D. (1981). The mammalian fauna of Madura Cave, Western Australia. Part IV. *Fieldiana: Geology, New Series* **6**: 1–72.

Lundelius, E.L., and Turnbull, W.D. (1982). The mammalian fauna of Madura Cave, Western Australia. Part V: Diprotodonta (Part). *Fieldiana: Geology, New Series* **11**: 1–32.

Lundelius, E.L., and Turnbull, W.D. (1984). The mammalian fauna of Madura Cave, Western Australia. Part VI, Macropodidae: Potoroinae. *Fieldiana: Geology, New Series* **14**: 1–63.

Lundelius, E.L., and Turnbull, W.D. (1989). The mammalian fauna of Madura Cave, Western Australia. Part VII, Macropodidae: Sthenurinae, Macropodinae, with a review of the marsupial portion of the fauna. *Fieldiana: Geology, New Series* **17**: 1–71.

Lundelius, E.L., and Turnbull, W.D. (1999). *Leporillus* (Rodentia: Muridae) from Madura Cave, Western Australia. *Proceedings of the Linnean Society of New South Wales* **121**: 129–146.

Lundelius, E.L., Turnbull, W.D. and May, S.R. (2025). The mammalian fauna of Madura Cave, Western Australia. Part IX, the placental mammals. *Records of the Western Australian Museum* **40**: 47–78. doi: 10.18195/issn.0312-3162.40.2025.047-078.

MacLucas, J. (1996). Nullarbor: Trip report 10th April to 4th May 1996. *CEGSA News* **41**(3): 7–86.

McAllan, I.A.W. (1997). More on early records of the 'cave owl' of the Nullarbor Plain. *The Australian Bird Watcher* **17**(4): 198–202.

McDowell, M.C., and Medlin, G.C. (2009). The effects of drought on prey selection of the barn owl (*Tyto alba*) in the Strzelecki Regional Reserve, north-eastern South Australia. *Australian Mammalogy* **31**(1): 47–55. doi: 10.1071/AM08115

McKenzie, N.L, Burbidge, A.A., Baynes, A., Gibson, L.A., Travouillon, K.J., Bullen, R.D., and Turpin, J.M. (2023). 2022 update shows Western Australia's mammals continue to decline. *Australian Mammalogy* **46**: AM23014. doi: 10.1071/AM23014

McKenzie, N.L., Rolfe, J.K., and Carter, D. (1987). Reptiles and amphibians. In: McKenzie, N.L., and Robinson, A.C. (eds), *A Biological Survey of the Nullarbor Region South and Western Australia in 1984*. South Australian Department of Environment and Planning, Western Australian Department of Conservation and Land Management, and Australian National Parks and Wildlife Service. Adelaide: South Australia. pp: 179–210.

Mead, J.I., Hollenshead, M., Swift, S.L., Bell, C.J., and Baynes, A. (2008). *Pygopus* (Squamata: Pygopodidae) from mid-Holocene cave deposits, Western and South Australia. *Records of the Western Australian Museum* **25**(1): 87–93. doi: 10.18195/issn.0312-3162.25(1).2008.087-093

Middleton, S.C., Davis, R.A., Travouillon, K.J., Hopkins, A.J.M., Mills, H.R., and Umbrello, L.S. (2025). Revised phylogeography of the common brushtail possum (*Trichosurus vulpecula*) reveals new insights into genetic structure across Australia. *Zoological Journal of the Linnean Society* **204**: zlaf026. doi: 10.1093/zoolinnean/zlaf026

Newman-Martin, J., Travouillon, K.J., Warburton, N., Barham, M., and Blyth, A.J. (2023). Taxonomic review of the genus *Dasycercus* (Dasyuromorphia: Dasyuridae) using modern and subfossil material; and the description of three new species. *Alcheringa: An Australasian Journal of Palaeontology* **47**(4): 624–661. doi: 10.1080/03115518.2023.2262083

Newman-Martin, J., Travouillon, K.J., Warburton, N., Barham, M., and Blyth, A.J. (2025). Description of the subfossil species *Bettongia haoucharae* sp. nov.; with a taxonomic review of the *Bettongia penicillata* (Diprotodontia:Potoroidae) species complex. *Zootaxa* **5690**(1): 1–69. doi: 10.11646/zootaxa.5690.1.1

Poulter, N. (2020). Prostate Pit 6N-1369: Nullarbor Plain. *Caves Australia* **211**: 22–27.

Prideaux, G.J., Long, J.A., Ayliffe, L.K., Hellstrom, J.C., Pillans, B., Boles, W.E., Hutchinson, M.N., Roberts, R.G., Cupper, M.L., Arnold, L.J., Devine, P.D., and Warburton, N.M. (2007). An arid-adapted middle Pleistocene vertebrate fauna from south-central Australia. *Nature* **445**: 422–425. doi: 10.1038/nature05471

Prideaux, G.J., and Warburton, N.M. (2008). A new Pleistocene tree-kangaroo (Diprotodontia: Macropodidae) from the Nullarbor Plain of south-central Australia. *Journal of Vertebrate Paleontology* **28**: 463–478.

Prideaux, G. J., and Warburton, N. (2009). *Bohra nullarbora* sp. nov., a second tree-kangaroo (Marsupialia: Macropodidae) from the Pleistocene of the Nullarbor Plain, Western Australia. *Records of the Western Australian Museum* **25**(2): 165–179. doi: 10.18195/issn.0312-3162.25(2).2009.165-179

Ramm, T., Gray, J.A., Hipsley, C.A., Hocknull, S., Melville, J., and Müller, J. (2025). Are modern cryptic species detectable in the fossil record? A case study on agamid lizards. *Systematic Biology* **74**(3): 373–394. doi: 10.1093/sysbio/syae067

Richards, J.D., and Short, J. (1996). History of the disappearance of native fauna from the Nullarbor Plain through the eyes of long-time resident Amy Crocker. *The Western Australian Naturalist* **21**(2): 89–96.

Scarsbrook, L., Verry, A.J., Walton, K., Hitchmough, R.A., and Rawlence, N.J. (2023). Ancient mitochondrial genomes recovered from small vertebrate bones through minimally destructive DNA extraction: Phylogeography of the New Zealand gecko genus *Hoplodactylus*. *Molecular Ecology* **32**(11): 2964–2984. doi: 10.1111/mec.16434

Smith, B., and Vague, A.-L. (2016). The denning behaviour of dingoes (*Canis dingo*) living in a human-modified environment. *Australian Mammalogy* **39**(2): 161–168. doi: 10.1071/AM16027.

Stanisic, J., Shea, M,, Potter, D., and Griffiths, O. (2018) *Australian land snails volume 2. A field guide to southern, central and western species*. Mauritius: Bioculture Press.

Storr, G.M., Hanlon, T.M.S., and Harold, G. (1981) Herpetofauna of the shores and hinterland of the Great Australian Bight, Western Australia. *Records of the Western Australian Museum* **9**(1): 23–39.

Storr, G.M., Smith, L.A., and Johnstone, R.E. (1983). *Lizards of Western Australia II. Dragons and Monitors*. Western Australian Museum, Perth.

Storr, G.M., Smith, L.A., and Johnstone, R.E. (2002). *Snakes of Western Australia*. Revised Edition. Western Australian Museum, Perth.

Tarburton, M.K. (1986). A comparison of the flight behaviour of the White-rumped Swiftlet and the Welcome Swallow. *Bird Behaviour* **6**(2): 72–84.

Travouillon, K.J., and Phillips, M.J. (2018). Total evidence analysis of the phylogenetic relationships of bandicoots and bilbies (Marsupialia: Peramelemorphia): reassessment of two species and description of a new species. *Zootaxa* **4378**(2): 224–256. doi: 10.11646/zootaxa.4378.2.3

Travouillon, K.J., Simões, B.F., Portela Miguez, R., Brace, S., Brewer, P., Stemmer, D., Price, G.J., Cramb, J., and Louys, J. (2019). Hidden in plain sight: reassessment of the pig-footed bandicoot, *Chaeropus ecaudatus* (Peramelemorphia, Chaeropodidae), with a description of a new species from central Australia, and use of the fossil record to trace its past distribution. *Zootaxa* **4566**: zootaxa.4566.1.1 doi: 10.11646/zootaxa.4566.1.1

Woodhead, J.D., Sniderman, J.M.K., Hellstrom, J., Drysdale, R.N., Maas, R., White, N., White, S., and Devine, P. (2019). The antiquity of Nullarbor speleothems and implications for karst palaeoclimate archives. *Scientific Reports* **9**: 603. doi: 10.1038/s41598-018-37097-2

MANUSCRIPT RECEIVED 21 OCTOBER 2025; ACCEPTED 13 NOVEMBER 2025.